Universidad de Concepción

Facultad de Ciencias Ambientales
Programa de Doctorado en Ciencias Ambientales mención Sistemas Acuáticos Continentales

INTEGRATED ASSESSMENT OF CLIMATE CHANGE AND LAND-USE/LAND-COVER CHANGE ON FLOODS: INSIGHS FROM LANDSCAPE CONFIGURATION IN A TROPICAL BASIN

Tesis para optar al grado de

Doctor en Ciencias Ambientales con mención en Sistemas Acuáticos Continentales

Jorge René Hurtado Pidal

CONCEPCIÓN-CHILE
2023

Universidad de Concepción

Facultad de Ciencias Ambientales
Programa de Doctorado en Ciencias Ambientales mención Sistemas Acuáticos Continentales

EVALUACIÓN INTEGRADA DEL CAMBIO CLIMÁTICO Y EL CAMBIO DE USO/COBERTURA DEL SUELO EN INUNDACIONES. PERSPECTIVAS DESDE LA CONFIGURACIÓN DEL PAISAJE EN UNA CUENCA TROPICAL

Tesis para optar al grado de

Doctor en Ciencias Ambientales con mención en Sistemas Acuáticos Continentales

Jorge René Hurtado Pidal

Profesor Guía: Dr. Mauricio Aguayo Arias
Dpto. de Planificación Territorial, Facultad de Ciencias Ambientales
Universidad de Concepción

Profesor Co-Guía: Dr. Oscar Link Lazo
Dpto. de Ingeniería Civil, Facultad de Ingeniería
Universidad de Concepción

CONCEPCIÓN-CHILE

2023

Comisión Evaluadora de Tesis de Grado:

Dr. Mauricio Aguayo
Director de Tesis
Departamento de Planificación Territorial
Facultad de Ciencias Ambientales
Universidad de Concepción

Dr. Oscar Link
Cotutor de Tesis
Departamento de Ingeniería Civil
Facultad de Ingeniería
Universidad de Concepción

Dr. Octavio Rojas
Evaluador interno
Departamento de Planificación Territorial
Facultad de Ciencias Ambientales
Universidad de Concepción

Dra. Alejandra Stehr
Evaluador interno
Departamento de Ingeniería Civil
Facultad de Ingeniería
Universidad de Concepción

Dr. Bryan Valencia
Evaluador externo (Internacional)
Facultad de Ciencias de la Tierra y Agua
Universidad Regional Amazónica Ikiam

DEDICATORIA

A Emilia y Karina, pilares de mi vida.

A mis queridos padres, Jorge y Janeth.

“Solo podemos dominar la naturaleza si la obedecemos”

"We can only dominate nature if we obey it"

Francis Bacon

AGRADECIMIENTOS

Gracias Karina y Emilia por su paciencia, no he podido dedicarles mucho tiempo estos años, y sumado al hecho de estar en otro país, lejos de nuestras familias, a significado un sacrificio adicional para ustedes. Quiero agradecer también a mis papás, Jorge y Janeth y a mis hermanos, Fidel e Iván, por estar siempre pendientes y apoyándonos desde Ecuador. Es oportuno dar las gracias a mi familia política, Marianita y Bosquito, por su apoyo en este proyecto familiar. Gracias a los amigos de Concepción, no son muchos, pero si valiosos. Además, de forma general quiero agradecer a los coautores de las publicaciones de esta Tesis.

De forma especial quiero agradecer a mis profesores tutores Mauricio Aguayo y Oscar Link, superaron todas mis expectativas. Gracias por esas orientaciones precisas y oportunas, siento que hicimos un buen equipo, fue increíble recibirlos en Ecuador cuando fueron. Quiero agradecer a los evaluadores de esta tesis por sus valiosos comentarios. Gracias también a las instituciones que hicieron posible esta Tesis. Empiezo con la Universidad de Concepción y la Facultad de Ciencias Ambientales. Fue una experiencia muy bonita hacer el doctorado en esta Universidad. También quiero hacer un especial reconocimiento del trabajo que hacen las personas encargadas de la dirección del programa de doctorado, son personas muy comprometidas. Gracias a la Universidad Ikiam y a personas como Bryan V, Jorge C, Edgar E y Juseth Ch, por su buena predisposición para compartir información y colaboración en general. Y ahora llegó el momento de dar gracias a los financistas. Gracias a la Secretaría de Educación Superior, Ciencia, Tecnología e Innovación (SENESCYT) por ayudarme con parte del financiamiento para el doctorado. De manera especial gracias a la Agencia Nacional de Investigación y Desarrollo de Chile (ANID), fueron un salvavidas cuando más lo necesité.

CURRICULUM VITAE

Jorge René Hurtado Pidal

Formación académica

Doctorado en Ciencias Ambientales con mención en Sistemas Acuáticos Continentales, Universidad de Concepción, Concepción, Chile (2019-2023).

Magister en Geomática, Universidad Nacional de La Plata, La Plata, Argentina (2014).

Ingeniero Geógrafo y Del Medio Ambiente, Universidad de las Fuerzas Armadas (ESPE), Sangolquí, Ecuador (2008).

Publicaciones

Relacionadas al proyecto de doctorado

Hurtado-Pidal, J., Acero Triana, J. S., Espitia-Sarmiento, E., & Jarrín-Pérez, F. (2020). Flood Hazard Assessment in Data-Scarce Watersheds Using Model Coupling, Event Sampling, and Survey Data. Water. https://doi.org/10.3390/w12102768

Hurtado-Pidal, J., Acero Triana, J. S., Aguayo, M., Link, O., Valencia, B., Espitia-Sarmiento, E., Conicelli, B. (2022). Is Forest location more important than forest fragmentation for flood regulation?. Ecological Engineering. https://doi.org/10.1016/j.ecoleng.2022.106764

Hurtado-Pidal, J., Aguayo, M., Link, O (2023). Analysis of the combined effects of climate change and land-use/land-cover change on floods. *En preparación*.

No relacionadas al proyecto de doctorado

Chancay, J. E., **Hurtado-Pidal, J.,** & Espitia-Sarmiento, E. (2023). Comparación Entre Un Modelo Hidrológico Distribuido y Otro Semi-Distribuido Para Simular Crecidas En La Amazonía Ecuatoriana. Memorias del XXX Congreso Latinoamericano de Hidráulica (Vol. 2, pp. 747–748). IAHR. ISBN 978-90-832612-3-2

Rifo, C., **Hurtado-Pidal, J.,** & Link, O. (2023). General Or Local Scour Exceedance?. Analysis Of The Cancura Bridge Collapse In Chile. Memorias del XXX Congreso Latinoamericano de Hidráulica (Vol. 3, pp. 254–255). IAHR. ISBN 978-90-832612-4-9

Participación en eventos científicos

Hurtado-Pidal, J., Aguayo, M. (2021). Evaluación del patrón espacial de la cobertura de bosque en relación a la generación de caudales por lluvias intensas. Aplicación en una cuenca de la Amazonía Ecuatoriana. Presentación oral en modalidad online. XLI Congreso Nacional y XXVI Internacional de Geografía. Valparaíso (Chile), entre el 18 y 22 de octubre de 2021.

Chancay, J. E., **Hurtado-Pidal, J.,** & Espitia-Sarmiento, E. (2023). Comparación Entre Un Modelo Hidrológico Distribuido y Otro Semi-Distribuido Para Simular Crecidas En La Amazonía Ecuatoriana. Presentación oral en modalidad online. XXX Congreso Latinoamericano de Hidráulica. Iguazú (Brasil), entre el 7 y 11 de noviembre de 2022.

Rifo, C., **Hurtado-Pidal, J.,** & Link, O. (2023). General Or Local Scour Exceedance?. Analysis Of The Cancura Bridge Collapse In Chile. Presentación oral en modalidad online. XXX Congreso Latinoamericano de Hidráulica. Iguazú (Brasil), entre el 7 y 11 de noviembre de 2022.

Hurtado-Pidal, J. (2023). ¿Es la localización del bosque más importante que su fragmentación para la regulación de inundaciones?. Presentación oral en modalidad online. Simposio Internacional de Ciencias Forestales. Bosque, Agua y Biodiversidad. Loja (Ecuador), entre el 13 y 15 de febrero del 2023.

Hurtado-Pidal, J., Aguayo, M., & Link, O. (2023). Interacciones y efectos por localización del cambio climático y de cobertura del suelo sobre inundaciones repentinas. Aplicación en una cuenca de la Amazonía Ecuatoriana. Presentación oral. IV Reunión Bienal IALE-CHILE: “Transiciones Socioecológicas para paisajes Sustentables y Resilientes”. Concepción (Chile), entre el 10 y 13 de mayo del 2023.

Hurtado-Pidal, J., Aguayo, M., & Link, O. (2023). Contribuciones y efectos por localización del cambio climático y de cobertura del suelo sobre inundaciones repentinas. Aplicación en una cuenca de la Amazonía Ecuatoriana. Presentación oral en modalidad online. III Congreso Nacional de Geografía. Expandiendo

horizontes disciplinares desde el pensamiento espacial. Quito (Ecuador), entre el 1 y 3 de junio del 2023.

Líneas de investigación

Principal: Cambio global, sociedad y agua.
Secundaria: Biodiversidad, servicios ecosistémicos y agua.

Experiencia en docencia

Docencia

Personal docente en la Universidad Regional Amazónica Ikiam (Ecuador). Asignaturas: Hidráulica General, Hidráulica de Ríos. Período: noviembre de 2017 hasta enero de 2019.

Ayudantías

Ayudante del curso 'SIG avanzado' de la Universidad de Concepción. Encargado del diseño, desarrollo y evaluación de prácticas para estudiantes de pre y postgrado. Período: 2021-2022. Profesor responsable, Dr. Mauricio Aguayo

Ayudante del curso 'Modelación Hidrológica Distribuida con el Modelo TETIS'. Organizado por la Universidad de Concepción (Escuelas de Verano UdeC) en colaboración con la Universidad Politécnica de Valencia (UPV, España). Fechas: enero de 2021 y enero de 2023. Profesor responsable, Dr. Mauricio Aguayo.

Becas y reconocimientos

Secretaría de Educación Superior, Ciencia, Tecnología e Innovación de Ecuador (SENESCYT). Adjudicación de beca en el **Programa de Becas Internacionales de Postgrado 2018** (Nro. Contrato CZ02-000837-2018). Convocatoria 2018.

Agencia Nacional de Investigación y Desarrollo de Chile (ANID). Adjudicación de beca en el **Concurso de Beca Doctorado Nacional** (Nro. Beca 21210172). Año académico 2021.

ANID. Adjudicación para **Gastos Operacionales del Proyecto de Tesis Doctoral**. Segundo llamado 2021.

ANID. Adjudicación de extensión de beca para **Redacción de Tesis Doctoral.** Primer llamado 2023.

FINANCIAMIENTO

Esta Tesis fue realizada con el financiamiento de:

Agencia Nacional de Investigación y Desarrollo (ANID), Chile
Programa de Formación de Capital Humano Avanzado
Beca de Doctorado Nacional
Folio Nro. 21210172

Secretaría de Educación Superior, Ciencia, Tecnología e Innovación (SENESCYT), Ecuador
Programa de Becas Internacionales de Postgrado 2018
Nro. Contrato CZ02-000837-2018

CONTENTS

LIST OF FIGURES

CHAPTER III

CHAPTER IV

CHAPTER V

APPENDIX II

LIST OF TABLES

CHAPTER III

CHAPTER IV

CHAPTER V

SUMMARY

Climate change and land-use/land-cover change (LUCC) are among the main anthropogenic factors affecting flood risk, as they change the frequency and magnitude of floods. Specifically, native forest deforestation in tropical humid basins reduces the forest capacity for flood regulation during small and medium-size storms events. Also, while climate change affects at regional scales, the LUCC influences occur at a smaller, local scale. Consequently, forest protection and reforestation are considered a nature-based solutions (NbS) for flood regulation, especially on small basins (<100 Km^2). However, there are few studies that analyze the combined effects of both forcings (i.e., climate change and LUCC) on floods, and generally they focus on the discharge at the basin outlet only. Thus, the continuous variation of interactions in the stream network has not been identified yet. On the other hand, little is known about the effects of different deforestation spatial patterns over floods. Together, these knowledge gaps limit the understanding of the ecosystem services provided by the forest for flood regulation within the context of NbS and climate change adaptation. Therefore, this research evaluates the effects of LUCC on floods distinguishing forest location and forest fragmentation in a humid tropical basin within the Ecuadorian Amazon. Additionally, it analyzes the individual and combined effects of climate change and LUCC on floods across the basin's altitudinal gradient.

In the first stage (Chapter III), this study applied the use of storm event sampling and flood-survey data to validate a modeling framework for flood hazard assessment in data-scarce watersheds. Specifically, the hydrologic modeling system (HEC-HMS) was coupled with the Nays2Dflood hydrodynamic solver to simulate the system response to several storm events including one, that flooded urban areas located within the basin. In the second stage (Chapter IV), the spatially-distributed hydrological model TETIS was calibrated and validated using nine storm samples in order to evaluate the effects of forest location and forest fragmentation on floods. The TETIS model was applied to simulate the influence of five LUCC scenarios, including forest location and forest fragmentation. The Kruskal-Wallis and the *post-hoc* Dunn tests were used to analyze the differences between scenarios. In the third stage (Chapter V), LUCC scenarios were prepared with two homogeneous land cover types, forest and agriculture, while precipitation scenarios were obtained through the Global Climate Model (GCM) IPSL SSP5-8.5 (CMIP6). The hydrological response of the scenarios was evaluated at 42 points across the stream network using the TETIS model previously calibrated. The individual and combined effects of climate change and LUCC were analyzed using absolute differences and the aforementioned statistical tests, including the Sheirer-Ray-Hare test.

Results from the coupled approach, showed satisfactory model performance in simulating streamflow and water depths. In almost all events, the Nash-Sutcliffe coefficient (NSE) was within the range $0.40 \leq NSE \leq 0.95$, while the range of Percent Bias (PBIAS) was $-3.67\% \leq PBIAS \leq 23.4\%$. Forest location and forest fragmentation had greater influence on overland flow than on stormflows at the basin outlet. However, forest location had more influence than forest fragmentation over both, overland flow and storm flows. Deforestation of the upper basin represented the worst scenario for flood regulation. In addition, the climate change effect on floods was more homogeneous than the LUCC effect, across the altitudinal gradient of the basin. Moreover, the relative influence of deforestation on stormflows was greater than that of climate change in the upper part of the basin, while in the lower part of the basin, the climate change was more important than LUCC for flood changes. For small floods the altitudinal range from 590 to 906 meters above sea level (m.a.s.l) was identified as a transitional area in terms of influence of deforestation on stormflows. However, a relatively stable threshold of absolute differences in peak flows and stormflow volume was obtained at 590 m.a.s.l. Finally, a slightly and statistically non-significant interaction between climate change and LUCC was identified, with an antagonistic effect in the lower part.

In conclusion, native forest protection and/or reforestation, in the upper part of the basin are crucial for flood risk mitigation during small and moderate events, while maintaining several ecosystems services through implementation of NbS. The flood magnitude changes in the lower part of the basin are closely related to the scale effect and the sensitivity of the ecosystem in the upper part. Moreover, the importance of forest for flood regulation will be even greater in the future due to the climate change-induced precipitation projections. However, as storm intensity and catchment area increases, the capacity of forest to regulate floods decreases in the downstream direction and in a non-linear manner. Thus, the NbS needs to be integrated to other strategies within a broader context in order to achieve an effective flood management. The applied methodology can be used by modelers and decision-makers for flood impact assessment under climate change and LUCC scenarios in data-scarce watersheds. Moreover, the results improve our understanding of ecosystem services of Andean foothills forests and provide guidelines to implement NbS for flood regulation and climate change adaptation.

Keywords: hydrological modeling, TETIS, Floods, climate change, land-use/land-cover changes, nature-based solutions, Ecuadorian Amazon.

RESUMEN

El cambio climático y el cambio de uso/cobertura del suelo (LUCC; por sus siglas en inglés) están entre los principales forzantes antrópicos que afectan la frecuencia y magnitud del riesgo de inundación. Específicamente, la deforestación de bosques nativos en cuencas húmedas tropicales reduce la capacidad de regulación de inundaciones (crecidas hidrológicas) durante eventos de tormentas pequeñas y medianas. Mientras que el cambio climático afecta a escalas regionales, la influencia del LUCC ocurre a una escala local más pequeña. En consecuencia, la protección y reforestación de bosques se consideran soluciones basadas en la naturaleza (SbN) para la regulación de inundaciones, especialmente en cuencas pequeñas (<100 Km2). Sin embargo, hay pocos estudios que analizan los efectos combinados del cambio climático y LUCC en las inundaciones, y generalmente se centran solo en el caudal a la salida de la cuenca. Por lo tanto, la variación continua de las interacciones en la red fluvial aún no ha sido identificada. Por otro lado, se sabe poco acerca de los efectos de diferentes patrones espaciales de deforestación en las inundaciones. Estas brechas de conocimiento limitan la comprensión de los servicios ecosistémicos proporcionados por los bosques para la regulación de inundaciones en el contexto de las SbN y la adaptación al cambio climático. Por lo tanto, este estudio evalúa los efectos del LUCC en las inundaciones distinguiendo la ubicación y fragmentación del bosque en una cuenca húmeda tropical dentro de la Amazonía ecuatoriana. Además, analiza los efectos individuales y combinados del cambio climático y el LUCC en las inundaciones a lo largo del gradiente altitudinal de la cuenca.

En la primera etapa (Capítulo III), este estudio utilizó un muestreo de eventos de tormenta y datos de inundaciones en terreno para validar un marco metodológico de modelación de peligrosidad en cuencas con escasez de datos. El modelo HEC-HMS se acopló con el modelo hidrodinámico Nays2Dflood para simular la respuesta del sistema a varios eventos de tormentas, incluido uno que inundó áreas urbanas en de la cuenca. En la segunda etapa (Capítulo IV), se calibró y validó el modelo hidrológico distribuido TETIS utilizando nueve eventos de tormentas para evaluar los efectos de la ubicación y fragmentación del bosque en los caudales de crecida. El modelo TETIS se aplicó para simular la influencia de cinco escenarios LUCC, considerando diferente localización y fragmentación del bosque. Se utilizó el test estadístico de Kruskal-Wallis y el test *post-hoc* de Dunn para analizar las diferencias entre los escenarios. En la tercera etapa (Capítulo V), se prepararon escenarios homogéneos de LUCC con dos escenarios, bosque y agricultura, mientras que los escenarios de precipitación se obtuvieron a través del Modelo Climático Global

(GCM; por sus siglas en inglés) IPSL SSP5-8.5 (CMIP6). La respuesta hidrológica de los escenarios se evaluó en 42 puntos a lo largo de la red fluvial utilizando el modelo TETIS previamente calibrado. Los efectos individuales y combinados del cambio climático y el LUCC se analizaron utilizando diferencias absolutas y los tests estadísticos ya mencionados, incluido el test de Sheirer-Ray-Hare.

Los resultados del enfoque acoplado mostraron un rendimiento satisfactorio de los modelos en la simulación de caudales y niveles de agua. En casi todos los eventos, el coeficiente de Nash-Sutcliffe (NSE) estuvo dentro del rango $0.40 \leq NSE \leq 0.95$, mientras que el rango de Sesgo Porcentual (PBIAS) fue $-3.67\% \leq PBIAS \leq 23.4\%$. Los patrones espaciales de LUCC tuvieron una influencia mayor en la escorrentía superficial que en los caudales de tormenta en la salida de la cuenca. Sin embargo, la localización del bosque tuvo más influencia que la fragmentación tanto en la escorrentía superficial como en los caudales de tormenta. La deforestación de la parte alta de la cuenca representó el peor escenario para la regulación de inundaciones. Por otro lado, el efecto del cambio climático en las inundaciones fue más homogéneo que el efecto del LUCC a lo largo del gradiente altitudinal de la cuenca. Además, la influencia relativa de la deforestación en la parte alta de la cuenca sobre el caudal de tormenta, fue mayor que la del cambio climático, mientras que en la parte baja, el cambio climático fue más importante. Para inundaciones pequeñas, el rango altitudinal de 590 a 906 metros sobre el nivel del mar (m.s.n.m) fue identificado como un área de transición en términos de la influencia de la deforestación en los caudales de tormenta. Sin embargo, se obtuvo un umbral relativamente estable de diferencias absolutas en caudales máximos y volumen de caudal a 590 m.s.n.m. Finalmente, se identificó una interacción leve y estadísticamente no significativa entre el cambio climático y el LUCC, con un efecto antagonico en la parte baja.

En conclusión, la protección y/o reforestación de bosque nativo en la parte alta de la cuenca es crucial para la mitigación del riesgo de inundaciones, durante eventos pequeños y moderados. Al mismo tiempo se mantienen varios servicios ecosistémicos mediante la implementación de SbN. Los cambios en la magnitud de las inundaciones en la parte baja de la cuenca, están estrechamente relacionados con el efecto de escala y la sensibilidad del ecosistema en la parte superior. En este sentido, la importancia del bosque para la regulación de inundaciones será aún mayor en el futuro debido a las proyecciones de precipitación por cambio climático. Sin embargo, a medida que aumenta la intensidad de las tormentas y el área de captación, la capacidad del bosque para regular inundaciones disminuye en dirección aguas abajo y de manera no lineal. Por lo tanto, las SbN deben integrarse con otras estrategias dentro de un contexto más amplio para lograr una gestión

efectiva de inundaciones. La metodología aplicada puede ser utilizada por modeladores y tomadores de decisiones para la evaluación del impacto de inundaciones bajo escenarios de cambio climático y de LUCC en cuencas con escasez de datos. Estos resultados mejoran la comprensión de los servicios ecosistémicos de los bosques de las estribaciones Andes-Amazonía y proporcionan pautas para implementar SbN para la regulación de inundaciones y la adaptación al cambio climático.

Palabras clave: modelación hidrológica, TETIS, inundaciones, cambio climático, cambio de uso/cobertura del suelo, soluciones basadas en la naturaleza, Amazonía Ecuatoriana.

CHAPTER I

INTRODUCTION

1. Introduction

1.1. Deforestation and Floods. Implications for Ecuadorian Amazon

Flooding is the most common type of natural hazard. During the 2000-2017 period, it affected more than 86 million people worldwide (EM-DAT, 2023). Flash floods are a type of flood that causes the most severe damage in terms of fatalities and economic losses (Jonkman, 2005; UNISDR, 2017). Climate change and land-use/land-cover change (LUCC), such as deforestation, are among the main drivers than can exacerbate flood magnitude and frequency (Bronstert et al., 2002; Chang & Franczyk, 2008; IPCC, 2021). The interaction between climate change and LUCC on floods is non-lineal and complex scale-dependent processes within the basin (Blöschl et al., 2007; Rogger et al., 2017). Moreover, the effect of different LUCC spatial patterns makes it even more difficult to predict the results of these interactions (Hou et al., 2018). It is therefore paramount understand the individual and combined effects of climate change and LUCC on floods to apply land-cover based solutions for flood risk management and climate change adaptation (Blöschl et al., 2019; Dadson et al., 2017; Lane, 2017).

Globally the deforestation rate per year has decreased from 10.6 million hectares in the 1900s to 6.5 million hectares between 2010 and 2015 (UNEP, 2019). In Ecuador deforestation rates decreased between 1900 and 2010 (Sierra, 2013). However, native forest has experienced a decline from 51.5% in 1990 to 50.9% in 2014 (Ministerio de Ambiente, 2015). Approximately 74% of this native forest is located within the Ecuadorian Amazon Region (EAR). Among the main drivers or factors promoting deforestation in the EAR are: proximity to roads and populated centers (access to markets), population density, land tenure and primary education (Kleemann et al., 2022; Mena et al., 2006; Sierra, 2013; Southgate et al., 1991). In the Tena River Basin (TRB), natural coverage (native forest and herbaceous vegetation) decreased from 17027 hectares in 1990 to 16219 hectares to 2014, representing a reduction of 5 % approximately (Ministerio de Ambiente, 2015). In this regard, the presence of the protected area Colonso-Chalupas Biological Reserve (RBCC) since 2014, with 9154 hectares (38 % of TRB) helps to decrease deforestation rates within the TRB (Cuenca et al., 2018; Kleemann et al., 2022).

However, the deforestatioin within the EAR and TRB remains a serious problem that compromises several ecosystem services, including water flow regulation associated with river flooding. This is explained by the close relationship between water and the landscape (H. Gao et al., 2018). This becomes even more

relevant considering that ecosystems and forests are key elements in establishing climate change adaptation measures (Cohen-Shacham et al., 2019). Furthermore, the loss of native forest has been recognized as a significant factor contributing to changes in flood risk (Q. Gao & Yu, 2017). Consequently, the implementation of forest protection and reforestation measures has been recognized as nature-based solutions (NbS) to complement the efforts for floods management (Dadson et al., 2017; Ilieva et al., 2018; Lane, 2017). Moreover, the NbS are especially relevant for Tropical Andean Regions as forest are related to several ecosystem services such as water regulation and supply, carbon sequestration, soil erosion control (Bonnesoeur et al., 2019).

1.2. General Relationships Between Forest and Floods

The Tropical Andean Forest (TAF) serves as a natural barrier where interception may account for 40% of total precipitation (Fleischbein et al., 2006). Moreover, the presence of trees and root systems in TAF enhances the soil water retention capacity, reducing the amount of water entering the stream network (Ataroff & Rada, 2000; Qi & Liu, 2019; Tobón, 2008, 2021). The relatively high saturated hydraulic conductivity by *Andisols* with high organic matter content, enhances the Infiltration capacity (Sánchez et al., 2018). All these characteristics together make TAF special ecosystems capable of acting as natural buffers against floods (Bonnesoeur et al., 2019; Tobón, 2008). However, the flood regulation capacity of forest is limited to small and medium size storms (Bathurst et al., 2011; Birkel et al., 2012; Iacob et al., 2017; Salazar et al., 2012). For instance, Bathurst et al. (2020) indicate that forest reach the maximum capacity to mitigate floods with moderate return periods of 5-20 years. Also, Birkel et al. (2012) found, in a humid basin in Costa Rica, small effect of LUCC on peak flows for discharges with return period > 1-year. Nevertheless, downstream lowland areas would still be prone to flooding, even if the forests upstream remained undisturbed (Laurance, 2007). Moreover, as soil moisture increases the effect of forest on high flows is lower (Bathurst et al., 2020; Bronstert et al., 2002; Sriwongsitanon & Taesombat, 2011).

The LUCC and its relationship with floods have different spatial and temporal scales (Chang & Franczyk, 2008). Anthropogenic activities such as forest management, agricultural practices (including weed burning), drainage, and others can modify chemical-biological interactions as well as spatial connectivity, thus affecting flooding (Rogger et al., 2017). However, the topography and land-cover are among the main features that define a landscape (H. Gao et al., 2018). In this regard, the forest location and forest fragmentation (spatial patterns), under certain conditions, can influence the runoff and flooding process (Kim & Park, 2016; Liu et

al., 2020). Forest location refers to the presence of aggregated forest coverage on different slopes (Hou et al., 2018). On the other hand, forest fragmentation is the conversion of continuous forest to disaggregated mosaic of forest patches (Fahrig, 2003). Some studies found differences on high flows when forest is located at different slopes (Descheemaeker et al., 2006; Hou et al., 2018; Jourgholami et al., 2020). In this regard, the evidence suggests a greater effect of LUCC in the upper basin than the lower part (Edokpa et al., 2022; Hung et al., 2020; Olang & Fürst, 2011). However, the proportion of forest area is important. Bathurst et al. (2011) suggests that changes in peak discharge can be observed from a minimum alteration of 20-30% in the forested area. Furthermore, locate dense vegetation near watercourses has the greater effect on floods (Dadson et al., 2017). Nevertheless, it is expected that flood attenuation decreases with the downstream distance to the perturbation (Lane, 2017). Moreover, due to scale effect, as watershed area increases the influence of LUCC on high flows becomes smaller (Blöschl et al., 2007; Dadson et al., 2017). Similarly, with the increase in watershed size, hydraulic processes in the channel become more important than slope runoff processes (i.e., overland flow, interflow) when determining response times (lag-time) in relation to water movement (Asano & Uchida, 2018). Thus, on small watersheds (<100 km^2) riparian vegetation and floodplains in the lower parts of the basin can contribute to flood reduction, desynchronizing flow, by increasing roughness and lag-time (Lane, 2017). For instance, Dixon et al. (2016) found 19% of reduction on peak flows for riparian forest restoration of 20-40% of the total catchment area. However, NbS focusing on channel and flood plain storage is only effective for small flood events and inadequate for larger ones (Metcalfe et al., 2017).

Finally, few studies have related the landscape spatial metrics, to hydrological response of the basin. For instance, Boongaling et al. (2018) indicates that connectivity, aggregation, and size of forest patches within the landscape are the metrics most closely related to overland flow and sediment load. Moreover, Boongaling et al. (2018) suggest that forest fragmentation increases overland flow and reduces the base flow. However, the study conducted by Kim & Park, (2016) in Texas, found that the role of connectivity in surface runoff is not clear, as they obtained contradictory results in some cases. Nevertheless, they found that metrics related to size and shape were correlated with runoff. Another study carried out in humid tropical catchments in Puerto Rico suggest that fragmentation may increase freshwater supply, whereas raise large discharges during extreme events (Q. Gao & Yu, 2017).

1.3. Climate Change and Floods. Implications for Ecuadorian Amazon

For high emission scenarios (CMIP5: RCP8.5; CMIP6: SSP5-8.5) derived from General Circulation Models (GCMs), the short-duration and high-intensity precipitation events are projected to become more intense, leading to increased global flood occurrences (Hirabayashi et al., 2013; IPCC, 2021; Merz et al., 2014; Vu et al., 2017). However, when discussing floods and precipitation, it is crucial to consider the co-dependence of climate and landscape. In this regard, some studies suggest that floods are more responsive to the spatial variability rather than the temporal variability of precipitation (Perdigão & Blöschl, 2014). Thus, the effect of spatial variability becomes more apparent as the watershed size increases. Furthermore, the interaction between soil surface conditions and precipitation must be considered (Bronstert et al., 2002). For instance, in some catchments, soil moisture is the major control on runoff generation processes (Blöschl, 2022).

Although an increase in global-scale flash floods would be expected under climate change scenarios, increasing temperatures would enhance precipitation intensity and surface runoff (Yin et al., 2018); other authors argue that an increase in temperature does not necessarily result in more floods, and it cannot be directly linked to a global-scale increase in flooding (Wasko & Sharma, 2017). Despite the rise in extreme precipitation events in various regions worldwide, the occurrence of floods does not exhibit an equal response. This can be partly explained by the fact that temperature increase in certain cases leads to a decrease in antecedent moisture conditions, thereby enhancing soil infiltration capacity (Sharma et al., 2018). Furthermore, it should be noted that the influence of antecedent moisture diminishes in smaller basins (Johnson et al., 2016; Sharma et al., 2018). However, the relationship between temperature, precipitation, and floods within the context of climate change and flash floods remains a topic of ongoing debate within the scientific community, lacking a general consensus at present (Wasko et al., 2019; Yin et al., 2019). This suggests that the effect of climate change on floods cannot be generalized, emphasizing the need for case-specific studies.

The climate in Ecuador is mainly influenced by the Pacific Ocean, the Andes Mountains, and the Amazon Rainforest, from which large moisture masses originate (Junquas et al., 2022). Specifically, the foothills such as the eastern slope of the Andes Mountains, are influenced significantly by the Intertropical Convergence Zone (ITCZ; Vargas et al., 2022) and by moist air masses from the eastern part of the Amazon basin. Therefore, the combination of orographic effect and the influence of the ITCZ favor the formation of convective storms in foothill basins such as TRB. Among the most significant impacts of climate change in Ecuador are: temperature

increases, glacier retreat, prolonged droughts, and changes in precipitation patterns (Cadilhac et al., 2017). The Amazon basin is prone to future extreme events related to floods (Hirabayashi et al., 2013). Palomino-Lemus et al., and Solman (2017; 2013) indicate that the average annual precipitation would decrease in the Amazon, but with an increase in the northwest region, near the foothills of the Andes Mountains. Similarly, the average annual runoff would increase (Pabón-Caicedo et al., 2020; Sorribas et al., 2016).

On the other hand, an increase in precipitation is projected in the tropical Andes of Ecuador (Sarmiento & Kooperman, 2019). Furthermore, increasing trends in maximum flows and decreasing trends in minimum flows are expected (Pabón-Caicedo et al., 2020). However, the studies on precipitation projections due to climate change in South America are based on GCMs and Regional Circulation Models (RCMs). Thus, part of the uncertainty associated with GCMs or RCMs is due to the weak representation of orographic effects or relief with coarse resolutions (Buytaert et al., 2010; Sarmiento & Kooperman, 2019), especially for rainfall hotspots with greater topographical gradient, such as Andes-Amazonian foothills (Espinoza et al., 2015).

1.4. Individual and Combined Effects of Climate Change and LUCC on Floods

Climate change and LUCC simultaneously impact hydrological processes at the basin scale. However, since the impacts acts at different spatial scales, the analysis of their individual contributions is necessary for watershed planning and management (Lian et al., 2020; Zhang et al., 2018). Blöschl et al. (2007) hypothesized that climate change impact on floods across different basin scales, is more homogeneous than LUCC. Moreover, they indicate that at smaller scales, LUCC has a larger impact than climate variability on hydrological response. Depending mainly on data availability and research purpose, several methodologies exist to separately identify these contributions (Yang et al., 2017). However, hydrological modeling and paired catchment analysis are among the most common (Zhang et al., 2018). Given the increasing data availability, development of distributed hydrological models and computing capabilities, the hydrological modeling approach have been widely used (Hung et al., 2020; Lamichhane & Shakya, 2019; Yang et al., 2017). This approach combines hypothetical scenarios ("what-if approach") and the one-factor-at-a-time analysis ("OFAT method").

The experimental design based on hydrological modeling combines different scenarios (i.e.: base scenario, LUCC-based scenarios and climate change-based scenarios), to assess the individual and combined effects on hydrological variables.

Previous studies (Chawla & Mujumdar, 2015; Tian et al., 2022; Zhang et al., 2018) have examined the individual and combined effects of climate change and LUCC on floods using hydrological modeling. In this regard, the interaction is one of the main characteristics related to the combined effects of climate change and LUCC. Specifically, interaction refers to the relationship between two or more variables that affects the response variable in a non-additive or non-independent manner (Dunne, 2010; Rothman, 1976). Thus, the interaction can be either synergistic or antagonistic. Synergistic interaction occurs when the combined effect of two variables (e.g., climate change and LUCC) exceeds the sum of their individual effects, resulting in an amplified outcome such as increased peak flows or runoff volume. Conversely, antagonistic interaction occurs when the combined effect is less than the sum of their individual effects, leading to a diminished outcome. Some studies have reported both synergistic interactions (Hung et al., 2020; Tian et al., 2022) and antagonistic interactions (Lamichhane & Shakya, 2019) between climate change and LUCC regarding hydrological response at basin scale.

1.5. Flood risk Management and Land Planning in Ecuador

The flood risk management in Ecuador is under the responsibility of the Risk Management Secretariat (SGR). However, the risk management in Ecuador is decentralized through different institutions that comprise the National Decentralized System for Risk Management, including the decentralized autonomous governments (GADs) on both levels, cantonal and provincial. According to the competencies established by the Constitution of the Republic of Ecuador and other laws such as the Organic Code for Territorial Organization, and the National Plan for Risk Reduction; the SGR generates various instruments, one of which is the Risk Reduction Agendas (SGR, 2018). The Risk Reduction Agendas is aimed at integrating and mainstreaming risk management into planning, aligning with the actors of the SNDGR to achieve their objectives. In this sense, the policy generated by the SGR recognizes the GADs as key actors in risk reduction since, based on their competencies, they can link the Risk Reduction Agendas to the Territorial Planning and Development Plans (SGR, 2019).

The risk management model proposed by the SGR considers both prospective and corrective risk management. Additionally, the SGR recommends that the GADs, during the diagnostic stage of the Territorial Planning and Development Plans, generate prospective risk scenarios that incorporate climate projections proposed by the Ministry of Environment (MAE), such as heavy rainfall scenarios. Furthermore, SGR indicates that climate change is a trigger factor for the generation of floods and landslides (SGR, 2019). In addition to GADs, SGR and MAE (Vice Ministry of Water),

other institutions are involved within the food risk management such as the National Institute of Meteorology and Hydrology (INAMHI) through the national monitoring network and more recently with GeoGloWS Portal (INAMHI, 2023).

1.6. Research Proposal

a. Related to flood management and data scarcity in TRB

Hydrological and hydrodynamic models are widely used tools for water resources planning and flood management (Díez-Herrero et al., 2009). The reliability of hydrological and hydrodynamic models depends on model formulations and input data quality (Smart, 2018; Teng et al., 2017). However, in developing countries, the availability of long-term and quality of hydrometeorological observations, is a constrain (Ochoa-Tocachi et al., 2016), especially on remote regions such as the Ecuadorian Amazon. The data-scarcity of reliable input data hinders the model´s capacity to correctly simulate the hydrological response of a basin under different scenarios (e.g., climate change and LUCC). Therefore, flash flood hazard assessment requires method strategies to cope with data scarcity, such as event sampling (Correa et al., 2016) and survey data (Ciervo et al., 2015). Consequently, the first research question is: **Can event sampling and survey data cope with data scarcity for flash flood hazard assessment where robust monitoring networks are not available?**

b. Related to forest spatial patterns and floods

Forest location and forest fragmentation are common land-cover spatial patterns. Previous studies indicate that forest fragmentation and forest location have effects on runoff generation and high flows (e.g., Boongaling et al., 2018; Q. Gao & Yu, 2017; Hou et al., 2018). However, in some cases, this relationship is unclear and changes with the scale of analysis (Kim & Park, 2016). Additionally, previous analyses do not maintain a constant area of forest, since fragmentation is related to a reduction in forest area (Q. Gao & Yu, 2017). Similarly, the analysis of forest location on upper and lower basin, does not maintain the same proportion of forest on different slopes (Iacob et al., 2017; Salazar et al., 2012). Thus, in this context, the changes on flows can be the result of a combination of both variables, forest spatial pattern (i.e., fragmentation and location) and forest area. Furthermore, previous studies do not compare simultaneously the effects of location and fragmentation on floods. In consequence, the effect of different forest spatial patterns on floods remains unknown, which hinders the integration of NbS with land-planning processes for natural flood management. Therefore, there is a need to evaluate,

within the same experiment, both spatial patterns, while maintaining the same proportion of forest area. In this regard, the second research question is: **Is the forest location more important than forest fragmentation for flood regulation?**

c. Related to individual and combined effects between climate change and LUCC on floods

Climate change and LUCC are among the main drivers that can affects the occurrence of flood in frequency and magnitude. Since climate change and LUCC can affect the hydrological processes at different spatial and temporal scales (Blöschl et al., 2007; Bronstert, 2004; Chang & Franczyk, 2008) it is important to analyze both individual and combined contributions (Lian et al., 2020). One of the main methods of analysis is through hydrological modeling (Zhang et al., 2018). However, previous studies have a coarse temporal and spatial scale. In other words, the analysis is generally conducted at monthly or annual time scales and also evaluates mean values within the basin or using few sampling points. Therefore, very little is known about the dynamics of the interactions between climate change and LUCC on floods across the altitudinal gradients within the basins. This knowledge gap difficult the application of NbS for flood management in the context of climate change adaptation. Hence, the third research question is: **How is the variation of individual and combined effects of climate change and LUCC on floods across the altitudinal gradient in the basin?**

2. Introducción

A continuación, se presenta una traducción al castellano de la sección anterior titulada ‘Introduction’:

2.1. Deforestación e Inundaciones. Implicaciones para la Amazonía Ecuatoriana

Las inundaciones son uno de los tipos más comunes de peligro natural. Durante el período 2000-2017, afectaron a más de 86 millones de personas en todo el mundo (EM-DAT, 2023). Las inundaciones repentinas son el tipo de inundación que causa más daños en términos de fatalidades y pérdidas económicas (Jonkman, 2005; UNISDR, 2017). El cambio climático y el cambio en el uso/cobertura del suelo (LUCC, por sus siglas en inglés), como la deforestación, se encuentran entre los principales forzantes o *drivers* que pueden incrementar la magnitud y frecuencia de las inundaciones (Bronstert et al., 2002; Chang y Franczyk, 2008; IPCC, 2021). La interacción entre el cambio climático y el LUCC en las inundaciones, es un proceso

no lineal y complejo, dependiente de la escala en la cuenca (Blöschl et al., 2007; Rogger et al., 2017). Además, el efecto de diferentes patrones espaciales de LUCC hace aún más difícil predecir los resultados de estas interacciones (Hou et al., 2018). Por lo tanto, es fundamental comprender los efectos individuales y combinados del cambio climático y el LUCC en las inundaciones para aplicar soluciones basadas en la cobertura del suelo para la gestión del riesgo de inundacion y la adaptación al cambio climático (Blöschl et al., 2019; Dadson et al., 2017; Lane, 2017).

A nivel mundial, la tasa de deforestación anual ha disminuido de 10.6 millones de hectáreas en la década de 1900 a 6.5 millones de hectáreas entre 2010 y 2015 (UNEP, 2019). En Ecuador, las tasas de deforestación disminuyeron entre 1900 y 2010 (Sierra, 2013). Sin embargo, el bosque nativo ha experimentado un declive, pasando del 51.5% en 1990 al 50.9% en 2014 (Ministerio de Ambiente, 2015). Aproximadamente el 74% de este bosque nativo se encuentra en la Región Amazónica Ecuatoriana (RAE). Entre los principales impulsores o factores que promueven la deforestación en la RAE están: la proximidad a carreteras y centros poblados (acceso a mercados), densidad poblacional, la tenencia de la tierra y la educación primaria (Kleemann et al., 2022; Mena et al., 2006; Sierra, 2013; Southgate et al., 1991). En la Cuenca del Río Tena (CRT), la cobertura natural (bosque nativo y vegetación herbácea) disminuyó de 17027 hectáreas en 1990 a 16219 hectáreas en 2014, lo que representa una reducción de aproximadamente el 5% (Ministerio de Ambiente, 2015). En este sentido, la presencia de la Reserva Biológica Colonso-Chalupas (RBCC) desde 2014, con 9154 hectáreas (38% de la CRT), contribuye a disminuir las tasas de deforestación en la CRT (Cuenca et al., 2018; Kleemann et al., 2022).

Sin embargo, la deforestación dentro de la RAE y la CRT sigue siendo un problema grave que compromete diversos servicios ecosistémicos, incluida la regulación del flujo de agua asociada a inundaciones fluviales. Esto se explica por la estrecha relación entre el agua y el paisaje (H. Gao et al., 2018). Esto cobra aún más relevancia considerando que los ecosistemas y los bosques son elementos clave para establecer medidas de adaptación al cambio climático (Cohen-Shacham et al., 2019). Además, la pérdida de bosque nativo ha sido reconocida como un factor significativo que contribuye a cambios en el riesgo de inundacion (Q. Gao y Yu, 2017). En consecuencia, la implementación de medidas de protección forestal y reforestación ha sido reconocida como parte de las soluciones basadas en la naturaleza (SbN) para complementar los esfuerzos en la gestión de inundaciones (Dadson et al., 2017; Ilieva et al., 2018; Lane, 2017). Además, las SbN son especialmente relevantes para las Regiones Tropicales Andinas, ya que los bosques están relacionados con varios servicios ecosistémicos como la regulación

y el suministro de agua, la captura de carbono, el control de la erosión del suelo (Bonnesoeur et al., 2019).

2.2. Relaciones Generales Entre Bosque e Inundaciones

El Bosque Tropical Andino (BTA) actúa como una barrera natural donde la interceptación puede representar el 40% de la precipitación total (Fleischbein et al., 2006). Además, la presencia de árboles y sistemas radiculares en el BTA aumenta la capacidad de retención de agua en el suelo, reduciendo la cantidad de agua que ingresa a la red de arroyos (Ataroff y Rada, 2000; Qi y Liu, 2019; Tobón, 2008, 2021). La conductividad hidráulica saturada relativamente alta de los *Andisoles* con un alto contenido de materia orgánica mejora la capacidad de infiltración (Sánchez et al., 2018). Todas estas características en conjunto hacen que el BTA sea un ecosistema especial capaz de actuar como amortiguador natural contra las inundaciones (Bonnesoeur et al., 2019; Tobón, 2008). Sin embargo, la capacidad de regulación de inundaciones del bosque se limita a tormentas de tamaño pequeño y mediano (Bathurst et al., 2011; Birkel et al., 2012; Iacob et al., 2017; Salazar et al., 2012). Por ejemplo, Bathurst et al., 2020 indican que el bosque alcanza su capacidad máxima para mitigar inundaciones con períodos de retorno moderados de 5-20 años. Además, Birkel et al. (2012) encontraron en una cuenca húmeda de Costa Rica un efecto pequeño del LUCC en los caudales máximos para períodos de retorno > 1 año. Sin embargo, las zonas bajas de las cuencas seguirían siendo propensas a inundaciones, incluso si los bosques aguas arriba permanecieran intactos (Laurance, 2007). Además, a medida que aumenta la humedad del suelo, el efecto del bosque en los caudales altos es menor (Bathurst et al., 2020; Bronstert et al., 2002; Sriwongsitanon y Taesombat, 2011).

La relación entre el LUCC y las inundaciones presenta diferentes escalas espaciales y temporales (Chang y Franczyk, 2008). Actividades antropogénicas como la gestión forestal, prácticas agrícolas (incluida la quema de maleza) y drenaje pueden modificar las interacciones químicas-biológicas y la conectividad espacial, afectando así las inundaciones (Rogger et al., 2017). Sin embargo, la topografía y la cobertura del suelo se encuentran entre las principales características que definen un paisaje (H. Gao et al., 2018). En este sentido, la localización y fragmentación del bosque (patrones espaciales), bajo ciertas condiciones, pueden influir en los procesos de escorrentía e inundaciones (Kim y Park, 2016; Liu et al., 2020). La localización del bosque se refiere a la presencia de cobertura forestal agregada en diferentes pendientes (Hou et al., 2018). Por otro lado, la fragmentación del bosque es la conversión de un bosque continuo en un mosaico desagregado de parches de bosque (Fahrig, 2003). Algunos estudios han encontrado diferencias en los

caudales altos cuando el bosque se encuentra en diferentes pendientes (Descheemaeker et al., 2006; Hou et al., 2018; Jourgholami et al., 2020). En este sentido, la evidencia sugiere un mayor efecto del LUCC en la parte superior de la cuenca que en la parte inferior (Edokpa et al., 2022; Hung et al., 2020; Olang y Fürst, 2011). Sin embargo, la proporción del área forestal también es importante. Bathurst et al. (2011) sugieren que se pueden observar cambios en el caudal máximo a partir de una alteración mínima del 20-30% en el área forestal. Por otro lado, ubicar vegetación densa cerca de los cursos de agua tiene un mayor efecto en las inundaciones (Dadson et al., 2017). No obstante, se espera que la atenuación de las inundaciones disminuya a medida que aumenta la distancia aguas abajo de la perturbación (Lane, 2017). Además, debido al efecto de escala, a medida que aumenta el área de la cuenca, la influencia del LUCC en los caudales altos disminuye (Blöschl et al., 2007; Dadson et al., 2017). Así mismo, con el aumento del tamaño de la cuenca, los procesos hidráulicos en el canal se vuelven más importantes que los procesos de escorrentía en laderas (i.e., escorrentía superficial, interflujo) al determinar los tiempos de respuesta de la cuenca (Asano y Uchida, 2018). Por lo tanto, en cuencas pequeñas (<100 km2), la vegetación ribereña y las llanuras de inundación en las partes bajas de la cuenca pueden contribuir a la reducción de inundaciones, desincronizando el flujo al aumentar la rugosidad y el tiempo de retardo (Lane, 2017). Por ejemplo, Dixon et al. (2016) encontraron una reducción del 19% en los flujos máximos debido a la restauración del bosque ribereño, que cubría del 20 al 40% del área total de captación. Sin embargo, las SbN centradas en el cauce y almacenamiento en las llanuras de inundación son efectivas solo para eventos de inundación pequeños e inadecuadas para los más grandes (Metcalfe et al., 2017).

Finalmente, pocos estudios han relacionado las métricas espaciales del paisaje con la respuesta hidrológica de la cuenca. Por ejemplo, Boongaling et al. (2018) indican que la conectividad, agregación y tamaño de los parches de bosque dentro del paisaje son las métricas más estrechamente relacionadas con el flujo superficial y la carga de sedimentos. Además, Boongaling et al. (2018) sugieren que la fragmentación del bosque aumenta el flujo superficial y reduce el flujo base. Sin embargo, el estudio realizado por Kim y Park (2016) en Texas (EU) encontró que el papel de la conectividad en la escorrentía superficial no es claro, ya que obtuvieron resultados contradictorios en algunos casos. Sin embargo, encontraron que las métricas relacionadas con el tamaño y la forma estaban más correlacionadas con la escorrentía. Otro estudio realizado en cuencas húmedas tropicales en Puerto Rico sugiere que la fragmentación puede aumentar tanto el caudal base como los caudales altos durante eventos extremos (Q. Gao y Yu, 2017).

2.3. Cambio Climático e Inundaciones. Implicaciones para la Amazonía Ecuatoriana

Para los escenarios de emisiones altas (CMIP5: RCP8.5; CMIP6: SSP5-8.5) derivados de Modelos de Circulación General (MCGs), se proyecta que los eventos de precipitación de corta duración y alta intensidad se vuelvan más intensos (IPCC, 2021). Esto, a su vez, llevará a un aumento en la frecuencia de inundaciones a nivel global (Hirabayashi et al., 2013; Merz et al., 2014; Vu et al., 2017). Sin embargo, al discutir inundaciones y precipitaciones, es crucial considerar la interdependencia entre el clima y el paisaje. En este sentido, algunos estudios sugieren que las inundaciones responden más a la variabilidad espacial que a la variabilidad temporal de la precipitación (Perdigão y Blöschl, 2014). Por lo tanto, el efecto de la variabilidad espacial se hace más evidente a medida que aumenta el tamaño de la cuenca. Además, se debe considerar la interacción entre las condiciones de la superficie del suelo y la precipitación (Bronstert et al., 2002). Por ejemplo, en algunas cuencas, la humedad del suelo es el principal factor de control en los procesos de generación de escorrentía (Blöschl, 2022).

Aunque por un lado se espera un aumento en las inundaciones repentinas a escala global bajo escenarios de cambio climático por el incremento de las temperaturas e intensidad de la precipitación (Yin et al., 2018). Por otro lado, algunos autores argumentan que un aumento en la temperatura no necesariamente resulta en más inundaciones (Wasko y Sharma, 2017). A pesar del aumento en eventos de precipitación extrema en varias regiones en todo el mundo, la ocurrencia de inundaciones no muestra una respuesta igual. Esto se puede explicar en parte por el hecho de que, en ciertos casos, el aumento de temperatura conduce a una disminución en las condiciones de humedad previa, mejorando así la capacidad de infiltración del suelo (Sharma et al., 2018). Además, debe indicarse que la influencia de la humedad previa disminuye en cuencas más pequeñas (Johnson et al., 2016; Sharma et al., 2018). Sin embargo, la relación entre temperatura, precipitación e inundaciones en el contexto del cambio climático e inundaciones repentinas sigue siendo un tema de debate continuo en la comunidad científica, careciendo de un consenso general en la actualidad (Wasko et al., 2019; Yin et al., 2019). Esto sugiere que el efecto del cambio climático en las inundaciones no puede generalizarse, destacando la necesidad de estudios específicos para cada caso.

El clima en Ecuador está principalmente influenciado por el Océano Pacífico, la Cordillera de los Andes y la Selva Amazónica, de donde provienen grandes masas de humedad (Junquas et al., 2022). Específicamente, las estribaciones como la vertiente oriental de la Cordillera de los Andes están influenciadas de manera

significativa por la Zona de Convergencia Intertropical (ZCIT; Vargas et al., 2022) y por masas de aire húmedo provenientes de la parte oriental de la cuenca amazónica. Por lo tanto, la combinación del efecto orográfico y la influencia de la ZCIT favorecen la formación de tormentas convectivas en cuencas de estribaciones como la CRT. Entre los impactos más significativos del cambio climático en Ecuador se encuentran: aumentos de temperatura, retroceso de los glaciares, sequías prolongadas y cambios en los patrones de precipitación (Cadilhac et al., 2017). La cuenca amazónica es propensa a futuros eventos extremos relacionados con inundaciones (Hirabayashi et al., 2013). Palomino-Lemus et al. y Solman (2017; 2013) indican que la precipitación anual promedio disminuiría en la Amazonía, pero con un aumento en la región noroeste, cerca de las estribaciones de la Cordillera de los Andes. De manera similar, el caudal anual promedio aumentaría en esta zona (Pabón-Caicedo et al., 2020; Sorribas et al., 2016).

Por otro lado, se proyecta un aumento en la precipitación en los Andes tropicales de Ecuador (Sarmiento y Kooperman, 2019). Además, se esperan tendencias crecientes en los caudales máximos y tendencias decrecientes en los caudales mínimos (Pabón-Caicedo et al., 2020). Sin embargo, los estudios sobre proyecciones de precipitación debido al cambio climático en América del Sur se basan en MCGs y Modelos de Circulación Regional (MCRs). Por lo tanto, parte de la incertidumbre asociada con los MCGs o MCRs se debe a la representación débil del efecto orográfico o el relieve con resoluciones gruesas (Buytaert et al., 2010; Sarmiento y Kooperman, 2019). Esto ocurre especialmente en áreas de alta precipitación con un mayor gradiente topográfico, como las estribaciones Andes-Amazonía (Espinoza et al., 2015).

2.4. Efectos Individuales y Combinados del Cambio Climático y LUCC en Inundaciones

El cambio climático y el LUCC afectan simultáneamente los procesos hidrológicos a nivel de cuenca. Sin embargo, debido a que los impactos actúan en diferentes escalas espaciales, el análisis individual de sus contribuciones es necesario para la planificación y gestión de cuencas hidrográficas (Lian et al., 2020; Zhang et al., 2018). Blöschl et al. (2007) propusieron la hipótesis de que el impacto del cambio climático en las inundaciones en diferentes escalas es más homogéneo que el del LUCC. Además, indican que, a escalas más pequeñas, el LUCC tiene un impacto mayor que la variabilidad climática en la respuesta hidrológica. Dependiendo principalmente de la disponibilidad de datos y el propósito de la investigación, existen varias metodologías para identificar estas contribuciones por separado (Yang et al., 2017). Sin embargo, el modelado hidrológico, el análisis de

cuencas emparejadas, enfoques conceptuales, diseños experimentales y enfoques analíticos se encuentran entre los más comunes (Zhang et al., 2018). Debido a la creciente disponibilidad de datos, de capacidades de cómputo y al desarrollo de modelos hidrológicos distribuidos, el enfoque con modelos hidrológicos se ha utilizado ampliamente (Hung et al., 2020; Lamichhane & Shakya, 2019; Yang et al., 2017). Este enfoque combina escenarios hipotéticos ("what-if approach" en inglés) y el análisis de un factor a la vez (“one-factor-at-a-time análisis” en inglés).

El diseño experimental basado en modelado hidrológico combina diferentes escenarios (i.e.: escenario base, escenarios basados en LUCC y escenarios basados en cambio climático) para evaluar los efectos individuales y combinados sobre las variables hidrológicas. Estudios previos (Chawla y Mujumdar, 2015; Tian et al., 2022; Zhang et al., 2018) han examinado los efectos individuales y combinados del cambio climático y el LUCC en inundaciones utilizando modelado hidrológico. En este sentido, la interacción es una de las principales características relacionadas con los efectos combinados del cambio climático y el LUCC. Específicamente, la interacción se refiere a la relación entre dos o más variables que afecta a la variable de respuesta de manera no aditiva o no independiente (Dunne, 2010; Rothman, 1976). Por lo tanto, la interacción puede ser sinérgica o antagonista. La interacción sinérgica ocurre cuando el efecto combinado de dos variables (e.g., cambio climático y LUCC) supera la suma de sus efectos individuales, lo que lleva a un efecto amplificado, como aumentos en los caudales máximos o el volumen de escorrentía. Por el contrario, la interacción antagonica ocurre cuando el efecto combinado es menor que la suma de sus efectos individuales, lo que lleva a un efecto disminuido. Algunos estudios han informado tanto interacciones sinérgicas (Hung et al., 2020; Tian et al., 2022) como interacciones antagonistas (Lamichhane y Shakya, 2019) entre el cambio climático y el LUCC con respecto a la respuesta hidrológica a nivel de cuenca.

2.5. Gestion del Riesgo de Inundaciones y Planificación Territorial en Ecuador

La gestión del riesgo de inundaciones en Ecuador está a cargo de la Secretaría de Gestión de Riesgos (SGR). Sin embargo, la gestión del riesgo en Ecuador se descentraliza a través de diferentes instituciones que conforman el Sistema Nacional Descentralizado de Gestión de Riesgos, incluyendo los gobiernos autónomos descentralizados (GAD) a nivel cantonal y provincial. De acuerdo con las competencias establecidas por la Constitución de la República del Ecuador y otras leyes, como el Código Orgánico de Organización Territorial, y el Plan Nacional de Reducción de Riesgos; la SGR genera varios instrumentos, uno de los cuales es

la Agenda de Reducción de Riesgos (SGR, 2018). La Agenda de Reducción de Riesgos tiene como objetivo integrar y incorporar la gestión del riesgo en la planificación, alineándose con los actores del SNDGR para alcanzar sus objetivos. En este sentido, la política generada por la SGR reconoce a los GAD como actores clave en la reducción del riesgo, ya que, en función de sus competencias, pueden vincular las Agendas de Reducción de Riesgos con la Planificación Territorial y los Planes de Desarrollo (SGR, 2019).

El modelo de gestión de riesgos propuesto por la SGR considera tanto la gestión del riesgo prospectiva como la correctiva. Además, la SGR recomienda que los GAD, durante la etapa de diagnóstico de los Planes de Ordenamiento Territorial y Desarrollo, generen escenarios prospectivos de riesgo. A su vez, estos escenarios deberían incorporar las proyecciones climáticas propuestas por el Ministerio del Ambiente (MAE), como los escenarios de lluvias intensas. Por otro lado, la SGR señala que el cambio climático es un factor desencadenante en la generación de inundaciones y deslizamientos (SGR, 2019). Además de los GAD, la SGR y el MAE (con el Viceministerio de Agua), otras instituciones están involucradas en la gestión de riesgos hídricos. Por ejemplo, el Instituto Nacional de Meteorología e Hidrología (INAMHI) a través de la red de monitoreo nacional y más recientemente con el Portal GeoGloWS (INAMHI, 2023).

2.6. Propuesta de Investigación

a. Relacionado a la gestión de inundaciones y datos escasos en la cuenca

Los modelos hidrológicos e hidrodinámicos son herramientas ampliamente utilizadas para la planificación de recursos hídricos y la gestión de inundaciones (Díez-Herrero et al., 2009). La confiabilidad de estos modelos depende de las formulaciones del modelo y la calidad de los datos de entrada (Smart, 2018; Teng et al., 2017). Sin embargo, en países en desarrollo, la disponibilidad de observaciones hidrometeorológicas a largo plazo y de calidad es limitada (Ochoa-Tocachi et al., 2016), especialmente en regiones remotas como la Amazonía Ecuatoriana. La escasez de datos confiables de entrada dificulta la capacidad del modelo para simular correctamente la respuesta hidrológica de una cuenca bajo diferentes escenarios (e.g., cambio climático y LUCC). Por lo tanto, la evaluación del peligro de inundaciones repentinas requiere estrategias metodológicas para enfrentar la escasez de datos, como el muestreo de eventos (Correa et al., 2016) y los datos de levantados en terreno (Ciervo et al., 2015). En consecuencia, la primera pregunta de investigación es: **¿Permite el muestreo de eventos y los datos de terreno manejar la escasez de datos para la evaluación del peligro de**

inundaciones repentinas en lugares donde no están disponibles redes de monitoreo robustas?

b. Relacionado a los patrones espaciales del bosque e inundaciones

La localización y fragmentación del bosque son patrones espaciales comunes de la cobertura del suelo. Estudios anteriores indican que la fragmentación y localización del bosque tienen efectos en la generación de escorrentía y caudales altos (por ejemplo, Boongaling et al., 2018; Q. Gao y Yu, 2017; Hou et al., 2018). Sin embargo, en algunos casos, esta relación es poco clara y cambia con la escala de análisis (Kim y Park, 2016). Por otro lado, los análisis previos no mantienen un área constante de bosque, ya que la fragmentación está relacionada con una reducción en el área forestal (Q. Gao y Yu, 2017). Del mismo modo, los análisis sobre la localización del bosque en la parte alta y baja de la cuenca no mantienen la misma proporción de bosque en las diferentes pendientes (Iacob et al., 2017; Salazar et al., 2012). En este contexto, los cambios identificados en los caudales, pueden ser el resultado de una combinación de ambas variables, patrón espacial del bosque (i.e., fragmentación y localización) y área forestal. Además, los estudios anteriores no hacen una comparación simultánea de los efectos de la localización y la fragmentación sobre las inundaciones. En consecuencia, no se conoce sobre el efecto de los diferentes patrones espaciales del bosque sobre los caudales altos, lo que dificulta la integración de SbN con procesos de planificación territorial para la gestión natural de inundaciones. Por lo tanto, es necesario evaluar, dentro del mismo experimento, ambos patrones espaciales, manteniendo la misma proporción de área forestal. En este sentido, la segunda pregunta de investigación es: **¿Es la localización del bosque más importante que la fragmentación para la regulación de inundaciones?**

c. Relacionado a los efectos individuales y combinados del cambio climático y LUCC en las inundaciones

El cambio climático y el LUCC se encuentran entre los principales forzantes que pueden afectar la ocurrencia de inundaciones en términos de frecuencia y magnitud. Dado que el cambio climático y el LUCC pueden afectar los procesos hidrológicos a diferentes escalas espaciales y temporales (Blöschl et al., 2007; Bronstert, 2004; Chang y Franczyk, 2008), es importante analizar tanto las contribuciones individuales como combinadas (Lian et al., 2020). Uno de los principales métodos de análisis es a través de la modelización hidrológica (Zhang et al., 2018). Sin embargo, los estudios anteriores tienen una escala temporal y espacial gruesa. En otras palabras, el análisis generalmente se realiza en escala de

tiempo mensual o anual y con valores medios a nivel de cuenca, o el mejor de los casos, utilizando pocos puntos de muestreo. Por lo tanto, se sabe muy poco sobre la dinámica de las interacciones entre el cambio climático y el LUCC en las inundaciones a lo largo de los gradientes altitudinales dentro de las cuencas. Esta brecha de conocimiento dificulta la aplicación de las SbN para la gestión de inundaciones en el contexto de la adaptación al cambio climático. En este contexto, la tercera pregunta de investigación es: **¿Cómo es la variación del efecto individual y combinado del cambio climático y el LUCC en las inundaciones a lo largo del gradiente altitudinal de la cuenca?**

CHAPTER II

HYPOTHESIS AND OBJECTIVES

1. Hypothesis and Objectives

1.1. Hypothesis

The following hypothesis related to main research questions are proposed:

H1. The influence of LUCC on flood regulation is greater in the upper basin and decrease in downstream direction, and the aggregated forest patches on the upper basin have more influence on flood regulation than fragmentation across the basin.

H2. Climate change effects across the basin are more homogeneous than LUCC, and the combined effects are greater in the upper basin and decrease in downstream direction in a non-linear manner.

1.1.1. Predictions

1) The deforestation of native forest in the upper basin will be the worst scenario for flood regulation.

2) The influence of LUCC on floods in the upper basin is greater than the influence of climate change.

1. 2. Objectives

To evaluate the hypothesis, the objectives of this research are:

1.2.1. General Objective

Analyze the combined effects of climate change and LUCC on floods in a tropical basin, with a specific emphasis on landscape configuration and the role of native forests for flood regulation.

1.2.2. Specific Objectives

1) Analyze past flash floods in the basin using model coupling, storm sampling, and survey data.

2) Analyze the effect of different deforestation spatial patterns, such as, forest location and forest fragmentation for flood regulation, using hypothetical scenarios.

3) Analyze the individual and combined effect of climate change and LUCC on floods across the altitudinal gradient in the basin.

1.3. Research Strategy

This research was carried out in three consecutive stages that allowed the achievement of the proposed objectives. The objective 1 was addressed in Chapter III, and among the main purposes of this chapter was the validation of existing data for flood hazard assessments through hydrological and hydrodynamic modelling. Then, in the following stages, hypothetical scenarios were evaluated using as a reference the hazard assessment of chapter III. The Chapter IV analyzed the effect of forest location and forest fragmentation on floods maintaining the same proportion of forest area in the basin (50%). Thus, on the experiment design of Chapter IV, the effect of forest area was isolated, and did not consider the scale effect on stormflow, since the analysis focused on the basin outlet. Finally, on the next stage, the Chapter V analyzed scale effects using 42 stormflow sampling sites across the basin. The chapter V had an experiment design that isolate the effect of spatial variability of LUCC (same land cover for each scenario) and explicitly analyzed the scale effect of climate change and LUCC across the basin. Therefore, Chapters IV and V, were complementary to analyze both the spatial pattern and scale effect of LUCC, including the interaction with climate change on floods.

The TRB located in the Ecuadorian Amazon was selected as the study area. The basin includes flood-prone areas, particularly in the downstream city of Tena, where multiple significant flash flood incidents have occurred in the past decade (GADM-TENA, 2021). Various factors, such as intense rainfall, saturated soils, and steep terrain in the upper basin, contribute to the increased risk of flash flooding (Jodar-Abellan et al., 2019; Nikolopoulos et al., 2011). Furthermore, the TRB is expected to be significantly affected by climate change, with projected alterations in precipitation patterns, rising temperatures, and more extreme weather events. Consequently, conducting hydrological research in the TRB is crucial due to its vulnerability to flash floods, as well as the opportunity to enhance the management of ecosystem services and NbS within the basin.

1. Hipótesis y Objetivos

A continuación, se presenta una traducción al castellano de la sección anterior titulada ‘Hypothesis and Objectives’:

2.1. Hipótesis

Se proponen las siguientes hipótesis relacionadas con las principales preguntas de investigación:

H1. La influencia del LUCC en la regulación de inundaciones es mayor en la cuenca alta y disminuye en dirección aguas abajo, y los parches de bosque agregados en la cuenca alta tienen más influencia en la regulación de inundaciones que la fragmentación a lo largo de la cuenca.

H2. Los efectos del cambio climático en toda la cuenca son más homogéneos que los del LUCC, y los efectos combinados son mayores en la cuenca alta y disminuyen en dirección aguas abajo de manera no lineal.

2.1.1. Predicciones

1) La deforestación del bosque nativo en la cuenca alta será el peor escenario para la regulación de inundaciones.

2) La influencia del LUCC en las inundaciones de la cuenca alta es mayor que la influencia del cambio climático.

2. 2. Objetivos

Para evaluar las hipótesis, los objetivos de esta investigación son:

2.2.1. Objetivo General

Analizar los efectos combinados del cambio climático y el LUCC en las inundaciones de una cuenca tropical, con énfasis en la configuración del paisaje y el rol del bosque nativo para la regulación de inundaciones.

2.2.2. Objetivos Específicos

1) Analizar crecidas repentinas pasadas en la cuenca utilizando modelos acoplados, muestreo de tormentas y datos de campo.

2) Analizar el efecto de diferentes patrones espaciales de deforestación, como la localización y la fragmentación forestal, en la regulación de inundaciones, utilizando escenarios hipotéticos.

3) Analizar el efecto individual y combinado del cambio climático y el LUCC en las inundaciones a lo largo del gradiente altitudinal en la cuenca.

2.3. Estrategia de Investigación

Esta investigación se llevó a cabo en tres etapas consecutivas que permitieron alcanzar los objetivos propuestos. El objetivo 1 se abordó en el Capítulo III, y uno de los principales propósitos de este capítulo fue la validación de los datos existentes para la evaluación de peligros de inundación a través de la modelización hidrológica e hidrodinámica. Luego, en las etapas siguientes, se evaluaron escenarios hipotéticos utilizando como referencia los resultados del Capítulo III. El Capítulo IV analizó el efecto de la localización y fragmentación forestal en las inundaciones, manteniendo la misma proporción de área forestal en la cuenca (50%). Por lo tanto, en el diseño experimental del Capítulo IV, se aisló el efecto del área forestal y no se consideró el efecto de escala sobre los caudales de crecida, ya que el análisis se centró en la salida de la cuenca. Finalmente, en la siguiente etapa, en el Capítulo V, se analizó los efectos de escala utilizando 42 sitios de muestreo de caudales de crecida en toda la cuenca. El Capítulo V tuvo un diseño experimental que aisló el efecto de la variabilidad espacial del LUCC (cobertura del suelo homogénea) y analizó explícitamente el efecto de escala del cambio climático y el LUCC a lo largo de toda la cuenca. Por lo tanto, los Capítulos IV y V fueron complementarios para analizar tanto el patrón espacial como el efecto de escala del LUCC, incluida la interacción con el cambio climático en la generación de crecidas repentinas.

La CRT, ubicada en la Amazonía Ecuatoriana, fue seleccionada como área de estudio. La cuenca incluye áreas propensas a inundaciones, especialmente aguas abajo en la ciudad de Tena, donde han ocurrido múltiples inundaciones repentinas en la última década (GADM-TENA, 2021). Factores como las lluvias intensas, los suelos saturados y el terreno empinado en la cuenca alta, contribuyen al aumento del riesgo de inundaciones repentinas (Jodar-Abellan et al., 2019; Nikolopoulos et al., 2011). Además, se prevé que a futuro la CRT se vea significativamente afectada por el cambio climático, con alteraciones en los patrones de temperatura,

precipitación y eventos climáticos más extremos. En este contexto, realizar investigaciones hidrológicas en la CRT es crucial debido a su vulnerabilidad a las inundaciones repentinas, así como a la oportunidad de mejorar la gestión de servicios ecosistémicos y de SbN dentro de la cuenca.

CHAPTER III

FLOOD HAZARD ASSESSMENT IN DATA-SCARCE WATERSHEDS USING MODEL COUPLING, EVENT SAMPLING, AND SURVEY DATA

This chapter is based on:

Hurtado-Pidal, J., Acero Triana, J. S., Espitia-Sarmiento, E., & Jarrín-Pérez, F. (2020). Flood Hazard Assessment in Data-Scarce Watersheds Using Model Coupling, Event Sampling, and Survey Data. Water. https://doi.org/10.3390/w12102768

Flood Hazard Assessment in Data-Scarce Watersheds Using Model Coupling, Event Sampling, and Survey Data

Jorge Hurtado-Pidal [1,] *, Juan S. Acero Triana [2], Edgar Espitia-Sarmiento [3] and Fernando Jarrín-Pérez [4]

[1] Department of Territorial Planning, Faculty of Environmental Sciences and EULA-Centre, Universidad de Concepción, 4070386 Concepción, Chile

[2] Department of Agricultural and Biological Engineering, University of Illinois, 1304 West Pennsylvania Avenue, Urbana, IL 61801, USA; jsa2@illinois.edu

[3] Water and Aquatic Resources Research Group (GIRHA), Universidad Regional Amazónica Ikiam, 150101 Tena, Ecuador; edgar.espitia@ikiam.edu.ec

[4] Department of Biological & Agricultural Engineering, Texas A&M University, TX 77843, USA; fjarrin@tamu.edu

Abstract

The application of hydrologic and hydrodynamic models in flash flood hazard assessment is mainly limited by the availability of robust monitoring systems and long-term hydro-meteorological observations. Nevertheless, several studies have demonstrated that coupled modeling approaches based on event sampling (short-term observations) may cope with the lack of observed input data. This study evaluated the use of storm events and flood-survey reports to develop and validate a modeling framework for flash flood hazard assessment in data-scarce watersheds. Specifically, we coupled the hydrologic modeling system (HEC-HMS) and the Nays2Dflood hydrodynamic solver to simulate the system response to several storm events including one, equivalent in magnitude to a 500-year event, that flooded the City of Tena (Ecuador) on 2 September, 2017. Results from the coupled approach showed satisfactory model performance in simulating streamflow and water depths ($0.40 \leq$ Nash-Sutcliffe coefficient ≤ 0.95; $-3.67\% \leq$ Percent Bias $\leq 23.4\%$) in six of the eight evaluated events, and a good agreement between simulated and surveyed flooded areas (Fit Index = 0.8) after the 500-year storm. The proposed methodology can be used by modelers and decision-makers for flood impact assessment in data-scarce watersheds and as a starting point for the establishment of flood forecasting systems to lessen the impacts of flood events at the local scale.

Keywords: flood hazard assessment; data scarcity; model coupling; event sampling; survey data

1. Introduction

The assessment of natural hazards, such as flash floods, remains a challenging issue in environmental sciences [1]. Flash floods caused by extreme rainfall events associated with climate change have increased in the past few years [2–4]. Thus, the development and implementation of measures that diminish flash flood impacts and safeguard people and civil infrastructure are imperative. In this context, numerical models have been found to be reliable tools for flash flood hazard assessment. Specifically, hydrological and hydrodynamic models have been widely applied to describe flash flood dynamics at the watershed scale and project potential impacts on urban areas. Hydrological models (e.g., HEC-HMS, SWAT, MIKE 11, HBV, Top Model) have been widely used to simulate precipitation-runoff processes due to the ease of their implementation [1]. Although these models can accurately estimate streamflow patterns across complex watersheds, they do not provide a comprehensive representation of water flow in riverbanks and floodplains. On the other hand, hydrodynamic models (e.g., MIKE 21, LISFLOOD-FP, DELFT-2D, IBER, Nays2Dflood), which are based on more complex formulations, can represent streamflow data in terms of water depths and flow velocities across river channels and floodplains [5–9] but with a larger expense in computational and data resources [10,11]. External coupling approaches that combine hydrological and hydrodynamic models have shown satisfactory performance in representing flood extents while requiring a reduced computational burden and data [12–16]. The information generated by combining these models may be used to reconstruct historical flood events or evaluate the plausible response of the hydrologic system to present or future stressors (e.g., climate and land-use changes) [17]. Given that hydrologic and hydrodynamic models play a crucial role in the design of flooding control structures, flood risk management, and mitigation policy-making, they need to be tested from a strict scientific point of view [18–22]. Model reliability depends on two key factors, namely, the model formulation that describes the system and the input data used to set up the model [11,23–26].

In developing countries, the availability and quality of hydrometeorological data represent a significant constraint for the implementation of hydrological and hydrodynamic models due to the absence of robust monitoring networks and the lack of long-term hydro-meteorological observations [27]. The scarcity of reliable input data hinders the models' ability to represent the hydrological dynamics.

Consequently, the application of hydrological and hydrodynamic models in data-scarce environments is prone to equifinality (i.e., to generate a similar systemic response under distinct model parameterizations) and high uncertainty, even after a successful calibration/validation process [28]. In other terms, modeling outputs under data scarcity conditions may not enhance the basic understanding of the processes taking place in the hydrologic system and appropriately represent the watershed's natural characteristics [29].

In the absence of long-term observations, event sampling data may provide sufficient information to perform hydrological and hydrodynamic simulations. In this sense, several studies have found that the degree of hydrological information obtained by processing data from several storm events is comparable to that obtained by processing long-term data series [30–36]. The implementation of externally coupled models with event sampling data for flood hazard assessment may be quite relevant in zones with high spatial precipitation variability such as those located in the Andes-Amazon transition [37], where monitoring networks are sparse and recently established.

This study evaluated the potential use of event sampling and survey data for flash flood hazard assessment in data-scarce watersheds. Specifically, this study was geared to (1) implement a coupled framework to simulate in-stream flow and flow velocity and water depths across floodplains against short precipitation-runoff events in the data-scarce Tena River Watershed in Ecuador, and (2) evaluate the ability of the modeling framework to recreate the flood intensity due to a 500-year precipitation event that flooded the city of Tena on 2 September, 2017. Despite the fact that this city, like many others in the Amazon Basin, has experienced several flood events during recent years (2008, 2010, 2016, 2017) that have caused fatalities and significant economic losses [38,39], no flood management system has been implemented. The methodology and findings from this study may be used in similar watersheds with scarce data and for the establishment of flood forecasting systems.

2. Materials and Methods

2.1. Study Area

The study area comprises the Tena River Basin (TRB) and the Pano River Basin (PRB), which converge on the city of Tena (Napo province, Ecuador) and cover a drainage area of 235 km^2 (Figure 3.1). The basins depict a very steep relief with a terrain elevation ranging from 500 to 2500 m above mean sea level (mamsl; Figure 3.1c) and an average slope of approximately 22.4%. The main stem of each

river extends for 28 and 25 km for TRB and PRB, respectively, with a mean slope of 7%. The domain for the flood hazard assessment in the city of Tena considered a river segment of 1.7 km (Figure 3.1d) that has a mean slope of 0.03%. Its width and bankfull area are equal to 50 m and 362 m^2, respectively, and its bed is composed of coarse material such as gravels (~5 cm) and cobbles (~25 cm). TRB and PRB have similar characteristics in terms of their geology, morphology, soil composition, land use, and climate. Both basins are part of a tertiary cretaceous sedimentary basin with predominant alluvial deposits. The soils, classified as hydrated *Andisols* formed in volcanic ash, that are predominantly sandy clay and sandy loam in the upper and lower parts of the watershed, respectively [40], remain saturated most of the time. This is explained by the low evapotranspiration rates of the cloud forest located in the upper part of the watershed [41], which, together with shrubs and herbaceous plants, cover 65% of the area. The lower part, on the other hand, is covered by secondary forest, pasture, and crops such as corn, cacao, and cassava (35%) [42].

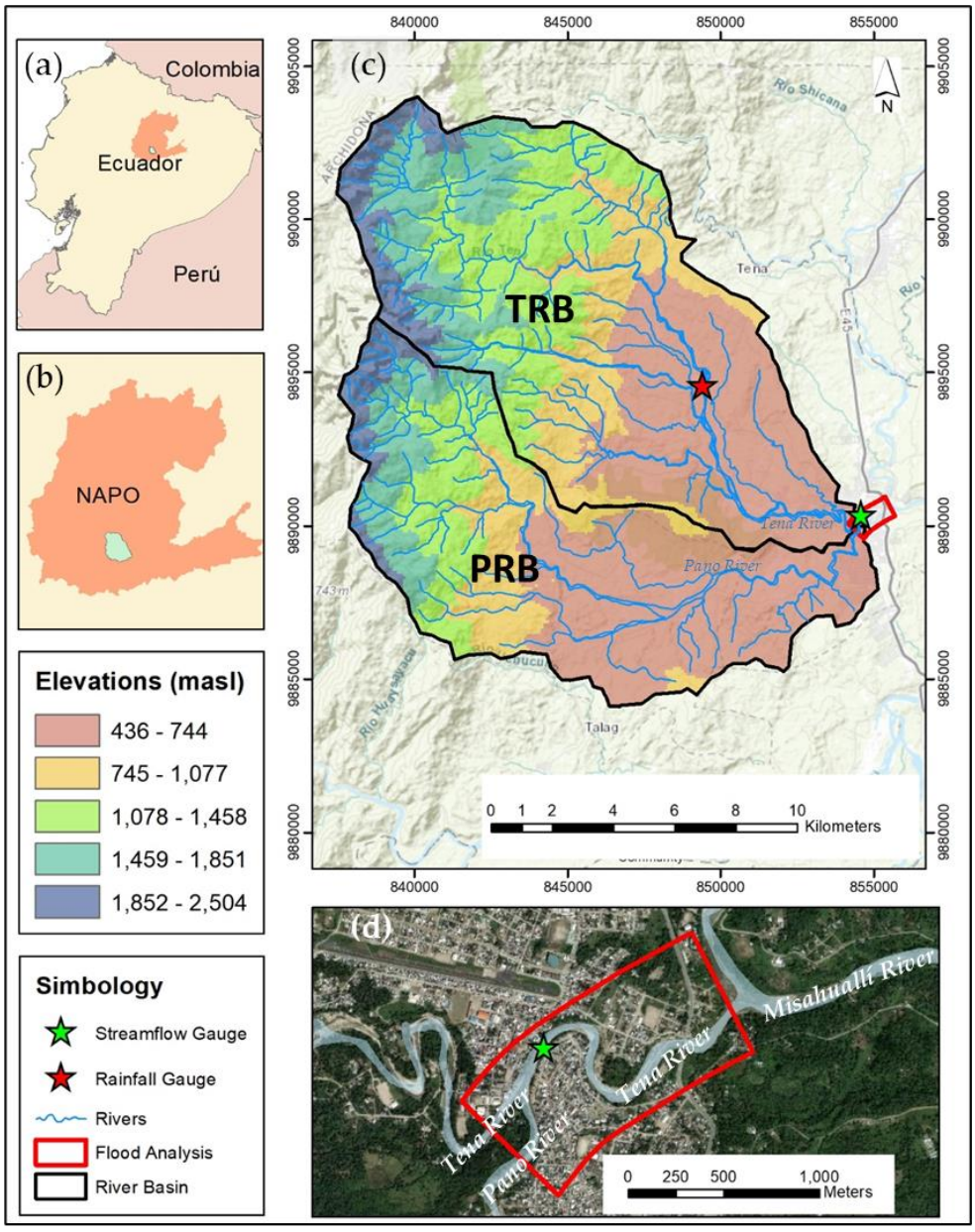

Figure 3.1. General features of the study area. (a) Location of the Napo province in Ecuador; (b) study area within the Napo province; (c) terrain elevation and location of the precipitation and streamflow gauges; (d) domain used for flood hazard assessment (red polygon) in the city of Tena.

In accordance with the Köppen climate classification, the study area can be defined as tropical rainforest (Af), i.e., the climate is strongly influenced by humid air masses coming from the remaining portion of the vast Amazon Basin in the east [43]. The mean annual precipitation in the city of Tena is estimated at 3500 mm, while in the upper zone of the study area, it could exceed 4000 mm. The mean

annual temperature is approximately 25 °C [38]. The city has experienced a disorderly urban growth in recent decades that has occupied areas susceptible to flooding (low terraces), where nowadays approximately 3000 people live [44]. Several climate scenarios for this region have projected a progressive increase in the occurrence of extreme precipitation events until the end of the century [45–48], which may imply a higher flood risk.

2.2. Data

Soil characteristics and land cover data for the TRB and PRB were derived from thematic maps of the SIGTIERRAS project (STP), available at the spatial scale of 1:25,000 [42]. The watershed morphological parameters for the hydrological modeling (Table 3.1) were derived from a 30-m digital elevation model (DEM) produced by the SRTM (Shuttle Radar Topographic Mission) [49], while the topography of the river segment and floodplains for the hydrodynamic modeling were derived from a 5-m DEM surveyed by the STP through Aerial Photogrammetry. In the latter, the topography of the main channel was adjusted with ground control points, and false elevation values were corrected [42]. It is important to note that the DEM described the terrain elevation, and consequently, it did not represent objects and obstacles such as buildings.

Table 3.1. Morphological and hydrological parameters of PRB and TRB.

Parameter	Description [Units]	PRB	TRB
A	Drainage area [km^2]	99.96	134.86
P	Perimeter [km]	54.97	54.13
El_min	Minimum elevation [m]	499.00	499.00
El_max	Maximum elevation [m]	2494.00	2448.00
El_ave	Mean elevation [m]	982.00	1087.00
Sl_min	Minimum slope [%]	0.00	0.00
Sl_max	Maximum slope [%]	95.93	106.23
Sl_ave	Mean slope [%]	24.09	27.51
Lh	Hydraulic length [km]	25.43	27.99
Le	Equivalent length [km]	23.17	20.48
Lr	Relative length of the largest reach (Lh / A^0.5) [-]; Lr > 1: elongated basin, Lr < 1: basins prone to floods	2.54	2.41
CN	Curve number for saturated conditions [-]	90.00	87.00
Tc	Time of concentration [minutes]	180.00	190.00
Lag	Lag time [minutes]	108.00	114.00
Bf	Baseflow [m^3/s]	6.00	9.00

Hydrometeorological monitoring initiatives in the watershed started in 2013 with the foundation of the Ikiam University, which installed an automatic weather station and an automatic radar streamflow gauge [50] in 2015 and 2018, respectively (Figure 3.1). These gauges record precipitation, streamflow, water depth, and flow velocity patterns using a one-minute time step. The data is available at http://meteorologia.ikiam.edu.ec:3838/meteoviewer/. The streamflow gauging station is a SOMMER RQ-30, which comprises a radar sensor for water level and flow velocity measurement [50]. The cross-section area (A) is computed as a function of the water level, and then used to calculate the streamflow (Q = A x V x k; k = correction factor). A discharge table is generated from the cross-section areas and the k-factors as a function of the water level corrected by a reference measurement. The cross section of the channel at the measuring point was determined with a detailed topographic survey.

Given that this study focuses on flash flood hazard assessment, for the calibration and validation of the modeling framework, we only considered storm events that have generated a significant streamflow. These were events that generated a streamflow over 211 m^3/s. This streamflow threshold was defined following the methodology proposed by Reynolds et al. [30], using the annual minimum from monthly maximum records instead of the annual mean. This obeyed the short time-series available for the streamflow (1 year; Figure 3.2). As a result, eight events were selected for the period between July 2018 and May 2019 (Table 3.2). E1 and E8 were the storm events with the longest durations (48 h), while E3 the event with the shortest (20 h) (Table 3.2). Likewise, the maximum and minimum peak flows were recorded for E1 (714.2 m^3/s) and E3 (234.8 m^3/s), respectively (Table 3.2).

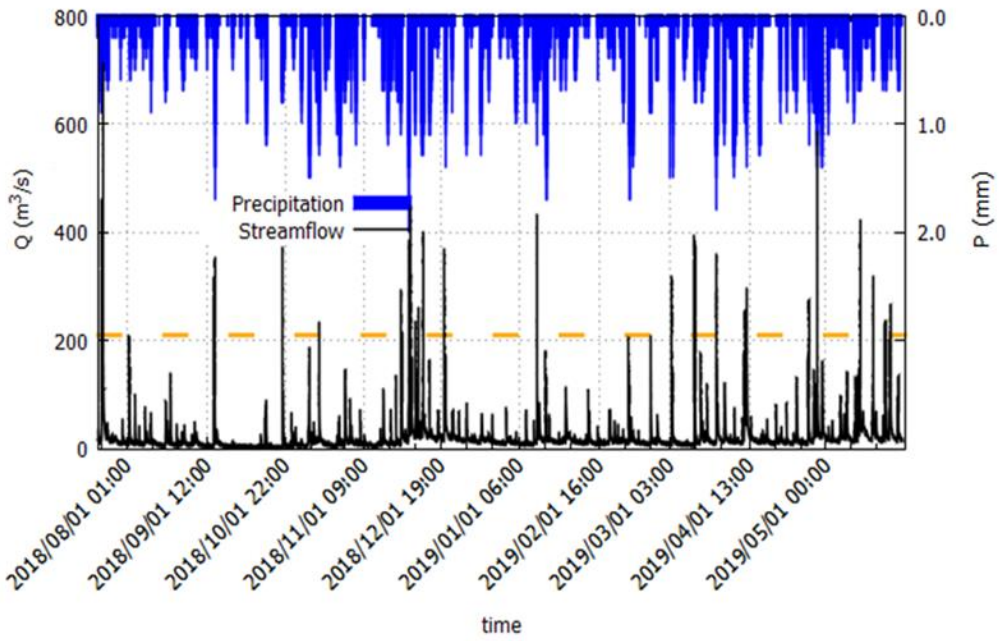

Figure 3.2. Time series of precipitation (P) and streamflow (Q) from July 2018 to May 2019. The orange dashed line represents the 211 m^3/s threshold for storm event selection.

Table 3.2. Duration and peak flow of the eight storm events considered for model calibration and validation.

Event	Start (Date, Time)	End (Date, Time)	Duration (Hours)	Peak Flow (m^3/s)
E1	21 Jul 2018, 12:00	23 Jul 2018, 12:00	48	714.20
E2	03 Sep 2018, 12:00	04 Sep 2018, 18:00	30	356.00
E3	14 Oct 2018, 12:00	15 Oct 2018, 08:00	20	234.80
E4	24 Nov 2018, 00:00	24 Nov 2018, 24:00	24	403.30
E5	07 Jan 2019, 12:00	08 Jan 2019, 12:00	24	435.60
E6	10 Mar 2019, 06:00	11 Mar 2019, 06:00	24	395.60
E7	27 Apr 2019, 00:00	27 Apr 2019, 24:00	24	589.80
E8	13 May 2019, 00:00	14 May 2019, 24:00	48	424.40

In September 2017, an extreme precipitation event flooded the city of Tena. It had a duration of 13 h with a 1.25-h period that registered a maximum intensity of 120 mm/h. In accordance with a study of heavy precipitation events in Ecuador developed by the National Hydrometeorological Institute (INAMHI) [51], the characteristics of the 2017 extreme event were equivalent to those of an event with a 500-year return period. This INAMHI study used a meteorological station located 10 km to the northeast of our study area and with more than 50 years of records to

determine the characteristics of precipitation events with different return periods. Among them, a 500-year event was described as that with a maximum intensity of 120 mm/h for a period of at least 1.25 h. In order to reproduce the flooding generated by the 2017 event and evaluate whether it may serve as a starting point for the establishment of a regional flood forecasting system, we employed our modeling framework to cope with the lack of streamflow records for the period when this 500-year event took place.

2.3. Hydrological Modeling

We set up a lumped HEC-HMS model (4.2.1 version) [52] to simulate streamflow in the main stem of PRB and TRB using the curve number (CN) and the synthetic unit hydrograph methods, both of which were developed by the Soil Conservation Service (SCS; now NRCS) [53–55]. The resulting hydrographs for PRB and TRB were combined without implementing any routing technique at the junction of the rivers in the city of Tena (Figure 3.1d). The CN is defined in terms of land cover, soil type, and antecedent soil moisture conditions. The latter is a crucial parameter that may reduce or increase the soil infiltration capacity [56], and hence, affect the amount of runoff. Initial values of CN, time of concentration (tc), and lag time (lag) were derived from previous studies performed in the study area, DEM processing, and the analysis of precipitation and streamflow time series, and then adjusted during calibration. According to Fernandez et al. [57], CN values of 90 for PRB and 87 for TRB (Table 3.1) accurately represent the soil saturated and the high surface runoff conditions in the basins. The tc, representing the hypothetical time that water would require to reach the watershed outlet from the remotest point [54], was expressed in terms of the river channel length and the elevation difference between the highest and lowest points of each basin using the Kirpich's equation [58]. The lag, which corresponds to the delay or time difference between the peak precipitation and peak streamflow, was calculated as 60% of tc [52]. The initial lag values for PRB and TRB were equal to 108 and 114 minutes, respectively. All the initial hydrological parameters used in this study are shown in Table 3.1.

The built-in automatic parameter estimation algorithm within the HEC-HMS interface [59] was employed for model calibration, where the model was calibrated for event E1 and validated for events E2-8. The goodness-of-fit of the model was evaluated by comparing the observed and simulated streamflow using the Nash-Sutcliffe efficiency coefficient (NSE) and the Percent Bias (PBIAS). The NSE indicates how well the observed and simulated data fit a 1:1 line [60], while the PBIAS measures the average tendency of the simulated data to underestimate or overestimate the streamflow compared to the observations [22]. The model

parameters were adjusted until the model reached a ‘very good’ performance in accordance with the Moriasi et al. [21] ratings, where the model performance metrics were computed considering all values at one-minute time steps over the event duration (Table 3.2).

2.4. Hydrodynamic Modeling

Nays2Dflood solver (3.0.0 version) [8] was used for hydrodynamic modeling. Nays2Dflood is an open-source flood flow solver for two-dimensional unsteady flow problems. It implements the continuity and momentum equations in a curvilinear coordinate system where water depths and flow velocities are the main model outputs [61,62]. For the domain used for flood hazard assessment in the city of Tena, we employed a 1-km^2 structured grid that comprises 10,000 × 10-m square cells (Figure 3.3). This simulation area encompassed the overflown section of the main channel and the urban areas that are more prone to flooding. The upstream boundary conditions were defined using the hydrographs generated by the hydrologic model for the Tena and Pano rivers (Figure 3.3a) while the downstream boundary conditions, located before the confluence of the Tena and Misahuallí rivers (Figure 3.1), were set as free outflow. Free outflow means the simulation results for the grid cells adjacent to the boundary grid cells are given to the boundary grid cells as their boundary condition [8]. Specifically, the initial water depth was set to 0.5 m, which corresponds to the water depth at the baseflow. Additionally, model calculations were performed using a time step of 0.05 s with the model outputs being printed every 60 s.

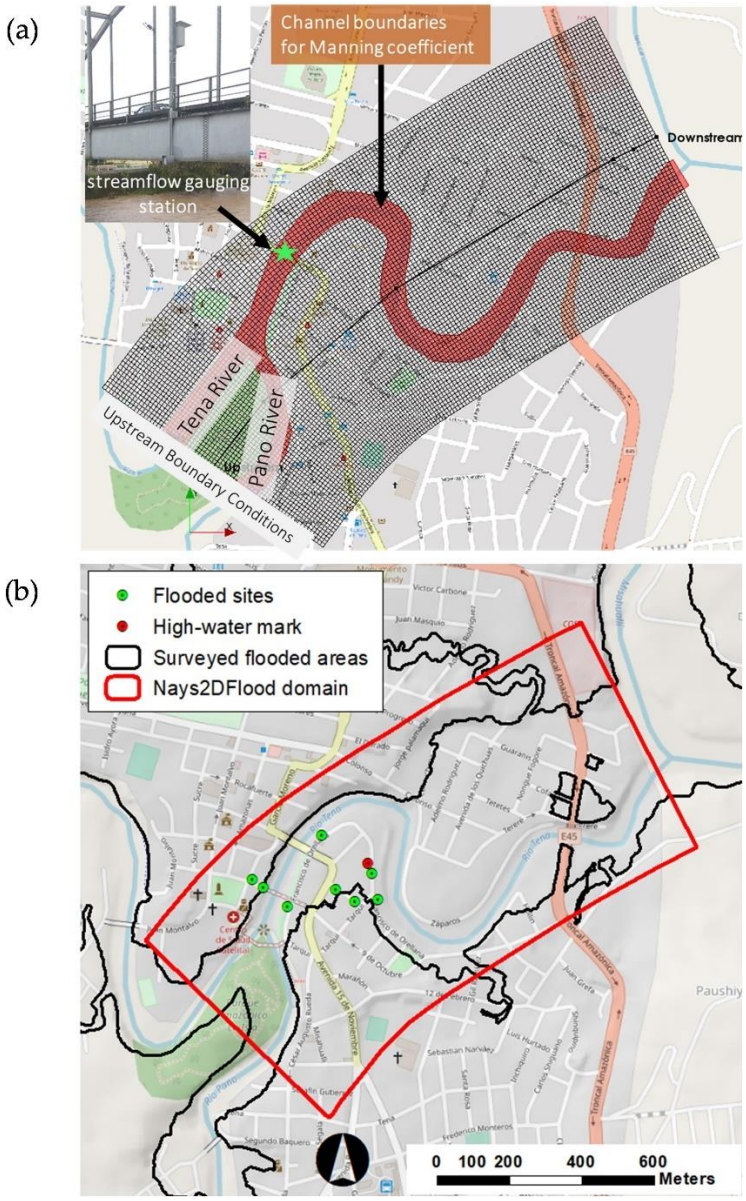

Figure 3.3. Hydrodynamic domain and control points for calibration and validation. (**a**) Modeling domain for the hydrodynamic simulations and location of the streamflow gauging station; (**b**) Polygon of flooded areas (black line), additional control points of flooded sites (greenish dots), and high-water mark (reddish dot) used to validate the results of the hydrodynamic model in simulating the 2017 flood event.

The cell roughness characteristics were estimated by comparing aerial photographs and land cover data with tabulated roughness values. Among all the parameters, the Manning's coefficient (n) is one of the most important for hydrodynamic modeling [11]. It represents the average flow resistance in the water profile [8]. We used an initial n value of 0.025 (natural channels with no vegetation)

for the main channel [63]. For the floodplains, an equivalent Manning coefficient was implemented resembling the roughness of pavement and other urban areas (n = 0.05) [64]. Given that Nays2Dflood employs an implicit finite difference scheme to solve the advection equation, during the simulation, the water flow variables need to be spatially interpolated at each time step. Specifically, this study used the constrained interpolation profile (CIP), which is a high-order, accurate method that fits a third-order polynomial to reduce numerical diffusion. One of the CIP advantages is that a small number of adjacent cells is required to obtain an accurate estimation of the advection terms [12].

There are several techniques for the calibration and validation of hydrodynamic models based on single or multiple data sources such as remote sensing, survey data, and historical records [65–69]. In this study, the coefficient of Manning was manually adjusted until the error between the observed and simulated water depths and flow velocities was the minimum possible at the radar streamflow gauge located in the main channel (Figure 3.1). It is important to note that during flash flood events, the kinematic wave (gravitational forces) prevails over the dynamic wave (inertial forces). Therefore, the use of flow velocities and water depths is suitable for calibrating the Manning's coefficient for the main channel, where the flow is predominantly one-dimensional [70,71]. The calibration and validation of the Manning's coefficient of the river reach took into account the six storm events that were calibrated and validated for the hydrologic model (i.e., E1-E3, E5, E6, and E8) and one that occurred in 2017. Events E4 and E7 were not considered because of the unsatisfactory performance of HEC-HMS in simulating their streamflow patterns (Figure 3.4). The same model metrics (NSE and PBIAS) used for the hydrological modeling were used to evaluate the performance of Nays2Dflood.

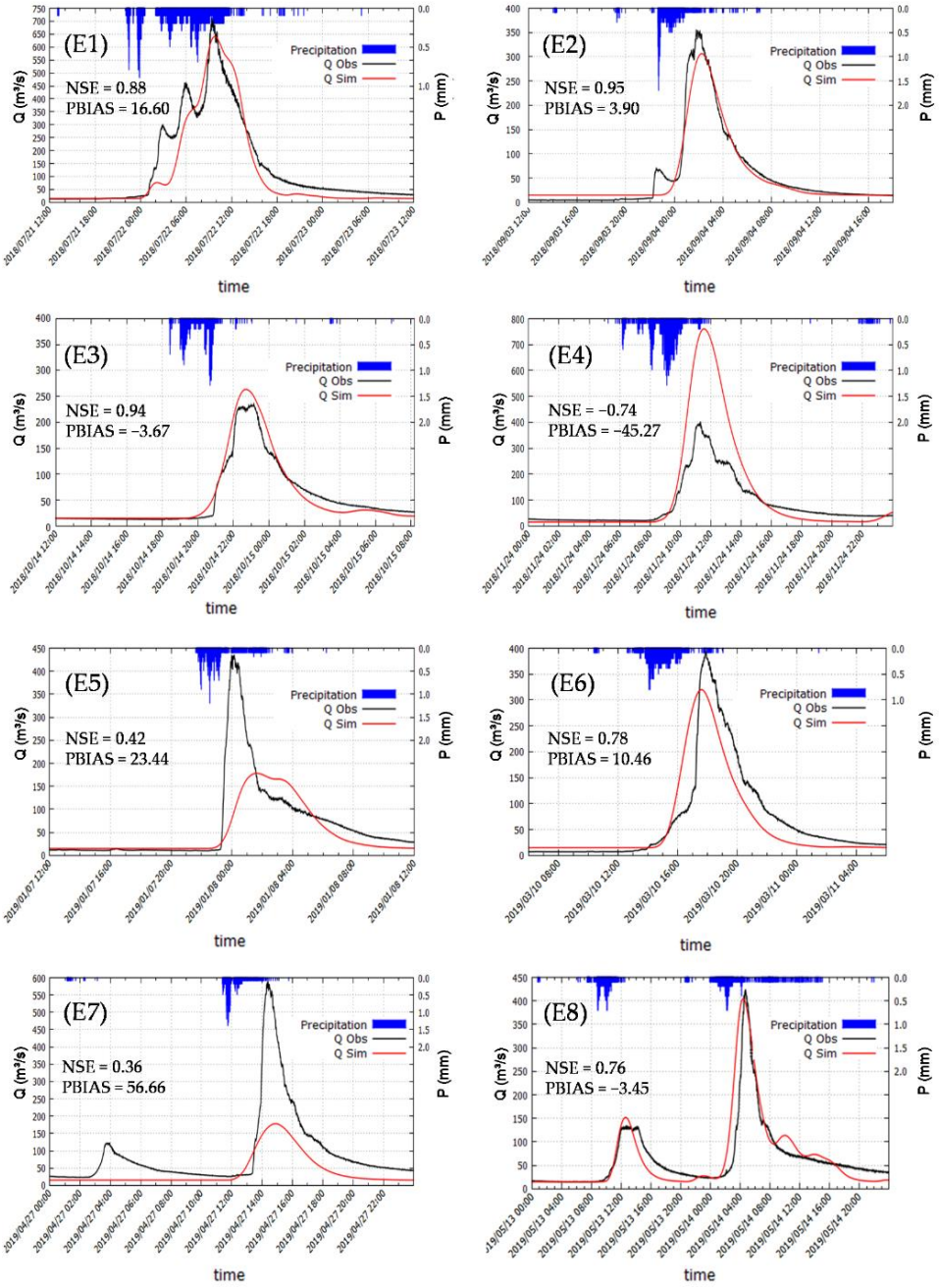

Figure 3.4. Observed (black line) and simulated (red line) streamflow (m^3/s) for the calibration and validation events (E1-E8).

In addition to the water depths and flow velocities at the gauging station, we used a polygon of flooded areas, additional control points of flooded sites, and a high-water mark (Figure 3.3b) to validate the performance of the model in simulating the 2017 extreme event. The flooded areas generated by the hydrodynamic model were evaluated using the fit index (better known as F index) [65,72], which measures the degree of overlap between the observed and simulated flooded areas from 0 to

1, where F = 1 represents a perfect overlap, and F = 0 represents no overlap. The F index is computed by dividing the spatial intersection between the observed and simulated flood areas by their spatial union.

2.5. Flood Hazard Mapping

The most relevant physical characteristics of flood events are flow velocity, water depth, and duration, which may determine their intensity and destructive capacity, and hence, may provide a measure of its hazard [73,74]. We built flood intensity maps for the 2017 flood event, postprocessing the results from the hydrodynamic simulations in GIS tools and using the flood intensity categories proposed by Cançado et al. [75] (Table 3.3). The flood hazard mapping was only implemented for the 2017 event because, within the available precipitation records, this flood event had survey data (flooded areas and points) which was useful for validation.

Table 3.3. Flood intensity as a function of flow velocities and water depth.

Flood Intensity	Depth (D) [m]-Velocity (V) [m/s]
High	D > 1.5 or V > 1.5
Medium	0.5 < D < 1.5 or 0.5 < V < 1.5
Low	0.1 < D < 0.5 and 0.1 < V < 0.5

3. Results and Discussion

3.1. HEC-HMS Calibration

The performance of HEC-HMS in simulating the streamflow at one-minute time steps showed satisfactory results (Table 3.4 and Figure 3.4). In accordance with the Moriasi et al. [21] guidelines for calibrating hydrologic models, the NSE (0.88) and PBIAS (16.6%) for the calibration event (E1; Figure 3.4) indicated a good fit between the observed and simulated streamflow. Similarly, in four (E2, E3, E6, E8) of the seven validation events, the hydrologic model had a satisfactory performance (0.76 ≤ NSE ≤ 0.95; −3.67% ≤ PBIAS ≤ 10.46%; Figure 3.4). Since high performance metrics are difficult to achieve using a one-minute time step, and the Moriasi et al. [21] performance ratings are for monthly time-step evaluations, we considered that our model had also an acceptable performance in simulating event E5, which obtained a NSE of 0.42 and a PBIAS of 23.44% (Figure 3.4).

Table 3.4. Observed and simulated peak flow, time at peak, and runoff volume for events E1-E8.

Event	Observed			Simulated		
	Time at Peak (Time)	Peak Flow (m^3/s)	Runoff Volume (mm)	Time at Peak (Time)	Peak Flow (m^3/s)	Runoff Volume (mm)
E1	09:24	714.20	100.66	09:47	641.10	83.96
E2	01:49	356.00	25.34	02:16	306.30	24.52
E3	23:09	234.80	16.92	22:42	263.70	17.54
E4	11:19	403.30	30.25	11:33	760.80	43.94
E5	00:09	435.60	24.1	01:36	178.10	18.45
E6	17:54	395.60	25.21	17:36	319.90	22.57
E7	14:24	589.80	33.76	14:53	178.10	14.63
E8	04:40	424.40	48.01	04:24	404.60	49.67

This was supported by other studies [76,77] that have stated that simulations with a daily (or smaller time steps) NSE as low as 0.4 may be considered acceptable. Consequently, five of the seven validation events had satisfactory results. Despite the fact that the performance of the model was not validated in two events (E4 and E7; Figure 3.4), our modeling framework was reliable in 71.4% (75% if considering the calibration event as well) of the cases, making it suitable for flood modeling. The low performance in the aforementioned two events may be explained by the spatial variability of the precipitation across the study area, which could not be fully described by the single weather station available for this study. Recall that precipitation is not monitored in PRB; this may explain some of the differences between the observed and simulated streamflow. Despite these limitations, the results were promising, taking into account the data-scarce condition of the study area and the fact that nowadays, flood prediction systems have not been deployed by the local authorities. The time difference between the observed and simulated peak flow ranged from −27 minutes to 87 minutes, with a mean value of 15 minutes, where the highest error was observed for E5 (Table 3.4).

The latter may imply some limitations for flood progress monitoring and forecasting, and a late response to such events from the local authorities. We believe that the modeling errors were related to the difficulty of describing the spatio-temporal patterns of every precipitation event that occurred across PRB and TRB due to the lack of multiple monitoring points. However, the results showed that in most of the cases, the single precipitation gauge available in the study area was able

to provide sufficient information for simulating the streamflow in the Tena River. More efforts should be made to improve the monitoring system in the study area.

The adjusted CN values for PRB and TRB were 84 and 81, respectively, being very close to the initial assumption. The optimum lag time values, on the other hand, were 125 minutes for PRB and 130 minutes for TRB, approximately 15% greater than the initial values. Similar results for the lag time were obtained in previous studies based on morphometric analyses [57]. The high CN and low lag values indicated a fast watershed response to precipitation. This was explained by the combined effect of intense precipitation patterns, steep slopes, and high-water storage capacity of clay and loam soil types. Recall that soils are saturated most of the time due to the humid environment and the cloud forest in the upper part of the study area, which has low evapotranspiration rates and allows the soil to remain moist [41]. Moreover, steep hillslopes in the upper zones of PRB and TRB facilitate surface runoff [78,79]. Under these conditions, surface runoff may be generated by both infiltration and saturation excess [80–82]. It is important to note that although TRB and PRB are densely forested, the ability of this cover to attenuate floods is limited [83,84].

3.2. Nays2Dflood Calibration and Reconstruction of the 500-Year Flood Event

The Manning coefficient for the channel and the floodplains was simultaneously calibrated and validated. As a result, a value of 0.05 for both generated the best results (highest performance metrics; Figures 5 and Figure 3.7c). Our findings matched those from other studies that estimated an equivalent Manning's n for urban floodplains [64,72,85]. Moreover, several studies have found that the calibrated Manning coefficient for the channel and floodplains can be very similar under certain conditions. For example, Mosquera-Machado et al. [86] obtained Manning's n values of 0.056 and 0.048 for the floodplains and channel, respectively, in a flood hazard study in Colombia. Horrit and Bates [65] also obtained similar values for the Manning coefficient in both the channel and floodplains of 0.02 and 0.05 using the TELEMAC and the LISFLOOD-FP models, respectively. In our case, the same value of Manning's n for the river channel and floodplains may be explained by the coarse bed material of the channel (gravel and cobble) [87] and the urban cover of the floodplains, which have similar roughness characteristics.

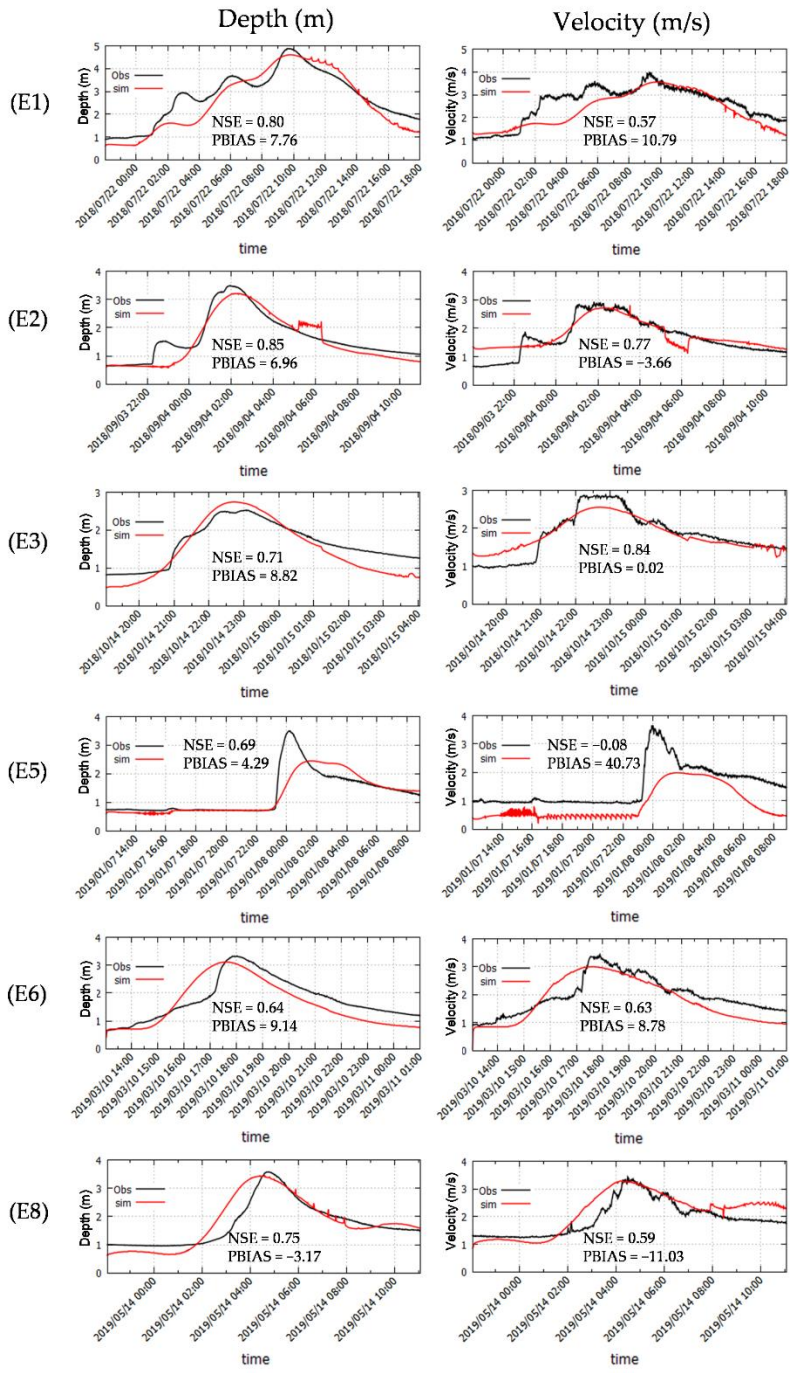

Figure 3.5. Observed (black line) and simulated (reddish line) water depth (m) and flow velocity (m/s) for the calibration and validation events (E1-E3, E5, E6, E8).

The Nays2Dflood showed satisfactory results in simulating water depths and flow velocity in the main channel (Figure 3.5). For the water depths over the

calibration and validation events (E1-E3, E5, E6, E8), the NSE values ranged between 0.64 and 0.85, while the PBIAS varied from −3.17% to 8.62% (Figure 3.5). Overall, the model was able to simulate the magnitude and timing of the water depths with a general tendency to underestimate its magnitude by 5.6%, which represents 'very good' performance in conformity with the Moriasi et al. [21] performance ratings. For the flow velocity, the NSE (0.57–0.84) and the PBIAS (−11.03–10.79%) described a reasonable goodness-of-fit in five of the six evaluated events (E1-E3, E6, E8; Figure 3.5). The model was not able to recreate the water velocity during event E5 (NSE = −0.08; PBIAS = 40.73%; Figure 3.5). This error in the flow velocity was associated with the low accuracy of the hydrologic model in simulating the streamflow for this event due to the complexity of describing precipitation patterns across the study area with a single weather station. However, we believe these limitations can be overcome in the near future by improving the precipitation monitoring network in the study area and/or using remote sensing data.

Given that there were no streamflow records for the precipitation event that flooded the city of Tena in September 2017, they were recreated using the calibrated HEC- HMS model (Figure 3.6a). At the junction of the Pano and Tena rivers, the simulated peak flow was equal to 1967 m^3/s (Figure 3.6a), i.e., 5.1% less than that estimated by Fernandez and Bateman [57] for the same area based on the precipitation event that INAMHI described with a 500-year return period [51].

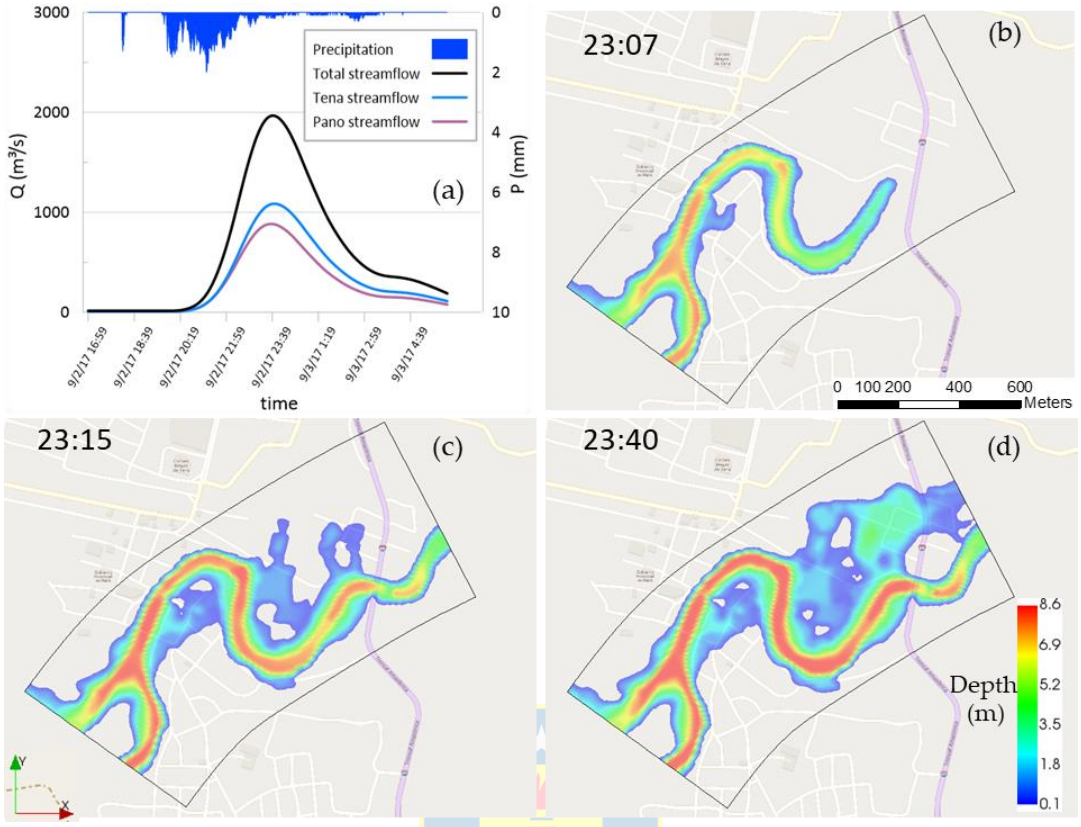

Figure 3.6. Spatio-temporal evolution of the flood event generated by the 500-year storm on September 2, 2017. (**a**) HEC-HMS-reconstructed hydrograph. Flood stage (**b**) at the beginning of the river overflow, (**c**) when the overflow took place along several river segments, and (**d**) at the time of peak flow.

According to the simulation results, the river started overflowing 150 m downstream of the confluence of the Pano and Tena rivers at 23:07 (111 minutes after the peak precipitation was observed; Figures 6a–b), and only 8 minutes later (23:15), several river segments near the meanders were overflowing simultaneously. Moreover, when the peak flow was observed (23:40), most of the floodplains were almost covered. These results may help stakeholders to develop flood emergency plans that consider evacuation plans, the establishment of early warnings, the construction of levees, or urban planning strategies to relocate vulnerable communities.

As mentioned in 2.4, the Nays2Dflood results were further validated using survey data of the flooded areas and control points of flooded sites. A high agreement between the simulated and observed flooded areas was obtained based on the fit index (F = 0.8). Additionally, six of the eight control points of flooded sites were within the simulated flooded areas, and the simulated water depth (1.23 m)

matched that observed in a high-water mark (1.2 m) left on a building after the flood event (Figure 3.7c).

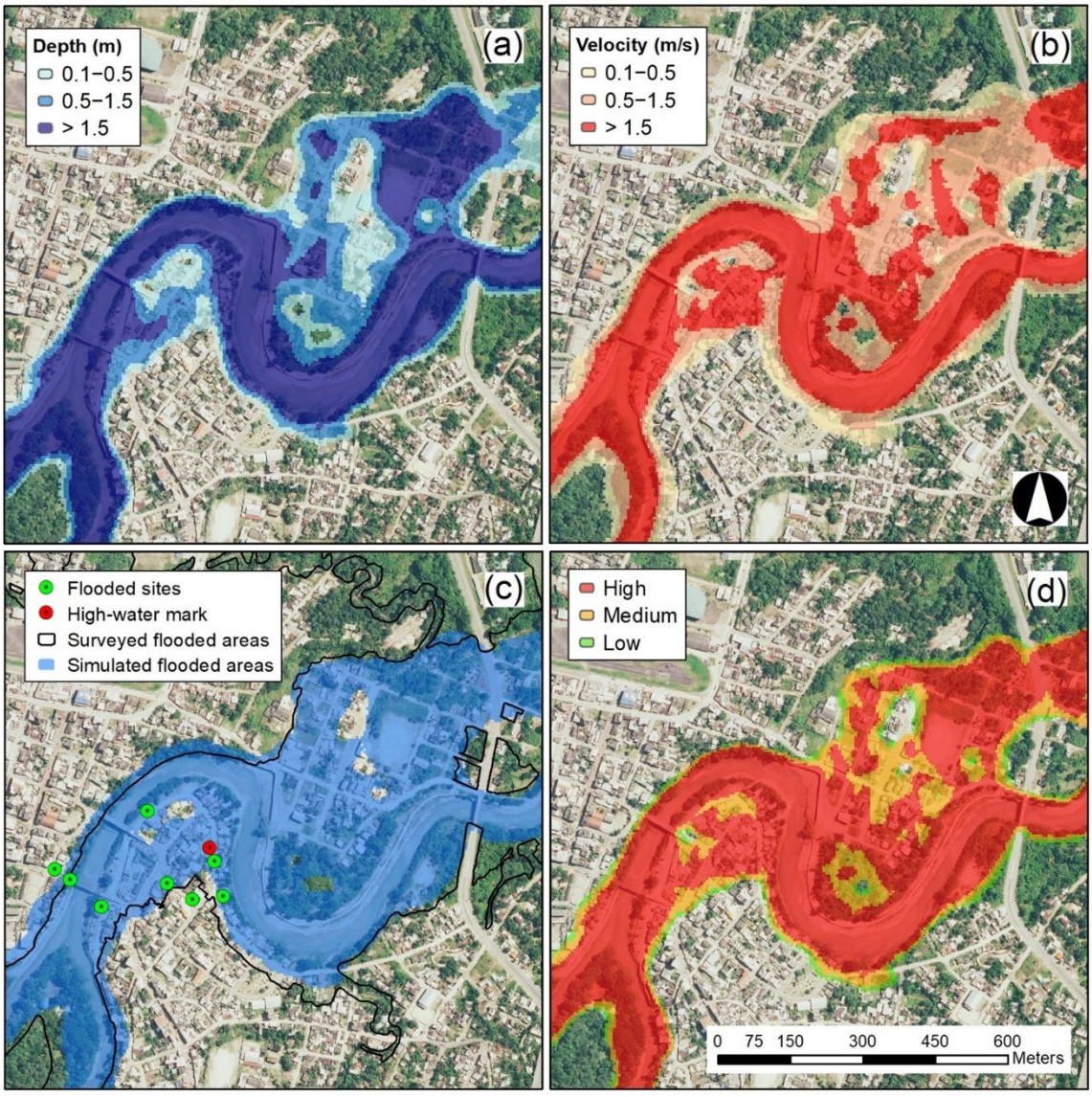

Figure 3. 7. Reconstructed 500-year flood event. (a) water depths; (b) flow velocities; (c) simulated flood extent against surveyed flooded areas (black line) and control points of flooded sites (greenish dots), and location of the high-water mark (reddish dot); (d) flood intensity map as a function of flow velocity and water depth in compliance with Cançado et al. [75] guidelines (Table 3.3).

The values reported In Figure 3.7 correspond to the instant at which the peak flow in the channel was reached (11:40 pm; Figure 3.6a). The flood intensity map (Figure 3.7d) indicated that 71% of the flooded areas (40.9 ha) were under a high

intensity, while 23% and 6% were under medium and low intensity, respectively. The flood intensity map also showed that the Bellavista and El Tereré neighborhoods were the most affected, being within high flood intensity areas (water depth > 1.5 m or flow velocity > 1.5 m/s). Accordingly, the maximum water depths in the floodplains were approximately 2 m and 4 m in the Bellavista and El Tereré neighborhoods, respectively, while the maximum water depth in the main channel was 8.5 m. The maximum flow velocity in the floodplains, on the other hand, was approximately 3 m/s across both neighborhoods, while in the main channel, a maximum of 9.4 m/s was reached (Figure 3.7). These areas with medium and high flood intensities may represent a threat to individuals and hinder evacuation and rescue tasks, given that at a water depth of at least 0.3 m and a flow velocity of 2.0 m/s, humans and cars become unstable [88,89]. Moreover, a water depth of 1.5 m may represent a damage factor of 0.84 on South American residential buildings [90]. Governmental reports stated that one person died and 1312 people, 324 houses, 36 private goods, and three public goods were affected during this extreme flood event [91].

4. Conclusions

This study coupled HEC-HMS and Nays2Dflood with event sampling and survey data to simulate the hydrologic response of data-scarce watersheds for a flood hazard assessment in the city of Tena. The results showed that this approach is suitable for calibrating and validating hydrologic and hydrodynamic models and recreating extreme flood events. Our modeling framework was reliable in simulating the streamflow and water depths of the main channel in 75% of the evaluated storm events, indicating that under certain conditions, data from a single precipitation gauge can accurately represent the spatio-temporal patterns of precipitation across the study area. Additionally, survey data such as polygons of flooded areas, control points of flooded sites, and high-water marks can provide sufficient information to constrain hydrodynamic models in the two-dimensional space. We appropriately reproduced an extreme flood event that occurred in September 2017 due to a 500-year precipitation event, where streamflow records were not available. According to our flood intensity map, 94% of the floodplains were under medium or high intensity, which may represent a threat to life, hinder evacuation and rescue tasks, and significantly damage residential and civil infrastructure.

The framework that we developed in this study facilitated the evaluation of the possible impacts of flood events on urban areas located in watersheds where robust monitoring networks are not available. Despite the assumptions that long-term data and multiple monitoring points are required for flood hazard assessment and the establishment of flood forecasting systems, we found that event sampling and survey

data can cope with data scarcity and pave the way for flood research and the establishment of flood monitoring/forecasting systems in developing countries while their monitoring systems are being improved. This will enable stakeholders to formulate timely adaptation and mitigating plans to lessen the impacts of flood events at the local scale.

Author Contributions: Conceptualization, J.H.-P., F.J.-P., E.E.-S. and J.S.A.T.; Data curation, E.E.-S.; Formal analysis, J.H.-P.; Writing—original draft, J.H.-P. and F.J.-P.; Writing—review & editing, J.H.-P., F.J.-P., E.E.-S. and J.S.A.T. All authors have read and agreed to the published version of the manuscript.

Acknowledgments: The authors would like to acknowledge Universidad Regional Amazónica Ikiam for providing access to its hydro-meteorological and survey data archive. Special thanks to Jorge Celi for his assistance for the development of this work. Also, authors would like to acknowledge the Municipality of Tena for providing information about flooded areas and the Secretary of Higher Education, Science, Technology, and Innovation for its financial support of the PhD scholarships of Jorge Hurtado and Fernando Jarrin. Lastly, the authors would like to acknowledge the reviewers of the manuscript for their valuable feedback.

Conflicts of Interest: The authors declare no conflict of interest.

References

1. Jain, S.K.; Mani, P.; Jain, S.K.; Prakash, P.; Singh, V.P.; Tullos, D.; Kumar, S.; Agarwal, S.P.; Dimri, A.P. A Brief Review of Flood Forecasting Techniques and Their Applications. *Int. J. River Basin Manag.* **2018**, *16*, 329–344, doi:10.1080/15715124.2017.1411920.

2. IPCC. *AR5 Climate Change 2013: The Physical Science Basis—IPCC*; 2013. Cambridge University Press, Cambridge, United Kingdom and New York, NY, USA, 1535 pp.

3. Merz, B.; Aerts, J.; Arnbjerg-Nielsen, K.; Baldi, M.; Becker, A.; Bichet, A.; Blöschl, G.; Bouwer, L.M.; Brauer, A.; Cioffi, F.; et al. Floods and Climate: Emerging Perspectives for Flood Risk Assessment and Management. *Nat. Hazards Earth Syst. Sci.* **2014**, *14*, 1921–1942, doi:10.5194/nhess-14-1921-2014.

4. Yin, J.; Gentine, P.; Zhou, S.; Sullivan, S.C.; Wang, R.; Zhang, Y.; Guo, S. Large Increase in Global Storm Runoff Extremes Driven by Climate and Anthropogenic Changes. *Nat. Commun.* **2018**, *9*, 4389, doi:10.1038/s41467-018-06765-2.

5. Merkuryeva, G.; Merkuryev, Y.; Sokolov, B.V.; Potryasaev, S.; Zelentsov, V.A.; Lektauers, A. Advanced River Flood Monitoring, Modelling and Forecasting. *J. Comput. Sci.* **2015**, *10*, 77–85, doi:10.1016/j.jocs.2014.10.004.

6. Díez-Herrero, A.; Huerta, L.L.; Isidro, M.L. *A Handbook on Flood Hazard Mapping Methodologies*; Geological Survey of Spain: Madrid, Spain, 2009; Volume 2.

7. Bates, P.D.; De Roo, A.P.J. A Simple Raster-Based Model for Flood Inundation Simulation. *J. Hydrol.* **2000**, *236*, 54–77, doi:10.1016/S0022-1694(00)00278-X.

8. Shimizu, Y.; Inoue, T.; Suzuki, E.; Kawamura, S.; Iwasaki, T.; Hamaki, M.; Omura, K.; Kakegawa, E.; Yoshida, T. *Nays2Dflood—Solver Manual*; The International River Interface Cooperative (Iric): Hokkaido, Japan, 2015; pp. 1–51.

9. Bladé, E.; Cea, L.; Corestein, G.; Escolano, E.; Puertas, J.; Vázquez-Cendón, E.; Dolz, J.; Coll, A. Iber: Herramienta de Simulación Numérica Del Flujo En Ríos. *Int. J. Numer. Methods Calc. Des. Eng. (RIMNI)* **2014**, *30*, 1–10, doi:10.1016/j.rimni.2012.07.004. (In Spanish)

10. Fernández-Pato, J.; Caviedes-Voullième, D.; García-Navarro, P. Rainfall/Runoff Simulation with 2D Full Shallow Water Equations: Sensitivity Analysis and Calibration of Infiltration Parameters. *J. Hydrol.* **2016**, *536*, 496–513, doi:10.1016/J.JHYDROL.2016.03.021.

11. Smart, G.M. Improving Flood Hazard Prediction Models. *Int. J. River Basin Manag.* **2018**, *16*, 449–456, doi:10.1080/15715124.2017.1411923.

12. Rai, P.K.; Dhanya, C.T.; Chahar, B.R. Coupling of 1D Models (SWAT and SWMM) with 2D Model (IRIC) for Mapping Inundation in Brahmani and Baitarani River Delta. *Nat. Hazards* **2018**, *92*, 1821–1840, doi:10.1007/s11069-018-3281-4.

13. Hanif, A.; Dhanasekar, A.; Keene, A.; Li, H.; Carlson, K. Flood Risk Assessment Methodology for Planning under Climate Change Scenarios and the Corresponding Change in Land Cover. *J. Water Clim. Chang.* **2019**, https://doi.org/10.2166/wcc.2019.016.

14. Mishra, B.K.; Rafiei Emam, A.; Masago, Y.; Kumar, P.; Regmi, R.K.; Fukushi, K. Assessment of Future Flood Inundations under Climate and Land Use Change Scenarios in the Ciliwung River Basin, Jakarta. *J. Flood Risk Manag.* **2018**, *11*, S1105–S1115, doi:10.1111/jfr3.12311.

15. Liu, Z.; Zhang, H.; Liang, Q. A Coupled Hydrological and Hydrodynamic Model for Flood Simulation. *Hydrol. Res.* **2019**, *50*, 589–606, doi:10.2166/nh.2018.090.

16. Zhang, Y.; Zhou, J.; Lu, C. Integrated Hydrologic and Hydrodynamic Models to Improve Flood Simulation Capability in the Data-Scarce Three Gorges Reservoir Region. *Water* **2020**, *12*, 1462, doi:10.3390/w12051462.

17. Chang, H.; Franczyk, J. Climate Change, Land-Use Change, and Floods: Toward an Integrated Assessment. *Geogr. Compass* **2008**, *2*, 1549–1579, doi:10.1111/j.1749-8198.2008.00136.x.

18. Barbedo, J.; Miguez, M.; van der Horst, D.; Marins, M. Enhancing Ecosystem Services for Flood Mitigation: A Conservation Strategy for Peri-Urban Landscapes? *Ecol. Soc.* **2014**, *19*, 54, doi:10.5751/ES-06482-190254.

19. Tsakiris, G. Flood Risk Assessment: Concepts, Modelling, Applications. *Nat. Hazards Earth Syst. Sci.* **2014**, *14*, 1361–1369, doi:10.5194/nhess-14-1361-2014.

20. De Roo, A.; Schmuck, G.; Perdigao, V.; Thielen, J. The Influence of Historic Land Use Changes and Future Planned Land Use Scenarios on Floods in the Oder Catchment. *Phys. Chem. Earth, Parts A/B/C* **2003**, *28*, 1291–1300, doi:10.1016/J.PCE.2003.09.005.

21. Moriasi, D.N.; Arnold, J.G.; Van Liew, M.W.; Bingner, R.L.; Harmel, R.D.; Veith, T.L.; Harmel, D.; Veith, T.L. Model Evaluation Guidelines for Systematic Quantification of Accuracy in Watershed Simulations. *Trans. ASABE* **2007**, *50*, 885–900, doi:10.13031/2013.23153.

22. Gupta, H.V.; Sorooshian, S.; Yapo, P.O. Status of Automatic Calibration for Hydrologic Models: Comparison with Multilevel Expert Calibration. *J. Hydrol. Eng.* **1999**, *4*, 135–143, doi:10.1061/(ASCE)1084-0699(1999)4:2(135).

23. Teng, J.; Jakeman, A.J.J.; Vaze, J.; Croke, B.F.W.F.W.; Dutta, D.; Kim, S. Flood Inundation Modelling: A Review of Methods, Recent Advances and Uncertainty Analysis. *Environ. Model. Softw.* **2017**, *90*, 201–216, doi:10.1016/j.envsoft.2017.01.006.

24. Peña, F.; Nardi, F. Floodplain Terrain Analysis for Coarse Resolution 2D Flood Modeling. *Hydrol.* **2018**, *5*, 52, doi:10.3390/hydrology5040052.

25. Papaioannou, G.; Loukas, A.; Vasiliades, L.; Aronica, G.T. Flood Inundation Mapping Sensitivity to Riverine Spatial Resolution and Modelling Approach. *Nat. Hazards* **2016**, *83*, 117–132, doi:10.1007/s11069-016-2382-1.

26. Caviedes-Voullième, D.; García-Navarro, P.; Murillo, J. Influence of Mesh Structure on 2D Full Shallow Water Equations and SCS Curve Number Simulation of Rainfall/Runoff Events. *J. Hydrol.* **2012**, *448–449*, 39–59, doi:10.1016/J.JHYDROL.2012.04.006.

27. Boongaling, C.G.K.; Faustino-Eslava, D.V.; Lansigan, F.P. Modeling Land Use Change Impacts on Hydrology and the Use of Landscape Metrics as Tools for Watershed Management: The Case of an Ungauged Catchment in the Philippines. *Land Use Policy* **2018**, *72*, 116–128, doi:10.1016/j.landusepol.2017.12.042.

28. Acero Triana, J.S.; Chu, M.L.; Guzman, J.A.; Moriasi, D.N.; Steiner, J.L. Beyond Model Metrics: The Perils of Calibrating Hydrologic Models. *J. Hydrol.* **2019**, *578*, 124032, doi:10.1016/j.jhydrol.2019.124032.

29. Johnston, R.; Smakhtin, V. Hydrological Modeling of Large River Basins: How Much Is Enough? *Water Resour. Manag.* **2014**, *28*, 2695–2730, doi:10.1007/s11269-014-0637-8.

30. Reynolds, J.E.; Halldin, S.; Seibert, J.; Xu, C.Y.; Grabs, T. Robustness of Flood-Model Calibration Using Single and Multiple Events. *Hydrol. Sci. J.* **2019**, *6667*, 842–853, doi:10.1080/02626667.2019.1609682.

31. McIntyre, N.; Lee, H.; Wheater, H.; Young, A.; Wagener, T. Ensemble Predictions of Runoff in Ungauged Catchments. *Water Resour. Res.* **2005**, *41*, 1–14, doi:10.1029/2005WR004289.

32. Perrin, C.; Oudin, L.; Andreassian, V.; Rojas-Serna, C.; Michel, C.; Mathevet, T. Impact of Limited Streamflow Data on the Efficiency and the Parameters of Rainfall-Runoff Models. *Hydrol. Sci. J.* **2007**, *52*, 131–151, doi:10.1623/hysj.52.1.131.

33. Seibert, J.; McDonnell, J.J. Gauging the Ungauged Basin: Relative Value of Soft and Hard Data. *J. Hydrol. Eng.* **2015**, *20*, A4014004, doi:10.1061/(ASCE)HE.1943-5584.0000861.

34. Correa, A.; Windhorst, D.; Crespo, P.; Célleri, R.; Feyen, J.; Breuer, L. Continuous versus Event-Based Sampling: How Many Samples Are Required for Deriving General Hydrological Understanding on Ecuador's Páramo Region? *Hydrol. Process.* **2016**, *30*, 4059–4073, doi:10.1002/hyp.10975.

35. Seibert, J.; Beven, K.J. Gauging the Ungauged Basin: How Many Discharge Measurements Are Needed? *Hydrol. Earth Syst. Sci.* **2009**, *13*, 883–892, doi:10.5194/hess-13-883-2009.

36. Juston, J.; Seibert, J.; Johansson, P.-O. Temporal Sampling Strategies and Uncertainty in Calibrating a Conceptual Hydrological Model for a Small Boreal Catchment. *Hydrol. Process.* **2009**, *23*, 3093–3109, doi:10.1002/hyp.7421.

37. Espinoza, J.C.; Chavez, S.; Ronchail, J.; Junquas, C.; Takahashi, K.; Lavado, W. Rainfall Hotspots over the Southern Tropical Andes: Spatial Distribution, Rainfall Intensity, and Relations with Large-Scale Atmospheric Circulation. *Water Resour. Res.* **2015**, *51*, 3459–3475, doi:10.1002/2014WR016273.

38. GAD-TENA. *Actualización Plan de Desarrollo y Ordenamiento Territorial de Tena*; Gobierno Municipal de Tena: Tena, Ecuador, 2014.

39. Cruz-Cueva, G. Elaboración de Un Plan de Contingencia Por Inundación Del Río Tena En Los Barrios: Bellavista Las Hierbitas Tereré y Barrio Central de La Ciudad de Tena; PUCE, Quito, Ecuador, 2016. (In Spanish)

40. Moreno, J.; Yerovi, F.; Herrera, M.; Yánez, D.; Espinosa, J.; Sánchez, D.; Merlo, J.; Haro, R.; Acosta, M.; Bernal, G. *Soils from the Amazonia*; Springer: Madison, USA. 2018; pp. 79–111, doi:10.1007/978-3-319-25319-0_3.

41. Tobón, C. *Los Bosques Andinos y El Agua;* ECOBONA: Quito, Ecuador, 2008.

42. MAGAP-SIGTIERRAS. Generación de Geoinformación para la Gestión del Territorio a Nivel Nacional. Available online: metadatos.sigtierras.gob.ec (accessed on 12 July 2020). (In Spanish)

43. Cadilhac, L.; Torres, R.; Calles, J.; Vanacker, V.; Calderón, E. Desafíos Para La Investigación Sobre El Cambio Climático En Ecuador. *Neotrop. Biodivers.* **2017**, *3*, 168–181, doi:10.1080/23766808.2017.1328247.

44. INEC. Censo de 51merica51t y Vivienda 2010. Available online: https://www.ecuadorencifras.gob.ec/estadisticas/ (accessed on 12 July 2020). (In Spanish)

45. Palomino-Lemus, R.; Córdoba-Machado, S.; Gámiz-Fortis, S.R.; Castro-Díez, Y.; Esteban-Parra, M.J. Climate Change Projections of Boreal Summer Precipitation over Tropical America by Using Statistical Downscaling from CMIP5 Models. *Environ. Res. Lett.* **2017**, *12*, 124011, doi:10.1088/1748-9326/aa9bf7.

46. Hirabayashi, Y.; Mahendran, R.; Koirala, S.; Konoshima, L.; Yamazaki, D.; Watanabe, S.; Kim, H.; Kanae, S. Global Flood Risk under Climate Change. *Nat. Clim. Chang.* **2013**, *3*, 816–821, doi:10.1038/nclimate1911.

47. Sorribas, M.V.; Paiva, R.C.D.D.; Melack, J.M.; Bravo, J.M.; Jones, C.; Carvalho, L.; Beighley, E.; Forsberg, B.; Costa, M.H. Projections of Climate Change Effects on Discharge and Inundation in the Amazon Basin. *Clim. Chang.* **2016**, *136*, 555–570, doi:10.1007/s10584-016-1640-2.

48. Armenta, E.; Villa, L.; Jácome, P. *Proyecciones Climáticas De Precipitación Y Temperatura Para Ecuador, Bajo Distintos Escenarios De Cambio Climático.*; Ministerio de Ambiente: Quito, Ecuador, 2016. (In Spanish)

49. USGS. EarthExplorer. Available online: https://earthexplorer.usgs.gov/ (accessed on 6 June 2020).

50. Sommer Messtechnick. *RQ-30, RQ-30a, Discharge Measurement System User Manual*.; Sommer GmbH: Koblach, Austria, **2014.** Available online: https://www.sommer.at/en/products/water/rq-30-rq-30a (accessed on 12 July 2020)

51. INAMHI. *Determinación de Ecuaciones Para El Cálculo de Intensidades Máximas de Precipitación*; Instituto Nacional de Meteorología e Hidrología (INAMHI): Quito, Ecuador, 2019. Available online: www.serviciometeorologico.gob.ec/Publicaciones/Hidrologia/ESTUDIO_DE_INTENSIDADES_V_FINAL.pdf (accessed on 12 July 2020). (In Spanish)

52. Scharffenberg, B.; Bartles, M.; Braurer, T.; Fleming, M.; Karlovits, G. *Hydrologic Modeling System HEC-HMS User's Manual*; No. 4.2; Hydrologic Engineering Center: Davis, CA, USA, 2016. Available online: https://www.hec.usace.army.mil/software/hec-hms/documentation/HEC-HMS_Users_Manual_4.2.pdf (accessed on 12 July 2020).

53. Hawkins, R.H.; Ward, T.J.; Woodward, D.E.; Van Mullem, J.A. *Curve Number Hydrology*; American Society of Civil Engineers (ASCE): Reston, USA, 2008; doi:10.1061/9780784410042.

54. Cronshey, R. *Urban Hydrology for Small Watersheds*; U.S. Dept. of Agriculture, Soil Conservation Service, Engineering Division; United States Department of Agriculture (USDA): Washington, DC, USA, 1986.

55. Merwade, V. *Terrain Processing and HMS-Model Development Using GeoHMS Load the Data to ArcMap*; Purdue University: West Lafayette, USA, 2012. Available online:

https://web.ics.purdue.edu/~vmerwade/education/geohms.pdf (accessed on 12 July 2020).

56. Bondelid, T.R.; McCuen, R.H.; Jackson, T.J. Sensitivity of SCS Models to Curve Number Variation. *J. Am. Water Resour. Assoc.* **1982**, *18*, 111–116, doi:10.1111/j.1752-1688.1982.tb04536.x.

57. Fernandez Nualart, M.; Bateman Pinzon, A. *Recuperación Paisajística y Estudio de Inundabilidad Del Sistema Hídrico a Su Paso Por Tena*; Polytechnic University of Catalonia (UPC): Barcelona, Spain, 2004. (In Spanish)

58. Vélez Upegui, J.J.; Botero Gutiérrez, A. Estimación Del Tiempo de Concentración y Tiempo de Rezago En La Cuenca Experimental Urbana de La Quebrada San Luis, Manizales. *Dyna* **2011**, *165*, 59. (In Spanish)

59. Scharffenberg, W.A. Model Optimization. In *Hydrologic Modeling System HEC-HMS, User Manual*; US-Army-Corps-Engineers, Ed.; Hydrologic Engineering Center: Davis, CA, USA, 2016; pp. 383–419.

60. Nash, J.E.; Sutcliffe, J.V. River Flow Forecasting through Conceptual Models Part I—A Discussion of Principles. *J. Hydrol.* **1970**, *10*, 282–290, doi:10.1016/0022-1694(70)90255-6.

61. Shokory, J.A.N.; Tsutsumi, J.G.; Sakai, K. Flood Modeling and Simulation Using IRIC: A Case Study of Kabul City. *E3S Web Conf.* **2016**, *7*, 04003, doi:10.1051/e3sconf/20160704003.

62. Kumar, S.; Kaushal, D.R.R.; Gosain, A.K.K. Hydrodynamic Simulation of Urban Stormwater Drain (Delhi City, India) Using IRIC Model. *J. Appl. Res. Technol.* **2018**, *16*, 67–78, doi:10.22201/ICAT.16656423.0.16.1.704.

63. Chow, V. *Hidráulica de Canales Abiertos*; McGraw Hill: Bogotá, Colombia, 1994. (In Spanish)

64. van der Sande, C.J.; de Jong, S.M.; de Roo, A.P.J. A Segmentation and Classification Approach of IKONOS-2 Imagery for Land Cover Mapping to Assist Flood Risk and Flood Damage Assessment. *Int. J. Appl. Earth Obs. Geoinf.* **2003**, *4*, 217–229, doi:10.1016/S0303-2434(03)00003-5.

65. Horritt, M.S.S.; Bates, P.D.D. Evaluation of 1D and 2D Numerical Models for Predicting River Flood Inundation. *J. Hydrol.* **2002**, *268*, 87–99, doi:10.1016/S0022-1694(02)00121-X.

66. Timbe, L.; Willems, P. Desempeño de Modelos Hidráulicos 1D y 2D Para La Simulación de Inundaciones. *Maskana* **2011**, *2*, 91–98. (In Spanish)

67. Domeneghetti, A.; Castellarin, A.; Tarpanelli, A.; Moramarco, T. Investigating the Uncertainty of Satellite Altimetry Products for Hydrodynamic Modelling. *Hydrol. Process.* **2015**, *29*, 4908–4918, doi:10.1002/hyp.10507.

68. Ciervo, F.; Papa, M.N.; Medina, V.; Bateman, A. Simulation of Flash Floods in Ungauged Basins Using Post-Event Surveys and Numerical Modelling. *J. Flood Risk Manag.* **2015**, *8*, 343–355, doi:10.1111/jfr3.12103.

69. Mtamba, J.; van der Velde, R.; Ndomba, P.; Zoltán, V; Mtalo, F. Use of Radarsat-2 and Landsat TM Images for Spatial Parameterization of Manning's Roughness Coefficient in Hydraulic Modeling. *Remote Sens.* **2015**, *7*, 836–864, doi:10.3390/rs70100836.

70. Ponce, V.M. Kinematic Wave Controversy. *J. Hydraul. Eng.* **1991**, *117*, 511–525, doi:10.1061/(ASCE)0733-9429(1991)117:4(511).

71. Barati, R.; Rahimi, S.; Akbari, G.H. Analysis of Dynamic Wave Model for Flood Routing in Natural Rivers. *Water Sci. Eng.* **2012**, *5*, 243–258, doi:10.3882/j.issn.1674-2370.2012.03.001.

72. Liu, Z.; Merwade, V.; Jafarzadegan, K. Investigating the Role of Model Structure and Surface Roughness in Generating Flood Inundation Extents Using One- and Two-Dimensional Hydraulic Models. *J. Flood Risk Manag.* **2019**, *12*, e12347, doi:10.1111/jfr3.12347.

73. Neto, A.; Batista, L.; Coutinho, R. Methodologies for Generation of Hazard Indicator Maps and Flood Prone Areas: Municipality of Ipojuca/PE. *Rev. Bras. Recur. Hídricos* **2016**, *21*, 377–390, doi:10.21168/rbrh.v21n2.p377-390.

74. Courtel, F.; López, J.; Bello, M.; Noya, M. Mapas de Amenaza Por Inundaciones y Aludes Torrenciales En El Valle de Caracas. In Proceedings of the 32nd Congreso Latinoamericano De Hidráulica, Ciudad Guayana, Venezuela, 01−05 October 2006. (In Spanish)

75. Cançado, V.; Brasil, L.; Nascimento, N.; Guerra, A. Flood Risk Assessment in an Urban Area: Measuring Hazard and Vulnerability. In Proceedings of the 11th International Conference on Urban Drainage, Edinburgh, Scotland, UK, 31 August – 5 September 2008; Iwa Publishing: Edinburgh, Scotland, UK, 2008; pp. 1–10.

76. Da Silva, M.G.; De-Oliveira, A.; de Jesus Neves, R.J.; Nascimento, A.; Almeida, C.; Faccioli, G.G. Sensitivity Analysis and Calibration of Hydrological Modeling of the Watershed Northeast Brazil. *J. Environ. Prot.* **2015**, *6*, 837–850, doi:10.4236/jep.2015.68076.

77. van Liew, M.W.; Arnold, J.G.; Bosch, D.D. Problems and Potential of Autocalibrating a Hydrologic Model. *Trans. ASAE* **2005**, *48*, 1025–1040, doi:10.13031/2013.18514.

78. Bin, L.; Xu, K.; Xu, X.; Lian, J.; Ma, C. Development of a Landscape Indicator to Evaluate the Effect of Landscape Pattern on Surface Runoff in the Haihe River Basin. *J. Hydrol.* **2018**, *566*, 546–557, doi:10.1016/J.JHYDROL.2018.09.045.

79. Asano, Y.; Uchida, T. The Roles of Channels and Hillslopes in Rainfall/Run-off Lag Times during Intense Storms in a Steep Catchment. *Hydrol. Process.* **2018**, *32*, 713–728, doi:10.1002/hyp.11443.

80. Beven, K.; Binley, A. The Future of Distributed Models: Model Calibration and Uncertainty Prediction. *Hydrol. Process.* **1992**, *6*, 279–298, doi:10.1002/hyp.3360060305.

81. Johnson, F.; White, C.J.; van Dijk, A.; Ekstrom, M.; Evans, J.P.; Jakob, D.; Kiem, A.S.; Leonard, M.; Rouillard, A.; Westra, S. Natural Hazards in Australia: Floods. *Clim. Chang.* **2016**, *139*, 21–35, doi:10.1007/s10584-016-1689-y.

82. Iacob, O.; Brown, I.; Rowan, J. Natural Flood Management, Land Use and Climate Change Trade-Offs: The Case of Tarland Catchment, Scotland. *Hydrol. Sci. J.* **2017**, *62*, 1931–1948, doi:10.1080/02626667.2017.1366657.

83. Bathurst, J.C.; Iroumé, A.; Cisneros, F.; Fallas, J.; Iturraspe, R.; Novillo, M.G.; Urciuolo, A.; de Bièvre, B., Borges, V.G.; Coello, C.; et al. Forest Impact on Floods Due to Extreme Rainfall and Snowmelt in Four Latin American Environments 1: Field Data Analysis. *J. Hydrol.* **2011**, *400*, 281–291, doi:10.1016/J.JHYDROL.2010.11.044.

84. Dadson, S.J.; Hall, J.W.; Murgatroyd, A.; Acreman, M.; Bates, P.; Beven, K.; Heathwaite, L.; Holden, J.; Holman, I.P.; Lane, S.N.; et al. A Restatement of the Natural Science Evidence Concerning Catchment-Based 'Natural' Flood Management in the UK. *Proc. R. Soc. A Math. Phys. Eng. Sci.* **2017**, *473*, 20160706, doi:10.1098/rspa.2016.0706.

85. Hejl, H.; Kans, L. Roughness Coefficient for Flooded Urban Areas. *J. Res. U.S. Geol. Surv.* **1977**, *5*, 541–545.

86. Mosquera-Machado, S.; Ahmad, S. Flood Hazard Assessment of Atrato River in Colombia. *Water Resour. Manag.* **2007**, *21*, 591–609, doi:10.1007/s11269-006-9032-4.

87. Arcement, G.; Schneider, V. *Guide for Selecting Manning's Roughness Coefficients for Natural Channels and Flood Plains*; United States Geological Survey (USGS): Denver, CO, USA 1989

88. Xia, J.; Falconer, R.A.; Lin, B.; Tan, G. Numerical Assessment of Flood Hazard Risk to People and Vehicles in Flash Floods. *Environ. Model. Softw.* **2011**, *26*, 987–998, doi:10.1016/j.envsoft.2011.02.017.

89. Bocanegra, R.A.; Vallés-Morán, F.J.; Francés, F. Review and Analysis of Vehicle Stability Models during Floods and Proposal for Future Improvements. *J. Flood Risk Manag.* **2020**, *13.* Doi:10.1111/jfr3.12551.

90. Huizinga, J.; de Moel, H.; Szewczyk, W. *Glob. Flood Depth-Damage Functions: Methodology and the database with guidelines*; Publications Office of the European Union: Luxemburg, 2017; doi:10.2760/16510.

91. Servicio Nacional de Gestión de Riesgos y Emergencias (SNGRE). COE Cantonal Toma Resoluciones Ante emergencia en Tena. Boletín de Prensa. Available online: https://www.gestionderiesgos.gob.ec/coe-cantonal-toma-resoluciones-ante-emergencia-en-tena/ (accessed 25 August 2020). (In Spanish)

CHAPTER IV

IS FOREST LOCATION MORE IMPORTANT THAN FOREST FRAGMENTATION FOR FLOOD REGULATION?

This chapter is based on:

Hurtado-Pidal, J., Acero Triana, J. S., Aguayo, M., Link, O., Valencia, B., Espitia-Sarmiento, E., Conicelli, B. (2022). Is Forest location more important than forest fragmentation for flood regulation?. Ecological Engineering. https://doi.org/10.1016/j.ecoleng.2022.106764

Is Forest location more important than forest fragmentation for flood regulation?

Jorge Hurtado-Pidal[a], Juan S. Acero Triana[b], Mauricio Aguayo[a], Oscar Link[c], Bryan G. Valencia[d], Edgar Espitia-Sarmiento[d], Bruno Conicelli[d]

[a] Department of Territorial Planning and EULA-Center, Universidad de Concepción, Chile

[b] Department of Environmental Sciences, University of California Riverside, USA

[c] Department of Civil Engineering, Universidad de Concepción, Chile

[d] Department of Water and Earth Sciences, Universidad Regional Amazónica Ikiam, Ecuador

Abstract

Native forest deforestation has been identified as one of the main land cover changes affecting flood risk specially during small and moderate storm events. In this regard, forest protection and reforestation are considered a nature-based solution (NbS) for flood regulation. However, there is a lack of knowledge about the effects of different deforestation spatial patterns over floods. Effects of land cover changes on floods in a humid tropical basin within the Ecuadorian Amazon are assessed distinguishing forest location and forest fragmentation. The hydrological distributed model TETIS was applied to simulate the hydrological response of a basin to extreme storms having return periods of 1, 10 and 100 years, considering five land cover scenarios. The model was calibrated and validated using nine storm samples collected at a gauge station during the years 2018 and 2020. The simulated overland flow in hillslopes and stormflows within the river channel were analyzed to i) assess the statistical differences among all land use scenarios with the Kruskal-Wallis test; ii) assess the statistical differences among pairs of both location and fragmentation scenarios through the post-hoc evaluation Dunn test; iii) assess the statistical differences in relation to the baseline. Obtained results indicate that stormflow is less sensitive than overland flow to land cover changes. Forest location have more influence than forest fragmentation over both, overland flow and storm flows. Deforestation of the upper basin represents the worst scenario for flood regulation, thus protection of existing forest, as well as reforestation of deforested areas located in the upper watersheds is a priority for flood risk mitigation and forest

conservation. The results enhance our understanding of ecosystem services provided by tropical Andean foothills forests.

Keywords: TETIS, overland flow, stormflow, land cover change, tropical humid basin, Ecuador

1. Introduction

Between January 1975 and June 2002, freshwater floods, including flash floods, killed 176,864 people producing 2.27 billion losses worldwide (Jonkman, 2005; Merz et al., 2014; UNISDR, 2017). The synergy between land cover and climate change will likely increase, exacerbating flood risk (Chang and Franczyk, 2008; De Roo et al., 2003; Güneralp et al., 2015; Hirabayashi et al., 2013; IPCC, 2021; Yin et al., 2018). Native forest deforestation has been identified as one of the main land cover changes affecting flood risk (Gao and Yu, 2017). Consequently, there is a general concern in searching for land cover based solutions to approach flood risk management as land cover is a fundamental hydrological driver (Barbedo et al., 2014; Bin et al., 2018; Blöschl et al., 2007; Lane, 2017; Rogger et al., 2017).

Forest protection and reforestation are considered a nature-based solution (NbS) for flood regulation (Dadson et al., 2017; Ilieva et al., 2018; Seddon et al., 2020). NbS gained much attention in Tropical Andean regions as forests also provide ecosystem services, such as carbon storage, soil erosion control, and water regulation (Ataroff and Rada, 2000; Bonnesoeur et al., 2019; Tobón, 2021, 2008). For instance, the forest can intercept up to 30% of the rainfall (FAO-CIFOR, 2005), returning it into the atmosphere through evaporation. Therefore, soil moisture is reduced by forests through evapotranspiration or enhanced infiltration, especially in tropical regions. Forests can also delay the overland flow acting as a water flow obstacle that increases the terrain roughness (Iacob et al., 2017; Shuttleworth et al., 2019; Yang et al., 2016). Therefore, forest protection and reforestation are related to the buffering effect of forest over floods affecting the overland flow in hillslopes and the stormflows within the river channels (Dadson et al., 2017; Lane, 2017; Van Noordwijk et al., 2017). At the same time, implementing such NbS provides the possibility to increase or conserve areas covered with native forest and fight global biodiversity loss.

Experimental catchments and simulation modeling demonstrated the forest potential to reduce peak flows during small and moderate storm events (Bathurst et al., 2020; Salazar et al., 2012), which is consistent with the literature (Bathurst et al., 2011; Hamilton, 1987; Laurance, 2007). An essential attribute affecting flow

reduction is forest fragmentation and patch location (Kim and Park, 2016; Liu et al., 2020). Forest fragmentation is defined as the conversion of continuous forest into a mosaic of forest patches (Fahrig, 2003). Forest location is described as the arboreal vegetation within discrete categories of slopes and altitudes (Hou et al., 2018). Field experiments performed in humid tropical catchments in Puerto Rico suggest that fragmentation intensifies medium- and large-scale floods (Gao and Yu, 2017). Moreover, Boongaling et al. (2018) argued that forest fragmentation increases the overland flow while reducing the base flow. Also, a number of investigations (Descheemaeker et al., 2006; Hümann et al., 2011; Jourgholami et al., 2020; Zhang et al., 2014) have shown that the forest location in different slopes may affect the storm and peak flow at the basin outlet. For example, Iacob et al. (2017) have shown through model simulations that forest plantations in lowlands reduce peak flows during small and medium-size storms compared to large ones. According to Hou et al. (2018) forests located in the lower part of a basin can more efficiently mitigate floods than forests in the upper part of the basin.

However, there is a lack of scientific evidence to clarify the effects of deforestation on floods distinguishing forest fragmentation, location, and area reduction. To evaluate the effects of forest fragmentation and forest location on floods, in our study the percentage of the basin covered by forest remained constant, and forest fragmentation and location were varied among different simulation scenarios, which were constructed following two spatial patterns, namely: random forest fragmentation and forest location by slopes. A comparative analysis of floods obtained for the different deforestation scenarios is presented to establish the relative importance among different deforestation spatial patterns, allowing NbS to be optimized for flood management setting priorities for native forest protection and reforestation areas.

2. Materials and Methods

2.1. Study Area

The Tena River Basin (TRB) lies in the Napo province (Ecuador; Figure 4.1) in the Eastern Andes. It comprises a drainage area of approximately 240 km² at the Pano and Tena Rivers junction. The TRB is part of the Napo River Basin that is one of the main tributaries of the Amazon River. The terrain elevation across the TRB ranges from 500 to 2500 m.a.s.l. It has a mean slope of 40% and 9% in the upper and lower parts. Following the Köppen-Geiger climate classification, the basin has a tropical rainforest climate (Af; Kottek et al., 2006) with a mean annual temperature

of 23°C. The annual precipitation ranges from 2400 to 5300 mm (Ikiam-University, 2021), describing a bimodal regime that peaks between June and November.

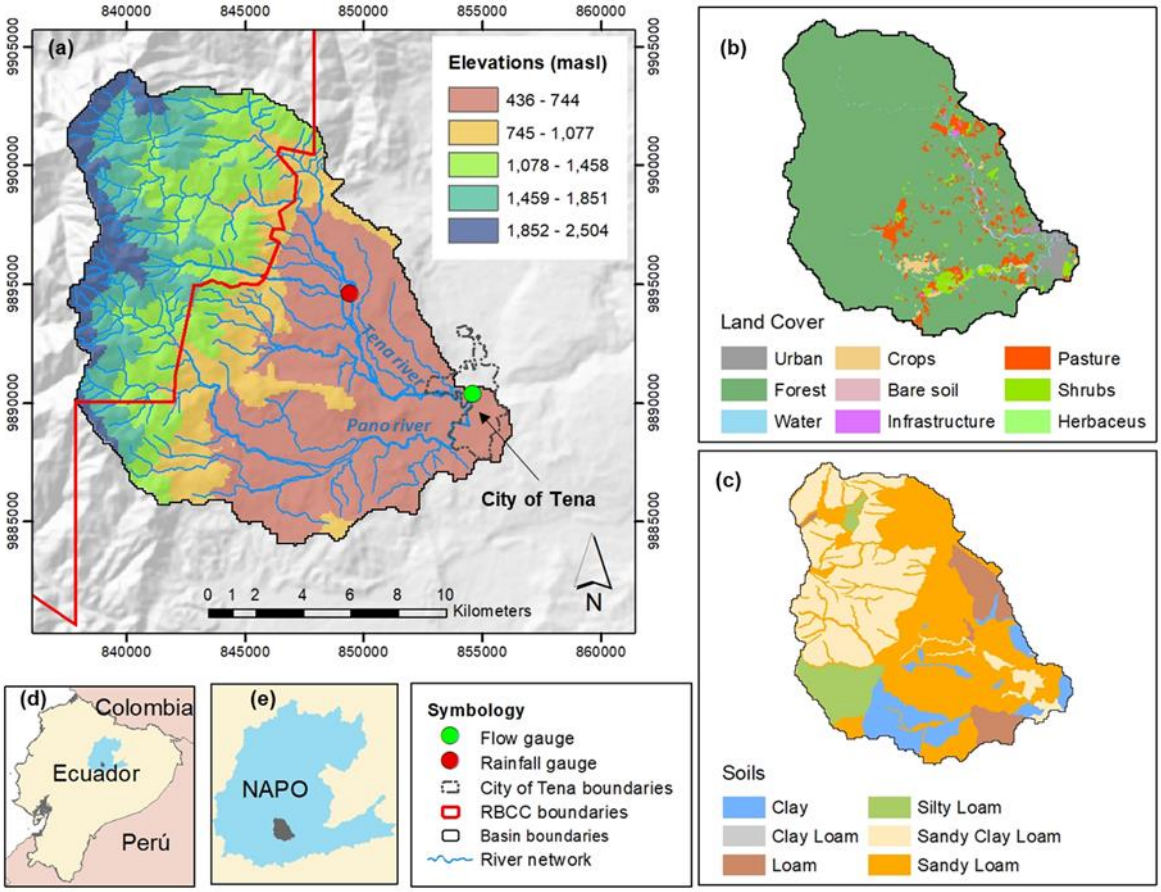

Figure 4.1. Main features of the TRB. (a) Terrain elevation and monitoring network; (b) land cover 2016 (scenario baseline) and; (c) soil textures; Location of the TRB in (d) Ecuador and I Napo province. RBCC in the symbology (red polygon) are the acronym in Spanish of Colonso-Chalupas Biological Reserve.

The geology of the upper basin is composed of Paleozoic-Mesozoic granites. The lower basin contains sandstones and limestones from the Cretaceous and Paleogene periods. Fluvial deposits from the Quaternary period are also common in the lower basin (MAGAP-SIGTIERRAS, 2016). The soils are primarily *Andisols*, with sandy clays and sandy loams across the basin (Figure 4.1c). Soils extend to a maximum depth of 1.5 m, with high organic content (~6%) within the first 0.5 m (MAGAP-SIGTIERRAS, 2016). Due to this feature, soils in the TRB have a high water retention capacity and reduced infiltration rates (Moreno et al., 2018). Native forest (87%) covers most of the basin, followed by grassland, scrubland, and herbaceous vegetation (7%). Urban areas represent 3% of the basin and agricultural

lands 1% (Figure 4.1b). Corn, cacao, and cassava are cultivated in the lower part of the basin, close to urban areas.

The upper basin is part of the Colonso-Chalupas Biological Reserve (RBCC) that retains primary forests (Cuenca et al., 2018). The city of Tena (Figure 4.1c), located in the lower part of the watershed, has more than 23000 inhabitants living in flood-prone areas (INEC, 2010). High-intensity precipitation events, moist soils, and steep relief in the upper basin increase the risk of flash flooding (Hurtado-Pidal et al., 2020; Jodar-Abellan et al., 2019).

2.2. Hydro-meteorological records

Despite meteorological and hydrological records (i.e., rainfall gauge and flow gauge, depict in Figure 4.1c) started in 2015 and 2018 respectively, we used rainfall and flow records from July 2018 to July 2020 because data loss was minor during these years (0.001% for rainfall and 8% for flow). The rainfall and streamflow data are available at 1-minute intervals (Hurtado-Pidal et al., 2020; Ikiam-University, 2021; Sommer-gmbh, 2014). However, these data series were resampled to 10-minute intervals to optimize the modeling framework.

High-flow events were identified using a flow threshold of 342.5 m^3/s that was defined following Reynolds et al. (2019) and the top 75% of maximum monthly flows. All the analyses were conducted in R environment (R-Development-Core-Team, 2020). As a result, nine events were identified (Table 4.1) having a minimum and maximum peak flow of 347 (E2) and 751 (E5) m^3/s, respectively, and a duration range between one and two days. Although the events are spread along the year, July is the month with more events (3 events) than the other months.

Because evapotranspiration is negligible during short flash floods, it was excluded as a variable (Adamovic et al., 2016; Segura-Beltrán et al., 2016).

Table 4.1. Main characteristics of observed and simulated storm events. Note that differences correspond a statistical metrics presented by Nikolopoulos et al. (2011), were positive values denote overestimation of the model.

Event	Start	Duration	Observed			Simulated			Differences		
			Time at peak	Peak flow	Stormflow volume	Time at peak	Peak flow	Stormflow volume	Time at peak	Peak flow	Stormflow volume
	(date, time)	(hours)	(time)	(m^3/s)	(Hm^3)	(time)	(m^3/s)	(Hm^3)	(min)	(%)	(%)
E1	21 Jul 2018, 12:00	48	09:30	689.04	23.66	09:40	600.31	20.40	10	-12.88	-13.78
E2	03 Sep 2018, 12:00	30	02:10	346.92	5.94	02:30	362.35	5.94	20	4.45	0.00
E3	10 Mar 2019, 06:10	24	18:00	387.08	5.92	17:50	370.69	5.71	-10	-4.23	-3.55
E4	13 May 2019, 00:00	48	04:50	417.23	11.29	04:40	393.29	11.05	-10	-5.74	-2.13
E5	18 Jul 2019, 15:00	30	03:10	751.75	12.93	03:00	839.09	9.50	-10	11.62	-26.53
E6	27 Jul 2019, 06:00	24	22:00	494.22	7.89	22:40	244.70	3.73	40	-50.49	-52.72
E7	04 Aug 2019, 00:00	30	12:30	437.17	10.68	13:30	483.57	11.08	60	10.61	3.75
E8	14 Nov 2019, 16:00	24	05:50	628.97	10.42	06:00	939.35	14.13	10	49.35	35.60
E9	18 Jun 2020, 17:00	30	00:30	484.57	17.94	00:20	546.92	14.69	-10	12.87	-18.12

2.3. Hydrologic modeling

The flood simulations were carried out using the conceptual and spatially-distributed hydrological model with physically based parameters TETIS (Francés et al., 2007). TETIS has been previously applied for simulation of humid and mountain environments with similar conditions to the study area (Siswanto and Francés, 2019), including study cases located in the Colombian Andes (Peña et al., 2016). Moreover, TETIS has been successfully applied for flood studies by several authors (Beneyto et al., 2020; McGrane et al., 2017; Segura-Beltrán et al., 2016; Velásquez et al., 2020). The simulations included five deforestation scenarios following the parameterization of TETIS model, for hillslopes and river channel, recommended by Francés et al. (2007), Vélez et al. (2009), Barrientos et al. (2020) and Buendía et al. (2016). Raster maps of overland flow and the stormflow hydrograph at the basin outlet corresponding to the instant with maximum rainfall intensity were obtained and compared for the different simulation scenarios.

Land cover and soil properties (Figure 4.1b, 1c) were derived from vector maps at spatial scale 1:25000, obtained free from SIGTIERRAS project (STP) of Ecuadorian Government (MAGAP-SIGTIERRAS, 2016). Lithology vector map at spatial scale 1:250000, was obtained from the Geological Institute of Ecuador

(INIGEMM). Catchment morphometric parameters, were derived from Digital Elevation Model (DEM). Specifically, we used the 90 m version of the SRTM (Shuttle Radar Topographic Mission) that has a minimum vertical accuracy of 16 m and absolute error (90% confidence) of 9.73 m worldwide (Mukul et al., 2017). Despite its original resolution (90 m), the DEM was resampled to 100 m, and all model parameters in TRB were estimated using a 100 x 100 m mesh, achieving a good compromise between spatial resolution and computation time.

Parameters maps such as slope, flow direction, flow accumulation and overland flow velocity required by TETIS were obtained from DEM. The overland flow velocity was calculated using the kinematic wave approximation for hillslopes proposed by Francés et al. (2007).

Soil properties such as texture class, organic matter content, soil deep and salinity, contained into the corresponding vector map database (i.e. shapefile) were used to estimate soil parameter maps. The static storage parameter map, was obtained by the sum of the available water content of soil and superficial storage of roughness topography and pounds. In turn, available water content was calculated by the difference between field capacity and the wilting point. Both of these parameters were calculated as a function of soil texture class, organic matter, salinity, and gravel content, following the pedo-transfer functions by Saxton and Rawls (2006). Available water content was multiplied by the minimum between soil and root depth. The superficial storage, was calculated from land cover and slope maps following Francés et al. (2007) and Vélez et al. (2009). Infiltration capacity and percolation capacity were obtained from shallow (0-20 cm) and deep (20-50 cm) soil properties respectively, following the pedo-transfer functions of Saxton and Rawls (2006). Also, considering the hydrologic expertise and available data, the interflow and base flow velocities were estimated from infiltration and percolation values respectively. Regarding groundwater outflow this parameter was estimated based on literature values according to lithological characteristics of geological formations in the catchment, taking into account the degree of fracturing and macro porosity (Puricelli, 2008). In addition, land cover types (Figure 4.1b), were used to estimate the canopy interception capacity using reference values for similar vegetation types published by Herwitz (1985), Fleischbein et al. (2006) and Gomez-Peralta et al. (2008).

The parameters to implement the geomorphological kinematic wave method, for flow propagation in stream network, were those recommended by Leopold and Maddock (1953), Francés et al. (2007), and Vélez et al. (2009). The model was run at the event scale using a split storm sampling following Hurtado-Pidal et al. (2020).

2.4. Hydrologic model calibration and validation

Calibration and validation of the model was made through the comparison between observed and simulated stormflows at the mouth basin (flow gauge location, Figure 4.1a). The model was calibrated for event E1 and validated for events E2-E9 using the baseline land cover scenario (Land cover 2016).

The efficiency index, NSE (Nash and Sutcliffe, 1970) and the Percent Bias (PBIAS) were used to evaluate the model´s performance, following the guidelines by Moriasi et al. (2007). Additionally, deviations in time at peak (min), peak flow (%) and stormflow volume (%) were computed following Nikolopoulos et al. (2011).
Calibration started by adjusting manually the correction factors (CFs) in order to find acceptable values based on NSE and PBIAS evaluation. After the first approximation of CFs values, the calibration was performed automatically using the SCE-UA (Shuffled Complex Evolution—University of Arizona) optimization algorithm (Duan et al., 1994) with the NSE index as objective function. Finally, the CFs values obtained during the calibration process (Table 4.2), were used for both, model validation and scenarios evaluation.

Table 4.2. Correction factors, limits for possible values, and final values obtained with SCE-UA algorithm in TETIS for TRB.

Correction factor	Lower Limit	Upper Limit	Initial Value	Final Value
Soil static storage	0.1	1	0.5	0.102
Evapotranspiration	-	-	-	1
Infiltration capacity	0	0.6	0.3	0.4
Overland flow velocity	-	-	-	0.1
Percolation capacity	0	1	0.1	0.001
Interflow velocity	0	1000	500	296.504
Groundwater outflow capacity	-	-	-	0.01
Base flow velocity	0	1000	500	854.192
Channel flow velocity	0	1	0.5	0.468

Note that overland flow velocity and groundwater outflow capacity were not calibrated because those parameters were uninfluential according to preliminary results obtained during the sensitivity analysis.

2.5. Hydrologic model performance

Figure 4.2 and Table 4.1 show model performance in the calibration and validation events.

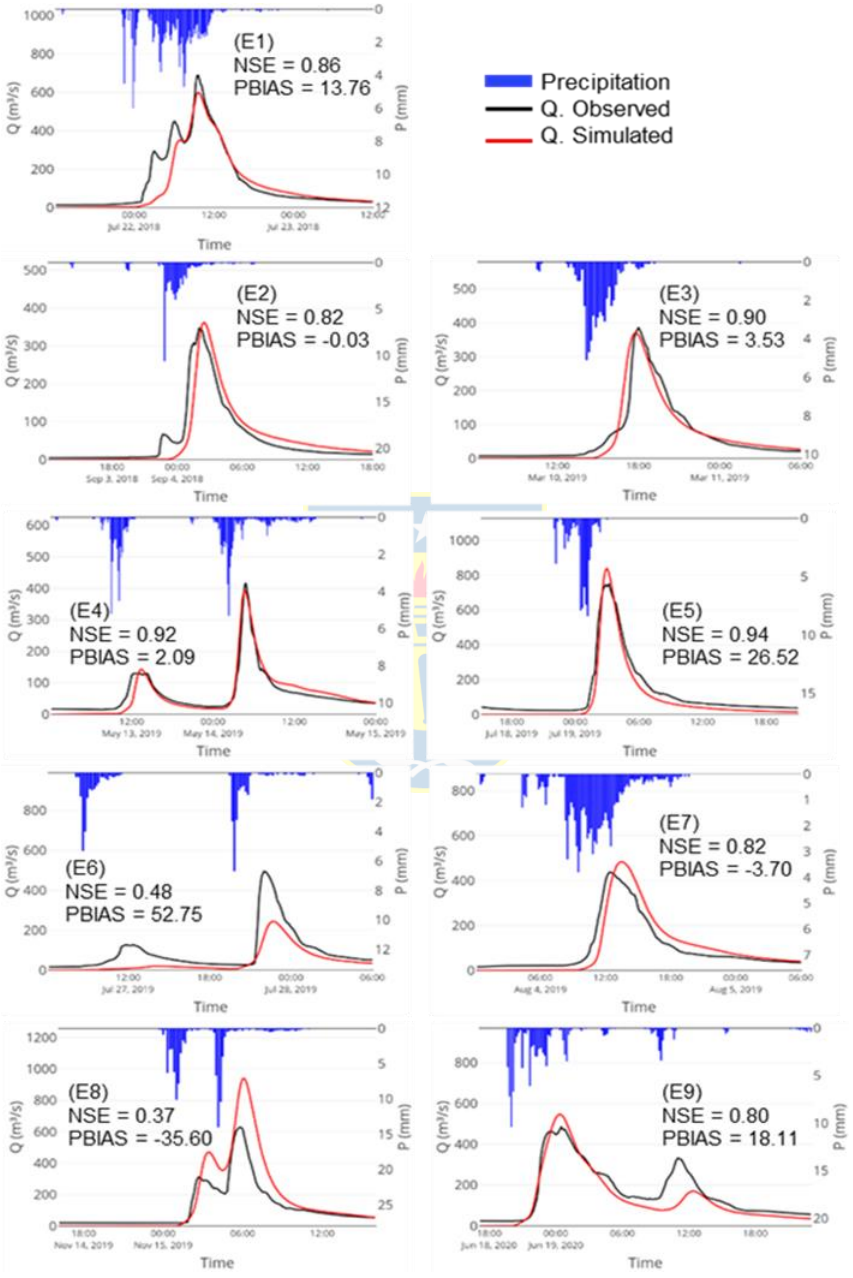

Figure 4.2. Stormflow hydrographs. Observed (black solid lines) and simulated (red solid lines) stormflow against precipitation (blue bars) for the calibration (E1) and validation (E1-9) events.

For the calibration event (E1, Figure 4.2) the model obtained a NSE of 0.86 and PBIAS of 13.76 % indicating a good fit between observations and simulations of stormflow. For the validation events, in six (E2-5, E7, E9) of the eight events, the model has a satisfactory performance (0.80≤NSE≤0.94; -3.70≤PBIAS≤26.52; Fig 2). The events E6 and E8 had the lower performance (NSE<0.5; -35.60≤PBIAS≤52.75; Fig 2).

In addition, considering both calibration and validation events, the mean absolute differences (deviations) in time at peak (min), peak flow (%) and stormflow volume (%) were 20, 18.02 and 17.35 respectively (Table 4.1). In the case of time to peak, 20 minutes can be considered a very good fit, since our simulations have a 10-minute time step. Together these results suggest that, despite data scarcity in the region, the hydrological model has an acceptable confidence level, in order to make simulations to evaluate scenarios proposed in this study.

Regarding to static storage in the soil, the effective parameter was calibrated using a CF of 0.1 (10% of the fist estimation) (Table 4.2). The average value of the effective static storage in the soil within the basin was only 10 mm. Therefore, the soil was highly saturated during the storms. Finally, according to the simulations of the stormflows, approximately 39 % correspond to overland flow, 60% correspond to interflow and base flow was virtually absent (< 1%).

2.6. Design storms

Design storms were used to evaluate the influence of different deforestation patterns on floods. Storms having return periods of 1 (Rp1), 10 (Rp10) and 100 (Rp100) years were obtained from the equations proposed by the National Hydrometeorological Institute (INAMHI, 2019), and the non-symmetric altering blocks method (Chow et al., 1988). The maximum rainfall intensity for Rp1, Rp10 and Rp100 was 14, 22 and 35 mm/10 min respectively.

2.7. Deforestation scenarios

The impact of deforestation was investigated distinguishing the effects of forest fragmentation through random scenarios S1 and S2, and of forest location through slope scenarios S3 and S4. In all scenarios the forest cover was 50% of the basin area. The observed situation in year 2016 was considered as the baseline case. Thus, a total of 5 land cover scenarios was considered: baseline, random scenario 1 (S1), random scenario 2 (S2), slope scenario 1 (S3) and slope scenario 2 (S4). The baseline scenario was used as a reference to quantify the effects of land cover

changes on floods. The model parameters changing among the scenarios are: canopy interception capacity and soil static storage, shown in Table 4.3. Note that in general the soil static storage has higher variations in comparison with canopy interception, especially among scenarios 3 and 4.

Table 4.3. Mean values of canopy interception and soil static storage in the basin for baseline and scenarios.

	Baseline	Scenario 1	Scenario 2	Scenario 3	Scenario 4
Canopy Interception (mm)	9.12	5.46	5.46	5.56	5.44
Soil Static Storage (mm)	100.94	81.72	81.98	83.51	80.56

The R environment (R-Development-Core-Team, 2020) was employed to built-up, both, fragmentation (random) and location (slope) scenarios. Specifically, the function 'randomHabitat' contained in the 'secr-package' (Efford, 2021) was used for fragmentation scenarios S1 and S2. The function has three parameters, namely: 'p', 'A' and 'minpatch', to control the degree of forest fragmentation, the proportion of basin area to be fragmented and the minimum size of patches (in pixels), respectively. In order to generate scenarios with different degree of fragmentation (p), but maintaining 50% of forest cover (A) and using a minimum patch size of 1 ha (minimum patch size of forest cover in the baseline map). The values of the parameters 'p', 'A' and 'minpatch' for scenario S1, were 0.1, 0.5 and 1 respectively, and the values for scenario S2, were 0.5, 0.5 and 1, respectively. Note that the only parameter changed was 'p', the degree of forest fragmentation (S1 with higher fragmentation than S2). Location scenarios S3 and S4, were defined using the 'While' loop function in R environment to find the slope threshold that correspond to the half basin area, obtaining a slope of 21.3%.

The degree of fragmentation of each scenario was determined with the landscape metric called 'contagion index' (%) (McGarigal, 2014) which is very common to evaluate the forest fragmentation (Boongaling et al., 2018; Riitters, 2018; Turner, 1989). Higher values of contagion index indicate a less fragmented landscape. In this regard, we use the functions within the 'landscapemetrics-package' (Hesselbarth et al., 2019) for R environment. Obtained values were 72.7, 5.12, 23.3, 29.4, 29.4 for baseline and S1-S4, respectively, confirming that S1 is more fragmented than S2, and that S3 and S4 have the same fragmentation level, while the baseline scenario is the less fragmented scenario. Figure 4.3 shows the fragmentation scenarios (3d, 3e) but also the location scenarios (3f, 3g).

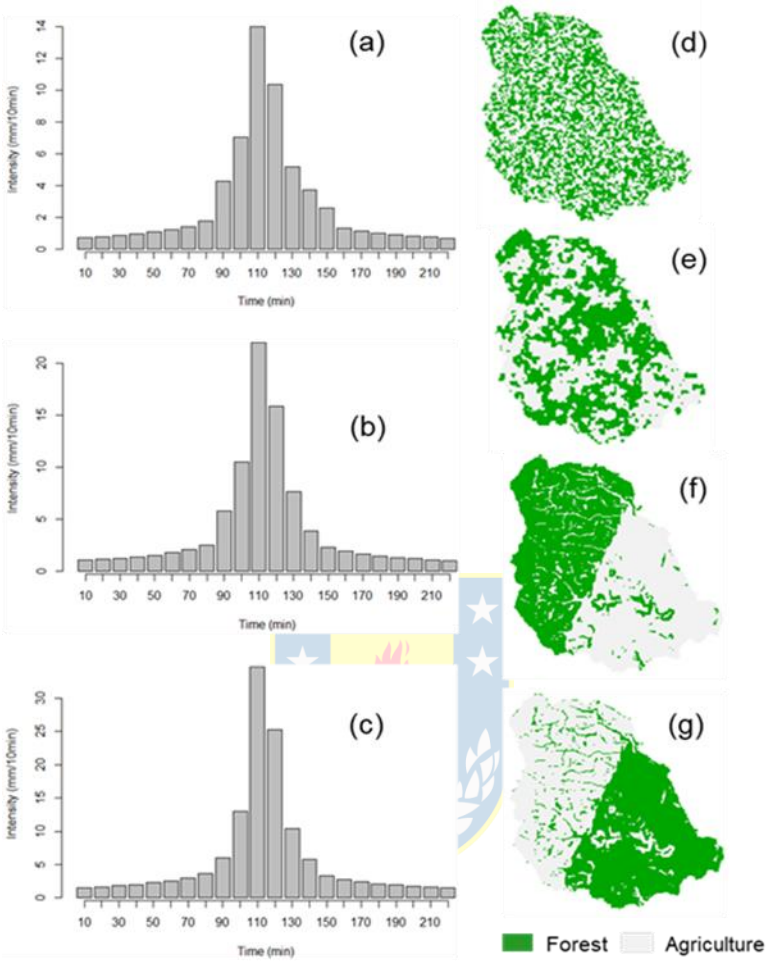

Figure 4.3. Rainfall and land cover scenarios. Left side: Design storms for three different return periods: 1 year (a), 10 years (b) and 100 years (c). Right side: Scenarios of deforestation with different spatial patterns: fragmentation (random deforestation) (d, e) and location (slope deforestation) (f, g). The Graphical Abstract of this paper also shows the scenarios of deforestation used.

2.8. Scenarios Analysis

The three design storms (Rp1, Rp10, Rp100) were combined with the land cover scenarios (baseline, S1-S4) to simulate both, the stormflow and the overland flow. Simulation results were analyzed to investigate the effects of forest location and forest fragmentation on floods, following three approximations described in the following sections.

Evaluation of inter-scenario differences, first approximation: for the three return periods, the absolute differences among all scenarios, regarding time to peak (min), peak flow (m^3/s) and overland flow volume (hm^3) were analyzed. Also the differences of stormflows and overland flow, among all scenarios (baseline, S1–S4), were evaluated statistically using the non-parametrical Kruskal-Wallis test (Kruskal and Wallis, 1952). Kruskal-Wallis test is the non-parametric alternative to the one-way analysis of variance (one-way ANOVA). Therefore, prior to its application the non-normality of the data (stormflow and overland flow) was verified using the Shapiro test (Shapiro and Wilk, 1965). Also, in Kruskal-Wallis test the null hypothesis was evaluated with a certain confidence level ($\alpha=0.05$). Hence, a p-value < 0.05 can be considered significant difference among scenarios. Note that this test has been applied in hydrological studies to evaluate the effects of land cover changes over floods (Jodar-Abellan et al., 2019; Singh et al., 2005). Additional details about this statistical test and its implementation can be found in (MacFarland and Yates, 2016).

Comparison of random and slope scenarios, second approximation: the absolute differences of peak flow, and overland flow, among pairs of random (S1–S2) and slope (S3–S4) scenarios were evaluated. Also, a statistical analysis among pairs was performed in order to discover significant differences. Therefore, after the Kruskal-Wallis test a post-hoc analysis was performed with Dunn test (Dunn, 1964). Similarly, to Jodar-Abellan et al. (2019), a 'BH' method was used to adjust the p-values. In addition, a Pearson's correlation test ($\alpha=0.05$) was performed in order to complement the comparisons among pairs. All statistical tests were achieved with R environment.

Comparison in relation to baseline, third approximation: Regarding to baseline a simple differences and relative differences both in peak flow and overland flow volume were evaluated for each scenario of deforestation and for the three return periods. In addition, the results from Dunn test were analyzed to discover significant differences in peak flow and overland flow volume among pairs respect to baseline. Finally, a spatial visualization of overland flow differences was obtained from subtraction of raster maps (Figure 4.7 in Results section). Note that raster maps of overland flow (mm), correspond to the instant of maximum rainfall intensity. Overland flow volume (Hm^3) was obtained by the sum of all pixels within the raster map.

3. Results

3.1. Inter-scenario differences

Figure 4.4 and Table 4.4 presents an overview of stormflow and overland flow for all scenarios. The time to peak was similar for all scenarios. For a given return period, differences in land cover have a negligible effect on the time to peak. The time to peak slightly decreased as the return period increases. Scenario S4 (deforestation in the upper basin) presented the maximum values of both peak flow and overland flow volume, for all return periods. From Figure 4.4, it can be seen that stormflow presents less differences than overland flow among scenarios. Differences in stormflow among the land use scenarios were not statistically significant (p-value > 0.05) for all return periods. However, in case of overland flow, differences among land cover scenarios were statistically significant (p-value < 0.0001) for all return periods. Overall, the results suggest that stormflow is less sensitive than overland flow to land cover changes.

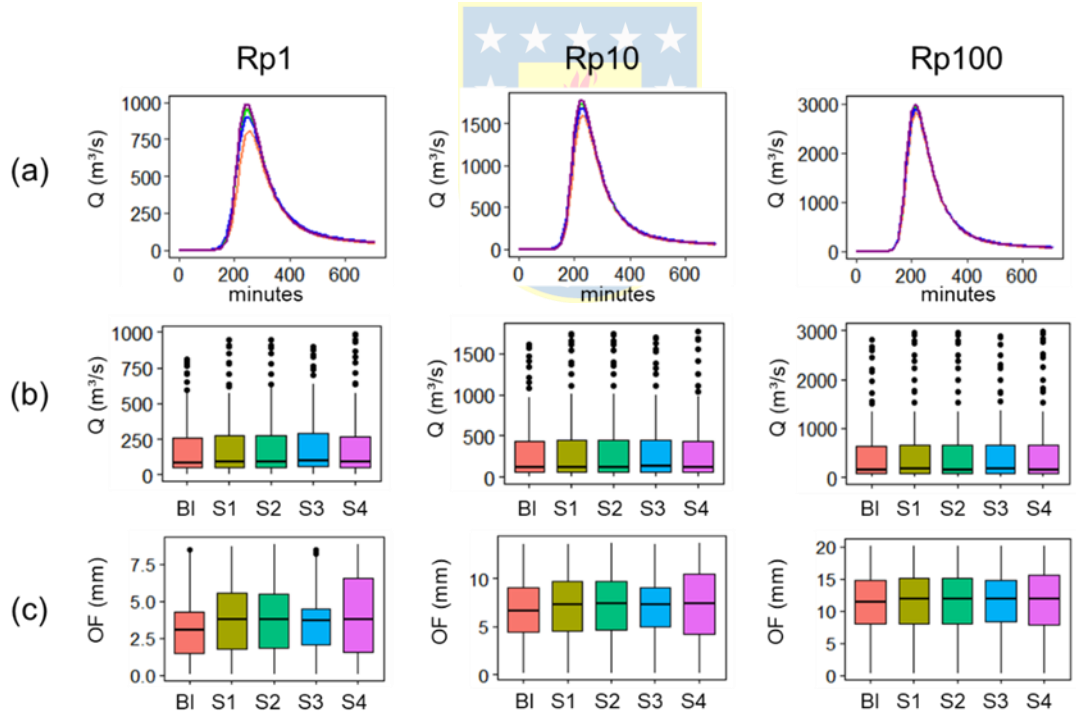

Figure 4.4. Hydrographs and Boxplots of five scenarios for three return periods (Rp1, Rp10, Rp100). (a) Hydrographs. Boxplots of (b) stormflow (Q) and (c) overland flow (OF).

Table 4.4. Time to peak, peak flow and overland flow volume of five scenarios for three return periods. Additionally, the p-Values of Kruskal-Wallis test, for storm flow and overland flow are presented.

	1-year return period			10-years return period			100-years return period		
	Time to peak	Peak flow	Overland flow volume	Time to peak	Peak flow	Overland flow volume	Time to peak	Peak flow	Overland flow volume
	(min)	(m^3/s)	(Hm^3)	(min)	(m^3/s)	(Hm^3)	(min)	(m^3/s)	(Hm^3)
Baseline	250	809.40	0.699	230	1604.17	1.553	210	2807.46	2.618
Scenario1	240	947.91	0.875	230	1734.99	1.667	210	2953.29	2.679
Scenario 2	250	946.17	0.878	230	1734.27	1.669	210	2952.63	2.682
Scenario 3	250	901.91	0.801	230	1692.43	1.628	210	2897.57	2.653
Scenario 4	240	991.59	0.944	220	1775.12	1.703	210	2998.72	2.702
p-value (stormflow)		0.986			0.996			0.997	
p-value (overland flow)		<0.0001			<0.0001			<0.0001	

In summary, the stormflow is less sensitive than overland flow regarding both forest location and forest fragmentation. Also, forest fragmentation scenarios S1 and S2 are more similar in comparison to forest location scenarios S3 and S4. Additionally, scenario S3 representing forest in upper basin is the most similar scenario respect to baseline. Consequently, S3 generates less peak flow and overland flow volume. Conversely, scenario S4 (forest in lower basin) is the most different scenario respect to baseline. Consequently, it generates more peak flow and overland flow volume. Overall, results suggest that floods are more affected by forest location than by forest fragmentation. However, the differences between effects caused by the different scenarios vanish as the return period of the design storm increases.

3.2. Differences between fragmentation (random) and location (slope) scenarios

Table 4.5a shows a comparison between fragmentation scenarios (S1, S2) and location scenarios (S3, S4). The mean value of absolute differences between fragmentation scenarios was 1 m^3/s and 0.003 Hm^3 for peak flow and overland flow volume, respectively. Also the mean value of absolute differences between location scenarios (S3, S4), was 91 m^3/s and 0.089 hm^3 for peak flow and overland flow volume, respectively. The absolute differences among return periods for these variables was relatively small or practically non-existent.

Table 4.5. (a) Differences between scenarios and respect to baseline both peak flow (m^3/s) and overland flow (hm^3) for three return periods. (b) Post-hoc Dunn test of stormflow and overland flow for the three return periods.

(a)	1-year return period		10-year return period		100-year return period	
	Peak flow difference (m^3/s)	Overland flow volume difference (Hm^3)	Peak flow difference (m^3/s)	Overland flow volume difference (Hm^3)	Peak flow difference (m^3/s)	Overland flow volume difference (Hm^3)
Scenario 1 – Scenario 2	1.75	0.003	0.71	0.002	0.66	0.003
Scenario 3 – Scenario 4	89.68	0.143	82.69	0.075	101.15	0.049
Baseline – Scenario 1	138.51	0.176	130.82	0.115	145.84	0.061
Baseline – Scenario 2	136.76	0.179	130.10	0.116	145.17	0.064
Baseline – Scenario 3	92.50	0.101	88.26	0.075	90.11	0.035
Baseline – Scenario 4	182.18	0.244	170.95	0.150	191.26	0.084

(b)	1-year return period		10-year return period		100-year return period	
	Stormflow p-value	Overland flow p-value	Stormflow p-value	Overland flow p-value	Stormflow p-value	Overland flow p-value
Scenario 1 – Scenario 2	0.958	0.480	0.972	0.810	0.975	0.728
Scenario 3 – Scenario 4	0.669	<0.0001	0.736	<0.0001	0.757	<0.0001
Baseline – Scenario 1	0.713	<0.0001	0.804	<0.0001	0.824	<0.0001
Baseline – Scenario 2	0.753	<0.0001	0.831	<0.0001	0.848	<0.0001
Baseline – Scenario 3	0.593	<0.0001	0.711	<0.0001	0.749	<0.0001
Baseline – Scenario 4	0.915	<0.0001	0.974	<0.0001	0.992	<0.0001

Table 4.5b show the results for the Dunn test. The p-values indicate that fragmentation scenarios (S1, S2) are not statistically different in both stormflow ($0.958 \leq$ p-value ≤ 0.975) and overland flow ($0.480 \leq$ p-value ≤ 0.810). Moreover, in relation to stormflow, location scenarios (S3, S4) are not different each other either ($0.669 \leq$ p-value ≤ 0.757). However, in terms of overland flow, location scenarios are statistically different (p-value < 0.0001). Note that p-values of stormflow for fragmentation scenarios are slightly higher than p-values of location scenarios, suggesting a bit more similarity among fragmentation scenarios. Pearson's correlation coefficient I of overland flow confirms the aforementioned result. Fragmentation scenarios show higher R than location scenarios, especially for Rp1 (Figure 4.5). Nevertheless, as the return period increased differences decreases, with R being the same (= 0.99) for Rp100.

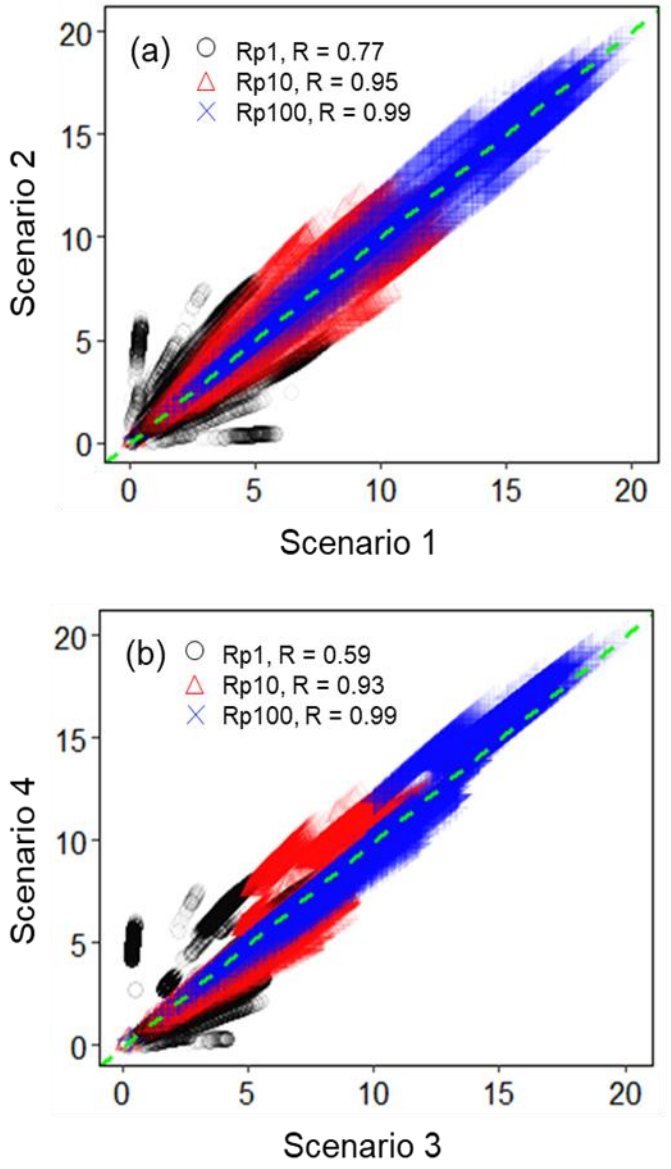

Figure 4.5. Scatterplots of overland flow (mm) simulated with TETIS at the moment of maximum rainfall intensity. (a) Fragmentation scenarios (S1, S2). (b) Location scenarios (S3, S4). The Pearson's correlation coefficient I with p-Value < 0.05 are presented for three return periods, 1-year (Rp1), 10-year (Rp10) and 100-year (Rp100). Black circles correspond to Rp1, red triangles to Rp10 and the blue crosses to Rp100. Green dashed line represents 1:1 line (slope =1).

In summary, these results show that, the pair of fragmentation scenarios are more similar to each other, respect to location scenarios. Therefore, slope deforestation (S3, S4) within the basin can cause higher effects on stormflow and

overland flow than random deforestation (S1, S2). However, in all cases, the difference between scenarios decrease as the return period increases.

3.3. Comparison of forest location and forest fragmentation scenarios with baseline

Table 4.5a and Figure 4.6 show differences between overland flow and storm flow for scenarios with respect to the baseline. Results indicate that scenario S3 is the most similar and conversely scenario S4 is most different to the baseline. Also fragmentation scenarios (S1, S2) are very similar, with intermediate values of peak flow and overland flow volume, between location scenarios (S3, S4). Likewise, both the peak flow and the overland flow volume, show a tendency to converge to a constant value as the return period increases.

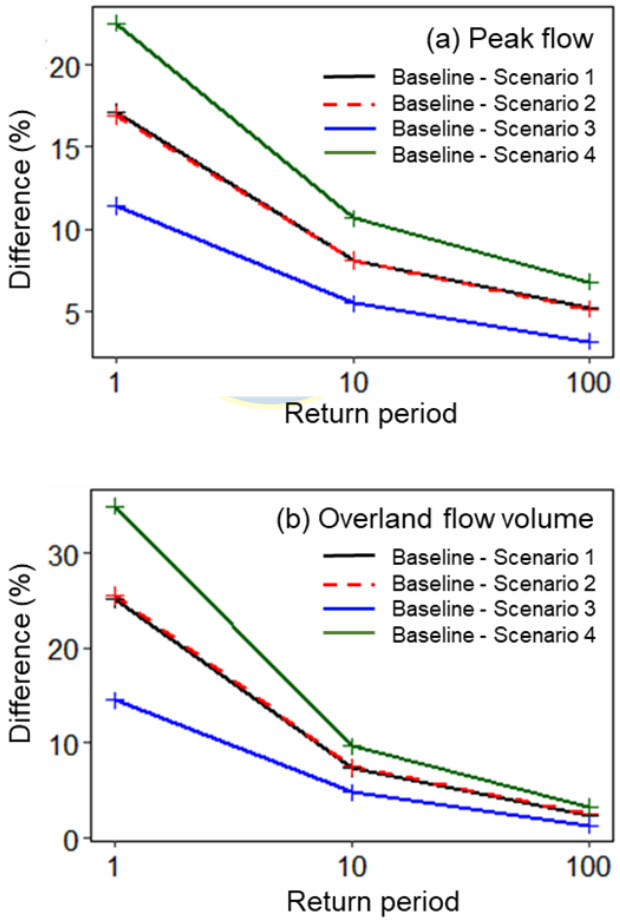

Figure 4.6. Percentage differences in (a) peak flow and (b) overland flow volume, between baseline and scenarios for the three return periods.

However, for 100-year return period, the relative difference of overland flow volume (around 2%) are less than relative difference of peak flow (around 5%), suggesting again that stormflow is less sensitive than overland flow to forest cover spatial pattern.

The post-hoc analysis with Dunn test show that differences in stormflow are not statistically significant among scenarios (p-value > 0.05) (Table 4.5b). However, in the case of overland flow, the differences are statistically significant (p-value < 0.0001) in all cases. Also, slight changes in the p-value for both stormflow and overland flow, confirms that scenario S3 is the most similar and conversely scenario S4 is most different to the baseline. Finally, the post-hoc analysis of stormflow confirms the similarity among fragmentation scenarios (S1, S2) with similar p-values. The p-values increased slightly as the return period increases, indicating that the difference between scenarios and the baseline decreases.

Figure 4.7 shows the overland flow difference among scenarios and baseline. The maximum and minimum differences are close to 4 and -6 mm respectively. According to our model setup, these differences are conditioned mainly by infiltration capacity, soil static storage, canopy interception and superficial storage. However, despite the dispersed deforestation in scenarios S1 and S2, the upper part of the TRB generated more overland flow than the lower part of the TRB, which can be explained by the greater infiltration capacity in this area. Also the values close to 0 (green color) prevalence as the storm intensity (or return period) increases.

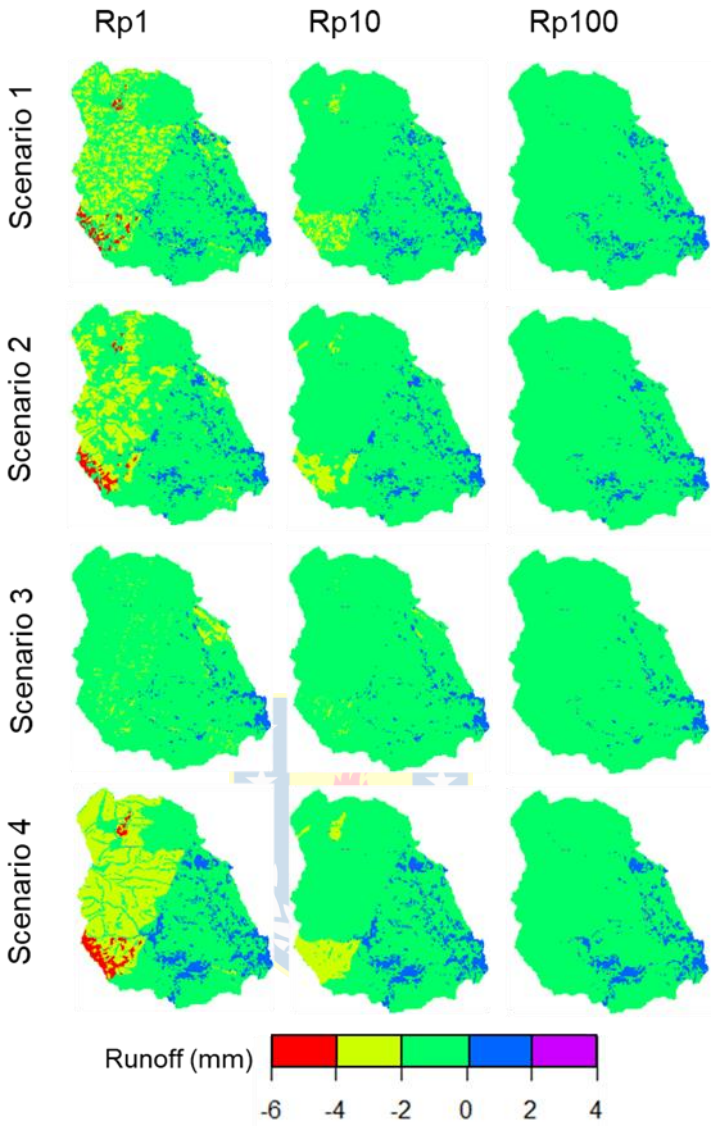

Figure 4.7. Overland flow difference between baseline and land cover scenarios, at the moment of maximum rainfall intensity for three return periods. Negative values (red, yellow and green) correspond to the situation where the scenarios generate more overland flow than baseline and conversely for positive values (blue and violet).

In summary, the storm flow was less sensitive than overland flow regarding forest spatial pattern. Also, fragmentation scenarios (S1, S2) were more similar in comparison to location scenarios (S3, S4). Additionally, the scenario S3 (forest in upper basin) was the most similar scenario respect to baseline. Consequently, it generates smaller peak flows and overland flow volume. Conversely, scenario S4 (forest in lower basin) is the most different respect to baseline. Consequently, it generates more peak flow and overland flow volume. Overall these results indicate

that, aggregated deforestation in steep slopes (S4), has the major implications for floods, rather than random or spread fragmentation within the basin. Differences between scenarios vanish as the storm return period increased.

4. Discussion

4.1. Hydrological Model Performance

Performance metrics NSE and PBIAS, as well as deviations, suggest that the hydrological model achieved a satisfactory level of confidence. VanLiew et al. (2005) establish that daily (or smaller time step) simulation, with NSE as low as 0.4 is acceptable. Also, Hurtado-Pidal et al. (2020) found similar NSE and PBIAS values during the calibration and validation process in the TRB using a 1-minute time step. Therefore, we consider that E6 and E8 had also an acceptable performance. In addition, the deviations in time to peak, peak flow and stormflow volume, obtained in our study, have been observed in other flash flood studies (Nikolopoulos et al., 2011; Segura-Beltrán et al., 2016).

The low effective static storage in the soil (10 mm), during the hydrological model calibration, indicates a high level of saturation. This condition was reported in previous studies in the basin (Chancay and Espitia-Sarmiento, 2021; Hurtado-Pidal et al., 2020). Specifically, Hurtado-Pidal et al. (2020) reported high values of Curve Number (CN), of 84 and 81 for Pano and Tena River Basins respectively. Finally, our study found a higher contribution of interflow (60%) respect to overland flow (39 %) during storms. The predominance of interflow during storms were stablished by several studies (Asano and Uchida, 2018; Gomi et al., 2008; Whipkey, 2010). Moreover, Birch et al. (2021) found that interflow contribution is over 50% during storm flows in forested catchments of the humid tropics.

4.2. Deforestation and floods in humid catchments

We presented for the first time an evaluation of floods produced with different spatial patterns of deforestation in a humid tropic catchment, distinguishing the effects of forest location and forest fragmentation. This is a significant step forward in the understanding of the influence of forest location and forest fragmentation over floods. In particular, our results show that the spatial pattern of deforestation (i.e. by slope and random) can cause a significant difference in the spatial distribution of overland flow during intense storms. However, stormflow was found to be less sensitive to the spatial pattern of deforestation, showing non-significant differences among scenarios. Obtained differences in the time to peak flow among all scenarios

was relatively low (10 minutes) in line with previous findings of the low influence of land cover in tropical humid catchments on floods and time to peak (Asano and Uchida, 2018; Bathurst et al., 2020; Birkel et al., 2012).

Through the comparison of stormflow and overland flow among scenarios, this research showed that the influence of the spatial pattern of forest cover decreases as storm intensity increases. This is consistent with Buendia et al. (2016), Dadson et al. (2017), Laurance (2007) and Soulsby et al. (2017). For a return period of 10-yr, we found an increase in the peak flow from deforestation scenarios, that ranges between 5-10% respect to the baseline. In contrast, Cosandey et al. (2005) and Horton et al. (2021), reported reductions (afforestation) and raising (deforestation) of about 5 and 25% for 10-years peak floods, respectively. Also, Salazar et al. (2012) found a peak reduction around 30% for annual peak floods, while this study stablishes, for annual events, a peak flood variation around 23% for S3 (worst scenario). According to Bathurst et al. (2020), the mitigation effect of forest varies between catchments, reaching the maximum capacity with moderate return periods of 5-20 years. However, this author also indicates, that peak flow moderation depends on soil moisture. Therefore, our results are consistent with previous research, showing a reduction effect for low and moderate floods, until 10-year events.

In our model, the overland flow depends on the land cover change through the initial abstractions. Conversely, the stormflow, simulated at the outlet basin, is the result of the flow routed downstream through river channels. As a consequence, the relatively low sensitivity of stormflow (including time to peak), to deforestation in TRB, may be partly explained by soil moisture conditions and hydrological connectivity. According to Bracken and Croke (2007), the hydrological connectivity determines the generation of stormflow during intense storms, and depends of soil moisture and stream network. Previous research (e.g. Bathurst et al., 2018; Sriwongsitanon and Taesombat, 2011) indicates that peak flow during small and middle size events is function of soil moisture; therefore, if the watershed is saturated the response is the same despite the differences in land cover. Birkel et al. (2012) found in a humid catchment in Costa Rica, that land cover change had relatively little effect on peak discharges with return periods greater than 1-year. Also, the variation in lag times is small when hillslopes are sufficiently wet. In this regard, Asano and Uchida (2018) suggest, that the catchment-scale variation in lag times can be explained almost entirely by channel processes. Therefore, since TRB is a humid catchment with very steep relief, hillslope deforestation would have low influence over both stormflow and time to peak during intense storm events.

The land cover change area, also determine the effect over stormflow. According to Bathurst et al. (2020), the threshold for measurable impact on peak flows is around 20% in land cover area. However, for statistical significance of differences the changes have to be drastic. For example, Jodar-Abellan et al. (2019) found significant stormflow differences, with p-values less than 0.05 using Kruskal-Wallis test, due to aggressive urbanization process, around 75% of basin areas. Considering in one hand, that urban areas generate more stormflow than agriculture areas (Liu et al., 2005), and in the other hand, our study represent a deforestation area of only 37 %, (i.e. from 87 % in baseline to 50 % in scenarios). Therefore, it is expected that changes in storm flow in TRB are lower or even statistically non-significant.

4.3. Spatial patterns of deforestation and floods

The most important finding in the current research, regarding deforestation spatial pattern, is that location is more important than fragmentation. Previous studies suggested that the fragmentation of vegetation does not show an obvious effect on floods (Hou et al., 2018; Kim and Park, 2016). In contrast, the location of forest in different slopes can alter the peak flows in a more obvious way (Hou et al., 2018; Iacob et al., 2017). In our study, effects of forest location and fragmentation on floods were evaluated separately. We showed for Andean catchments in the humid tropics, such as the TRB, that deforestation (by slope) in the upper basin it is the most unfavorable scenario regarding the hazardousness of floods. Which is explained by the lower infiltration capacity in the upper basin, composed mainly by soils with clay content and the lithological material such as granite, but also by the steep relief. Therefore, the hillslopes are actually the area with highest contribution to stormflows during more intense and larger storm events in agreement with several studies (Birch et al., 2021; Gomi et al., 2008; Hopp and McDonnell, 2009). Consequently, our results indicate that hillslopes should be reforested and protected with priority to mitigate flood risk and for native forest conservation.

Forest cover reduce small floods, while it has the capacity to generate more runoff during intense storms due to retention of soil moisture from previous storms due to the deep roots in forest zones (Sriwongsitanon and Taesombat, 2011). In addition, lower evapotranspiration rates, especially in the upper basin, due to the presence of cloud forest, can maintain the soil moisture (Ataroff and Rada, 2000; Cárdenas et al., 2017; Moreno et al., 2018). Hence, forest cover generates fast-responding storm flow by both overland flow and subsurface flow (Asano and Uchida, 2018; Chifflard et al., 2019; Crespo et al., 2011; Hopp and McDonnell, 2009).

In these conditions, the hillslopes are more sensitive to deforestation generating stormflows and overland flow during intense storm events.

Although there are several salient strengths of this work, such as the evaluation of floods for different spatial patterns of deforestation maintaining the same amount of forest cover, our findings may be extended in the future through the analysis of additional scenarios focusing on the role of riparian forest on floods.

4.4. Implications for Nature Based Solutions

Despite the potential of forest to reduce floods, especially in the upper basin, our finding suggests that the influence of forest cover to reduce floods vanishes as return period increases. Other studies also found, a convergence in the flood response of the basins, with higher storm events, despite the forest coverage (Bathurst et al., 2011; Salazar et al., 2012). Therefore, the use of Nature Based Solutions (NbS), such as protection and reforestation efforts for flood management, need to be integrated in a broader context of land-use planning and water resources management (Cohen-Shacham et al., 2019).

We demonstrate, regarding floods, the importance of the forest cover located in the upper basin, which is rich in biodiversity and part of the Colonso-Chalupas Biological Reserve. This would allow that NbS initiatives within the basin to be advanced within the wider context of an integrated catchment management strategy to deliver multiple ecosystem services.

5. Conclusions

The effect of land cover changes on floods considering forest location and forest fragmentation in a humid tropical basin within the Ecuadorian Amazon were analyzed through simulations of different land cover scenarios with the hydrological distributed model TETIS.

Forest location presented higher effects than forest fragmentation on both, overland flow and stormflows. However, stormflow was less sensitive than overland flow to analyzed land cover changes. Deforestation of the upper basin represented the worst scenario for flood regulation. Finally, as storm intensity increases the effect of land cover scenarios decreases. Moreover, forest location and forest fragmentation has more influence over flows during small and medium-size storms.

Obtained results enhance our understanding of ecosystem services provided by the tropical Andean foothills forests.

Acknowledgements

Financial support was provided by the National Secretary of Higher Education and Research of Ecuador (SENESCYT) and the National Agency of Research and Development of Chile (ANID, Grant N°21210172). The authors acknowledge Ikiam University to provide the hydrometeorological data for this research. Finally, thanks to anonymous reviewers for their insightful comments.

References

Adamovic, M., Branger, F., Braud, I., Kralisch, S., 2016. Development of a data-driven semi-distributed hydrological model for regional scale catchments prone to Mediterranean flash floods. J. Hydrol. 541, 173–189. https://doi.org/10.1016/J.JHYDROL.2016.03.032

Asano, Y., Uchida, T., 2018. The roles of channels and hillslopes in rainfall/run-off lag times during intense storms in a steep catchment. Hydrol. Process. 32, 713–728. https://doi.org/10.1002/hyp.11443

Ataroff, M., Rada, F., 2000. Deforestation Impact on Water Dynamics in a Venezuelan Andean Cloud Forest. https://doi.org/10.1579/0044-7447-29.7.440 29, 440–444. https://doi.org/10.1579/0044-7447-29.7.440

Barbedo, J., Miguez, M., van der Horst, D., Marins, M., 2014. Enhancing ecosystem services for flood mitigation: a conservation strategy for peri-urban landscapes? Ecol. Soc. 19, art54. https://doi.org/10.5751/ES-06482-190254

Barrientos, G., Herrero, A., Iroumé, A., Mardones, O., Batalla, R.J., 2020. Modelling the Effects of Changes in Forest Cover and Climate on Hydrology of Headwater Catchments in South-Central Chile. Water 12, 1828. https://doi.org/10.3390/w12061828

Bathurst, J., Birkinshaw, S., Johnson, H., Kenny, A., Napier, A., Raven, S., Robinson, J., Stroud, R., 2018. Runoff, flood peaks and proportional response in a combined nested and paired forest plantation/peat grassland catchment. J. Hydrol. 564, 916–927. https://doi.org/10.1016/J.JHYDROL.2018.07.039

Bathurst, J.C., Fahey, B., Iroumé, A., Jones, J., 2020. Forests and floods: Using field evidence to reconcile analysis methods. Hydrol. Process. 34, 3295–3310. https://doi.org/10.1002/HYP.13802

Bathurst, J.C., Iroumé, A., Cisneros, F., Fallas, J., Iturraspe, R., Novillo, M.G., Urciuolo, A., Bièvre, B. de, Borges, V.G., Coello, C., Cisneros, P., Gayoso, J., Miranda, M., Ramírez, M., 2011. Forest impact on floods due to extreme rainfall and snowmelt in four Latin American environments 1: Field data analysis. J. Hydrol. 400, 281–291. https://doi.org/10.1016/J.JHYDROL.2010.11.044

Beneyto, C., Aranda, J.Á., Benito, G., Francés, F., 2020. New Approach to Estimate Extreme Flooding Using Continuous Synthetic Simulation Supported by Regional Precipitation and Non-Systematic Flood Data. Water 2020, Vol. 12, Page 3174 12, 3174. https://doi.org/10.3390/W12113174

Bin, L., Xu, K., Xu, X., Lian, J., Ma, C., 2018. Development of a landscape indicator to evaluate the effect of landscape pattern on surface runoff in the Haihe River Basin. J. Hydrol. 566, 546–557. https://doi.org/10.1016/J.JHYDROL.2018.09.045

Birch, A.L., Stallard, R.F., Bush, S.A., Barnard, H.R., 2021. The influence of land cover and storm magnitude on hydrologic flowpath activation and runoff generation in steep tropical catchments of central Panama. J. Hydrol. 596, 126138. https://doi.org/10.1016/J.JHYDROL.2021.126138

Birkel, C., Soulsby, C., Tetzlaff, D., 2012. Modelling the impacts of land-cover change on streamflow dynamics of a tropical rainforest headwater catchment. Hydrol. Sci. J. 57, 1543–1561. https://doi.org/10.1080/02626667.2012.728707

Blöschl, G., Ardoin-Bardin, S., Bonell, M., Dorninger, M., Goodrich, D., Gutknecht, D., Matamoros, D., Merz, B., Shand, P., Szolgay, J., 2007. At what scales do climate variability and land cover change impact on flooding and low flows? Hydrol. Process. 21, 1241–1247. https://doi.org/10.1002/HYP.6669

Bonnesoeur, V., Locatelli, B., Guariguata, M.R., Ochoa-Tocachi, B.F., Vanacker, V., Mao, Z., Stokes, A., Mathez-Stiefel, S.L., 2019. Impacts of forests and forestation on hydrological services in the Andes: A systematic review. For. Ecol. Manage. 433, 569–584. https://doi.org/10.1016/J.FORECO.2018.11.033

Boongaling, C.G.K., Faustino-Eslava, D. V., Lansigan, F.P., 2018. Modeling land use change impacts on hydrology and the use of landscape metrics as tools for watershed management: The case of an ungauged catchment in the Philippines. Land use policy 72, 116–128. https://doi.org/10.1016/j.landusepol.2017.12.042

Bracken, L.J., Croke, J., 2007. The concept of hydrological connectivity and its contribution to understanding runoff-dominated geomorphic systems. Hydrol. Process. 21, 1749–1763. https://doi.org/10.1002/HYP.6313

Buendia, C., Bussi, G., Tuset, J., Vericat, D., Sabater, S., Palau, A., Batalla, R.J., 2016. Effects of afforestation on runoff and sediment load in an upland Mediterranean catchment. Sci. Total Environ. 540, 144–157. https://doi.org/10.1016/J.SCITOTENV.2015.07.005

Cárdenas, M.F., Tobón, C., Buytaert, W., 2017. Contribution of occult precipitation to the water balance of 84meric ecosystems in the Colombian Andes. Hydrol. Process. 31, 4440–4449. https://doi.org/10.1002/HYP.11374

Chancay, J.E., Espitia-Sarmiento, E.F., 2021. Improving Hourly Precipitation Estimates for Flash Flood Modeling in Data-Scarce Andean-Amazon Basins: An Integrative Framework Based on Machine Learning and Multiple Remotely Sensed Data. Remote Sens. 2021, Vol. 13, Page 4446 13, 4446. https://doi.org/10.3390/RS13214446

Chang, H., Franczyk, J., 2008. Climate Change, Land-Use Change, and Floods: Toward an Integrated Assessment. Geogr. Compass 2, 1549–1579. https://doi.org/10.1111/j.1749-8198.2008.00136.x

Chifflard, P., Blume, T., Maerker, K., Hopp, L., Meerveld, I. van, Graef, T., Gronz, O., Hartmann, A., Kohl, B., Martini, E., Reinhardt-Imjela, C., Reiss, M., Rinderer, M., Achleitner, S., 2019. How can we model subsurface stormflow at the catchment scale if we cannot measure it? Hydrol. Process. 33, 1378–1385. https://doi.org/10.1002/HYP.13407

Chow, V. Te, Maidment, D.R., Mays, L.W., 1988. Applied hydrology. McGraw-Hill.

Cohen-Shacham, E., Andrade, A., Dalton, J., Dudley, N., Jones, M., Kumar, C., Maginnis, S., Maynard, S., Nelson, C.R., Renaud, F.G., Welling, R., Walters, G., 2019. Core principles for successfully implementing and upscaling Nature-based Solutions. Environ. Sci. Policy 98, 20–29. https://doi.org/10.1016/J.ENVSCI.2019.04.014

Cosandey, C., Andréassian, V., Martin, C., Didon-Lescot, J.F., Lavabre, J., Folton, N., Mathys, N., Richard, D., 2005. The hydrological impact of the 84merica84trico forest: a review of French research. J. Hydrol. 301, 235–249. https://doi.org/10.1016/J.JHYDROL.2004.06.040

Crespo, P.J., Feyen, J., Buytaert, W., Bücker, A., Breuer, L., Frede, H.G., Ramírez, M., 2011. Identifying controls of the rainfall–runoff response of small catchments in the

tropical Andes (Ecuador). J. Hydrol. 407, 164–174. https://doi.org/10.1016/J.JHYDROL.2011.07.021

Cuenca, P., Peñuela Mora, M.C., Maisincho, L., Celi, J., Gonzales, J., Chapalbay, R., 2018. Hacia un manejo adaptativo de la Reserva Biológica Colonso Chalupas y su zona de amortiguamiento. Sistematización de la aplicación de la metodología Manejo Adaptativo de Riesgo y Vulnerabilidad en Sitios de Conservación (MARISCO). GIZ, Quito-Ecuador.

Dadson, S.J., Hall, J.W., Murgatroyd, A., Acreman, M., Bates, P., Beven, K., Heathwaite, L., Holden, J., Holman, I.P., Lane, S.N., O'Connell, E., Penning-Rowsell, E., Reynard, N., Sear, D., Thorne, C., Wilby, R., 2017. A restatement of the natural science evidence concerning catchment-based 'natural' flood management in the UK. Proc. R. Soc. A Math. Phys. Eng. Sci. 473, 20160706. https://doi.org/10.1098/rspa.2016.0706

De Roo, A., Schmuck, G., Perdigao, V., Thielen, J., 2003. The influence of historic land use changes and future planned land use scenarios on floods in the Oder catchment. Phys. Chem. Earth, Parts A/B/C 28, 1291–1300. https://doi.org/10.1016/J.PCE.2003.09.005

Descheemaeker, K., Nyssen, J., Poesen, J., Raes, D., Haile, M., Muys, B., Deckers, S., 2006. Runoff on slopes with restoring vegetation: A case study from the Tigray highlands, Ethiopia. J. Hydrol. 331, 219–241. https://doi.org/10.1016/J.JHYDROL.2006.05.015

Duan, Q., Sorooshian, S., Gupta, V.K., 1994. Optimal use of the SCE-UA global optimization method for calibrating watershed models. J. Hydrol. 158, 265–284. https://doi.org/10.1016/0022-1694(94)90057-4

Dunn, O.J., 1964. Multiple Comparisons Using Rank Sums. Technometrics 6, 241–252. https://doi.org/10.1080/00401706.1964.10490181

Efford, M., 2021. Spatially Explicit Capture-Recapture [R package secr version 4.4.7].

Fahrig, L., 2003. Effects of Habitat Fragmentation on Biodiversity. Annu. Rev. Ecol. Evol. Syst. 34, 487–515. https://doi.org/10.1146/annurev.ecolsys.34.011802.132419

FAO-CIFOR, 2005. Forests and floods: drowning in fiction or thriving on facts? World.

Fleischbein, K., Wilcke, W., Valarezo, C., Zech, W., Knoblich, K., 2006. Water budgets of three small catchments under montane forest in Ecuador: experimental and modelling approach. Hydrol. Process. 20, 2491–2507. https://doi.org/10.1002/HYP.6212

Francés, F., Vélez, J.I., Vélez, J.J., 2007. Split-parameter structure for the automatic calibration of distributed hydrological models. J. Hydrol. 332, 226–240. https://doi.org/10.1016/J.JHYDROL.2006.06.032

Gao, Q., Yu, M., 2017. Reforestation-induced changes of landscape composition and configuration modulate freshwater supply and flooding risk of tropical watersheds. PloSOne12, e0181315. https://doi.org/10.1371/journal.pone.0181315

Gomez-Peralta, D., Oberbauer, S.F., McClain, M.E., Philippi, T.E., 2008. Rainfall and cloud-water interception in tropical montane forests in the eastern Andes of Central Peru. For. Ecol. Manage. 255, 1315–1325. https://doi.org/10.1016/J.FORECO.2007.10.058

Gomi, T., Sidle, R.C., Miyata, S., Kosugi, K., Onda, Y., 2008. Dynamic runoff connectivity of overland flow on steep forested hillslopes: Scale effects and runoff transfer. Water Resour. Res. 44, 8411. https://doi.org/10.1029/2007WR005894

Güneralp, B., Güneralp, I., Liu, Y., 2015. Changing global patterns of urban exposure to flood and drought hazards. Glob. Environ. Chang. 31, 217–225. https://doi.org/10.1016/j.gloenvcha.2015.01.002

Hamilton, L.S., 1987. What are the impacts of Himalayan deforestation on the Ganges-Brahmaputra lowlands and delta? Assumptions and facts. Mt. Res. Dev. 7, 256–263. https://doi.org/10.2307/3673202

Herwitz, S.R., 1985. Interception storage capacities of tropical rainforest canopy trees. J. Hydrol. 77, 237–252. https://doi.org/10.1016/0022-1694(85)90209-4

Hesselbarth, M.H.K., Sciaini, M., With, K.A., Wiegand, K., Nowosad, J., 2019. Landscapemetrics: an open-source R tool to calculate landscape metrics. Ecography (Cop.). 42, 1648–1657. https://doi.org/10.1111/ECOG.04617

Hirabayashi, Y., Mahendran, R., Koirala, S., Konoshima, L., Yamazaki, D., Watanabe, S., Kim, H., Kanae, S., 2013. Global flood risk under climate change. Nat. Clim. Chang. 3, 816–821. https://doi.org/10.1038/nclimate1911

Hopp, L., McDonnell, J.J., 2009. Connectivity at the hillslope scale: Identifying interactions between storm size, bedrock permeability, slope angle and soil depth. J. Hydrol. 376, 378–391. https://doi.org/10.1016/J.JHYDROL.2009.07.047

Horton, A.J., Nygren, A., Diaz-Perera, M.A., Kummu, M., 2021. Flood severity along the Usumacinta River, Mexico: Identifying the anthropogenic signature of tropical forest conversion. J. Hydrol. X 10, 100072. https://doi.org/10.1016/J.HYDROA.2020.100072

Hou, J., Guo, K., Liu, F., Han, H., Liang, Q., Tong, Y., Li, P., 2018. Assessing Slope Forest Effect on Flood Process Caused by a Short-Duration Storm in a Small Catchment. Water 10, 1256. https://doi.org/10.3390/w10091256

Hümann, M., Schüler, G., Müller, C., Schneider, R., Johst, M., Caspari, T., 2011. Identification of runoff processes – The impact of different forest types and soil properties on runoff formation and floods. J. Hydrol. 409, 637–649. https://doi.org/10.1016/J.JHYDROL.2011.08.067

Hurtado-Pidal, J., Acero Triana, J.S., Espitia-Sarmiento, E., Jarrín-Pérez, F., 2020. Flood Hazard Assessment in Data-Scarce Watersheds Using Model Coupling, Event Sampling, and Survey Data. Water 12, 2768. https://doi.org/10.3390/w12102768

Iacob, O., Brown, I., Rowan, J., 2017. Natural flood management, land use and climate change trade-offs: the case of Tarland catchment, Scotland. Hydrol. Sci. J. 62, 1931–1948. https://doi.org/10.1080/02626667.2017.1366657

Ikiam-University, 2021. Ikiam Hydromet Service [WWW Document]. URL http://hidrometeorologia.ikiam.edu.ec/ (accessed 10.27.21).

Ilieva, L., McQuistan, C., Van-Breda, A., Rodriguez, A., Guevara, O., Cordero, D., Renaud, F., 2018. Adoptando soluciones basadas en la naturaleza para la reducción del riesgo de inundación en América Latina.

INAMHI, 2019. Determinación de ecuaciones para el cálculo de intensidades máximas de precipitación. Quito – Ecuador. https://doi.org/www.serviciometeorologico.gob.ec/Publicaciones/Hidrologia/ESTUDIO_DE_INTENSIDADES_V_FINAL.pdf

INEC, 2010. Censo de 87merica87t y Vivienda – 2010 [WWW Document]. URL https://www.ecuadorencifras.gob.ec/banco-de-informacion/

IPCC, 2021. Climate Change 2021: The Physical Science Basis. Contribution of Working Group I to the Sixth Assessment Report of the Intergovernmental Panel on Climate Change.

Jodar-Abellan, A., Valdes-Abellan, J., Pla, C., Gomariz-Castillo, F., 2019. Impact of land use changes on flash flood prediction using a sub-daily SWAT model in five Mediterranean ungauged watersheds (SE Spain). Sci. Total Environ. 657, 1578–1591. https://doi.org/10.1016/J.SCITOTENV.2018.12.034

Jonkman, S.N., 2005. Global Perspectives on Loss of Human Life Caused by Floods. Nat. Hazards 2005 342 34, 151–175. https://doi.org/10.1007/S11069-004-8891-3

Jourgholami, M., Karami, S., Tavankar, F., Lo Monaco, A., Picchio, R., 2020. Effects of Slope Gradient on Runoff and Sediment Yield on Machine-Induced Compacted Soil in Temperate Forests. For. 2021, Vol. 12, Page 49 12, 49. https://doi.org/10.3390/F12010049

Kim, H.W., Park, Y., 2016. Urban green infrastructure and local flooding: The impact of landscape patterns on peak runoff in four Texas MSAs. Appl. Geogr. 77, 72–81. https://doi.org/10.1016/J.APGEOG.2016.10.008

Kottek, M., Grieser, J., Beck, C., Rudolf, B., Rubel, F., 2006. World map of the Köppen-Geiger climate classification updated. Meteorol. Zeitschrift 15, 259–263. https://doi.org/10.1127/0941-2948/2006/0130

Kruskal, W.H., Wallis, W.A., 1952. Use of Ranks in One-Criterion Variance Analysis. J. Am. Stat. Assoc. 47, 583–621. https://doi.org/10.1080/01621459.1952.10483441

Lane, S.N., 2017. Natural flood management. Wiley Interdiscip. Rev. Water 4, e1211. https://doi.org/10.1002/wat2.1211

Laurance, W.F., 2007. Forests and floods. Nat. 2007 4497161 449, 409–410. https://doi.org/10.1038/449409a

Leopold, L., Maddock, T., 1953. The hydraulic geometry of stream channels and some physiographic implications. Prof. Pap. https://doi.org/10.3133/PP252

Liu, J., Liu, X., Wang, Y., Li, Y., Jiang, Y., Fu, Y., Wu, J., 2020. Landscape composition or configuration: which contributes more to catchment hydrological flows and variations? Landsc. Ecol. 2020 357 35, 1531–1551. https://doi.org/10.1007/S10980-020-01035-3

Liu, Y.B., De Smedt, F., Hoffmann, L., Pfister, L., 2005. Assessing land use impacts on flood processes in complex terrain by using GIS and modeling approach. Environ. Model. Assess. 2004 94 9, 227–235. https://doi.org/10.1007/S10666-005-0306-7

MacFarland, T.W., Yates, J.M., 2016. Kruskal–Wallis H-Test for Oneway Analysis of Variance (ANOVA) by Ranks. Introd. To Nonparametric Stat. Biol. Sci. Using R 177–211. https://doi.org/10.1007/978-3-319-30634-6_6

MAGAP-SIGTIERRAS, 2016. Generación de Geoinformación para la Gestión del Territorio a Nivel Nacional [WWW Document]. URL metadatos.sigtierras.gob.ec

McGarigal, K., 2014. Landscape Pattern Metrics, in: Wiley StatsRef: Statistics Reference Online. Wiley. https://doi.org/10.1002/9781118445112.stat07723

McGrane, S.J., Hutchins, M.G., Miller, J.D., Bussi, G., Kjeldsen, T.R., Loewenthal, M., 2017. During a winter of storms in a small UK catchment, hydrology and water quality responses follow a clear rural-urban gradient. J. Hydrol. 545, 463–477. https://doi.org/10.1016/J.JHYDROL.2016.12.037

Merz, B., Aerts, J., Arnbjerg-Nielsen, K., Baldi, M., Becker, A., Bichet, A., Blöschl, G., Bouwer, L.M., Brauer, A., Cioffi, F., Delgado, J.M., Gocht, M., Guzzetti, F., Harrigan, S., Hirschboeck, K., Kilsby, C., Kron, W., Kwon, H.-H., Lall, U., Merz, R., Nissen, K., Salvatti, P., Swierczynski, T., Ulbrich, U., Viglione, A., Ward, P.J., Weiler, M., Wilhelm, B., Nied, M., 2014. Floods and climate: emerging perspectives for flood risk assessment and management. Nat. Hazards Earth Syst. Sci. 14, 1921–1942. https://doi.org/10.5194/nhess-14-1921-2014

Moreno, J., Yerovi, F., Herrera, M., Yánez, D., Espinosa, J., Sánchez, D., Merlo, J., Haro, R., Acosta, M., Bernal, G., 2018. Soils from the Amazonia. Pp. 79–111. https://doi.org/10.1007/978-3-319-25319-0_3

Moriasi, D.N., Arnold, J.G., Van Liew, M.W., Bingner, R.L., Harmel, R.D., Veith, T.L., Harmel, D., Veith, T.L., 2007. Model Evaluation Guidelines for Systematic Quantification of Accuracy in Watershed Simulations. Trans. ASABE 50, 885–900. https://doi.org/10.13031/2013.23153

Mukul, Manas, Srivastava, V., Jade, S., Mukul, Malay, 2017. Uncertainties in the Shuttle Radar Topography Mission (SRTM) Heights: Insights from the Indian Himalaya and Peninsula. Sci. Reports 2017 71 7, 1–10. https://doi.org/10.1038/srep41672

Nash, J.E., Sutcliffe, J. V., 1970. River flow forecasting through conceptual models part I – A discussion of principles. J. Hydrol. 10, 282–290. https://doi.org/10.1016/0022-1694(70)90255-6

Nikolopoulos, E.I., Anagnostou, E.N., Borga, M., Vivoni, E.R., Papadopoulos, A., 2011. Sensitivity of a mountain basin flash flood to initial wetness condition and rainfall variability. J. Hydrol. 402, 165–178. https://doi.org/10.1016/J.JHYDROL.2010.12.020

Peña, L.E., Barrios, M., Francés, F., 2016. Flood quantiles scaling with upper soil hydraulic properties for different land uses at catchment scale. J. Hydrol. 541, 1258–1272. https://doi.org/10.1016/J.JHYDROL.2016.08.031

Puricelli, M.M., 2008. Estimación y distribución de parámetros del suelo para la modelación hidrólogica. Riunet. https://doi.org/10.4995/THESIS/10251/2904

R-Development-Core-Team, 2020. R: A Language and Environment for Statistical Computing.

Reynolds, J.E., Halldin, S., Seibert, J., Xu, C.Y., Grabs, T., 2019. Robustness of flood-model calibration using single and multiple events. Hydrol. Sci. J. 6667. https://doi.org/10.1080/02626667.2019.1609682

Riitters, K., 2018. Pattern metrics for a transdisciplinary landscape ecology. Landsc. Ecol.2018 349 34, 2057–2063. https://doi.org/10.1007/S10980-018-0755-4

Rogger, M., Agnoletti, M., Alaoui, A., Bathurst, J.C., Bodner, G., Borga, M., Chaplot, V., Gallart, F., Glatzel, G., Hall, J., Holden, J., Holko, L., Horn, R., Kiss, A., Kohnová, S., Leitinger, G., Lennartz, B., Parajka, J., Perdigão, R., Peth, S., Plavcová, L., Quinton, J.N., Robinson, M., Salinas, J.L., Santoro, A., Szolgay, J., Tron, S., van den Akker, J.J.H., Viglione, A., Blöschl, G., 2017. Land use change impacts on floods at the catchment scale: Challenges and opportunities for future research. Water Resour. Res. 53, 5209–5219. https://doi.org/10.1002/2017WR020723

Salazar, S., Francés, F., Komma, J., Blume, T., Francke, T., Bronstert, A., Blöschl, G., 2012. A comparative analysis of the effectiveness of flood management measures based on the concept of “retaining water in the landscape” in different European hydro-climatic regions. Nat. Hazards Earth Syst. Sci. 12, 3287–3306. https://doi.org/10.5194/nhess-12-3287-2012

Saxton, K.E., Rawls, W.J., 2006. Soil Water Characteristic Estimates by Texture and Organic Matter for Hydrologic Solutions. Soil Sci. Soc. Am. J. 70, 1569–1578. https://doi.org/10.2136/SSSAJ2005.0117

Seddon, N., Chausson, A., Berry, P., Girardin, C.A.J., Smith, A., Turner, B., 2020. Understanding the value and limits of nature-based solutions to climate change and other global challenges. Philos. Trans. R. Soc. B 375. https://doi.org/10.1098/RSTB.2019.0120

Segura-Beltrán, F., Sanchis-Ibor, C., Morales-Hernández, M., González-Sanchis, M., Bussi, G., Ortiz, E., 2016. Using post-flood surveys and geomorphologic mapping to evaluate hydrological and hydraulic models: The flash flood of the Girona River (Spain) in 2007. J. Hydrol. 541, 310–329. https://doi.org/10.1016/J.JHYDROL.2016.04.039

Shapiro, S.S., Wilk, M.B., 1965. An analysis of variance test for normality (complete samples). Biometrika 52, 591–611. https://doi.org/10.1093/BIOMET/52.3-4.591

Shuttleworth, E.L., Evans, M.G., Pilkington, M., Spencer, T., Walker, J., Milledge, D., Allott, T.E.H., 2019. Restoration of blanket peat moorland delays stormflow from hillslopes

and reduces peak discharge. J. Hydrol. X 2, 100006. https://doi.org/10.1016/J.HYDROA.2018.100006

Singh, V.P., Wang, S.X., Zhang, L., 2005. Frequency analysis of nonidentically distributed hydrologic flood data. J. Hydrol. 307, 175–195. https://doi.org/10.1016/j.jhydrol.2004.10.029

Siswanto, S.Y., Francés, F., 2019. How land use/land cover changes can affect water, flooding and sedimentation in a tropical watershed: a case study using distributed modeling in the Upper Citarum watershed, Indonesia. Environ. Earth Sci. 2019 7817 78, 1–15. https://doi.org/10.1007/S12665-019-8561-0

Sommer-gmbh, 2014. RQ-30, RQ-30a, Discharge Measurement System User Manual [WWW Document]. URL http://www.sommer.at/en/products/water/rq-30-rq-30a

Soulsby, C., Dick, J., Scheliga, B., Tetzlaff, D., 2017. Taming the flood—How far can we go with trees? Hydrol. Process. 31, 3122–3126. https://doi.org/10.1002/HYP.11226

Sriwongsitanon, N., Taesombat, W., 2011. Effects of land cover on runoff coefficient. J. Hydrol. 410, 226–238. https://doi.org/10.1016/J.JHYDROL.2011.09.021

Tobón, C., 2021. Ecohydrology of Tropical Andean Cloud Forests. Andean Cloud For. 61–87. https://doi.org/10.1007/978-3-030-57344-7_4

Tobón, C., 2008. Los bosques andinos y el agua, Serie#4. Ed, Publicación de ECOBONA. Programa regional ECOBONA – INTERCOOPERATION, CONDESAN, Quito.

Turner, M.G., 1989. Landscape Ecology: The Effect of Pattern on Process. Annu. Rev. Ecol. Syst. 20, 171–197. https://doi.org/10.1146/annurev.es.20.110189.001131

UNISDR, 2017. Words into Action Guidelines: National Disaster Risk Assessment Hazard Specific Risk Assessment 4. Flood Hazard and Risk Assessment.

Van Noordwijk, M., Tanika, L., Lusiana, B., 2017. Flood risk reduction and flow buffering as ecosystem services – Part 1: Theory on flow persistence, flashiness and base flow. Hydrol. Earth Syst. Sci. 21, 2321–2340. https://doi.org/10.5194/HESS-21-2321-2017

VanLiew, M.W., Arnold, J.G., Bosch, D.D., 2005. Problems and potential of autocalibrating a hydrologic model. Trans. ASAE 48, 1025–1040. https://doi.org/10.13031/2013.18514

Velásquez, N., Hoyos, C.D., Vélez, J.I., Zapata, E., 2020. Reconstructing the 2015 Salgar flash flood using radar retrievals and a conceptual modeling framework in an

ungauged basin. Hydrol. Earth Syst. Sci. 24, 1367–1392. https://doi.org/10.5194/HESS-24-1367-2020

Vélez, J.J., Puricelli, M., López Unzu, F., Francés, F., 2009. Parameter extrapolation to ungauged basins with a hydrological distributed model in a regional framework. Hydrol. Earth Syst. Sci. 13, 229–246. https://doi.org/10.5194/HESS-13-229-2009

Whipkey, R., 2010. Subsurface stormflow from forested slopes. Int. Assoc. Sci. Hydrol. Bull. 10, 74–85. https://doi.org/10.1080/02626666509493392

Yang, X., Chen, H., Wang, Y., Xu, C.-Y., 2016. Evaluation of the effect of land use/cover change on flood characteristics using an integrated approach coupling land and flood analysis. Hydrol. Res. 47, 1161–1171. https://doi.org/10.2166/nh.2016.108

Yin, J., Gentine, P., Zhou, S., Sullivan, S.C., Wang, R., Zhang, Y., Guo, S., 2018. Large increase in global storm runoff extremes driven by climate and anthropogenic changes. Nat. Commun. 9, 4389. https://doi.org/10.1038/s41467-018-06765-2

Zhang, X., Yu, G.Q., Li, Z. Bin, Li, P., 2014. Experimental Study on Slope Runoff, Erosion and Sediment under Different Vegetation Types. Water Resour. Manag. 28, 2415–2433. https://doi.org/10.1007/S11269-014-0603-5/FIGURES/13

CHAPTER V

ANALYSIS OF THE COMBINED EFFECTS OF CLIMATE CHANGE AND LUCC ON FLOODS

This chapter is based on:

Hurtado-Pidal, J., Aguayo, M., Link, O. (**2023**). Analysis of the combined effects of climate change and land-use/land-cover change on floods in a humid tropical basin (*in prep.*)

Analysis of the combined effects of climate change and land-use/land-cover change on floods in a humid tropical basin

Jorge Hurtado-Pidal[a], Mauricio Aguayo[a], Oscar Link[b]

[a] Department of Territorial Planning and EULA-Center, Universidad de Concepción, Chile

[b] Department of Civil Engineering, Universidad de Concepción, Chile

Abstract

Climate change and land-use/land-cover change (LUCC) are among the largest anthropogenic forcings that alter floods, especially their frequency and magnitude. Although climate change can affect floods at regional spatial scales, LUCC effects on floods are local and occure at small spatial scales. Few studies analyzed the combined effects of LUCC and climate change forcing on floods focusing on the discharge at the basin outlet. Thus, the continuous variation of interactions in the stream network has not yet been identified. This constrain limits current understanding of the ecosystem services provided by the forest for flood regulation in the context of climate change, even though flood control using forest is an excellent nature-based solution for disaster mitigation. Therefore, this study evaluates the relative importance of and interactions between the effects of climate change and LUCC on floods for a humid tropical basin within the Ecuadorian Amazon. To achieve this goal, deforestation scenarios with two land cover types (forest and agriculture) were designed. Precipitation scenarios were obtained through the projected precipitation of the Global Climate Model (GCM) IPSL SSP5-8.5 (CMIP6). The hydrological response of the basin with the different LUCC and precipitation scenarios was simulated using the distributed hydrological model TETIS. The changes in stormflow were analyzed at 42 points across the stream network, using absolute differences and the statistical tests: Kruskal-Wallis, Dunn, and Sheirer-Ray-Hare tests. Our results show that the effect of climate change on floods is more homogeneous over the basin than that of LUCC. Floods in the upper part of the basin were more sensitive to LUCC, i.e., deforestation, while floods in the lower part of the basin were more sensitive to climate change than to LUCC. For a two-year return period (Rp2) the altitudinal range from 590 to 906 meters above sea level was identified as a transitional area where the influence of LUCC on stormflows appears. The threshold of absolute differences in peak flows and stormflow volume was 590 m.a.s.l. A slightly and statistically non-significant interaction between

climate change and LUCC was identified in the lower part. The magnitude of changes in stormflows in the lower part of the basin is closely related to the scale effect and the sensitivity of the ecosystem in the upper part. Therefore, native forest is crucial for downstream flow regulation and flood control, and its importance is expected to increase in the future due to the climate change-induced precipitation projections.

Keywords: TETIS, stormflow, land-use/land-cover change, climate change, interactions, floods, nature-based solutions, Ecuador.

1. Introduction

Flash floods are one of the most damaging natural hazards around the world causing multiple fatalities and economic loses (Jonkman, 2005; UNISDR, 2017). Climate change and land use/ land cover change (LUCC) are among the largest anthropogenic forcings driving floods. The deforestation of native forest, has been recognized as one of the main drivers that can exacerbate the occurrence and magnitude of floods (Chang & Franczyk, 2008). Moreover, flood prediction is difficult as it depends on non-linear and scale-dependent processes controlling the interactions between LUCC and climate change effects (Blöschl et al., 2007; Rogger et al., 2017). Consequently, it is imperative to understand the variations across the basin of the individual and combined effects of climate change and LUCC on floods for watershed planning and flood management.

Climate change is a significant factor increasing frequency and intensity of floods worldwide (Hirabayashi et al., 2013; IPCC, 2021). Future climate change scenarios for the northwestern Amazon basin are expected to be associated with rising temperatures and changing precipitation patterns. These changes will likely result in more frequent extreme weather events, such as heavy rainfall, which can trigger floods (Palomino-Lemus et al., 2017; Solman, 2013; Sorribas et al., 2016).

Forest protection and reforestation have been recognized as nature-based solutions (NbS) for flood management (Dadson et al., 2017; Ilieva et al., 2018; Lane, 2017). The Tropical Andean Forest (TAF) is a natural barrier that intercept part of the precipitation (Ataroff & Rada, 2000). The vegetation can enhance the surface rugosity and slow down the runoff, allowing it to be absorbed gradually by the soil and vegetation (Tobón, 2008, 2021). In particular, infiltration helps to reduce the amount of runoff and surface flow during rainfall events reducing downstream flood risk. Additionally, trees and other vegetation in TAF also help to retain water in the soil, increasing the soil's capacity to absorb water and reducing the amount of water

that flows into rivers and streams. These characteristics make the TAF special ecosystems that can act as a natural buffer against flooding, especially during small and medium-sized floods (Bonnesoeur et al., 2019; Bathurst et al., 2011, 2020; Birkel et al., 2012). Thus, the implementation of NbS in these areas allow the conservation of various ecosystem services related to biodiversity conservation, climate change adaptation and water resources management (Cohen-Shacham et al., 2016).

Climate change and LUCC simultaneously impact hydrological processes at the basin scale (Blöschl et al., 2007; Bronstert, 2004; Chang & Franczyk, 2008). However, since the impacts acts at different spatial scales, the analysis of their individual contributions is necessary for watershed planning and management (Lian et al., 2020; Zhang et al., 2018). The main methodologies to separate the individual contributions are: hydrological modeling, paired catchment, conceptual, experimental and analytical approaches (see: Yang et al., 2017 and Zhang et al., 2018). The hydrological modeling-based approach is combined with hypothetical scenarios ('what-if approach'; e.g., Iacob et al., 2017) and one-factor-at-a-time analysis ('OFAT method'; e.g., Zhang et al., 2018).

The experimental design based on hydrological modeling includes a base or reference scenario, to analyze the individual and combined contributions of climate change and LUCC on hydrological variables. Hydrological modeling has been used to decompose the individual effect of climate change and LUCC on floods (Chawla & Mujumdar, 2015; Tian et al., 2022; Yang et al., 2017; Zhang et al., 2018). Synergies and antagonisms are key features of the combined effects of climate change and LUCC interactions. The interaction is the relationship between two or more variables that affects the outcome or response variable in a way that is not simply additive or independent (Dunne, 2010; Rothman, 1976). A synergistic interaction occurs when the combined effect of two variables (eg., climate change and LUCC) is greater than the sum of their individual effects, resulting in an amplified outcome (eg., peak flows, runoff volume). Conversely, an antagonistic interaction arises when the combined effect of two variables is less than the sum of their individual effects, leading to a diminished outcome. Some hydrological studies have reported both, synergistic and antagonistic interactions of climate change and LUCC on basin hydrological response (Hung et al., 2020; Tian et al., 2022; Lamichhane & Shakya, 2019). However, studies that analyzed interactions of climate change and LUCC, presented a coarse spatial scale, (i.e., mean values at basin scale or few sampling points). Additionally, climate change has a homogeneous effect on floods at the basin scalecompared with the LUCC effects that is a non-linear and complex scale-dependent process (Blöschl et al., 2007; Rogger et al., 2017). Moreover,

LUCC has a greater effect in the upper than in the lower basin. As a basin becomes larger, the effect of LUCC becomes smaller (Edokpa et al., 2022; Hurtado-Pidal et al., 2022; Olang & Fürst, 2011). Furthermore, the analysis of the contribution of climate change and LUCC is generally conducted at monthly or annual time scales. Consequently, it has not been possible to identify the variation of the interactions across the basin during floods. This limitation hinders understanding to improve the application of NbS for flood regulation within the context of climate change adaptation.

In consequence, the goal of this study is to evaluate the effects of climate change and LUCC on stormflows across an altitudinal gradient. To achieve this goal, we used the spatially-distributed hydrological model TETIS at event time scale, applying hypothetical scenarios of climate change and LUCC. The analysis was carried out using 42 stormflow sampling sites across the study area covering a full range of elevations. A comparative analysis of stormflows obtained for multiple scenarios is presented to determine the contributions and interaction of climate change and LUCC on floods.

The Tena River Basin (TRB), located within the Ecuadorian Amazon, was used as a study case. Many people in the basin live in flood-prone areas, especially in the city of Tena located in the downstream part of the basin, where at least three significant incidents related to flash floods occurred in the past decade (GADM-TENA, 2021). Moreover, some features such as high-intensity precipitation events, humid soils, and steep relief in the upper basin, increases the chance of flash flooding (Jodar-Abellan et al., 2019; Nikolopoulos et al., 2011). Additionally, the climate change is expected to have significant impact on TRB, including changes in precipitation patterns, increased temperatures, and more extreme weather events. Thus, the TRB is of critical importance for hydrological research due to its susceptibility to flash floods but also due to the opportunity to better manage the ecosystem services of the basin.

2. Materials and Methods

2.1. Study Area

The study was carried out in the TRB located in the foothills of the Eastern Andes in the Napo province, Ecuador (Figure 5.1b, 5.1c). It is a small watershed in the upper part of the Amazon basin, covering a drainage area of 240 km^2 at the junction of Tena and Pano rivers in the city of Tena (flow gauge; Figure 5.1a).

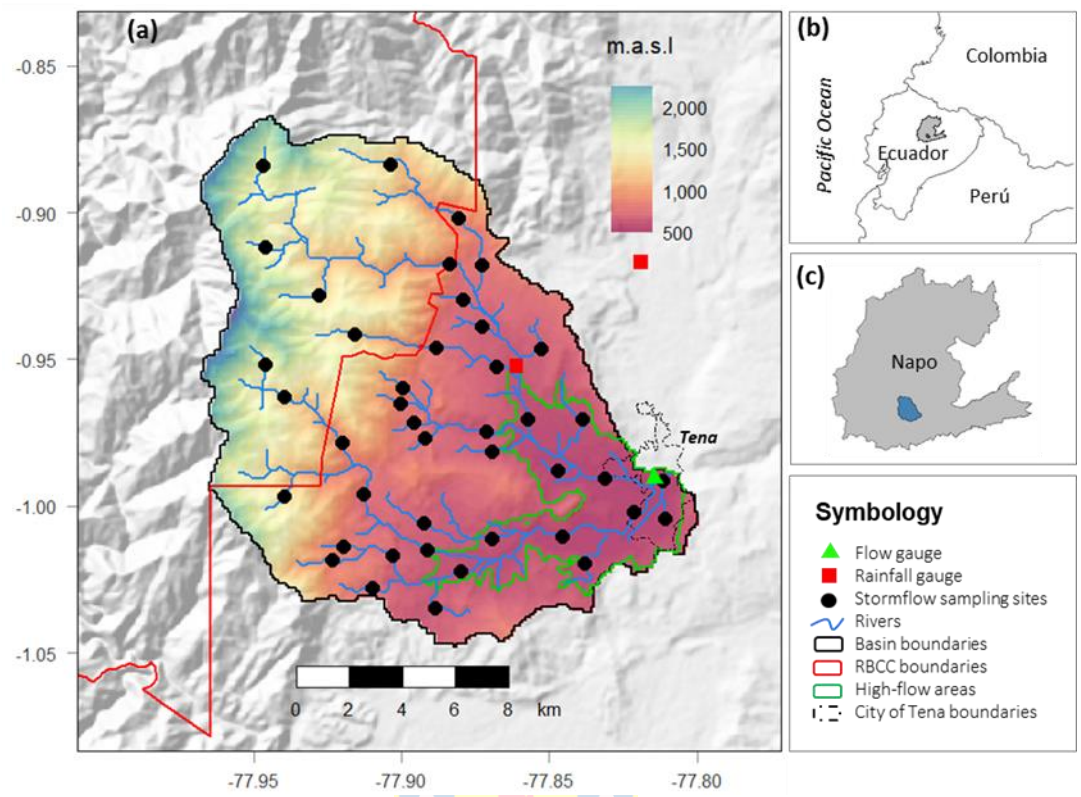

Figure 5.1. Main features of the TRB. (a) Terrain elevation, gauge stations, and stormflow sampling sites; Location of the TRB in (b) Ecuador and (c) Napo province. RBCC in the symbology (red polygon) refers to the Colonso-Chalupas Biological Reserve.

The terrain elevation within the TRB ranges from 500 to 2500 m.a.s.l, with a mean slope of 40% and 9% in the upper and lower regions, respectively. The mean annual temperature and precipitation are 23°C and 3500 mm, respectively. According to Köppen-Geiger climate classification (Kottek et al., 2006), the basin can be defined as tropical rainforest (Af). The climate in this area is influenced significantly by the Intertropical Convergence Zone (ITCZ; Vargas et al., 2022). Specifically, by moist air masses from the eastern part of the Amazon basin. Thus, the combination of orographic effect and the influence of the Intertropical Convergence Zone (ITCZ) favor the formation of convective storms in the basin. Therefore, it is common that the annual precipitation and rainfall intensities in this area reach 5000 mm and 65 mm/h respectively (Chancay & Espitia-Sarmiento, 2021; Ikiam-University, 2021). Although the base flow of the Tena river is 13 m^3/s at the basin outlet, it is common to record high flows of 700-800 m^3/s, at least once a year. This amount is approximately half of the bankfull discharge at the reach located downstream of the Tena and Pano rivers junction, as indicated by the flow gauge in Figure 5.1a. The geology of the basin consists of Paleozoic-Mesozoic granites in the

upper basin and sandstones and limestones from the Cretaceous and Paleogene periods in the lower basin. The soils are mainly Andisols, composed by sandy clays and sandy loams textures, with a maximum depth of 1.5 m. Also, the soils have a relatively high organic content (6%) within the first 0.5 m (MAGAP-SIGTIERRAS, 2016). Overall, these characteristics result in a high-water retention capacity with low infiltration rates (15.6 mm/h) (Hurtado-Pidal et al., 2022; Sánchez et al., 2018). The native forest cover most of the area (87%) and is located mainly in the upper basin, that is part of the Colonso-Chalupas Biological Reserve (Figure 5.1.a). Other land uses represent minor coverage, such as grassland, scrubs, crops (8%) and urban areas (3%), located in the lower part of the basin. Additional details of the study area can be found in Hurtado-Pidal et al. (2020, 2022).

2.2. Hydrological modeling

The stormflows were simulated at event time scale and 10 min time step using the spatially -distributed hydrological model with physically based parameters TETIS (Francés et al., 2007). TETIS has been widely used for flood studies including humid and mountain environments (Salazar et al., 2012; Siswanto & Francés, 2019). TETIS was previously calibrated and validated for the TRB (Hurtado-Pidal et al., 2022) showing good performance reproducing extreme events according to Moriasi et al. (2007) guidelines. Specifically, Hurtado-Pidal et al. (2022) reported values of $0.80 \leq$ Nash-Sutcliffe coefficient ≤ 0.94 and $-3.70 \leq$ Percent Bias ≤ 26.52. The parameterization of TETIS in TRB was caried out using soil, land cover/use and lithology maps at spatial scale 1:25.000 (MAGAP-SIGTIERRAS, 2016). The catchment morphometric parameters were obtained from 90 m version of SRTM-DEM and all raster parameters in TETIS were resampled to 100 x 100 m. Split time series of stream flow and rainfall of nine storm events recorded by gauge stations within the basin, from July 2018 to June 2020, were used for calibration and validation of TETIS in TRB. Thus, the effective parameters obtained from this parameterization and calibration were used in the simulations. Additionally, the parameters recommended by Frances et al. (2007) were utilized for the implementation of the kinematic wave approximation for flow routing in the streams network. Further details of parameterization of TETIS model (including calibration and validation) in TRB can be found in Hurtado-Pidal et al. (2022).

2.3. Climate change scenarios and data

The climate change scenarios of extreme precipitation were obtained following three sequential stages based on Vu et al. (2017) methodology as follows: Firstly, the bias correction was applied over precipitation series (raw-data) of three General

Circulation Models (GCM; SSP5-8.5), using the quantile mapping method (QM) with rain gauge observations. In the second stage, five probability distribution functions (PDF) were fitted for series of 30 years of maximum annual precipitation in 24 hours from both GCM-BC and observations. Finally, design storms were obtained for both, current climate (gauge observations) and future climate (GCM-BC), using three return periods: 2 (Rp2), 10 (Rp10) and 100 (Rp100) years.

2.3.1. Climate data

The observed daily precipitation was obtained from the M1219 meteorological station (Tena Hda. Chaupishungo) located close to the TRB (Figure 5.1a). The station maintained by the National Institute of Hydrology and Meteorology of Ecuador (INAMHI) was selected due to the high quality of data andrecording span (1981-2016 after homogenization) in relation to other gauge stations in the area (Figure 5.2a).

The Coupled Model Intercomparison Project Phase 6 (CMIP6) climate projections for the study area were downloaded from Copernicus (Copernicus, 2021). Specifically, three GCM were selected; IPSL (CM6A-LR, France; Boucher et al., 2020), MIROC (MIROC-ES2L, Japan; Hajima et al., 2020) and NorESM2 (NorESM2-MM, Norway; Seland et al., 2020). These GCM´s have been previously used to analyze reanalysis datasets and future scenarios of precipitation on Ecuador and the Northern Andes (Armenta et al., 2016; Campozano et al., 2017; Palomino-Lemus et al., 2017). Time series of daily precipitation were downloaded for the period from 1981 to 2010 and future climate from 2041 to 2070. Future climate projections are related to emission scenarios namely Shared Socioeconomic Pathways (SSP). In this study the SSP5-8.5 (very high emission scenario) was considered. Note that, the SSP5-8.5 (corresponding to RCP8.5) is commonly used for climate change impact assessment of floods (Liu et al., 2023; Mishra et al., 2018) and is suitable for our experiment goals since possible underestimation of precipitation rates is reduced.

2.3.2. Bias correction

The GCM precipitation raw-data have systematic deviation called ‘bias’ in frequency and intensity (Mishra et al., 2018; Piani et al., 2010). Bias correction (BC) techniques are routinely used to produce regional or local climate outputs from GCM´s (Heredia et al., 2018; Manzanas et al., 2020). Thus, Quantile Mapping (QM) bias correction (BC) method was employed to reduce the bias in frequency and intensity. The QM is a non-parametric BC method that can be applicable for all

possible distributions and have been widely used as a statistical downscaling technique to correct bias from climate models (e.g., see Campozano et al., 2016 and Fang et al., 2015). The QM uses empirical Cumulative Distribution Functions (CDF) of observed and modelled values instead of assuming parametric distributions. Thus, the modelled CDF is fitted to the observed CDF. More details of QM method can be found in (Gudmundsson et al., 2012).

The QM method was applied in R (R-Development-Core-Team, 2020) using the qmap-package (Gudmundsson, 2016; Gudmundsson et al., 2012). The daily data from 1981 to 2010 (30 years of daily data) were used as a common period of observations and simulations. Similarly to Tripathi et al. (2006), the data was split into 70 and 30 % for training and testing, respectively. Thus, the QM fitted function was applied for BC of future climate simulations. This procedure was repeated three times, one for each GCM. The Figure 5.2b, shows the CDFs fitted for each GCM with historical climate, using the testing data (30%). The 30-year time series of maximum annual precipitation (MAP, mm/day) for the observed (M1219) and three GCM-BC (IPSL, MIROC and NorESM2) under SSP5-8.5 scenario are shown in Figure 5.2c.

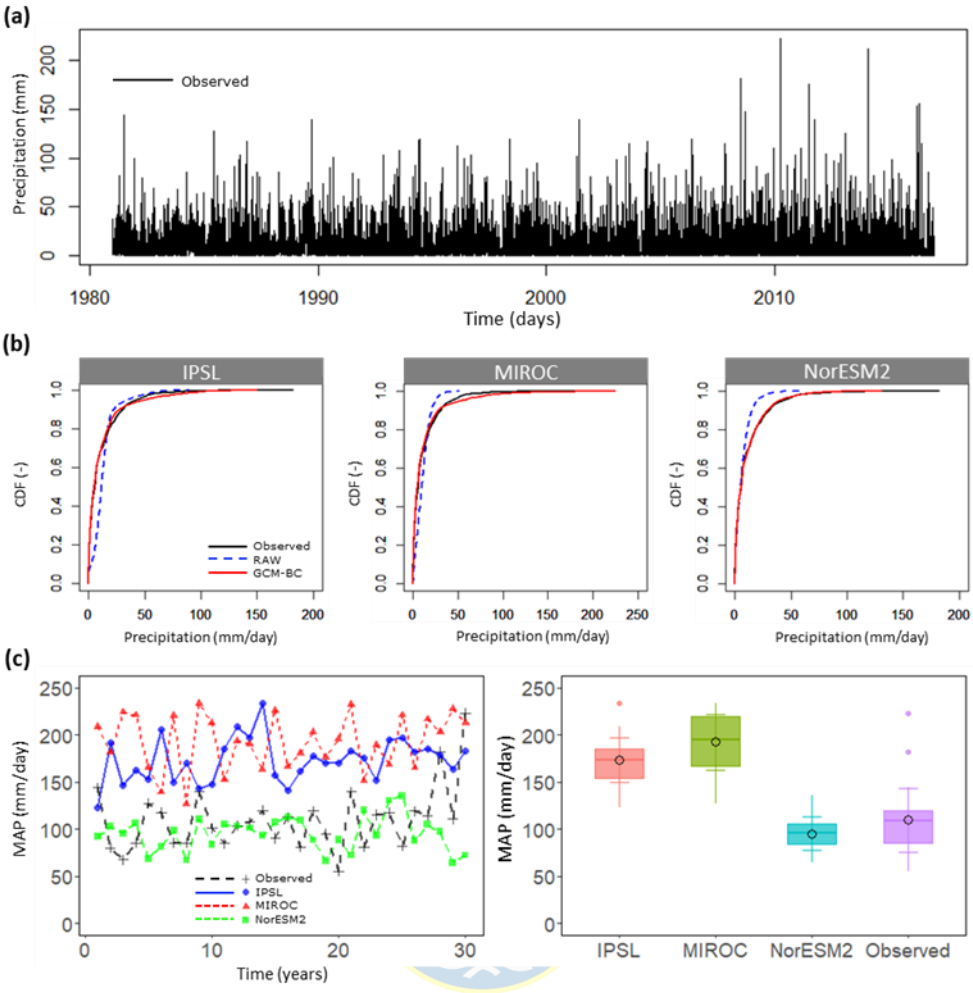

Figure 5.2. Precipitation intensity corrections of RAW GCM´s. (a) Observed daily precipitation from gauge M1219 (Tena Hda. Chaupishungo, the red square outside the basin in Figure 5.1.a); (b) CDF for three GCM´s (IPSL, MIROC and NorESM2, ensemble of current climate); (c) 30-year time series of MAP for observations (1980-2010) and future climate simulations (GCM-BC SSP5-8.5; 2041-2070); time series (left) and boxplots (right). Note that, the black circle in the boxplots represent the mean value of MAP.

Finally, the performance evaluation of three GCM-BC was carried out in order to select one GCM for the following stage (fitting distributions). Due to the purpose of the BC in this study is to fit frequency and intensity (overlapping observed and simulated CDF´s) rather than reproduce the daily time series. Thus, following the approach by Fang et al. (2015) and Manzanas et al. (2020), frequency-based statistics and the PDF score (-) were employed in the evaluation (see Table 5.1).

Table 5.1. Frequency-based statistics for the evaluation of GCM-BC simulations. Note that the observed and historical values correspond to the 30 % of testing data.

Frequency-based statistics	Observed	IPSL		MIROC		NorESM2	
		Historical	Future	Historical	Future	Historical	Future
mean (mm)	11.16	11.59	14.32	12.15	14.56	10.79	9.53
median (mm)	5.70	4.97	6.80	4.84	5.50	5.45	4.90
maximum (mm)	182.20	149.69	233.50	224.80	233.40	130.92	135.30
Standard Deviation (mm)	15.91	18.64	23.19	21.96	25.74	14.62	13.35
3rd quartile (mm)	15.00	14.30	17.30	13.65	15.50	14.87	12.70
PDF score (-)	-	0.88	-	0.88	-	0.95	-

The PDF score that ranges from 0 to 1 is a measure of the degree of overlap between two distributions, where 1 is a perfect coincidence. Although NorESM2 has the higher PDF score (0.95), in general terms, all GCM´s have a very good overlapping among distributions (>0.8). Also, the CFD of NorESM2 (Figure 2b) shows a slightly better fit. Additionally, while NorESM2 (-30%) and IPSL (-18%) underestimates the maximum values, the MIROC overestimates (23%). However, is important to note that future maximum value of NorESM2 is lower than observations. Thus, can´t be used for the evaluation of floods under scenarios of increasing precipitation due to climate change. Although the three GCM´s produced consistent results, enhaced overestimations and underestimations were produced by the MIROC and NoeESM2 respectively. The IPSL model was selected for the next stage as is produced the best performance and is considered the best performing model for Ecuador according to the Ministry of Environment (Armenta et al., 2016).

2.3.3. Fitting distributions

The extreme value distributions (EVD) are a type of probability density functions (PDF) used to model the behavior of extreme events such as floods or droughts (Gumbel, 1941; Kotz & Nadarajah, 2000). The observed (M1219) and simulated (IPSL) MAP were fitted to extreme value distributions using the maximum likelihood method (Engeland et al., 2004). Specifically, five distributions such as Gamma, Gumbel, log-Normal, Normal and Weibull, were fitted to obtain the MAP for three return periods: 2 (Rp2), 10 (Rp10) and 100 (Rp100) years (Figure 5.3). Additional details of distributions (e.g., definitions and equations) can be found in (Chow et al., 1988; Lima et al., 2021).

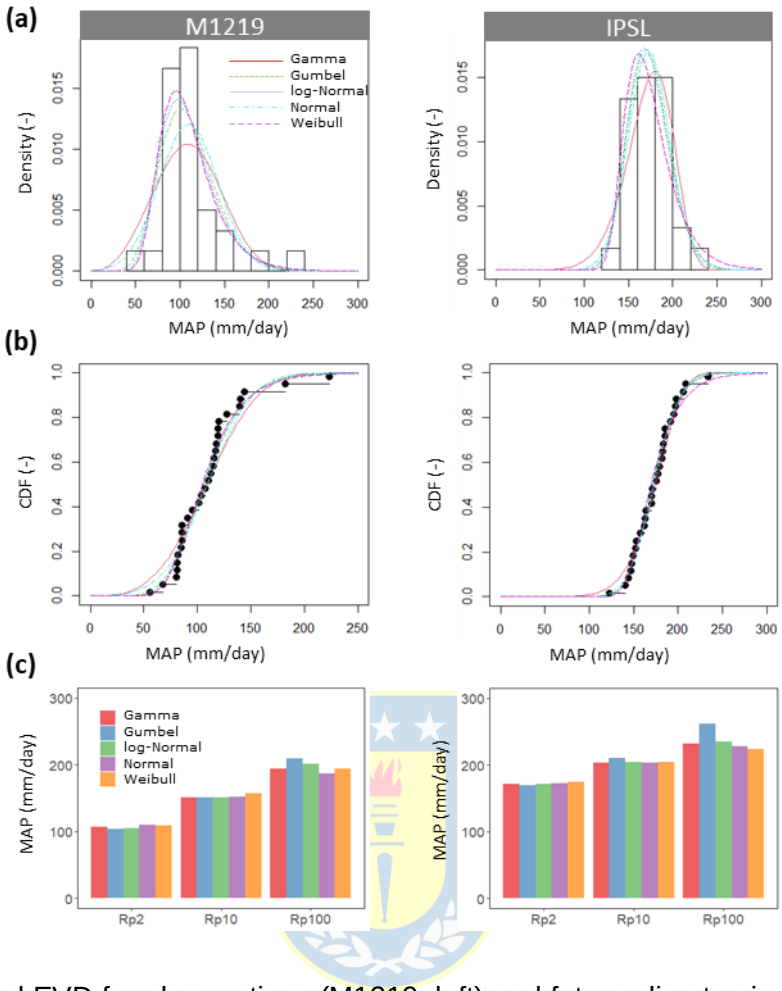

Figure 5.3. Fitted EVD for observations (M1219, left) and future climate simulations (IPSL, right). (a) Density plots; (b) CDF plots; (c) MAP for three return periods (Rp2, Rp10, Rp100).

An important aspect to consider when modeling probability distributions is the seasonality (Menéndez et al., 2009), as it can significantly affect the parameters and shape of the distribution over time. Thus, prior to fit distributions, the seasonality of MAP time series was corroborated with a certain confidence level ($\alpha = 0.05$) using the Dickey-Fuller test (Dickey & Fuller, 1979) implemented in tseries-package in R (Trapletti et al., 2023). Then, fitted distributions were obtained (Figure 5.3a, 5.3b), but also MAP for three return periods (Figure 5.3c).

The goodness of fit was evaluated for each probability distribution using the Kolmogorov-Smirnov (KS) test, Anderson-Darling (AD) test and Akaike´s Information Criterion (AIC) (Stephens, 2017). The KS and AD were evaluated with a confidence level of 0.05. With respect to AIC, the lower the value, the more parsimonious the model and better fitted to data. The fitted distributions (Fig. 5.3a, 5.3b) and the statistical test/criteria for the goodness of fit evaluation (Table 5.2)

were obtained using the functions implemented in the fitdistrplus-package in R (Delignette-Muller & Dutang, 2015).

Table 5.2. Goodness of fit statistics/criteria of fitted distributions.

Goodness of fit statistics/criteria	Observed					IPSL				
	Gamma	Gumbel	log-Normal	Normal	Weibull	Gamma	Gumbel	log-Normal	Normal	Weibull
Kolmogorov-Smirnov test (-)	0.14	0.11	0.12	0.18	0.18	0.07	0.11	0.07	0.08	0.10
Anderson-Darling test (-)	0.53	0.41	0.44	0.94	1.17	0.16	0.35	0.17	0.16	0.36
Akaike´s Information Criterion (-)	293.49	291.58	292.06	299.14	300.65	278.01	280.54	278.13	278.33	281.37

In general, all distributions had good performance (>0.05) with both KS and AD test. The AIC criterion indicates that log-Normal and Gumbel distributions performed slightly better for observations, while log-Normal and Normal distributions perform slightly better for IPSL. Thus, the log-Normal distribution was selected for design storms in the following section. Note that, all distributions have very similar performance, especially for Rp2 and Rp10 (Figure 5.3c).

2.3.4. Design storms

Design storms were used to evaluate the influence of climate change and LUCC on floods. Storm intensities for different return periods (Rp2, Rp10, Rp100) were obtained from the maximum annual precipitation and equations proposed by the National Hydrometeorological and Institute (INAMHI, 2019). Then, storms were constructed following the non-symmetric altering blocks method (Chow et al., 1988) with a total duration of 220 minutes, equivalent to concentration time of TRB (Hurtado-Pidal et al., 2020). For the current climate, the maximum rainfall intensity for Rp2, Rp10 and Rp100 was 16, 24 and 32 mm/10 min respectively. While for the future climate, the maximum rainfall intensity for Rp2, Rp10 and Rp100 was 27, 33 and 38 mm/10 min respectively (Figure 5.4).

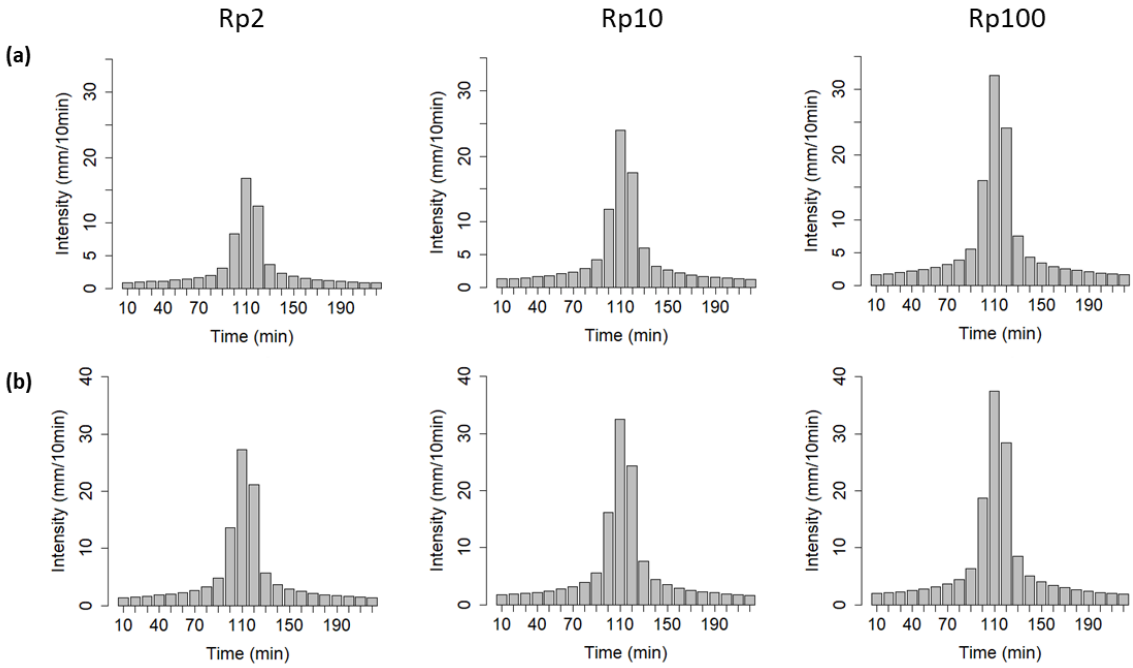

Figure 5.4. Design storms for three return periods (Rp2, Rp10, Rp100). (a) Current climate (observations, M1219). (b) Future climate (GCM-BC IPSL SSP5-8.5).

Note that the increment of maximum intensities due to climate change is 11, 9 and 5 mm/10 min for Rp2, Rp10 and Rp100 respectively. Thus, as the return period increases, the relative effect of climate change diminishes.

2.4. LUCC scenarios

The impact of LUCC (i.e., deforestation) was analyzed using two simple hypothetical scenarios: either a forest or agriculture covering the entire basin (what if approach). This approach has the advantage of isolating the effect of spatial variability of LUCC on the hydrological system since the entire basin has the same land cover. Moreover, this approach avoids the need to use a specific base line period, which could increase uncertainties in the analysis of contribution (Zhang et al., 2018). In addition, the contrast between scenarios is enhanced allowing the differentiation on stormflows changes. Thus, the scenario of forest with current climate (S1, Figure 5.5a) was established as base line scenario. Similarly to Hurtado-Pidal et al., 2022, the model parameters changing among the scenarios are: canopy interception capacity, and soil static storage. Evapotranspiration was not considered as a variable due to its negligible impact during short flash floods. Therefore, the mean values of canopy interception capacity and soil static storage were 10 and 105 mm for forest and 1 and 58 mm for agriculture, respectively.

2.5. Stormflow sampling sites

One advantage of using a fully spatially-distributed hydrological model such as TETIS is the ability to obtain outputs for any cell within the simulation domain (watershed). However, it is important to achieve a good compromise between the number of sampling sites and the stability of the results. Thus, a total of 42 points were automatically generated at intervals of 3 km to simulate the stormflows (m^3/s) along the TRB stream network (see Figure 5.1a). This systematic sampling allowed analyze the effect of climate change and LUCC at different scales along the altitudinal gradient. The 'st_line_sample' function from the 'sf-package' (Pebesma, 2023) in R was used for this purpose.

2.6. Scenarios analysis

The hydrological simulations were carried out following a factorial design of two variables, with two levels each one. This resulted in four (2^2) possible scenarios (combinations) between climate change and LUCC (Figure 5.5a) for three return periods. Following the methodology proposed by Zhang et al., 2018, the scenarios were used to separate (and combine) the effect of climate change and LUCC on stormflows with one-factor-at-a-time (OFAT) analysis. Since the S1 was established as the base line scenario, the pairs to evaluate the individual effect of climate change and LUCC were S2-S1 and S3-S1 scenarios, respectively. The combined effect was evaluated with S4-S1 scenarios. These scenarios were analyzed with two approaches described in the following sections.

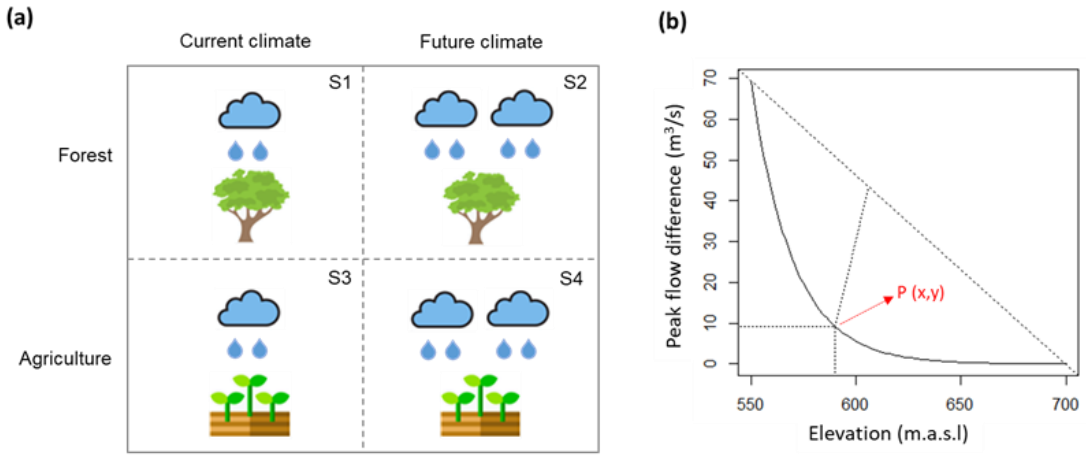

Figure 5.5. Schematic representation of (a) Scenarios: S1: forest with current climate, S2: forest with future climate, S3: agriculture with current climate, S4: agriculture with future

climate, (b) Point (x,y) of maximum curvature as a threshold of abrupt changes in peak flow (and stormflow volume) difference, where x-axis is the critical elevations and y-axis is the critical difference. Note that, the upper and lower basin, from maximum curvature, P(x,y), have small and high differences, respectively.

Evaluation of effects of climate change and LUCC with statistical tests: For the three return periods, the statistical differences of stormflows among scenarios S1 to S4 were analyzed using the non-parametric Kruskal-Wallis test (Kruskal & Wallis, 1952). The Kruskal-Wallis test is a non-parametric alternative to one-way ANOVA and has been applied to evaluate the effects of climate change and LUCC on floods when data was non-normal (Jodar-Abellan et al., 2019; Singh et al., 2005). Therefore, the non-normality of the stormflow series was corroborated with the Shapiro Test (Shapiro & Wilk, 1965). The null hypothesis in the Kruskal-Wallis test (no difference among scenarios) is generally evaluated with a confidence level of 0.05. However, this value was used only as a reference since our goal was to evaluate general change patterns in the altitudinal gradient, rather than a specific confidence level (i.e., $\alpha = 0.05$). This reasoning applies to the other tests (i.e.: Dunn and Scheirer-Ray-Hare tests). Further details about this statistical test can be found in (MacFarland & Yates, 2016).

The individual and combined contribution of climate change and LUCC was determined comparing the statistical differences among pairs: S2-S1 for climate change; S3-S1 for LUCC; and S4-S1 for both, climate change and LUCC. Therefore, after the Kruskal-Wallis test, a post-hoc analysis was carried out with Dunn test (Dunn, 1964) using the ´BH' method to adjust p-values, similarly to Hurtado-Pidal et al. (2022) and Jodar-Abellan et al. (2019). Additionally, as a complementary analysis, the contribution of independent variables (climate change and LUCC) over dependent variable (stormflows) and their interaction, was assessed with the Scheirer-Ray-Hare test (Sokal & Rohlf, 1969). This test is the non-parametric alternative to two-way ANOVA and is used to analyze the individual contribution and interactions among factors (variables) with two or more levels. Finally, the exponential decay equations were fitted to analyze the relationship among elevations (m.a.s.l, x-axis) and p-values (y-axis) for the three return periods. The coefficient of determination R^2 was used to measure the goodness of fit, which quantifies the proportion of the variance present in the observed data that can be explained by the model. R^2 ranges from 0 to 1, where higher values imply reduced error variance and values greater than 0.5 are considered acceptable (Moriasi et al., 2007).

Evaluation of effects of climate change and LUCC with absolute differences: For the three return periods, the absolute differences of peak flows (m^3/s) and stormflow volumes (SFV, Hm^3) were evaluated applying the methodology proposed by Yang et al. (2017) and Zhang et al. (2018) with the following equations:

$$\Delta Qp_C = \frac{1}{2}[(Qp_{L1}^{C2}) - (Qp_{L1}^{C1}) + (Qp_{L2}^{C2}) - (Qp_{L2}^{C1})] \quad (1)$$

$$\Delta Qp_L = \frac{1}{2}[(Qp_{L2}^{C1}) - (Qp_{L1}^{C1}) + (Qp_{L2}^{C2}) - (Qp_{L1}^{C2})] \quad (2)$$

$$\Delta Qp = \Delta Qp_C + \Delta Qp_L = Qp_{L2}^{C2} - Qp_{L1}^{C1} \quad (3)$$

where ΔQp_C, ΔQp_L and ΔQp are the individual and combined effect on peak flows (or SFV) of climate change, LUCC and climate change and LUCC, respectively. Note that L1, L2, C1, C2 are forest, agriculture, current climate and future climate respectively. Thus, for peak flows, Qp_{L1}^{C1}, Qp_{L1}^{C2}, Qp_{L2}^{C1}, Qp_{L2}^{C2} are the S1, S2, S3 and S4, respectively. Additionally, the interaction was assessed as follows:

$$IQp = (Qp_{L2}^{C2} - Qp_{L1}^{C1}) - \left((Qp_{L1}^{C2} - Qp_{L1}^{C1}) + (Qp_{L2}^{C1} - Qp_{L1}^{C1})\right) \quad (4)$$

The univariate exponential decay equations were fitted to analyze the differences and interactions of peak flows and SFV across the altitudinal gradient. As a complementary analysis, a lineal equation was fitted between SFV interaction and flow accumulation. The goodness of fit was assessed with the coefficient of determination R^2. Additionally, the maximum curvature was evaluated in the fitted exponential decay equations. The maximum curvature is proposed as a point of abrupt change in the differences of peak flows and SFV along the altitudinal gradient (Figure 5.5b). Thus, the point coordinates of maximum curvature are the critical-elevation (x-axis) and the critical-difference (y-axis). The maximum curvature point of exponential decay fitted equations, was determined with the 'maxcurv' function from the 'soilphysics-package' in R (Silva & Lima, 2017). Finally, the peak flows at the basin outlet were obtained, in order to analyze specifically the implications of climate change and LUCC for floods in the city of Tena. All statistical analysis and graphics were achieved with R.

3. Results

3.1. Effects of climate change and LUCC with Kruskal-Wallis test

The results of Kruskal-Wallis test to evaluate the effect of climate change and LUCC with three return periods (Rp2, Rp10, Rp100), are shown in Figure 5.6. The

fitted exponential decay equations indicate excellent performance, with R^2 values higher than 0.8 for Rp10 and Rp100. Thus, the pattern of changes across elevations is clear. The difference in stormflow among scenarios is higher in the upper basin (low p-values) indistinctly of the return period from elevations above 1250 m approximately (p-value ≈ 0.005). However, as the altitude decreases from medium to lower elevations within the basin (≈ < 1000 m.a.s.l), the scenarios become more similar. Additionally, as the storm intensifies, the differences between them further decrease. Using a confidence level of 0.05 as a reference, the Table 5.3 show the percentage of stormflow sampling sites with p-values below this value. For Rp2 almost all sampling sites (95%) has a statistically significant difference among scenarios. While, for Rp10 and Rp100 less than a half have p-values below 0.05, especially in the upper basin.

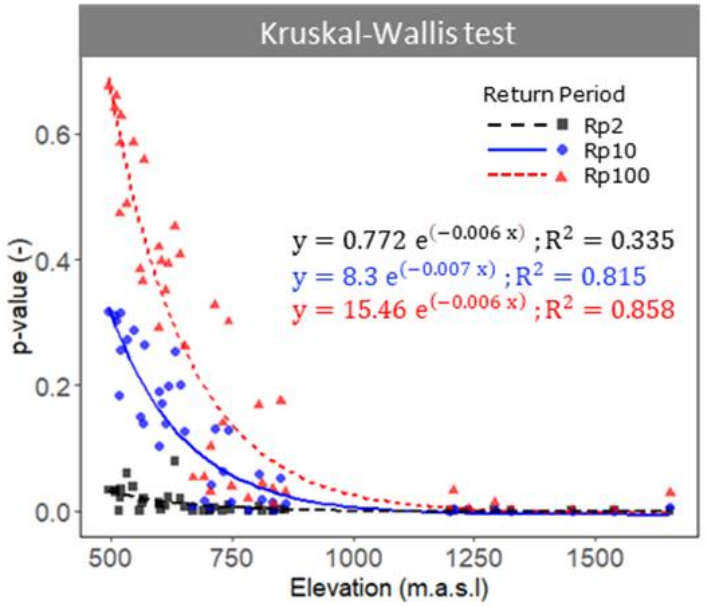

Figure 5.6. Relationship between p-values of Kruskal-Wallis test (y-axis) and elevations in the basin (x-axis) for three return periods; Rp2 (black dashed line and square points), Rp10 (blue solid line and circle points), Rp100 (red dashed line and triangle points).

Table 5.3. Percentage of stormflows sampling sites with p-values below 0.05.

Factor	Kruskal-Wallis test			Dunn Test			Scheirer-Ray-Hare test		
	Rp2	Rp10	Rp100	Rp2	Rp10	Rp100	Rp2	Rp10	Rp100
Climate change				0.24	0.00	0.00	1.00	0.12	0.00
LUCC	0.95	0.43	0.36	0.17	0.14	0.12	0.62	0.50	0.50
Climate change and LUCC				0.98	0.50	0.24	0.00	0.00	0.00

3.2. Effects of climate change and LUCC with Dunn test

Figure 5.7 shows the results of post-hoc analysis with Dunn test for evaluating both the individual and combined effects of climate change and LUCC on floods. For climate change effect (Figure 5.7a), the fitted exponential decay equations indicate satisfactory results in general terms, with R^2 values higher than 0.7 for Rp10 and Rp100. The effect of climate change is relatively homogeneous for Rp2, while the fitted curve for Rp100 and especially Rp10 shows an abrupt change in the gradient on the lower part of the basin (≈ < 750 m.a.s.l). Overall, the effect of climate change in the upper basin is higher than in the lower basin. Also, as storm is more intense the influence of climate change on floods becomes marginal. Regarding the significance level, only the Rp2 has sampling sites (24%, Table 3) with p-values below 0.05 (702 m.a.s.l).

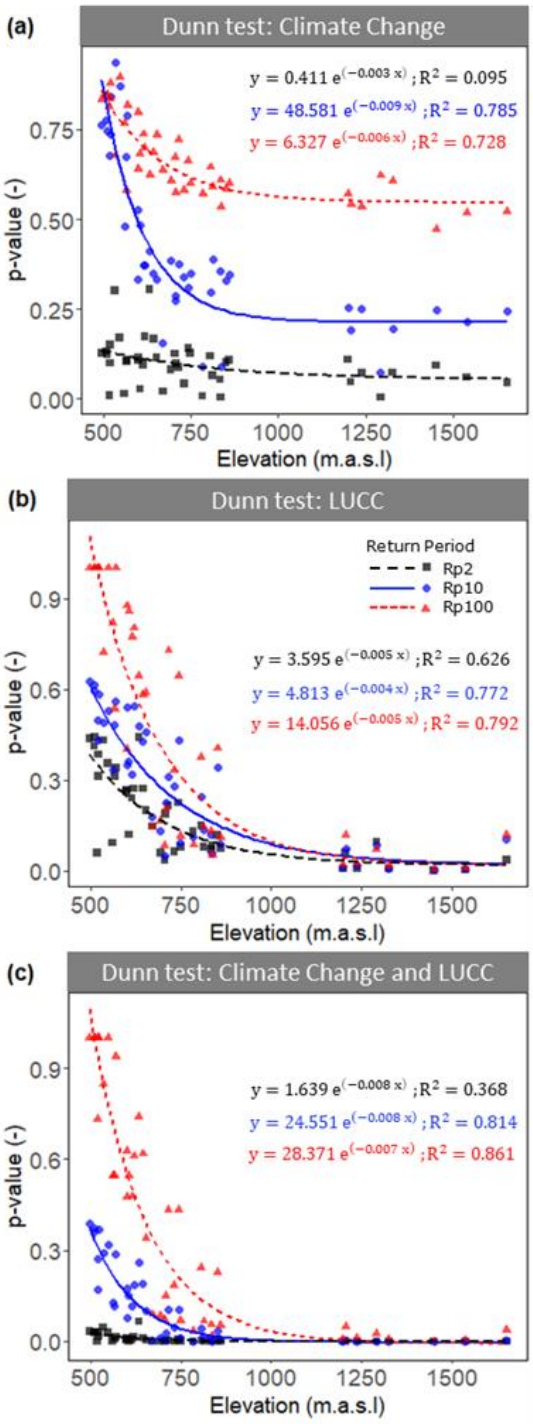

Figure 5.7. Relationship between p-values of Dunn test (y-axis) and elevations in the basin (x-axis) for three return periods in the evaluation of (a) Climate change, (b) LUCC and (c) Climate change and LUCC. Symbology description is the same as Figure 5.6.

The LUCC effect over stormflows with Dunn test (Figure 5.7b) show satisfactory fitted equations in all cases (R^2 > 0.6). The effect of LUCC is heterogeneous with higher effect in the upper part of the basin (e.g., for Rp2, p-value = 0.05, elevation = 874 m.a.s.l) and smaller effect in the lower part (p-values > 0.05). The stormflow sampling sites with p-values below 0.05 decreases progressively (Table 5.3) as storm increases (e.g. 17 and 12% for Rp2 and Rp100 respectively).

Figure 5.7c depicts the results of the combined effect of climate change and LUCC through the Dunn test. The fitted exponential decay equations indicate excellent performance for Rp100 and Rp10 (R^2 > 0.8), and moderate performance for Rp2 (R^2 = 0.4). Also, the combined effect is relatively homogeneous for Rp2 (p-values with lower dispersion) but heterogeneous for Rp10 and Rp100 (p-values with higher dispersion, Figure 5.8a). In this regard, the combined effect of climate change and LUCC is higher in the upper part of the basin, and the smaller in the lower part (e.g., for Rp2, p-value = 0.05, elevation = 906 m.a.s.l).

Note that for Rp2, almost all sampling sites (98%) has p-values below 0.05 for combined effect using Dunn test. However, as the storm intensity increases, the percentage of sampling sites with p-values below 0.05 is smaller (Table 5.3). Thus, these results suggest that smaller stormflows (Rp2) are more strongly affected by both climate change and LUCC.

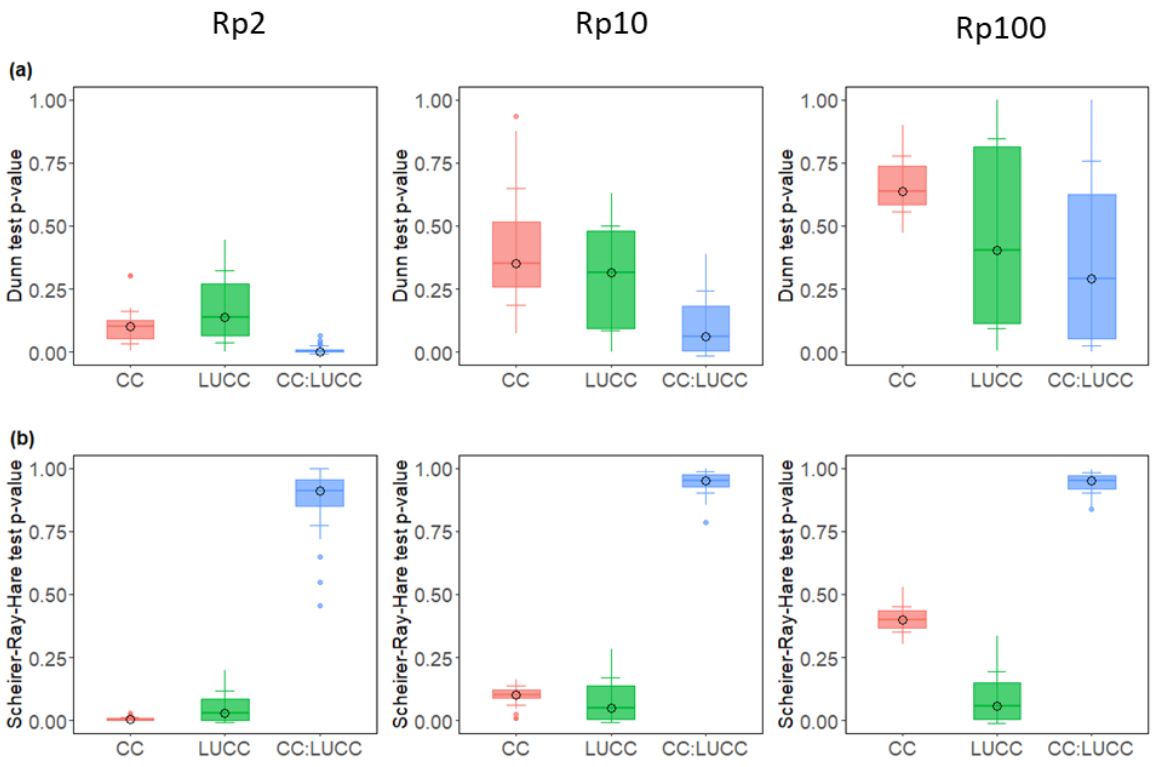

Figure 5.8. Boxplots of p-values from individual and combined effects of climate change (CC) and LUCC with three return periods (Rp2, Rp10, Rp100). (a) Dunn test and (b) Scheirer-Ray-Hare test. The black circle in the boxplots indicate the median value.

3.3. Effects of climate change and LUCC with Scheirer-Ray-Hare test

Figure 5.9 shows the results of the Scheirer-Ray-Hare test, which is the non-parametric analysis equivalent for a two-way ANOVA. The results show the individual effects of climate change and LUCC. The effect of climate change is relatively homogeneous across the gradient, with greater dispersion in the lower basin (Figure 5.9a). The effect of climate change is higher in the upper basin and smaller in the lower basin. Also, as storm is more intense the influence of climate change is smaller. Note that only for Rp2, all sampling sites (100%) have p-values below 0.05 (see Table 5.3).

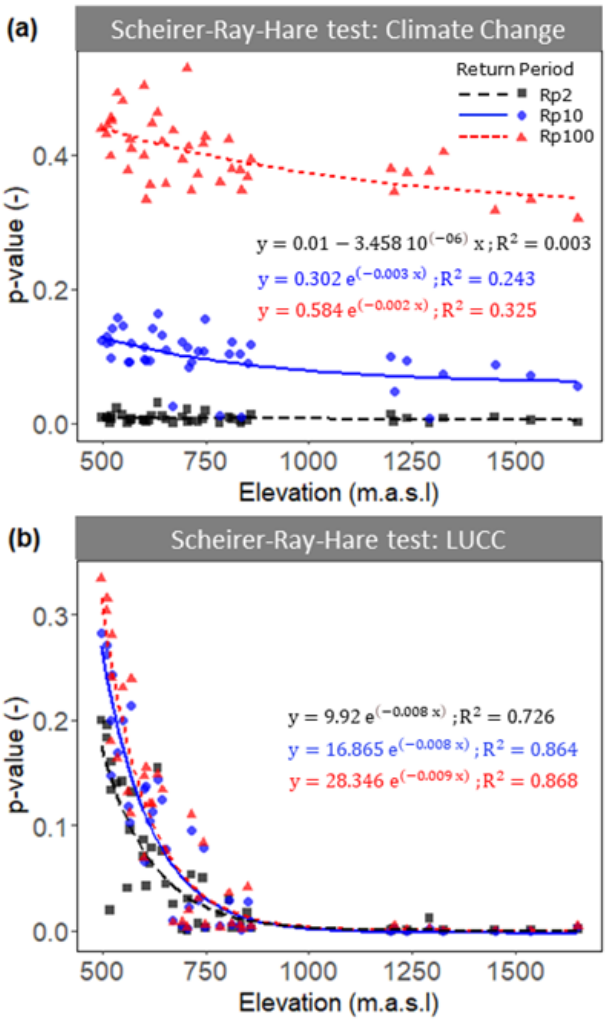

Figure 5.9. Relationship between p-values of Scheirer-Ray-Hare test (y-axis) and elevations in the basin (x-axis) for three return periods in the evaluation of (a) Climate change and (b) LUCC. Symbology description is the same as Figure 5.6.

The LUCC effect over stormflows with Scheirer-Ray-Hare test (Figure 5.9b) shows satisfactory fitted equations in all cases ($R^2 > 0.7$). The effect of LUCC varies across the basin, with a higher effect in the upper part (e.g., for Rp2, p-values = 0.05, elevation = 661 m.a.s.l) and a smaller effect in the lower part (p-values > 0.05). For Rp2, 60% of stormflow sampling sites have p-values below 0.05, whereas for Rp10 and Rp100, only 50% of sampling sites are below this confidence level (Table 5.3). Also, the combined effects of climate change and LUCC indicate no significant interaction between these factors (p-values > 0.05, Figure 5.8b, Table 5.3). However, a very small interaction is observed for Rp2 events, which decreases progressively with increasing storm intensity.

In summary, the results obtained with the three statistical tests (Kruskal-Wallis, Dunn, and Scheirer-Ray-Hare test's) indicate the same spatial pattern across elevations regarding the effects of climate change and LUCC over stormflows. In general terms, the stormflows in the upper part of the basin are more sensitive to perturbations triggered by climate change or LUCC and their combination, than those in the lower part. Additionally, when the factors are isolated, the climate change have greater influence for Rp2, and LUCC greater influence for Rp10 and Rp100 (Table 5.3). Also, the LUCC influence is higher in the upper than in the lower basin (≈ > 1000 m.a.s.l), regardless of the storm intensities. However, the effect of LUCC is more varied than climate change across elevations because of the p-value dispersion (Figure 5.8a and 5.8b). It is worth noting that the combined effect notably enhances the changes in the upper part of the basin, especially for Rp2 (98% of sampling sites with p-values < 0.05, as indicated in Table 5.3). Nevertheless, as storm intensity increases, the effect of these factors in the lower part of the basin becomes smaller.

3.4. Effects of climate change and LUCC with absolute differences

Figure 5.10 and Table 4 show the individual and combined effect of climate change and LUCC over peak flows (m^3/s) and SFV (Hm^3) from three return periods. The fitted exponential decay equations indicate in all cases satisfactory results (R^2 ≥ 0.7) for both variables (peak flows, SFV). Also, the individual effect of climate change produces greater differences, than those generated by LUCC (Figure 5.10a, 5.10b). However, as expected, the combined effect of these factors produces even higher differences for peak flows and SFV (Figure 5.10c, Figure 5.11).

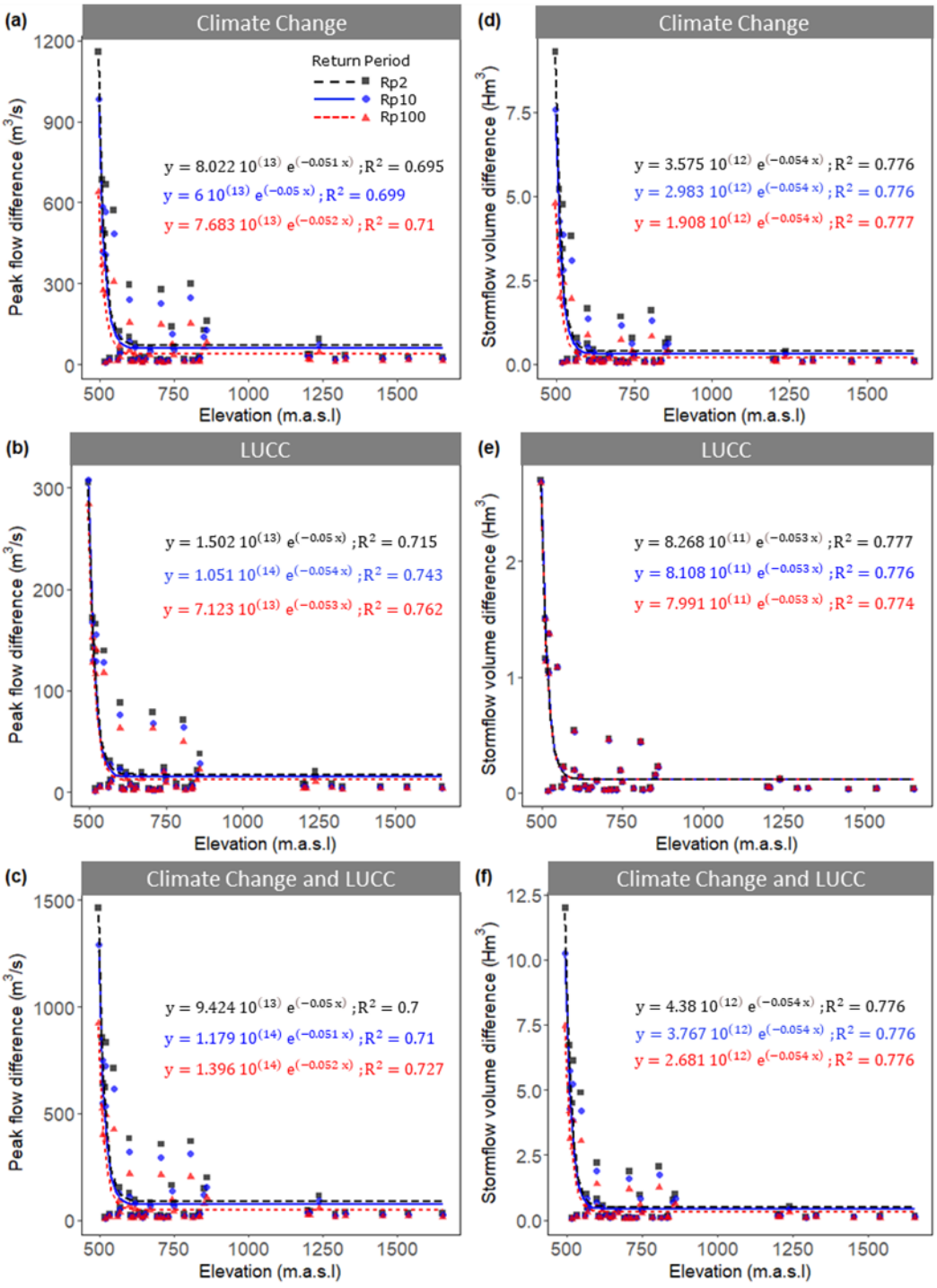

Figure 5.10. Relationship between absolute differences (y-axis) and elevations in the basin (x-axis) for three return periods in the evaluation of (a) Climate change, (b) LUCC and (c) Climate change and LUCC. The left and right panel correspond to peak flows difference and SFV difference respectively. Symbology description is the same as Figure 5.6.

Table 5.4. Coordinates (x,y) of maximum curvature related to abrupt changes in Figure 5.10. (a) critical elevation (m.a.s.l), (b) critical difference of peak flows (m^3/s) and SFV (Hm^3).

(a) Critical elevation (x-axis)						
Factor	Peak flow			Stormflow volume		
	Rp2	Rp10	Rp100	Rp2	Rp10	Rp100
Climate change	590.12	590.21	589.67	588.77	588.77	588.77
LUCC	590.39	588.86	589.10	588.95	588.98	588.98
Climate change and LUCC	590.18	589.88	589.49	588.83	588.83	588.83
(b) Critical difference (y-axis)						
Factor	Peak flow			Stormflow volume		
	Rp2	Rp10	Rp100	Rp2	Rp10	Rp100
Climate change	9.15	7.93	4.69	0.06	0.05	0.03
LUCC	2.56	1.96	1.91	0.02	0.02	0.02
Climate change and LUCC	11.70	9.85	6.59	0.08	0.07	0.05

In general terms, the critical elevations (threshold of changes by the maximum curvature) for peak flows and SFV are localized, in average, at 590 and 589 m.a.s.l respectively (Table 5.4a). In addition, as storm intensity increases the critical difference declines (Table 5.4b). However, the isolate effect of LUCC over SFV generates the same difference (0.2 Hm^3) regardless of storm intensity (Figure 5.10b, Figure 5.11b).

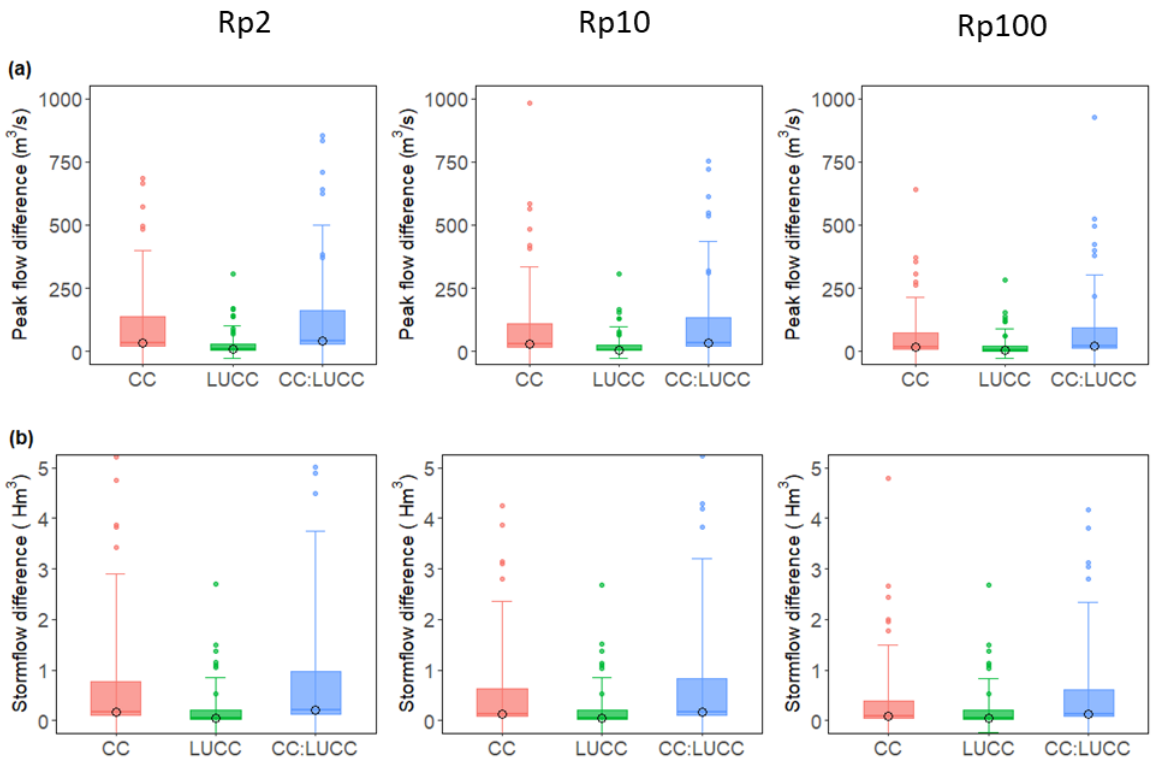

Figure 5.11. Boxplots of absolute differences from individual and combined effects of climate change (CC) and LUCC with three return periods (Rp2, Rp10, Rp100) for (a) peak flow difference and (b) stormflow volume difference. The median value is represented by the black circle in the box plots. Note that the y-axis was limited to enhance visualization of values near the mean: 0-1000 for peak flow and 0-5 for stormflow volume.

For Rp2 the combined results of break points of statistical tests (p-value = 0.05) and absolute differences (maximum curvature), allow the establishment of an altitudinal range from 590 to 906 m.a.s.l approximately. This is the transitional area in terms of influence (individual and combined with climate change) of LUCC on stormflows.

3.5. Interactions between climate change and LUCC with absolute differences

Figure 5.12 shows the interaction between climate change and LUCC, from stormflow volume with different return period. The fitted exponential and linear equations show an antagonistic interaction pattern. In other words, the individual sum of factors is greater than the combined effect. The fitted exponential equations (Figure 5.12a) show satisfactory results, especially for Rp10 and Rp100 ($R^2 \geq 0.7$). The interaction is very small, regardless the storm intensity, up to 590 m.a.s.l

(elevation for maximum curvature, Table 4). However, from this elevation to downstream the interaction increases slightly, especially for Rp2.

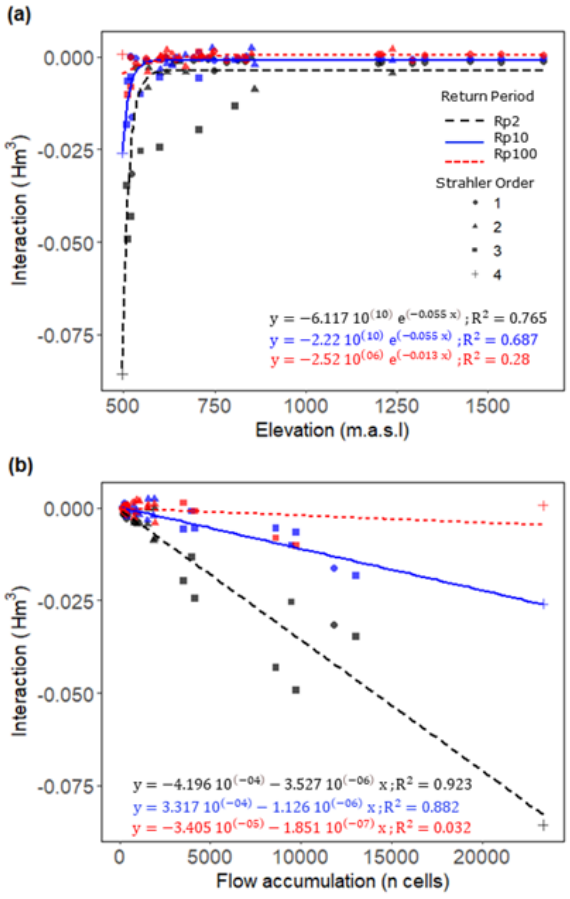

Figure 5.12. Relationship between climate change and LUCC interaction (y-axis, equation 1) using SFV with (a) elevation in the basin (x-axis), (b) flow accumulation (x-axis, drainage area expressed in number of cells of 100 x 100 m) for three return periods; Rp2 (black dashed line), Rp10 (blue solid line), Rp100 (red dashed line). Also, the Strahler order is represented by different point symbols; 1 (circle), 2 (triangle), 3 (square), 4 (plus).

The relationship of interactions between climate change and LUCC with flow accumulation (Figure 5.12b), fitted with linear equations, show satisfactory results overall, especially for Rp2 and Rp10 ($R^2 \geq 0.9$). The sampling sites with Strahler order 3 and 4 (downstream) show different level of interactions across return periods. In this regard, the Rp2 show higher interaction. However, Strahler order 1 and 2 (mainly upstream) show small interaction values for all return periods.

In summary, the results suggest that there is a very small antagonistic interaction between climate change and LUCC. This interaction increases slightly to

downstream as storm intensity decrease, especially for streams with Strahler order 3 and 4.

3.6. Effects of climate change and LUCC at the basin outlet

Finally, Table 5.5 shows the results of relative contribution (%) both the individual and combined effects, of climate change and LUCC over peak flows (m^3/s) at the basin outlet (city of Tena, Figure 5.1). The isolate effect of climate change is greater than LUCC effect, especially for Rp2 (131 %). However, as storm becomes more intense, the individual and combined effect of factors decline.

Table 5.5. Relative contribution of individual and combined effect of climate change (CC, %) and LUCC (%) over peak flows (m^3/s) at the basin outlet (TRB).

Rp	Forest		Agriculture		CC	LUCC	CC and LUCC
	Current	Future	Current	Future	effect (%)	effect (%)	effect (%)
Rp2	894	2066	1212	2358	131.10	35.57	163.76
Rp10	1683	2670	1996	2973	58.65	18.60	76.65
Rp100	2628	3285	2929	3552	25.00	11.45	35.16

Additionally, it is shown an antagonistic interaction with regard peak flows at the outlet, since the sum of the individual effect of factors are greater than the combined effect. For instance, Rp2 generates a change of 166.67 and 163.76 %, for individuals and combined effects respectively. However, in concordance with previous results, the difference among individual and combined effects decreases as storm intensity increase.

In summary, the results suggest that in the upper basin stormflows are more sensitive to LUCC, while in the lower basin stormflows are more sensitive to climate change. Therefore, even with the hypothetical scenario of whole basin covered by forest, the climate change will have a much greater contribution, especially for frequent storm events (Rp2). However, as storm intensity increases the interaction, and the relative effect of factors over peak flows decreases.

4. Discussion

4.1. Climate change projections in the Ecuadorian Amazon and implications for the city of Tena

Our results showed and increment of 28 % in mean daily precipitation between observed (M1219) and middle future simulated climate (2041-2070; IPSL SSP5-8.5). Segarra (2022) found an increment of 21 % in daily precipitation for Colonso basin (within the TRB) due to climate change under RCP8.5. However, the difference (28 v/s 21%) can be attributed to the fact that CMIP6 simulates, in general, more precipitation than CMIP5 (Kim et al., 2020). Moreover, one of the improvements of IPSL-CMIP6 is the capacity to better simulate extreme precipitations and reducing the dry Amazon basin bias (Boucher et al., 2020). However, despite the small discrepancies in magnitude, several studies consistently project an increase in precipitation in the northwest Amazon region, near the Andes foothills (Almazroui et al., 2021; Pabón-Caicedo et al., 2020; Palomino-Lemus et al., 2017; Sarmiento & Kooperman, 2019; Solman, 2013). The ensemble regional climate model of Ecuador under RCP8.5 also indicates a projected increase of approximately 15% in monthly precipitation for the north-central Ecuadorian Amazon region, as reported by the Environmental Ministry of Ecuador (Armenta et al., 2016). Additionally, mean annual runoff and floods are projected to increase in this region due to climate change (Hirabayashi et al., 2013; Sorribas et al., 2016). Our results about IPSL SSP5-8.5 middle future projections (2041-2070) are in agreement with the projections of precipitation intensity and floods for the study area.

The peak flow at the basin outlet changed from 894 to 2066 m^3/s for Rp2, with the considered climate change scenario (Table 5.5). Previous studies in TRB simulated, with different modeling approach, the flood occurred in the city of Tena in September 2017. For instance, Chancay & Espitia-Sarmiento (2021), simulated with GR4H model at hourly time step a peak flow of 1379 m^3/s. Also, Hurtado-Pidal et al. (2020) simulated with HEC-HMS model at minute time step a peak flow of 1967 m^3/s, for the same event. Thus, in the future (2041-2070), climate change alone has the capacity to produce floods in the city of Tena every two years on average, even when the entire basin is covered by forest.

In the base scenario (forest with current climate), the peak flow for Rp10 is 1683 m^3/s (Table 5.5) which is enough to overflow the channel banks and cause floods (Chancay & Espitia-Sarmiento, 2021). Therefore, due to climate change, it is probable that the frequency of floods will change from once every 10 years to at least once every 2 years, in average. In other words, the probabilities of producing floods in the city of Tena during any given year will change from 10 (current) to 50 % (future). Considering the numerous floods that have occurred in recent years (3 in the last 10 years), this scenario is even more discouraging from the perspective of the risk it poses to the inhabitants (GADM-TENA, 2021).

4.2. Individual effects of climate change and LUCC on floods

We presented for the first time an evaluation of the effect of climate change and LUCC across the altitudinal gradient in a humid tropic catchment distinguishing the individual and combined effect on stormflows. Despite the relatively high effect of LUCC on stormflows in the upper basin, our results also indicate that climate change has greater influence by absolute differences in peak flow and stormflow volume, SFV (Figure 5.10 and Figure 5.11). Although the effects of climate change and LUCC on floods are site-specific, it appears that, in general, climate change has a greater influence on key hydrological variables such as annual runoff. Shang et al. (2019) found a relative contribution from climate change and LUCC to the runoff generation over a basin in China of 87% and 53%, respectively. Additionally, Lian et al. (2020) reported that human activities such as LUCC and management practices account for 57% and 78% of runoff in two basins, respectively, while precipitation in non-flood season accounts for 84% and 172%, respectively. Furthermore, Lamichhane & Shakya, (2019) observed an increment in river runoff of 37% and 21% for the individual effects of climate change and LUCC, in a basin in Nepal, respectively. On the other hand, the individual effects of climate change and LUCC can be in the opposite direction, resulting in a decrease in mean annual runoff, such as the results reported by Krajewski et al. (2021), regarding a contribution on runoff reductions due to climate change and LUCC of up to 80% and 40%, respectively. Therefore, in general, the climate change has a greater contribution than LUCC to runoff and floods (Chawla & Mujumdar, 2015; Hung et al., 2020; Tian et al., 2022; Wang & Stephenson, 2018; Zhang et al., 2018). Specially for small LUCC variations below 20% of the basin area (Bathurst et al., 2020). However, even in landscapes dominated by saturation-excess overland flow, the processes of runoff are susceptible to scale (Edokpa et al., 2022). Thus, the effect of LUCC on stormflows is not only limited, but is gradually decreasing in the downstream direction which can be explained in part by the scale process (Rogger et al., 2017). In other words, even with large scale of intervention, such as deforestation, the greater the distance downstream the smaller will be the impact even when large scale deforestation takes place (Lane, 2017). Therefore, while LUCC is more important at smaller basins (e.g., < 100 km2), climate can have effects even at higher scales (Blöschl et al., 2007; Chang & Franczyk, 2008; Hung et al., 2020). Blöschl et al. (2007) and Dadson et al. (2017) indicate that the impact of LUCC on river flows is small compared with natural climate variability. Moreover, they indicate that at smaller scales, LUCC has a larger impact than climate variability on hydrological response. In this regard, this research showed that LUCC has a greater and significant influence on floods in the upper basin than climate change. Then, as the flow moves downstream the influence is reduced. Similar to Blöschl et al. (2007), the climate change showed a more

homogeneous effect than LUCC on stormflows across the altitudinal gradient, being more important climate change than LUCC in the downstream part of the study basin.

The higher effect of LUCC observed in the upper basin is explained by higher connectivity during storms due to soil moisture and steep slopes. Previous research in the TRB (Hurtado-Pidal et al., 2022) showed that deforestation in the upper part of the basin is the worst scenario regarding floods. Olang & Fürst, (2011), also found that upper basin deforestation produces the highest effects on peak flows due to the steep slopes. Additionally, Shuttleworth et al. (2019) found that restoration of upland basins in UK can contribute to natural flood management reducing peak flows by 27% and increasing lag times by 106%. The soil moisture and steep slopes play a determinant role in the flow connectivity and thus in the increment of subsurface stormflow rates (Blöschl, 2022; Crespo et al., 2011). The higher influence of LUCC in the upper basin is related to the scale processes and physical characteristics such as soil moisture, saturated soil conductivity and steep slopes that enhance basin connectivity (Asano & Uchida, 2018; Birch et al., 2021; Edokpa et al., 2022; Gomi et al., 2008; Hopp & McDonnell, 2009).

The obtained results also show that as storm becomes more intense the relative influence of forest cover on stormflows decrease, which is in agreement with other studies (Bathurst et al., 2020; Iacob et al., 2017; Laurance, 2007). Bathurst et al. (2011) conducted a study in Latin American basins using data analysis and model applications, which supported the hypothesis that the effect of forest cover decreases with increasing flood magnitude. Also, Birkel et al. (2012) showed for a humid catchment in Costa Rica that LUCC has relatively little effect on peak flows with return periods > 1-year.

4.3. Combined effects of climate change and LUCC on floods

The most important finding in the current research is related to the interaction between climate change and LUCC across the altitudinal gradient. The results using stormflow series show a statistically non-significant interaction (Scheirer-Ray-Hare test, p-value > 0.05). Also, the absolute differences of SFV indicate a slightly antagonistic effect in the lower part. These results together indicate a slightly but statistically non-significant interaction between climate change and LUCC. Some studies have show both antagoninstic and synergistic interactions at basin scale (e.g.: Hung et al., 2020; Lamichhane & Shakya, 2019). Lamichhane & Shakya, (2019) obtains an antagonistic interaction for future projections in annual river runoff, since the percentage of change for climate change, LUCC and combined were 37,

21, 12 %, respectively. In contrast, Hung et al. (2020) found at monthly time scale, an increase in peak discharges, respect to base line, of 118% for the combined effects, while the individual effect of climate change and LUCC, were 83 and 27 %, respectively (≈ 8 % due to synergistic interaction). However, differences can be attributed to the use of different time scales (i.e., event vs monthly time scales). This suggest that the nature of interaction between climate change and LUCC depends on the temporal time scales of hydrological processes. More research is needed in this regard.

Furthermore, the combined effect of climate change and LUCC over stormflows in the altitudinal gradient, is more like individual effect of LUCC (Fig 7b). Also, the Kruskal-Wallis test and the post-hoc Dunn test demonstrate that the combined effect of factors is crucial in the upper basin, regardless of rainfall intensity. However, as elevation decreases and rainfall intensity increases, the combined effect of climate change and LUCC on floods diminishes in a non-linear manner (exponential decay function).

4.4. Implications for ecosystem services to regulate floods

It is crucial to protect forests in the upper basins as forest provide irreplaceable flood regulation services especially with ongoing and projected climate change. Although for Rp2 the altitudinal range from 590 to 906 m.a.s.l approximately, would be the transitional area between upper and lower basin in terms of influence of LUCC on stormflows. The relatively stable critical elevation (≈ 590 m.a.s.l), associated with abrupt changes in peak flows and SFV, can aid in zoning the TRB for nature-based flood management strategies. Thus, we propose prioritizing the protection and/or restoration of hillslopes from 590 m.a.s.l to the upper part of the basin. Similarly, protecting the main channel and its influence areas, such as low terraces and riparian zones, from 590 m.a.s.l to the lower part of the basin, specifically the high-flow areas in Figure. 1a (green polygon). Although the critical elevation of 590 m.a.s.l is site specific, the methodology based on OFAT together with Zhang et al. (2018) equations can be replicated in other basins with abrupt changes in the altitudinal gradient such as TRB, in order to establish the zoning proposed in this study.

The zoning proposed in this study (High-flow areas in Fig. 1a) can enhance the management of ecosystem services for flood mitigation in TRB especially during small and medium storm events (≤ Rp2). Other flood management strategies such as the peri-urban landscapes planning can be based on our proposal (Barbedo et al., 2014). However, combining the ecosystem services and peri-urban planning are increasingly important in the context of climate change projections in the study area.

5. Conclusions

This study evaluates, through hypothetical scenarios and spatially-distributed hydrological modeling, the individual and combined effect of climate change and LUCC on stormflows across the altitudinal gradient in a humid tropic basin within the Ecuadorian Amazon.

A slightly and statistically non-significant interaction between climate change and LUCC was identified, with an antagonistic effect in the lower part. However, in practical terms can be considered a null interaction. The probabilities of producing floods downstream during any given year will change due to climate change from 10 to 50 % even with the hypothetical scenario of the entire basin being covered by forest. Additionally, climate change has more homogeneous effect than LUCC across the altitudinal gradient. However, the combined effect of factors is greater in the upper basin and decreases as storm intensity increases. Therefore, maintaining or restoring the native forest in the upper basin is crucial to help in the mitigation of climate change effects during small and medium-size storms. For Rp2 the altitudinal range from 590 to 906 m.a.s.l approximately, would be the transitional area between upper and lower basin in terms of influence of LUCC on stormflows. Nevertheless, the 590 m.a.s.l is the elevation where the abrupt changes of peak flow and stormflow volume occurs. Finally, a spatial zoning is proposed based in this elevation to prioritize the protection of hillslopes and river channel areas.

The results of this study provide clear guidelines for the application of NbS for flood regulation in humid tropical basins and enhance our understanding of ecosystem services in a context of climate change.

References

Almazroui, M., Ashfaq, M., Islam, M. N., Rashid, I. U., Kamil, S., Abid, M. A., O'Brien, E., Ismail, M., Reboita, M. S., Sörensson, A. A., Arias, P. A., Alves, L. M., Tippett, M. K., Saeed, S., Haarsma, R., Doblas-Reyes, F. J., Saeed, F., Kucharski, F., Nadeem, I., … Sylla, M. B. (2021). Assessment of CMIP6 Performance and Projected Temperature and Precipitation Changes Over South America. Earth Systems and Environment 2021 5:2, 5(2), 155–183. https://doi.org/10.1007/S41748-021-00233-6

Armenta, E., Villa, L., & Jácome, P. (2016). PROYECCIONES CLIMÁTICAS DE PRECIPITACIÓN Y TEMPERATURA PARA ECUADOR, BAJO DISTINTOS ESCENARIOS DE CAMBIO CLIMÁTICO.

Asano, Y., & Uchida, T. (2018). The roles of channels and hillslopes in rainfall/run-off lag times during intense storms in a steep catchment. Hydrological Processes, 32(6), 713–728. https://doi.org/10.1002/hyp.11443

Ataroff, M., & Rada, F. (2000). Deforestation Impact on Water Dynamics in a Venezuelan Andean Cloud Forest. Https://Doi.Org/10.1579/0044-7447-29.7.440, 29(7), 440–444. https://doi.org/10.1579/0044-7447-29.7.440

Barbedo, J., Miguez, M., van der Horst, D., & Marins, M. (2014). Enhancing ecosystem services for flood mitigation: a conservation strategy for peri-urban landscapes? Ecology and Society, 19(2), art54. https://doi.org/10.5751/ES-06482-190254

Bathurst, J. C., Fahey, B., Iroumé, A., & Jones, J. (2020). Forests and floods: Using field evidence to reconcile analysis methods. Hydrological Processes, 34(15), 3295–3310. https://doi.org/10.1002/HYP.13802

Bathurst, J. C., Iroumé, A., Cisneros, F., Fallas, J., Iturraspe, R., Novillo, M. G., Urciuolo, A., Bièvre, B. de, Borges, V. G., Coello, C., Cisneros, P., Gayoso, J., Miranda, M., & Ramírez, M. (2011). Forest impact on floods due to extreme rainfall and snowmelt in four Latin American environments 1: Field data analysis. Journal of Hydrology, 400(3–4), 281–291. https://doi.org/10.1016/J.JHYDROL.2010.11.044

Birch, A. L., Stallard, R. F., Bush, S. A., & Barnard, H. R. (2021). The influence of land cover and storm magnitude on hydrologic flowpath activation and runoff generation in steep tropical catchments of central Panama. Journal of Hydrology, 596, 126138. https://doi.org/10.1016/J.JHYDROL.2021.126138

Birkel, C., Soulsby, C., & Tetzlaff, D. (2012). Modelling the impacts of land-cover change on streamflow dynamics of a tropical rainforest headwater catchment. Hydrological Sciences Journal, 57(8), 1543–1561. https://doi.org/10.1080/02626667.2012.728707

Blöschl, G. (2022). Flood generation: Process patterns from the raindrop to the ocean. Hydrology and Earth System Sciences, 26(9), 2469–2480. https://doi.org/10.5194/HESS-26-2469-2022

Blöschl, G., Ardoin-Bardin, S., Bonell, M., Dorninger, M., Goodrich, D., Gutknecht, D., Matamoros, D., Merz, B., Shand, P., & Szolgay, J. (2007). At what scales do climate variability and land cover change impact on flooding and low flows? Hydrological Processes, 21(9), 1241–1247. https://doi.org/10.1002/HYP.6669

Bonnesoeur, V., Locatelli, B., Guariguata, M. R., Ochoa-Tocachi, B. F., Vanacker, V., Mao, Z., Stokes, A., & Mathez-Stiefel, S. L. (2019). Impacts of forests and forestation on

hydrological services in the Andes: A systematic review. Forest Ecology and Management, 433, 569–584. https://doi.org/10.1016/J.FORECO.2018.11.033

Boucher, O., Servonnat, J., Albright, A. L., Aumont, O., Balkanski, Y., Bastrikov, V., Bekki, S., Bonnet, R., Bony, S., Bopp, L., Braconnot, P., Brockmann, P., Cadule, P., Caubel, A., Cheruy, F., Codron, F., Cozic, A., Cugnet, D., D'Andrea, F., … Vuichard, N. (2020). Presentation and Evaluation of the IPSL-CM6A-LR Climate Model. Journal of Advances in Modeling Earth Systems, 12(7), e2019MS002010. https://doi.org/10.1029/2019MS002010

Bronstert, A. (2004). Rainfall-runoff modelling for assessing impacts of climate and land-use change. Hydrological Processes, 18(3), 567–570. https://doi.org/10.1002/HYP.5500

Campozano, L., Tenelanda, D., Sanchez, E., Samaniego, E., & Feyen, J. (2016). Comparison of Statistical Downscaling Methods for Monthly Total Precipitation: Case Study for the Paute River Basin in Southern Ecuador. Advances in Meteorology, 2016. https://doi.org/10.1155/2016/6526341

Campozano, L., Vázquez-Patiño, A., Tenelanda, D., Feyen, J., Samaniego, E., & Sánchez, E. (2017). Evaluating extreme climate indices from CMIP3&5 global climate models and reanalysis data sets: a case study for present climate in the Andes of Ecuador. International Journal of Climatology, 37, 363–379. https://doi.org/10.1002/JOC.5008

Chancay, J. E., & Espitia-Sarmiento, E. F. (2021). Improving Hourly Precipitation Estimates for Flash Flood Modeling in Data-Scarce Andean-Amazon Basins: An Integrative Framework Based on Machine Learning and Multiple Remotely Sensed Data. Remote Sensing 2021, Vol. 13, Page 4446, 13(21), 4446. https://doi.org/10.3390/RS13214446

Chang, H., & Franczyk, J. (2008). Climate Change, Land-Use Change, and Floods: Toward an Integrated Assessment. Geography Compass, 2(5), 1549–1579. https://doi.org/10.1111/j.1749-8198.2008.00136.x

Chawla, I., & Mujumdar, P. P. (2015). Isolating the impacts of land use and climate change on streamflow. Hydrology and Earth System Sciences, 19(8), 3633–3651. https://doi.org/10.5194/HESS-19-3633-2015

Chow, V. Te, Maidment, D. R., & Mays, L. W. (1988). Applied hydrology. McGraw-Hill.

Cohen-Shacham, E., Janzen, C., Maginnis, S., & Walters, G. (2016). Nature-based solutions to address global societal challenges (E. Cohen-Shacham, G. Walters, C. Janzen, & S. Maginnis (eds.)). IUCN International Union for Conservation of Nature. https://doi.org/10.2305/IUCN.CH.2016.13.en

Copernicus. (2021). CMIP6 climate projections. Copernicus Climate Change Service (C3S) Climate Data Store (CDS). https://doi.org/10.24381/cds.c866074c

Crespo, P. J., Feyen, J., Buytaert, W., Bücker, A., Breuer, L., Frede, H.-G., & Ramírez, M. (2011). Identifying controls of the rainfall–runoff response of small catchments in the tropical Andes (Ecuador). Journal of Hydrology, 407(1–4), 164–174. https://doi.org/10.1016/j.jhydrol.2011.07.021

Dadson, S. J., Hall, J. W., Murgatroyd, A., Acreman, M., Bates, P., Beven, K., Heathwaite, L., Holden, J., Holman, I. P., Lane, S. N., O'Connell, E., Penning-Rowsell, E., Reynard, N., Sear, D., Thorne, C., & Wilby, R. (2017). A restatement of the natural science evidence concerning catchment-based 'natural' flood management in the UK. Proceedings of the Royal Society A: Mathematical, Physical and Engineering Science, 473(2199), 20160706. https://doi.org/10.1098/rspa.2016.0706

Delignette-Muller, M. L., & Dutang, C. (2015). Fitdistrplus: An R Package for Fitting Distributions. Journal of Statistical Software, 64(4), 1–34. https://doi.org/10.18637/JSS.V064.I04

Dickey, D. A., & Fuller, W. A. (1979). Distribution of the Estimators for Autoregressive Time Series With a Unit Root. Journal of the American Statistical Association, 74(366), 427. https://doi.org/10.2307/2286348

Dunn, O. J. (1964). Multiple Comparisons Using Rank Sums. Technometrics, 6(3), 241–252. https://doi.org/10.1080/00401706.1964.10490181

Dunne, R. P. (2010). Synergy or antagonism-interactions between stressors on coral reefs. Coral Reefs, 29(1), 145–152. https://doi.org/10.1007/s00338-009-0569-6

Edokpa, D., Milledge, D., Allott, T., Holden, J., Shuttleworth, E., Kay, M., Johnston, A., Millin-Chalabi, G., Scott-Campbell, M., Chandler, D., Freestone, J., & Evans, M. (2022). Rainfall intensity and catchment size control storm runoff in a gullied blanket peatland. Journal of Hydrology, 609, 127688. https://doi.org/10.1016/J.JHYDROL.2022.127688

Engeland, K., Hisdal, H., & Frigessi, A. (2004). Practical extreme value modelling of hydrological floods and droughts: A case study. Extremes, 7(1), 5–30. https://doi.org/10.1007/S10687-004-4727-5/METRICS

Fang, G. H., Yang, J., Chen, Y. N., & Zammit, C. (2015). Comparing bias correction methods in downscaling meteorological variables for a hydrologic impact study in an arid area in China. Hydrology and Earth System Sciences, 19(6), 2547–2559. https://doi.org/10.5194/HESS-19-2547-2015

Francés, F., Vélez, J. I., & Vélez, J. J. (2007). Split-parameter structure for the automatic calibration of distributed hydrological models. Journal of Hydrology, 332(1–2), 226–240. https://doi.org/10.1016/J.JHYDROL.2006.06.032

GADM-TENA. (2021). ACTUALIZACIÓN PDOT 2020-2023. GADM-Tena. https://tena.gob.ec/index.php/tena/plan-de-desarrollo

Gomi, T., Sidle, R. C., Miyata, S., Kosugi, K., & Onda, Y. (2008). Dynamic runoff connectivity of overland flow on steep forested hillslopes: Scale effects and runoff transfer. Water Resources Research, 44(8), 8411. https://doi.org/10.1029/2007WR005894

Gudmundsson, L. (2016). Qmap: Statistical Transformations for Post-Processing Climate Model Output [R package qmap version 1.0-4] (1.0-4). Comprehensive R Archive Network (CRAN). https://cran.r-project.org/package=qmap

Gudmundsson, L., Bremnes, J. B., Haugen, J. E., & Engen-Skaugen, T. (2012). Technical Note: Downscaling RCM precipitation to the station scale using statistical transformations – a comparison of methods. Hydrology and Earth System Sciences, 16(9), 3383–3390. https://doi.org/10.5194/hess-16-3383-2012

Gumbel, E. J. (1941). The Return Period of Flood Flows. The Annals of Mathematical Statistics, 12(2), 163–190. http://www.jstor.org/stable/2235766

Hajima, T., Watanabe, M., Yamamoto, A., Tatebe, H., Noguchi, M. A., Abe, M., Ohgaito, R., Ito, A., Yamazaki, D., Okajima, H., Ito, A., Takata, K., Ogochi, K., Watanabe, S., & Kawamiya, M. (2020). Development of the MIROC-ES2L Earth system model and the evaluation of biogeochemical processes and feedbacks. Geoscientific Model Development, 13(5), 2197–2244. https://doi.org/10.5194/GMD-13-2197-2020

Heredia, M. B., Junquas, C., Prieur, C., & Condom, T. (2018). New Statistical Methods for Precipitation Bias Correction Applied to WRF Model Simulations in the Antisana Region, Ecuador. Journal of Hydrometeorology, 19(12), 2021–2040. https://doi.org/10.1175/JHM-D-18-0032.1

Hirabayashi, Y., Mahendran, R., Koirala, S., Konoshima, L., Yamazaki, D., Watanabe, S., Kim, H., & Kanae, S. (2013). Global flood risk under climate change. Nature Climate Change, 3(9), 816–821. https://doi.org/10.1038/nclimate1911

Hopp, L., & McDonnell, J. J. (2009). Connectivity at the hillslope scale: Identifying interactions between storm size, bedrock permeability, slope angle and soil depth. Journal of Hydrology, 376(3–4), 378–391. https://doi.org/10.1016/J.JHYDROL.2009.07.047

Hung, C. L. J., James, L. A., Carbone, G. J., & Williams, J. M. (2020). Impacts of combined land-use and climate change on streamflow in two nested catchments in the Southeastern United States. Ecological Engineering, 143, 105665. https://doi.org/10.1016/J.ECOLENG.2019.105665

Hurtado-Pidal, J., Acero Triana, J. S., Aguayo, M., Link, O., Valencia, B. G., Espitia-Sarmiento, E., & Conicelli, B. (2022). Is forest location more important than forest fragmentation for flood regulation? Ecological Engineering, 183, 106764. https://doi.org/10.1016/J.ECOLENG.2022.106764

Hurtado-Pidal, J., Acero Triana, J. S., Espitia-Sarmiento, E., & Jarrín-Pérez, F. (2020). Flood Hazard Assessment in Data-Scarce Watersheds Using Model Coupling, Event Sampling, and Survey Data. Water, 12(10), 2768. https://doi.org/10.3390/w12102768

Iacob, O., Brown, I., & Rowan, J. (2017). Natural flood management, land use and climate change trade-offs: the case of Tarland catchment, Scotland. Hydrological Sciences Journal, 62(12), 1931–1948. https://doi.org/10.1080/02626667.2017.1366657

Ikiam-University. (2021). Ikiam Hydromet Service. http://hidrometeorologia.ikiam.edu.ec/

Ilieva, L., McQuistan, C., Van-Breda, A., Rodriguez, A., Guevara, O., Cordero, D., & Renaud, F. (2018). Adoptando soluciones basadas en la naturaleza para la reducción del riesgo de inundación en América Latina (p. 24). https://solucionespracticas.org.pe/Adoptando-soluciones-basadas-en-la-naturaleza-para-la-reduccion-del-riesgo-de-inundacion-en-America-Latina

INAMHI. (2019). Determinación de ecuaciones para el cálculo de intensidades máximas de precipitación. https://doi.org/www.serviciometeorologico.gob.ec/Publicaciones/Hidrologia/ESTUDIO_DE_INTENSIDADES_V_FINAL.pdf

IPCC. (2021). Climate Change 2021: The Physical Science Basis. Contribution of Working Group I to the Sixth Assessment Report of the Intergovernmental Panel on Climate Change (p. 41). Cambridge University Press. https://www.ipcc.ch/report/ar6/wg1/

Jodar-Abellan, A., Valdes-Abellan, J., Pla, C., & Gomariz-Castillo, F. (2019). Impact of land use changes on flash flood prediction using a sub-daily SWAT model in five Mediterranean ungauged watersheds (SE Spain). Science of The Total Environment, 657, 1578–1591. https://doi.org/10.1016/J.SCITOTENV.2018.12.034

Jonkman, S. N. (2005). Global Perspectives on Loss of Human Life Caused by Floods. Natural Hazards 2005 34:2, 34(2), 151–175. https://doi.org/10.1007/S11069-004-8891-3

Kim, Y. H., Min, S. K., Zhang, X., Sillmann, J., & Sandstad, M. (2020). Evaluation of the CMIP6 multi-model ensemble for climate extreme indices. Weather and Climate Extremes, 29, 100269. https://doi.org/10.1016/J.WACE.2020.100269

Kottek, M., Grieser, J., Beck, C., Rudolf, B., & Rubel, F. (2006). World map of the Köppen-Geiger climate classification updated. Meteorologische Zeitschrift, 15(3), 259–263. https://doi.org/10.1127/0941-2948/2006/0130

Kotz, S., & Nadarajah, S. (2000). Extreme Value Distributions. Extreme Value Distributions. https://doi.org/10.1142/P191

Krajewski, A., Sikorska-Senoner, A. E., Hejduk, L., & Banasik, K. (2021). An Attempt to Decompose the Impact of Land Use and Climate Change on Annual Runoff in a Small Agricultural Catchment. Water Resources Management, 35(3), 881–896. https://doi.org/10.1007/S11269-020-02752-9/TABLES/4

Kruskal, W. H., & Wallis, W. A. (1952). Use of Ranks in One-Criterion Variance Analysis. Journal of the American Statistical Association, 47(260), 583–621. https://doi.org/10.1080/01621459.1952.10483441

Lamichhane, & Shakya. (2019). Integrated Assessment of Climate Change and Land Use Change Impacts on Hydrology in the Kathmandu Valley Watershed, Central Nepal. Water, 11(10), 2059. https://doi.org/10.3390/w11102059

Lane, S. N. (2017). Natural flood management. Wiley Interdisciplinary Reviews: Water, 4(3), e1211. https://doi.org/10.1002/wat2.1211

Laurance, W. F. (2007). Forests and floods. Nature 2007 449:7161, 449(7161), 409–410. https://doi.org/10.1038/449409a

Lian, J., Chen, H., Wang, F., Nie, Y., & Wang, K. (2020). Separating the relative contributions of climate change and ecological restoration to runoff change in a mesoscale karst basin. CATENA, 194, 104705. https://doi.org/10.1016/J.CATENA.2020.104705

Lima, A. O., Lyra, G. B., Abreu, M. C., Oliveira-Júnior, J. F., Zeri, M., & Cunha-Zeri, G. (2021). Extreme rainfall events over Rio de Janeiro State, Brazil: Characterization using probability distribution functions and clustering analysis. Atmospheric Research, 247, 105221. https://doi.org/10.1016/J.ATMOSRES.2020.105221

Liu, W., Feng, Q., Engel, B. A., Yu, T., Zhang, X., & Qian, Y. (2023). A probabilistic assessment of urban flood risk and impacts of future climate change. Journal of Hydrology, 618, 129267. https://doi.org/10.1016/J.JHYDROL.2023.129267

MacFarland, T. W., & Yates, J. M. (2016). Kruskal–Wallis H-Test for Oneway Analysis of Variance (ANOVA) by Ranks. Introduction to Nonparametric Statistics for the Biological Sciences Using R, 177–211. https://doi.org/10.1007/978-3-319-30634-6_6

MAGAP-SIGTIERRAS. (2016). Generación de Geoinformación para la Gestión del Territorio a Nivel Nacional. MAGAP (Ministerio de Agricultura y Ganadería). Metadatos.sigtierras.gob.ec

Manzanas, R., Fiwa, L., Vanya, C., Kanamaru, H., & Gutiérrez, J. M. (2020). Statistical downscaling or bias adjustment? A case study involving implausible climate change projections of precipitation in Malawi. Climatic Change, 162(3), 1437–1453. https://doi.org/10.1007/S10584-020-02867-3/FIGURES/6

Menéndez, M., Méndez, F. J., Izaguirre, C., Luceño, A., & Losada, I. J. (2009). The influence of seasonality on estimating return values of significant wave height. Coastal Engineering, 56(3), 211–219. https://doi.org/10.1016/j.coastaleng.2008.07.004

Mishra, B. K., Rafiei Emam, A., Masago, Y., Kumar, P., Regmi, R. K., & Fukushi, K. (2018). Assessment of future flood inundations under climate and land use change scenarios in the Ciliwung River Basin, Jakarta. Journal of Flood Risk Management, 11, S1105–S1115. https://doi.org/10.1111/jfr3.12311

Moriasi, D. N., Arnold, J. G., Van Liew, M. W., Bingner, R. L., Harmel, R. D., Veith, T. L., Harmel, D., & Veith, T. L. (2007). Model Evaluation Guidelines for Systematic Quantification of Accuracy in Watershed Simulations. Transactions of the ASABE, 50(3), 885–900. https://doi.org/10.13031/2013.23153

Nikolopoulos, E. I., Anagnostou, E. N., Borga, M., Vivoni, E. R., & Papadopoulos, A. (2011). Sensitivity of a mountain basin flash flood to initial wetness condition and rainfall variability. Journal of Hydrology, 402(3–4), 165–178. https://doi.org/10.1016/j.jhydrol.2010.12.020

Olang, L. O., & Fürst, J. (2011). Effects of land cover change on flood peak discharges and runoff volumes: model estimates for the Nyando River Basin, Kenya. Hydrological Processes, 25(1), 80–89. https://doi.org/10.1002/HYP.7821

Pabón-Caicedo, J. D., Arias, P. A., Carril, A. F., Espinoza, J. C., Borrel, L. F., Goubanova, K., Lavado-Casimiro, W., Masiokas, M., Solman, S., & Villalba, R. (2020). Observed and Projected Hydroclimate Changes in the Andes. Frontiers in Earth Science, 8, 61. https://doi.org/10.3389/FEART.2020.00061/BIBTEX

Palomino-Lemus, R., Córdoba-Machado, S., Gámiz-Fortis, S. R., Castro-Díez, Y., & Esteban-Parra, M. J. (2017). Climate change projections of boreal summer precipitation over tropical America by using statistical downscaling from CMIP5 models. Environmental Research Letters, 12(12), 124011. https://doi.org/10.1088/1748-9326/aa9bf7

Pebesma, E. (2023). Simple Features for R [R package sf version 1.0-12]. https://cran.r-project.org/package=sf

Piani, C., Haerter, J. O., & Coppola, E. (2010). Statistical bias correction for daily precipitation in regional climate models over Europe. Theoretical and Applied Climatology, 99(1–2), 187–192. https://doi.org/10.1007/S00704-009-0134-9/FIGURES/4

R-Development-Core-Team. (2020). R: A Language and Environment for Statistical Computing (4.0.2). CRAN. https://www.r-project.org/

Rogger, M., Agnoletti, M., Alaoui, A., Bathurst, J. C., Bodner, G., Borga, M., Chaplot, V., Gallart, F., Glatzel, G., Hall, J., Holden, J., Holko, L., Horn, R., Kiss, A., Kohnová, S., Leitinger, G., Lennartz, B., Parajka, J., Perdigão, R., … Blöschl, G. (2017). Land use change impacts on floods at the catchment scale: Challenges and opportunities for future research. Water Resources Research, 53(7), 5209–5219. https://doi.org/10.1002/2017WR020723

Rothman, K. (1976). The Estimation of Synergy or Antagonism. American Journal of Epidemiology, 103(5), 506–511. https://doi.org/10.1093/oxfordjournals.aje.a112252

Salazar, S., Francés, F., Komma, J., Blume, T., Francke, T., Bronstert, A., & Blöschl, G. (2012). A comparative analysis of the effectiveness of flood management measures based on the concept of “retaining water in the landscape” in different European hydro-climatic regions. Natural Hazards and Earth System Sciences, 12(11), 3287–3306. https://doi.org/10.5194/nhess-12-3287-2012

Sánchez, D., Merlo, J., Haro, R., Acosta, M., & Bernal, G. (2018). Soils from the Amazonia (J. Espinosa, J. Moreno, & G. Bernal (eds.); pp. 113–137). Springer. https://doi.org/10.1007/978-3-319-25319-0_4

Sarmiento, F. O., & Kooperman, G. J. (2019). A Socio-Hydrological Perspective on Recent and Future Precipitation Changes Over Tropical Montane Cloud Forests in the Andes. Frontiers in Earth Science, 7, 324. https://doi.org/10.3389/feart.2019.00324

Segarra, V. (2022). Evaluación de la oferta hídrica bajo escenarios de cambio climático en la microcuenca del río Colonso, Ecuador.

https://repositorio.ikiam.edu.ec/jspui/bitstream/RD_IKIAM/627/1/TT-H-IKIAM-000011.pdf

Seland, Ø., Bentsen, M., Olivié, D., Toniazzo, T., Gjermundsen, A., Graff, L. S., Debernard, J. B., Gupta, A. K., He, Y. C., Kirkeväg, A., Schwinger, J., Tjiputra, J., Schanke Aas, K., Bethke, I., Fan, Y., Griesfeller, J., Grini, A., Guo, C., Ilicak, M., … Schulz, M. (2020). Overview of the Norwegian Earth System Model (NorESM2) and key climate response of CMIP6 DECK, historical, and scenario simulations. Geoscientific Model Development, 13(12), 6165–6200. https://doi.org/10.5194/GMD-13-6165-2020

Shang, X., Jiang, X., Jia, R., & Wei, C. (2019). Land Use and Climate Change Effects on Surface Runoff Variations in the Upper Heihe River Basin. Water, 11(2), 344. https://doi.org/10.3390/w11020344

Shapiro, S. S., & Wilk, M. B. (1965). An analysis of variance test for normality (complete samples). Biometrika, 52(3–4), 591–611. https://doi.org/10.1093/BIOMET/52.3-4.591

Shuttleworth, E. L., Evans, M. G., Pilkington, M., Spencer, T., Walker, J., Milledge, D., & Allott, T. E. H. (2019). Restoration of blanket peat moorland delays stormflow from hillslopes and reduces peak discharge. Journal of Hydrology X, 2, 100006. https://doi.org/10.1016/J.HYDROA.2018.100006

Silva, A. R. da, & Lima, R. P. (2017). Determination of maximum curvature point with the R package soilphysics. International Journal of Current Research, 9(1), 45241–45245.

Singh, V. P., Wang, S. X., & Zhang, L. (2005). Frequency analysis of nonidentically distributed hydrologic flood data. Journal of Hydrology, 307(1–4), 175–195. https://doi.org/10.1016/j.jhydrol.2004.10.029

Siswanto, S. Y., & Francés, F. (2019). How land use/land cover changes can affect water, flooding and sedimentation in a tropical watershed: a case study using distributed modeling in the Upper Citarum watershed, Indonesia. Environmental Earth Sciences 2019 78:17, 78(17), 1–15. https://doi.org/10.1007/S12665-019-8561-0

Sokal, R. R., & Rohlf, F. J. (1969). Biometry: The Principles and Practice of Statistics in Biological Research (R. R. Sokal & F. J. Rohlf (eds.)). W. H. Freeman and Company.

Solman, S. A. (2013). Regional climate modeling over south 135merica: A review. Advances in Meteorology, 2013. https://doi.org/10.1155/2013/504357

Sorribas, M. V., Paiva, R. C. D. D., Melack, J. M., Bravo, J. M., Jones, C., Carvalho, L., Beighley, E., Forsberg, B., & Costa, M. H. (2016). Projections of climate change effects

on discharge and inundation in the Amazon basin. Climatic Change, 136(3–4), 555–570. https://doi.org/10.1007/s10584-016-1640-2

Stephens, M. A. (2017). Tests Based on EDF Statistics. Goodness-of-Fit Techniques, 97–194. https://doi.org/10.1201/9780203753064-4

Tian, J., Guo, S., Yin, J., Pan, Z., Xiong, F., & He, S. (2022). Quantifying both climate and land use/cover changes on runoff variation in Han River basin, China. Frontiers of Earth Science, 16(3), 711–733. https://doi.org/10.1007/S11707-021-0918-5/METRICS

Tobón, C. (2008). Los bosques andinos y el agua. In Publicación de ECOBONA (Serie#4). Programa regional ECOBONA – INTERCOOPERATION, CONDESAN. http://infobosques.com/portal/wp-content/uploads/2016/08/b6a77b5786ffc08556b4861b514e76d6.pdf

Tobón, C. (2021). Ecohydrology of Tropical Andean Cloud Forests. The Andean Cloud Forest, 61–87. https://doi.org/10.1007/978-3-030-57344-7_4

Trapletti, A., Hornik, K., & LeBaron, B. (2023). Time Series Analysis and Computational Finance [R package tseries version 0.10-54] (0.10-54). Comprehensive R Archive Network (CRAN). https://cran.r-project.org/package=tseries

Tripathi, S., Srinivas, V. V., & Nanjundiah, R. S. (2006). Downscaling of precipitation for climate change scenarios: A support vector machine approach. Journal of Hydrology, 330(3–4), 621–640. https://doi.org/10.1016/J.JHYDROL.2006.04.030

UNISDR. (2017). Words into Action Guidelines: National Disaster Risk Assessment Hazard Specific Risk Assessment 4. Flood Hazard and Risk Assessment. UNISDR.

Vargas, D., Pucha-Cofrep, D., Serrano-Vincenti, S., Burneo, A., Carlosama, L., Herrera, M., Cerna, M., Molnár, M., Jull, A. J. T., Temovski, M., László, E., Futó, I., Horváth, A., & Palcsu, L. (2022). ITCZ precipitation and cloud cover excursions control Cedrela nebulosa tree-ring oxygen and carbon isotopes in the northwestern Amazon. Global and Planetary Change, 211, 103791. https://doi.org/10.1016/J.GLOPLACHA.2022.103791

Vu, M. T., Raghavan, V. S., & Liong, S.-Y. (2017). Deriving short-duration rainfall IDF curves from a regional climate model. Natural Hazards, 85(3), 1877–1891. https://doi.org/10.1007/s11069-016-2670-9

Wang, H., & Stephenson, S. R. (2018). Quantifying the impacts of climate change and land use/cover change on runoff in the lower Connecticut River Basin. Hydrological Processes, 32(9), 1301–1312. https://doi.org/10.1002/hyp.11509

Yang, L., Feng, Q., Yin, Z., Wen, X., Si, J., Li, C., & Deo, R. C. (2017). Identifying separate impacts of climate and land use/cover change on hydrological processes in upper stream of Heihe River, Northwest China. Hydrological Processes, 31(5), 1100–1112. https://doi.org/10.1002/HYP.11098

Zhang, L., Nan, Z., Yu, W., Zhao, Y., & Xu, Y. (2018). Comparison of baseline period choices for separating climate and land use/land cover change impacts on watershed hydrology using distributed hydrological models. Science of The Total Environment, 622–623, 1016–1028. https://doi.org/10.1016/J.SCITOTENV.2017.12.055

CHAPTER VI

GENERAL DISCUSSION

1. General Discussion

1.1. Hydrologic and hydrodynamic modeling of September 2017 flood event

Flash floods are the main natural hazard in the city of Tena in the Ecuadorian Amazon. This is due to the combination of heavy rainfall, steep terrains (40% in the upper part), small drainage areas (≈ <135 km2), and saturated soils (~90%). From 1996 to 2017, floods in this area have affected 16,422 people and 923 households, causing thousands of victims and hundreds of destroyed homes. For instance, the September 2017 flood event alone, affected 974 inhabitants (GADM-TENA, 2021). This event supplied the essential data for its reconstruction, and thus was used as a reference to understand the main features of a flash flood in the city of Tena through hydrological and hydrodynamic modeling.

Performance metrics NSE and PBIAS suggest that the hydrological models used in Chapters III, IV and V (HEC-HMS, Hurtado-Pidal et al., 2020; and TETIS, Hurtado-Pidal et al., 2022; Hurtado-Pidal et al., 2023 in prep), achieved a satisfactory level of confidence according to Moriasi et al. (2007) guidelines. Moreover, VanLiew et al. (2005) established that daily or smaller time step simulations the NSE can be as low as 0.4 to be considered acceptable. Thus, despite the context of hydrometeorological data scarcity, the simulations with HEC-HMS and TETIS (1-minute and 10-minute time step, respectively) reproduced a reliable hydrological response during extreme events.

The HEC-HMS model allowed the reconstruction of the flood hydrograph of the flash flood event occurred in the city of Tena on 2 September 2017. According to the simulation, the peak flow of this event was 1967 m^3/s. Additionally, Chancay & Espitia-Sarmiento (2021) through the GR4H model, with hourly time step simulation, establish a peak flow of 1379 m^3/s for the same event. However, the differences can be attributed in part to the different time step simulations between HEC-HMS (1-minute) and GR4H (1-hour). For instance, the change of the GR4 model time step results in large and monotonous changes of the internal fluxes (Ficchì et al., 2019). Additionally, the simulation for TRB carried out by Chancay & Espitia-Sarmiento (2021) exhibits a - 27% difference with respect to the observed peak flow of 1896 m^3/s. Consequently, using this value as a reference (1896 m^3/s), the peak flow estimated by HEC-HMS (1967 m^3/s) is only overestimated by 4%.

The results with 2D hydrodynamic modeling (Nays2DFlood) for September 2017 flood event show satisfactory performance for both flow velocity (m/s) and flow

depth (m), according to Moriasi et al. (2007) guidelines applied for this task (Chapter III). Furthermore, a very good level of spatial agreement was achieved between the observed and modeled flood areas with the F index (0.8) proposed by Horritt and Bates (2002), as well as with control points (6/8). Therefore, the hydrodynamic reconstruction and maps derived from this simulation can be used as a reference for flood management in urban areas (with residential, commercial and tourism uses) within the city of Tena. The published maps in the Territorial Planning and Development Plans (TPDP) of the Municipality of Tena do not indicate flow levels or velocities within the flood-prone areas (GADM-TENA, 2021). It is highly probable that these maps are currently based on spatial analysis and geomorphic analysis using geographic information systems and digital elevation models. However, relying solely on flood-prone areas without considering flow levels and velocities limits urban planning for housing construction, design of infrastructure and public spaces, as well as flood contingency plans (Maranzoni et al., 2023).

In this regard, the flood intensity map indicates that 71 % of flooded areas were under high intensity flood (water depth > 1.5 m or flow velocity > 1.5 m/s). The maximum water depth and flow velocity in flooded areas were approximately, 4m and 3 m/s, respectively. Also, the medium intensity flood (0.5 < depth < 1.5 m; 0.5 < flow velocity < 1.5 m/s) reach 23% of flooded areas. Therefore, a scenario similar to the September 2017 flood event, implies that human lives, infrastructure and vehicles are at risk in 94% of the projected flooded areas (Bocanegra et al., 2020; Huizinga et al., 2017). These areas may require evacuation and rescue operations, as well as damage to residential buildings is also expected.

1.2. Climate change projections and implication for floods in the city of Tena

The results showed that the daily precipitation in the basin would change from 11.16 mm (historical) to 14.32 mm (future), which represents an increase of 28%. Additionally, there would also be a change in the precipitation range (maximum - minimum), shifting from 182.20 mm (historical) to 233.50 mm (future), meaning also an increase of 28% (in both periods, the minimum value is 0 mm). In general, climate change simulations related to high emission scenarios (SSP5-8.5, RCP8.5) indicate an increment in precipitation for the northwest Amazon including the Ecuadorian Amazon and Andes foothills (Almazroui et al., 2021; Armenta et al., 2016; Pabón-Caicedo et al., 2020; Palomino-Lemus et al., 2017; Sarmiento & Kooperman, 2019; Solman, 2013). Specifically, Segarra (2022) found an increment of 21% in daily precipitation for Colonso basin (within the TRB) due to climate change.

In the future (2041-2070), climate change alone has the capacity to produce floods in the city of Tena every two years on average (Rp2), even in the extreme scenario of the entire basin being covered by forest. Thus, the probabilities of producing floods in the city of Tena during any given year will change from 10 (current, Rp10) to 50 % (future, Rp2). These results are in agreement with Hirabayashi et al. (2013) that found a projected change in the range of 5 to 25 year in flood frequency for this region using the scenario RCP8.5. Moreover, is probably that these changes are already taking place due to the increase of flood events in recent years (at least 3 in the last 10 years; GADM-TENA, 2021).

1.3. LUCC spatial patterns and floods

Through the analysis of different LUCC spatial patterns, such as, fragmentation and location scenarios, the results of Chapter II shows that, deforestation in the upper basin produces the worst scenario for flood regulation (Hurtado-Pidal et al., 2022). Further, the effect of LUCC is higher in the upper basin and decreases progressively to downstream direction (Chapter V), which can be explained by scale processes (Rogger et al., 2017). However, the higher influence of LUCC in the upper basin is related not only to the scale processes but also to specific physical characteristics in this part of the basin that can enhance the connectivity, such as soil moisture, saturated soil conductivity and steep slopes (Asano & Uchida, 2018; Birch et al., 2021; Edokpa et al., 2022; Gomi et al., 2008; Hopp & McDonnell, 2009).

Additionally, the forest fragmentation scenarios show smaller influence than location scenarios. These results are in concordance with Hou et al. (2018) that found relatively low effect of fragmentation. Contrarily, Boongaling et al. (2018) and Gao & Yu, (2017) suggest that forest fragmentation is related to greater runoff and high flows. Nevertheless, previous studies (Boongaling et al., 2018; Q. Gao & Yu, 2017) do not considered the area of forest, in other words higher fragmentation is also related to forest loss. In our experiments the area of forest is constant (50% of the basin). Thus, the results presented in this research (Chapter IV) isolate the effect of forest loss on floods, and only considers the different LUCC spatial patterns.

The lower basin is characterized by smaller terrain slopes and higher infiltration capacity compared to the upper basin. As a result, the overland flow in this area is lower. Also, the lower basin has greater fragmentation of forest due to the presence of agriculture, infrastructure and other anthropic land covers. Thus, it is possible found in the lower basin, an inverse correlation, between fragmentation and overland flow (greater fragmentation with relatively lower overland flow). However, this inverse correlation does not represent causation.

In general terms, the soil infiltration capacity and terrain slopes would have more influence than LUCC in the response during small and middle size events. Previous research (e.g., Bathurst et al., 2018; Sriwongsitanon & Taesombat, 2011) indicates that peak flows regulation is function of soil moisture content and if the watershed is saturated the response is the same despite the differences in land cover. Moreover, as storm intensity increases the effect of LUCC decreases (Bathurst et al., 2020; Iacob et al., 2017; Laurance, 2007).

1.4. Effects of climate change and LUCC across the basin

This research presents a detailed analysis of variations of individual and combined effects of climate change and LUCC on floods across an altitudinal gradient in a tropical humid basin. The results in Chapter V, shows that climate change is more homogeneous than LUCC across the altitudinal gradient. Blöschl et al. (2007), hypothesized that as the spatial scale increases the impact of LUCC on hydrological response decreases progressively. In contrast, climate variability has a homogeneous impact across different spatial scale. In other words, at smaller scales, LUCC has a larger impact than climate variability on hydrological response.

The combined effects of climate change and LUCC on stormflows across altitudinal gradient, also follow a non-lineal pattern. Thus, the LUCC effect in the altitudinal gradient with an exponential decay function, prevails when the factors are combined. Moreover, changes localized in the upper basin produce larger effects than those produced downstream. These findings are in concordance to the results presented by Hung et al. (2020) and Olang & Fürst (2011) related to greater sensitivity of stormflows to LUCC in small watersheds or headwaters. Also, one of the more important findings shown in Chapter V is related to the interaction analysis. A slightly and statistically non-significant interaction between climate change and LUCC was identified, with an antagonistic effect in the lower part. Although some studies found either, synergistic (Hung et al., 2020) or antagonistic interactions between climate change and LUCC (e.g.: Lamichhane & Shakya, 2019), the differences could be attributed to modeling setups (e.g., event v/s monthly time scales).

The exponential decay function of absolute differences in the altitudinal gradient of the study basin, indicates a relatively stable point of abrupt changes located at 590 m.a.s.l. This elevation represents a threshold where the effect of climate change and LUCC on stormflows is notably greater. Abrupt changes occur in this part of the basin because, for the same elevation range (e.g., 50 m), the

difference in accumulated draining area is much greater in the lower part than in the upper part. Additionally, the results in Chapter V corroborate the findings shown in Chapter IV, regarding the decrease in the effect of LUCC as storm intensity increases. Nevertheless, the different rainfall intensities (Rp2, Rp10, Rp100) slightly alter the effect of LUCC on stormflows in the upper basin.

1.5. Implications for nature-based solutions and flood management

The results demonstrate the importance of the forest cover, located in the upper basin, which is part of the biological reverse Colonso-Chalupas (RBCC, Figure 5.1a in Chapter V), to regulate floods. Moreover, considering the unfavorable scenarios of climate change due to increased precipitation and flooding, the forest in the upper basin plays a key role as a nature-based solution for flood regulation. However, the results also indicate that, the influence of forest to regulate floods is limited to small and medium size storms (≤Rp2). In this regard, for Rp2 the altitudinal range from 590 to 906 m.a.s.l., approximately, would be the transitional area between upper and lower basin in terms of influence of LUCC on stormflows (Chapter V). In agreement with our findings, Birkel et al. (2012) found in a humid catchment in Costa Rica that LUCC has relatively little effect on peak flows with return periods > 1-year. Also, other studies emphasize the limited potential of forest to reduce floods with higher storm events (Bathurst et al., 2011; Iacob et al., 2017; Salazar et al., 2012). Therefore, the application of nature-based solutions related to the capacity of forest to regulate floods need to be completed with other initiatives for an effective flood management (Ilieva et al., 2018; Soulsby et al., 2017).

This research defined the areas of greatest flow change (high-flow areas in Figure 5.1a, Chapter V), based on a relatively stable critical elevation, localized at 590 m.a.s.l. In this elevation, abrupt changes on peak flows and stormflow volume occurs due to the effects of climate change and LUCC. Thus, based on the evidence, it is reasonable to prioritize the protection and/or restoration of hillslopes outside of these high-flow areas (>590 m.a.s.l.). While inside high-flow areas ≤590 m.a.s.l), can be established to prioritize the protection of river channel, low terraces and riparian zones. Additionally, initiatives within the basin can be based on this spatial zoning, such as peri-urban planning landscapes (Barbedo et al., 2014). This is important considering that 6000 inhabitants live within high-flow areas, most of them indigenous, with relatively high socioeconomic vulnerability (INEC, 2010).”

NbS and territorial planning (urban and peri-urban) can incorporate fluvial corridors (with flooding parks) as multifunctional landscapes for flood attenuation, recreation, conservation, among other purposes (Martín-Vide, 2015; Miguez et al.,

2015; Rotger, 2018). In this regard, the urban zoning contained within the TPDP of the Municipality of Tena (GADM-TENA, 2021) indicates that many flood-prone areas, close to the rivers Tena and Pano, are designated, as tourist development zones (A17) and conservation areas (A16). Therefore, the establishment of fluvial corridors is necessary and compatible with the urban zoning of the city of Tena serving effectively for both purposes (A17, A16). The establishment of NbS for risk management, and territorial planning, should be together with the hydrometeorological monitoring within the basin.

It is reasonable to assume that, during flood events, below 590 m.a.s.l., the stormflow volume is moving mainly in the river channel. Whereas above this elevation, an important percentage of water moves through interflow within the soil profile. Thus, in agreement with findings of Asano & Uchida, (2018), it is possible establish that, below 590 m.a.s.l., the response time of the basin (lag-time) during storm events, is defined by the channel processes. On the other hand, above 590 m.a.s.l., the lag is defined by both interflow and stream flow.

The results presented in Chapter III, indicate a fast hydrological response of the basin with short lag times during storm events. Additionally, the Chapter III suggest densifying precipitation monitoring to capture the spatial variability of non-homogeneous storms in the basin. Thus, hydrometeorological monitoring for water resources and flood management (early warning systems) is recommended prioritizing river flow gauging below 590 m.a.s.l and rainfall gauging for areas above 590 m.a.s.l. The Universidad Regional Amazónica (Ikiam) located within the basin has started working in this regard (Ikiam-University, 2021).

2. Discusión General

A continuación, se presenta una traducción al castellano de la sección anterior titulada ‘General Discussion’:

2.1. Modelacion hidrológica e hidrodinámica del evento de inundación de septiembre 2017

Las crecidas repentinas son la principal amenaza natural en la ciudad de Tena de la Amazonía Ecuatoriana. Esto se debe a la combinación de fuertes precipitaciones con relieves escarpados (40 % en la parte alta), áreas de drenaje pequeñas (≈<135 km2) y suelos saturados (~90%). Desde 1996 hasta 2017 las inundaciones en esta zona han afectado a 16422 personas y a 923 hogares, generando miles de damnificados y cientos de hogares destruidos. Por ejemplo,

solamente la inundación del 2 de septiembre de 2017 produjo 974 afectados (GADM-TENA, 2021). Este evento, al contar con información necesaria para su reconstrucción, fue usado de referencia para entender por medio de modelación hidrológica e hidrodinámica las características de una inundación en la ciudad de Tena.

Las métricas de desempeño NSE y PBIAS sugieren que los modelos hidrológicos utilizados en los Capítulos III, IV y V (HEC-HMS, Hurtado-Pidal et al., 2020; y TETIS, Hurtado-Pidal et al., 2022; Hurtado-Pidal et al., 2023 *in prep*), alcanzaron un nivel satisfactorio de confianza según las directrices de Moriasi et al. (2007). Además, VanLiew et al. (2005) establecen que en simulaciones diarias o con intervalos de tiempo más pequeños, el NSE puede ser tan bajo como 0.4 para considerarse aceptable. Por lo tanto, a pesar del contexto de escasez de datos hidrometeorológicos, las simulaciones con HEC-HMS y TETIS (con intervalos de tiempo de 1 minuto y 10 minutos, respectivamente) fueron confiables para reproducir la respuesta hidrológica durante eventos extremos.

El modelo HEC-HMS permitió la reconstrucción del hidrograma de crecida de la inundación repentina ocurrida en la ciudad de Tena el 2 de septiembre de 2017. Según la simulación, el caudal máximo de este evento fue de 1967 m^3/s. Además, Chancay y Espitia-Sarmiento (2021), a través del modelo GR4H con simulaciones de intervalo horario, establecen un caudal máximo de 1379 m3/s para el mismo evento. No obstante, estas diferencias pueden atribuirse, en parte, a los diferentes intervalos de tiempo usados las simulaciones de HEC-HMS (1 minuto) y GR4H (1 hora). Por ejemplo, el cambio en el intervalo de tiempo del modelo GR4H resulta en cambios significativos en los flujos internos del modelo (Ficchì et al., 2019). Además, la simulación de la cuenca del río Tena realizada por Chancay y Espitia-Sarmiento (2021), muestra una diferencia del -27% con respecto al caudal máximo observado de 1896 m3/s. De esta manera, utilizando este valor como referencia (1896 m3/s), el caudal máximo estimado por HEC-HMS (1967 m3/s) está sobreestimado solo en un 4%.

Los resultados con el modelo hidrodinámico Nays2DFlood para el evento de inundación de septiembre de 2017, muestran un rendimiento satisfactorio, tanto para velocidades (m/s) como para niveles de agua (m), según Moriasi et al. (2007) (Capítulo III). Además, se logró un buen nivel de concordancia espacial entre las áreas de inundación observadas y modeladas con el índice F (0.8) propuesto por Horritt y Bates (2002), así como con puntos de control (6/8). Por lo tanto, la reconstrucción hidrodinámica y los mapas derivados de esta simulación pueden ser utilizados como referencia para la gestión de inundaciones en áreas urbanas (con

usos residenciales, comerciales y turístico) dentro de la ciudad de Tena. Los mapas publicados en el Plan de Desarrollo y Ordenamiento Territorial (PDOT) de la municipalidad de Tena no indican niveles ni velocidades de flujo en las áreas inundables (GADM-TENA, 2021). Es muy posible que, actualmente, estos mapas estén basados en técnicas de análisis espacial y geomorfológico a partir de sistemas de información geográfica y modelos digitales de elevación. Sin embargo, utilizar simplemente el área inundable y no los niveles y velocidades del flujo, limita la planificación urbana para construcción de vivienda, diseño de equipamiento y espacios públicos, así como planes de contingencia por inundación (Maranzoni et al., 2023).

En este sentido, el mapa de intensidad de inundación indica que el 71 % de las áreas inundadas corresponden a una alta intensidad (niveles de agua > 1.5 m o velocidad del flujo > 1.5 m/s). Sin embargo, en las áreas inundadas, los valores máximos tanto de velocidades como de niveles de agua fueron alrededor de 4 m y 3 m/s, respectivamente. Además, la inundación con intensidad media (0.5 < niveles de agua < 1.5 m; 0.5 < velocidad del flujo < 1.5 m/s) cubrió el 23 % de las áreas inundadas. Por lo tanto, un escenario similar al evento de inundación de septiembre de 2017 implica que el 94% de las áreas inundadas proyectadas representan riesgo para vidas humanas, infraestructura y vehículos (Bocanegra et al., 2020; Huizinga et al., 2017). Estas áreas pueden requerir operaciones de evacuación y rescate, así como también podría esperarse daños en edificaciones residenciales.

2.2. Proyecciones de cambio climático e implicaciones para inundaciones en la ciudad de Tena

Los resultados mostraron que la precipitación diaria en la cuenca cambiaría de 11.16 mm (histórico) a 14.32 mm (futuro) lo que equivale a un incremento del 28%. Además, también habría un cambio en el rango (máximo - mínimo) de precipitación, pasando de 182.20 mm (histórico) a 233.50 mm (futuro) lo que significa también un incremento de 28% (en ambos períodos el valor mínimo es 0 mm). En general, las simulaciones de cambio climático relacionadas a escenarios con altas emisiones (SSP5-8.5, RCP8.5) indican un aumento de precipitación para el noroeste de la Amazonia, incluyendo la Amazonia ecuatoriana y las estribaciones de los Andes (Almazroui et al., 2021; Armenta et al., 2016; Pabón-Caicedo et al., 2020; Palomino-Lemus et al., 2017; Sarmiento & Kooperman, 2019; Solman, 2013). Específicamente, Segarra (2022) encontró un incremento del 21% en la precipitación diaria para la cuenca del Colonso (dentro de la TRB) debido al cambio climático.

En el futuro (2041-2070), el cambio climático por sí solo tendría la capacidad de producir inundaciones en la ciudad de Tena cada dos años en promedio (Rp2; período de retorno de 2 años), incluso en un escenario extremo con toda la cuenca cubierta de bosque. Por lo tanto, las probabilidades de que se produzcan inundaciones en la ciudad de Tena durante cualquier año cambiarían del 10% en la actualidad (Rp10; período de retorno de 10 años) al 50% en el futuro (Rp2). Estos resultados concuerdan con Hirabayashi et al. (2013), quienes encontraron un cambio proyectado en el rango de 5 a 25 años en la frecuencia de inundaciones para esta región utilizando el escenario RCP8.5. Además, es probable que estos cambios ya estén ocurriendo debido al aumento de eventos de inundaciones en los últimos años (al menos 3 en los últimos 10 años; GADM-TENA, 2021).

2.3. Patrones espaciales de la deforestación e inundaciones

Analizando diferentes patrones espaciales del cambio de uso/cobertura del suelo (LUCC), los resultados del Capítulo IV muestran que la deforestación en la cuenca alta es el peor escenario para la regulación de inundaciones (Hurtado-Pidal et al., 2022). Además, el efecto del LUCC es mayor en la cuenca alta y disminuye progresivamente hacia aguas abajo (Capitulo V), lo cual puede explicarse por procesos a escala (Rogger et al., 2017). Sin embargo, la mayor influencia del LUCC en la cuenca alta también se debe a las características específicas en esta parte que pueden mejorar la conectividad, como la humedad del suelo, la conductividad hidráulica y las pendientes pronunciadas (Asano & Uchida, 2018; Birch et al., 2021; Edokpa et al., 2022; Gomi et al., 2008; Hopp & McDonnell, 2009).

Por otro lado, los escenarios de fragmentación de bosque muestran una influencia menor que los escenarios de localización. Estos resultados concuerdan con Hou et al. (2018) que encontraron un efecto relativamente bajo de la fragmentación. Por el contrario, Boongaling et al. (2018) y Gao & Yu, (2017) sugieren que la fragmentación del bosque está relacionada con una mayor escorrentía y caudales altos. Sin embargo, los estudios anteriores (Boongaling et al., 2018; Q. Gao & Yu, 2017) no consideran la superficie, es decir, una mayor fragmentación de bosque también estaba relacionada con una menor superficie. En esta investigación, la superficie de bosque es constante (50% de la cuenca). Por lo tanto, los resultados presentados en esta investigación (Capítulo III) aíslan el efecto de la pérdida de bosque en las inundaciones y solo consideran los diferentes patrones espaciales de LUCC.

La cuenca baja se caracteriza por tener pendientes de terreno más pequeñas y una mayor capacidad de infiltración respecto a la parte alta. Como resultado, el

flujo superficial en esta parte es menor. Además, la cuenca baja tiene una mayor fragmentación del bosque debido a la presencia de agricultura, infraestructura y otras coberturas antrópicas. Por lo tanto, es posible encontrar en la cuenca baja una correlación inversa entre la fragmentación y el flujo superficial (mayor fragmentación con flujo superficial relativamente menor). Sin embargo, esta correlación inversa no representa una causalidad.

En términos generales, la capacidad de infiltración del suelo y las pendientes del terreno tendrían más influencia que el LUCC en la respuesta hidrológica de la cuenca durante eventos de pequeña y mediana magnitud. Investigaciones anteriores (por ejemplo, J. Bathurst et al., 2018; Sriwongsitanon & Taesombat, 2011) indican que la regulación de caudales de crecidas es una función del contenido de humedad del suelo. Además, si la cuenca está saturada, la respuesta es la misma independientemente de las diferencias en la cobertura del suelo. Finalmente, a medida que aumenta la intensidad de las tormentas, el efecto del LUCC disminuye (J. C. Bathurst et al., 2020; Iacob et al., 2017; Laurance, 2007).

2.4. Efectos del cambio climático y LUCC en la cuenca

Esta investigación presenta un análisis detallado de las variaciones de los efectos aislados y combinados del cambio climático y el LUCC en crecidas a lo largo de un gradiente altitudinal en una cuenca húmeda tropical. Los resultados en el Capítulo V muestran que el cambio climático es más homogéneo que el LUCC a lo largo del gradiente altitudinal. Blöschl et al. (2007) hipotetizaron que a medida que aumenta la escala espacial, el impacto del LUCC disminuye progresivamente en la respuesta hidrológica. Por otro lado, la variabilidad climática tiene un efecto más homogéneo en las diferentes escalas espaciales. En otras palabras, a escalas pequeñas, el LUCC tiene un impacto mayor que la variabilidad climática en la respuesta hidrológica.

Los efectos combinados del cambio climático y el LUCC en los caudales de crecida a lo largo del gradiente altitudinal también siguen un patrón no lineal. Así, el patron de exponencial descente que sigue el efecto del LUCC en el gradiente altitudinal prevalece también cuando los factores se combinan. Además, los cambios producidos en la cuenca alta producen mayores efectos sobre el caudal, que aquellos producidos en la cuenca baja. Estos hallazgos concuerdan con los resultados presentados por Hung et al. (2020) y Olang & Fürst (2011) relacionados con una mayor sensibilidad de los caudales de crecida al LUCC en cuencas pequeñas o de cabecera. También, uno de los hallazgos más importantes mostrados en el Capítulo V se relaciona con el análisis de interacción. Se encontró

una muy pequeña interacción antagónica entre el cambio climático y el LUCC. Esta interacción es mas pequeña en la cuenca alta y aumenta ligeramente hacia aguas abajo. Algunos estudios han encontrado interacciones sinérgicas (Hung et al. 2020) y antagónicas entre el cambio climático y el LUCC (por ejemplo, Lamichhane & Shakya, 2019). Sin embargo, las diferencias podrían atribuirse principalmente al uso de diferentes configuraciones en la modelación hidrológica (por ejemplo, escala de evento versus escala mensual).

La función exponencial descendente de las diferencias absolutas en el gradiente altitudinal de la cuenca de estudio indica un punto relativamente estable de cambios abruptos ubicado a 590 m.s.n.m. Esta elevación representa un umbral donde el efecto del cambio climático y el LUCC en los caudales de crecida es notablemente mayor. Los cambios abruptos ocurren en esta parte de la cuenca porque, para el mismo rango de elevación (por ejemplo, 50 m), la diferencia en el área de drenaje acumulada es mucho mayor en la parte inferior que en la parte superior. Además, los resultados en el Capítulo V corroboran los hallazgos mostrados en el Capítulo IV con respecto a la disminución del efecto del LUCC a medida que aumenta la intensidad de las tormentas. Sin embargo, en la cuenca alta las diferentes intensidades de lluvia (Rp2, Rp10, Rp100) alteran ligeramente el efecto del LUCC sobre los caudales de crecida.

2.5. Implicaciones para las soluciones basadas en la naturaleza y la gestión de inundaciones

Los resultados demuestran la importancia de la cobertura forestal, ubicada en la cuenca alta, que forma parte de la reserva biológica Colonso-Chalupas (RBCC, Figura 5.1a en el Capítulo V), para regular las inundaciones. Además, considerando los escenarios desfavorables del cambio climático debido al aumento de la precipitación e inundaciones, el bosque en la cuenca alta desempeña un papel clave como solución basada en la naturaleza (SbN) para la regulación de inundaciones. Sin embargo, los resultados también indican que la influencia del bosque para regular las inundaciones está limitada a tormentas pequeñas y moderadas (≤Rp2). En este sentido, para Rp2, aproximadamente el rango altitudinal de 590 a 906 m.s.n.m., sería el área de transición entre la cuenca alta y la cuenca baja en términos de influencia del LUCC en los caudales de crecida (Capítulo V). En concordancia con nuestros hallazgos, Birkel et al. (2012) encontraron en una cuenca húmeda en Costa Rica que el LUCC tiene un efecto relativamente pequeño en los caudales máximos con períodos de retorno > 1 año. Además, otros estudios enfatizan el potencial limitado del bosque para reducir inundaciones con eventos de tormenta mayores (J. C. Bathurst et al., 2011; Iacob et al., 2017; Salazar et al.,

2012). Por lo tanto, la aplicación de SbN relacionadas con la capacidad del bosque para regular crecidas debe complementarse con otras iniciativas para una gestión efectiva de inundaciones (Ilieva et al., 2018; Soulsby et al., 2017).

Esta investigación definió las áreas de mayor cambio de caudal (High-flow areas en la Figura 5.1a, Capítulo V), basadas en una elevación crítica relativamente estable, localizada a 590 m.s.n.m. En esta elevación ocurren cambios abruptos de caudal máximo y de volumen de caudal debido a los efectos del cambio climático y el LUCC. Por lo tanto, basándose en los resultados, es razonable dar prioridad a la protección y/o restauración de laderas fuera de estas áreas de mayor cambio de caudal (>590 m.s.n.m.). Mientras que dentro de las áreas (≤590 m.s.n.m), se puede establecer la prioridad de proteger el cauce del río, las terrazas bajas y las zonas ribereñas. Además, otras iniciativas dentro de la cuenca pueden basarse en esta zonificación espacial, como la planificación periurbana de paisajes (Barbedo et al., 2014). Esto es muy importante considerando que dentro de estas zonas viven aproximadamente 6000 personas, la mayoría de origen indígena con una vulnerabilidad socioeconómica relativamente alta (INEC, 2010).”

Las SbN y la planificación territorial (urbana y peri-urbana) pueden incluir parques fluviales como paisajes multifuncionales para amortiguar crecidas, recreación, conservación, entre otros (Martín-Vide, 2015; Miguez et al., 2015; Rotger, 2018). En este sentido la zonificación urbanística del PDOT de la municipalidad de Tena (GADM-TENA, 2021) indica que muchas de las áreas inundables cerca de los cauces, son áreas de desarrollo turístico (A17) y áreas de conservación (A16). Por lo tanto, el establecimiento de parques fluviales es necesario y compatible con la zonificación urbanística de la ciudad de Tena cumpliendo efectivamente con ambos propósitos (A17, A16). El establecimiento de SbN para la gestión de riesgos y planificación territorial en general, debe ir acompañado de monitoreo hidrometeorológico en la cuenca.

Es razonable suponer que, durante eventos de crecidas, por debajo de 590 m.s.n.m., el volumen de caudal de crecidas se desplaza principalmente en el cauce del río. Mientras que, por encima de esta elevación, un porcentaje importante de agua se mueve a través del perfil del suelo como interflujo. Por lo tanto, en concordancia con Asano & Uchida, (2018), es posible establecer que, por debajo de 590 m.s.n.m., el tiempo de respuesta de la cuenca (desfasaje) durante eventos de tormenta está definido por los procesos en el canal. Mientras que, por encima de los 590 m.s.n.m., el tiempo de respuesta está definido tanto por el interflujo como por el movimiento del agua en el canal.

Los resultados presentados en el Capítulo III indican una rápida respuesta hidrológica de la cuenca con tiempos de retraso cortos durante eventos de tormenta. Además, el Capítulo III sugiere una densificación de estaciones para el monitoreo de precipitación que permita capturar la variabilidad espacial de tormentas no homogéneas en la cuenca. Por lo tanto, es factible recomendar que el monitoreo hidrometeorológico priorize la medición de caudales por debajo de los 590 m.s.n.m. y el monitoreo de precipitación por encima de los 590 m.s.n.m. La Universidad Regional Amazónica (Ikiam) ubicada dentro de la cuenca de estudio ha comenzado a trabajar en este sentido (Ikiam-University, 2021).

CHAPTER VII

GENERAL CONCLUSIONS

1. General Conclusions

The general objective of this research was to analyze the combined effects of climate change and LUCC on floods in a tropical basin, with a specific emphasis on landscape configuration and the role of native forests for flood regulation. The hydrological models HEC-HMS (semi-distributed) and TETIS (fully spatially-distributed) as well as the hydrodynamic model Nays2DFlood (2D) were applied in this research in a complementary modelling framework. The event-sampling approach was used within the context of data-scarce watershed for a humid tropic basin of Ecuadorian Amazon. Specifically, the HEC-HMS and Nays2DFlood models were coupled to reproduce the flood event occurred in the city of Tena in September 2017 (Chapter III). On the other hand, the TETIS model was used to evaluate the effect of forest location and forest fragmentation on floods (Chapter IV) as well the individual and combined contribution of climate change and LUCC (Chapter V).

The results showed that the proposed approach was suitable for the calibration and validation of hydrological models and for the simulation of extreme flood events. Moreover, the results indicate that the HEC-HMS model, accuratelly reproduced the flood event occurred in the city of Tena in September 2017 (Chapter III). Also, regarding the effect of forest spatial patterns, the stormflows were more sensitive to forest location than forest fragmentation. Specifically, the deforestation in the upper basin is the worst scenario to regulate floods (Chapter IV). Therefore, the hypothesis H1 is accepted. However, even with the hypothetical scenario of the entire basin being covered by forest, the probabilities of producing floods in the city of Tena during any given year will change due to climate change from 10 (Rp10) to 50% (Rp2).

The interaction between climate change and LUCC is slightly and statistically non-significant with an antagonistic effect in the lower part. Therefore, in general, the interaction is null. Although the individual effect of climate change is more homogeneous than LUCC on floods, the combined effect is greater in the upper basin and decreases progressively to downstream direction in a non-lineal manner. Therefore, the hypothesis H2 is also accepted. Therefore, the native forest in the upper basin is crucial to mitigate climate change induced floods during small and medium-size storms (≤Rp2). However, as storm intensity increases the influence of forest cover decreases. Also, the 590 m.a.s.l is the elevation where the abrupt changes of peak flow and stormflow volume occurs. Thus, the forest protection/restauration is proposed using this critical elevation. Additionally,

hydrometeorological gauging efforts within the basin can be based on this threshold of abrupt changes.

The results of this research can be used by decision-makers and institutions related to water resources management, risk management, and territorial planning in general. The analyzed hypotheses contribute to the integrated knowledge of the interaction between climate change, deforestation, and floods, with a focus on landscape configuration in a tropical basin with a pronounced altitudinal gradient. Obtained results enhance our understanding of ecosystem services provided by the Andean-Amazonian foothills forests and provide guidelines for the implementation of NbS for flood regulation and climate change adaptation. Finally, the application of NbS related to the forest's capacity to regulate floods need to be integrated in a broader context with other initiatives for effective flood management.

2. Conclusiones Generales

A continuación, se presenta una traducción al castellano de la sección anterior titulada ‘General Conclusions’:

El objetivo general de esta investigación fue analizar los efectos combinados del cambio climático y el LUCC sobre las inundaciones de una cuenca tropical, con un énfasis en la configuración del paisaje y el rol del bosque nativo en la regulación de crecidas. Los modelos hidrológicos HEC-HMS (semi-distribuido) y TETIS (totalmente distribuido), así como el modelo hidrodinámico Nays2DFlood (2D), se aplicaron en esta investigación en un marco de modelado complementario. Se utilizó un enfoque de muestreo de eventos en el contexto de una cuenca con datos escasos de la Región Amazonia Ecuatoriana. Específicamente, los modelos HEC-HMS y Nays2DFlood se acoplaron para reproducir el evento de inundación ocurrido en la ciudad de Tena en septiembre de 2017 (Capítulo III). Por otro lado, el modelo TETIS se utilizó para evaluar el efecto de la localización y fragmentación del bosque en las crecidas (Capítulo IV), así como la contribución individual y combinada del cambio climático y el LUCC (Capítulo V).

Los resultados muestran que el enfoque propuesto fue adecuado para la calibración y validación de modelos hidrológicos, así como para la simulación de eventos extremos de inundación. Además, los resultados indican que el modelo HEC-HMS reprodujo adecuadamente el evento de inundación ocurrido en la ciudad de Tena en septiembre de 2017 (Capítulo III). Respecto al efecto que tienen los patrones espaciales del bosque, los resultados indican que los caudales de crecida fueron más sensibles a la localización del bosque que a su fragmentación.

Específicamente, la deforestación en la cuenca alta es el peor escenario para regular crecidas (Capítulo IV). Por lo tanto, la hipótesis H1 es verdadera. Sin embargo, incluso con el escenario hipotético de que toda la cuenca esté cubierta por bosque, las probabilidades de producir inundaciones en la ciudad de Tena cambiarían en el futuro debido al cambio climático de 10 (Rp10) a 50% (Rp2).

La interacción entre el cambio climático y el LUCC es muy pequeña y estadísticamente no significativa con un efecto ligeramente antagónico en la parte baja. Por lo tanto, de forma general la interacción es nula. Aunque el efecto aislado del cambio climático es más homogéneo que el del LUCC en las crecidas, el efecto combinado es mayor en la cuenca alta y disminuye hacia aguas debajo de manera no lineal. Por lo tanto, la hipótesis H2 también es verdadera. En este contexto, el bosque nativo en la cuenca alta es crucial para ayudar en la mitigación de los efectos del cambio climático en las crecidas durante tormentas pequeñas y moderadas (≤Rp2). Sin embargo, a medida que aumenta la intensidad de la tormenta, la influencia del bosque sobre las crecidas disminuye. En la elevación de 590 m.s.n.m. ocurren cambios abruptos en el caudal máximo y el volumen de caudal. Por lo tanto, se propone la protección/restauración del bosque utilizando esta elevación crítica. Además, los esfuerzos de medición hidrometeorológica dentro de la cuenca pueden basarse en este umbral de cambios abruptos.

Los resultados de esta investigación pueden ser usados por tomadores de decisiones e instituciones relacionadas a la gestión de recursos hídricos, gestión de riesgos y planificación territorial en general. Las hipótesis analizadas, contribuyen al conocimiento integrado de la interacción entre cambio climático, deforestación y crecidas con una mirada desde la configuración del paisaje en una cuenca tropical con marcado gradiente altitudinal. Los resultados obtenidos mejoran la comprensión de los servicios ecosistémicos de los bosques de las estribaciones Andino-Amazónicas y proporcionan directrices para la implementación de SbN para la regulación de crecidas y la adaptación al cambio climático. Finalmente, la aplicación de SbN relacionadas con la capacidad del bosque para regular crecidas debe complementarse con otras iniciativas para una gestión efectiva de inundaciones.

GENERAL REFERENCES

(Chapters I, II, VI)

Almazroui, M., Ashfaq, M., Islam, M. N., Rashid, I. U., Kamil, S., Abid, M. A., O'Brien, E., Ismail, M., Reboita, M. S., Sörensson, A. A., Arias, P. A., Alves, L. M., Tippett, M. K., Saeed, S., Haarsma, R., Doblas-Reyes, F. J., Saeed, F., Kucharski, F., Nadeem, I., … Sylla, M. B. (2021). Assessment of CMIP6 Performance and Projected Temperature and Precipitation Changes Over South America. Earth Systems and Environment 2021 5:2, 5(2), 155–183. https://doi.org/10.1007/S41748-021-00233-6

Armenta, E., Villa, L., & Jácome, P. (2016). PROYECCIONES CLIMÁTICAS DE PRECIPITACIÓN Y TEMPERATURA PARA ECUADOR, BAJO DISTINTOS ESCENARIOS DE CAMBIO CLIMÁTICO.

Asano, Y., & Uchida, T. (2018). The roles of channels and hillslopes in rainfall/run-off lag times during intense storms in a steep catchment. Hydrological Processes, 32(6), 713–728. https://doi.org/10.1002/hyp.11443

Ataroff, M., & Rada, F. (2000). Deforestation Impact on Water Dynamics in a Venezuelan Andean Cloud Forest. Https://Doi.Org/10.1579/0044-7447-29.7.440, 29(7), 440–444. https://doi.org/10.1579/0044-7447-29.7.440

Barbedo, J., Miguez, M., van der Horst, D., & Marins, M. (2014). Enhancing ecosystem services for flood mitigation: a conservation strategy for peri-urban landscapes? Ecology and Society, 19(2), art54. https://doi.org/10.5751/ES-06482-190254

Bathurst, J., Birkinshaw, S., Johnson, H., Kenny, A., Napier, A., Raven, S., Robinson, J., & Stroud, R. (2018). Runoff, flood peaks and proportional response in a combined nested and paired forest plantation/peat grassland catchment. Journal of Hydrology, 564, 916–927. https://doi.org/10.1016/J.JHYDROL.2018.07.039

Bathurst, J. C., Fahey, B., Iroumé, A., & Jones, J. (2020). Forests and floods: Using field evidence to reconcile analysis methods. Hydrological Processes, 34(15), 3295–3310. https://doi.org/10.1002/HYP.13802

Bathurst, J. C., Iroumé, A., Cisneros, F., Fallas, J., Iturraspe, R., Novillo, M. G., Urciuolo, A., Bièvre, B. de, Borges, V. G., Coello, C., Cisneros, P., Gayoso, J., Miranda, M., & Ramírez, M. (2011). Forest impact on floods due to extreme rainfall and snowmelt in four Latin American environments 1: Field data analysis. Journal of Hydrology, 400(3–4), 281–291. https://doi.org/10.1016/J.JHYDROL.2010.11.044

Birch, A. L., Stallard, R. F., Bush, S. A., & Barnard, H. R. (2021). The influence of land cover and storm magnitude on hydrologic flowpath activation and runoff generation in steep tropical catchments of central Panama. Journal of Hydrology, 596, 126138. https://doi.org/10.1016/J.JHYDROL.2021.126138

Birkel, C., Soulsby, C., & Tetzlaff, D. (2012). Modelling the impacts of land-cover change on streamflow dynamics of a tropical rainforest headwater catchment. Hydrological Sciences Journal, 57(8), 1543–1561. https://doi.org/10.1080/02626667.2012.728707

Blöschl, G. (2022). Flood generation: Process patterns from the raindrop to the ocean. Hydrology and Earth System Sciences, 26(9), 2469–2480. https://doi.org/10.5194/HESS-26-2469-2022

Blöschl, G., Ardoin-Bardin, S., Bonell, M., Dorninger, M., Goodrich, D., Gutknecht, D., Matamoros, D., Merz, B., Shand, P., & Szolgay, J. (2007). At what scales do climate variability and land cover change impact on flooding and low flows? Hydrological Processes, 21(9), 1241–1247. https://doi.org/10.1002/HYP.6669

Blöschl, G., Bierkens, M. F. P., Chambel, A., Cudennec, C., Destouni, G., Fiori, A., Kirchner, J. W., McDonnell, J. J., Savenije, H. H. G., Sivapalan, M., Stumpp, C., Toth, E., Volpi, E., Carr, G., Lupton, C., Salinas, J., Széles, B., Viglione, A., Aksoy, H., … Zhang, Y. (2019). Twenty-three unsolved problems in hydrology (UPH) – a community perspective. Hydrological Sciences Journal, 64(10), 1141–1158. https://doi.org/10.1080/02626667.2019.1620507

Bocanegra, R. A., Vallés-Morán, F. J., & Francés, F. (2020). Review and analysis of vehicle stability models during floods and proposal for future improvements. Journal of Flood Risk Management, 13(S1). https://doi.org/10.1111/jfr3.12551

Bonnesoeur, V., Locatelli, B., Guariguata, M. R., Ochoa-Tocachi, B. F., Vanacker, V., Mao, Z., Stokes, A., & Mathez-Stiefel, S. L. (2019). Impacts of forests and forestation on hydrological services in the Andes: A systematic review. Forest Ecology and Management, 433, 569–584. https://doi.org/10.1016/J.FORECO.2018.11.033

Boongaling, C. G. K., Faustino-Eslava, D. V., & Lansigan, F. P. (2018). Modeling land use change impacts on hydrology and the use of landscape metrics as tools for watershed management: The case of an ungauged catchment in the Philippines. Land Use Policy, 72(August 2016), 116–128. https://doi.org/10.1016/j.landusepol.2017.12.042

Bronstert, A. (2004). Rainfall-runoff modelling for assessing impacts of climate and land-use change. Hydrological Processes, 18(3), 567–570. https://doi.org/10.1002/HYP.5500

Bronstert, A., Niehoff, D., & Brger, G. (2002). Effects of climate and land-use change on storm runoff generation: present knowledge and modelling capabilities. Hydrological Processes, 16(2), 509–529. https://doi.org/10.1002/HYP.326

Buytaert, W., Vuille, M., Dewulf, A., Urrutia, R., Karmalkar, A., & Célleri, R. (2010). Uncertainties in climate change projections and regional downscaling in the tropical Andes: implications for water resources management. Hydrology and Earth System Sciences, 14(7), 1247–1258. https://doi.org/10.5194/hess-14-1247-2010

Cadilhac, L., Torres, R., Calles, J., Vanacker, V., & Calderón, E. (2017). Desafíos para la investigación sobre el cambio climático en Ecuador. Neotropical Biodiversity, 3(1), 168–181. https://doi.org/10.1080/23766808.2017.1328247

Chancay, J. E., & Espitia-Sarmiento, E. F. (2021). Improving Hourly Precipitation Estimates for Flash Flood Modeling in Data-Scarce Andean-Amazon Basins: An Integrative Framework Based on Machine Learning and Multiple Remotely Sensed Data. Remote Sensing 2021, Vol. 13, Page 4446, 13(21), 4446. https://doi.org/10.3390/RS13214446

Chang, H., & Franczyk, J. (2008). Climate Change, Land-Use Change, and Floods: Toward an Integrated Assessment. Geography Compass, 2(5), 1549–1579. https://doi.org/10.1111/j.1749-8198.2008.00136.x

Chawla, I., & Mujumdar, P. P. (2015). Isolating the impacts of land use and climate change on streamflow. Hydrology and Earth System Sciences, 19(8), 3633–3651. https://doi.org/10.5194/HESS-19-3633-2015

Ciervo, F., Papa, M. N., Medina, V., & Bateman, A. (2015). Simulation of flash floods in ungauged basins using post-event surveys and numerical modelling. Journal of Flood Risk Management, 8(4), 343–355. https://doi.org/10.1111/jfr3.12103

Cohen-Shacham, E., Andrade, A., Dalton, J., Dudley, N., Jones, M., Kumar, C., Maginnis, S., Maynard, S., Nelson, C. R., Renaud, F. G., Welling, R., & Walters, G. (2019). Core principles for successfully implementing and upscaling Nature-based Solutions. Environmental Science & Policy, 98, 20–29. https://doi.org/10.1016/J.ENVSCI.2019.04.014

Correa, A., Windhorst, D., Crespo, P., Célleri, R., Feyen, J., & Breuer, L. (2016). Continuous versus event-based sampling: how many samples are required for deriving general hydrological understanding on Ecuador's páramo region? Hydrological Processes, 30(22), 4059–4073. https://doi.org/10.1002/hyp.10975

Cuenca, P., Robalino, J., Arriagada, R., & Echeverría, C. (2018). Are government incentives effective for avoided deforestation in the tropical Andean forest? PLOS ONE, 13(9), e0203545. https://doi.org/10.1371/journal.pone.0203545

Dadson, S. J., Hall, J. W., Murgatroyd, A., Acreman, M., Bates, P., Beven, K., Heathwaite, L., Holden, J., Holman, I. P., Lane, S. N., O'Connell, E., Penning-Rowsell, E., Reynard, N., Sear, D., Thorne, C., & Wilby, R. (2017). A restatement of the natural science evidence concerning catchment-based 'natural' flood management in the UK. Proceedings of the Royal Society A: Mathematical, Physical and Engineering Science, 473(2199), 20160706. https://doi.org/10.1098/rspa.2016.0706

Descheemaeker, K., Nyssen, J., Poesen, J., Raes, D., Haile, M., Muys, B., & Deckers, S. (2006). Runoff on slopes with restoring vegetation: A case study from the Tigray highlands, Ethiopia. Journal of Hydrology, 331(1–2), 219–241. https://doi.org/10.1016/J.JHYDROL.2006.05.015

Díez-Herrero, A., Huerta, L. L., & Isidro, M. L. (2009). A handbook on flood hazard mapping methodologies (Issue 2). http://books.google.com/books?hl=en&lr=&id=4nXerdbeEogC&pgis=1

Dixon, S. J., Sear, D. A., Odoni, N. A., Sykes, T., & Lane, S. N. (2016). The effects of river restoration on catchment scale flood risk and flood hydrology. Earth Surface Processes and Landforms, 41(7), 997–1008. https://doi.org/10.1002/esp.3919

Dunne, R. P. (2010). Synergy or antagonism-interactions between stressors on coral reefs. Coral Reefs, 29(1), 145–152. https://doi.org/10.1007/s00338-009-0569-6

Edokpa, D., Milledge, D., Allott, T., Holden, J., Shuttleworth, E., Kay, M., Johnston, A., Millin-Chalabi, G., Scott-Campbell, M., Chandler, D., Freestone, J., & Evans, M. (2022). Rainfall intensity and catchment size control storm runoff in a gullied blanket peatland. Journal of Hydrology, 609, 127688. https://doi.org/10.1016/J.JHYDROL.2022.127688

EM-DAT. (2023). The international disasters database. https://www.emdat.be/

Espinoza, J. C., Chavez, S., Ronchail, J., Junquas, C., Takahashi, K., & Lavado, W. (2015). Rainfall hotspots over the southern tropical Andes: Spatial distribution, rainfall intensity, and relations with large-scale atmospheric circulation. Water Resources Research, 51(5), 3459–3475. https://doi.org/10.1002/2014WR016273

Fahrig, L. (2003). Effects of Habitat Fragmentation on Biodiversity. Annual Review of Ecology, Evolution, and Systematics, 34(1), 487–515. https://doi.org/10.1146/annurev.ecolsys.34.011802.132419

Ficchì, A., Perrin, C., & Andréassian, V. (2019). Hydrological modelling at multiple sub-daily time steps: Model improvement via flux-matching. Journal of Hydrology, 575, 1308–1327. https://doi.org/10.1016/J.JHYDROL.2019.05.084

Fleischbein, K., Wilcke, W., Valarezo, C., Zech, W., & Knoblich, K. (2006). Water budgets of three small catchments under montane forest in Ecuador: experimental and modelling approach. Hydrological Processes, 20(12), 2491–2507. https://doi.org/10.1002/HYP.6212

GADM-TENA. (2021). ACTUALIZACIÓN PDOT 2020-2023. GADM-Tena. https://tena.gob.ec/index.php/tena/plan-de-desarrollo

Gao, H., Sabo, J. L., Chen, X., Liu, Z., Yang, Z., Ren, Z., & Liu, M. (2018). Landscape heterogeneity and hydrological processes: a review of landscape-based hydrological models. Landscape Ecology, 33(9), 1461–1480. https://doi.org/10.1007/s10980-018-0690-4

Gao, Q., & Yu, M. (2017). Reforestation-induced changes of landscape composition and configuration modulate freshwater supply and flooding risk of tropical watersheds. PLOS ONE, 12(7), e0181315. https://doi.org/10.1371/journal.pone.0181315

Gomi, T., Sidle, R. C., Miyata, S., Kosugi, K., & Onda, Y. (2008). Dynamic runoff connectivity of overland flow on steep forested hillslopes: Scale effects and runoff transfer. Water Resources Research, 44(8), 8411. https://doi.org/10.1029/2007WR005894

Hirabayashi, Y., Mahendran, R., Koirala, S., Konoshima, L., Yamazaki, D., Watanabe, S., Kim, H., & Kanae, S. (2013). Global flood risk under climate change. Nature Climate Change, 3(9), 816–821. https://doi.org/10.1038/nclimate1911

Hopp, L., & McDonnell, J. J. (2009). Connectivity at the hillslope scale: Identifying interactions between storm size, bedrock permeability, slope angle and soil depth. Journal of Hydrology, 376(3–4), 378–391. https://doi.org/10.1016/J.JHYDROL.2009.07.047

Horritt, M. S. S., & Bates, P. D. D. (2002). Evaluation of 1D and 2D numerical models for predicting river flood inundation. Journal of Hydrology, 268(1–4), 87–99. https://doi.org/10.1016/S0022-1694(02)00121-X

Hou, J., Guo, K., Liu, F., Han, H., Liang, Q., Tong, Y., & Li, P. (2018). Assessing Slope Forest Effect on Flood Process Caused by a Short-Duration Storm in a Small Catchment. Water, 10(9), 1256. https://doi.org/10.3390/w10091256

Huizinga, J., de Moel, H., & Szewczyk, W. (2017). Global flood depth-damage functions : Methodology and the Database with Guidelines. In Joint Research Centre (JRC). https://doi.org/10.2760/16510

Hung, C. L. J., James, L. A., Carbone, G. J., & Williams, J. M. (2020). Impacts of combined land-use and climate change on streamflow in two nested catchments in the Southeastern United States. Ecological Engineering, 143, 105665. https://doi.org/10.1016/J.ECOLENG.2019.105665

Hurtado-Pidal, J., Acero Triana, J. S., Aguayo, M., Link, O., Valencia, B. G., Espitia-Sarmiento, E., & Conicelli, B. (2022). Is forest location more important than forest fragmentation for flood regulation? Ecological Engineering, 183, 106764. https://doi.org/10.1016/J.ECOLENG.2022.106764

Hurtado-Pidal, J., Acero Triana, J. S., Espitia-Sarmiento, E., & Jarrín-Pérez, F. (2020). Flood Hazard Assessment in Data-Scarce Watersheds Using Model Coupling, Event Sampling, and Survey Data. Water, 12(10), 2768. https://doi.org/10.3390/w12102768

Iacob, O., Brown, I., & Rowan, J. (2017). Natural flood management, land use and climate change trade-offs: the case of Tarland catchment, Scotland. Hydrological Sciences Journal, 62(12), 1931–1948. https://doi.org/10.1080/02626667.2017.1366657

Ikiam-University. (2021). Ikiam Hydromet Service. http://hidrometeorologia.ikiam.edu.ec/

Ilieva, L., McQuistan, C., Van-Breda, A., Rodriguez, A., Guevara, O., Cordero, D., & Renaud, F. (2018). Adoptando soluciones basadas en la naturaleza para la reducción del riesgo de inundación en América Latina (p. 24). https://solucionespracticas.org.pe/Adoptando-soluciones-basadas-en-la-naturaleza-para-la-reduccion-del-riesgo-de-inundacion-en-America-Latina

INAMHI. (2023). INAMHI GEOGloWS Portal. https://inamhi.geoglows.org/

INEC. (2010). Censo de Poblacion y Vivienda - 2010. INEC (Instituto Nacional de Estadísticas y Censos). https://www.ecuadorencifras.gob.ec/banco-de-informacion/

IPCC. (2021). Climate Change 2021: The Physical Science Basis. Contribution of Working Group I to the Sixth Assessment Report of the Intergovernmental Panel on Climate Change (p. 41). Cambridge University Press. https://www.ipcc.ch/report/ar6/wg1/

Jodar-Abellan, A., Valdes-Abellan, J., Pla, C., & Gomariz-Castillo, F. (2019). Impact of land use changes on flash flood prediction using a sub-daily SWAT model in five Mediterranean ungauged watersheds (SE Spain). Science of The Total Environment, 657, 1578–1591. https://doi.org/10.1016/J.SCITOTENV.2018.12.034

Johnson, F., White, C. J., van Dijk, A., Ekstrom, M., Evans, J. P., Jakob, D., Kiem, A. S., Leonard, M., Rouillard, A., & Westra, S. (2016). Natural hazards in Australia: floods. Climatic Change, 139(1), 21–35. https://doi.org/10.1007/s10584-016-1689-y

Jonkman, S. N. (2005). Global Perspectives on Loss of Human Life Caused by Floods. Natural Hazards 2005 34:2, 34(2), 151–175. https://doi.org/10.1007/S11069-004-8891-3

Jourgholami, M., Karami, S., Tavankar, F., Lo Monaco, A., & Picchio, R. (2020). Effects of Slope Gradient on Runoff and Sediment Yield on Machine-Induced Compacted Soil in Temperate Forests. Forests 2021, Vol. 12, Page 49, 12(1), 49. https://doi.org/10.3390/F12010049

Junquas, C., Heredia, M. B., Condom, T., Ruiz-Hernández, J. C., Campozano, L., Dudhia, J., Espinoza, J. C., Menegoz, M., Rabatel, A., & Sicart, J. E. (2022). Regional climate modeling of the diurnal cycle of precipitation and associated atmospheric circulation patterns over an Andean glacier region (Antisana, Ecuador). Climate Dynamics, 58(11–12), 3075–3104. https://doi.org/10.1007/S00382-021-06079-Y/FIGURES/13

Kim, H. W., & Park, Y. (2016). Urban green infrastructure and local flooding: The impact of landscape patterns on peak runoff in four Texas MSAs. Applied Geography, 77, 72–81. https://doi.org/10.1016/J.APGEOG.2016.10.008

Kleemann, J., Zamora, C., Villacis-Chiluisa, A. B., Cuenca, P., Koo, H., Noh, J. K., Fürst, C., & Thiel, M. (2022). Deforestation in Continental Ecuador with a Focus on Protected Areas. Land 2022, Vol. 11, Page 268, 11(2), 268. https://doi.org/10.3390/LAND11020268

Lamichhane, & Shakya. (2019). Integrated Assessment of Climate Change and Land Use Change Impacts on Hydrology in the Kathmandu Valley Watershed, Central Nepal. Water, 11(10), 2059. https://doi.org/10.3390/w11102059

Lane, S. N. (2017). Natural flood management. Wiley Interdisciplinary Reviews: Water, 4(3), e1211. https://doi.org/10.1002/wat2.1211

Laurance, W. F. (2007). Forests and floods. Nature 2007 449:7161, 449(7161), 409–410. https://doi.org/10.1038/449409a

Lian, J., Chen, H., Wang, F., Nie, Y., & Wang, K. (2020). Separating the relative contributions of climate change and ecological restoration to runoff change in a mesoscale karst basin. CATENA, 194, 104705. https://doi.org/10.1016/J.CATENA.2020.104705

Liu, J., Liu, X., Wang, Y., Li, Y., Jiang, Y., Fu, Y., & Wu, J. (2020). Landscape composition or configuration: which contributes more to catchment hydrological flows and variations? Landscape Ecology 2020 35:7, 35(7), 1531–1551. https://doi.org/10.1007/S10980-020-01035-3

Maranzoni, A., D'Oria, M., & Rizzo, C. (2023). Quantitative flood hazard assessment methods: A review. Journal of Flood Risk Management, 16(1), e12855. https://doi.org/10.1111/JFR3.12855

Martín-Vide, J. P. (2015). Restauración del río Besòs en Barcelona. Historia y lecciones. Ribagua, 2(1), 51–60. https://doi.org/10.1016/j.riba.2015.07.001

Mena, C. F., Bilsborrow, R. E., & McClain, M. E. (2006). Socioeconomic Drivers of Deforestation in the Northern Ecuadorian Amazon. Environmental Management, 37(6), 802–815. https://doi.org/10.1007/s00267-003-0230-z

Merz, B., Aerts, J., Arnbjerg-Nielsen, K., Baldi, M., Becker, A., Bichet, A., Blöschl, G., Bouwer, L. M., Brauer, A., Cioffi, F., Delgado, J. M., Gocht, M., Guzzetti, F., Harrigan, S., Hirschboeck, K., Kilsby, C., Kron, W., Kwon, H.-H., Lall, U., … Nied, M. (2014). Floods and climate: emerging perspectives for flood risk assessment and management. Natural Hazards and Earth System Sciences, 14(7), 1921–1942. https://doi.org/10.5194/nhess-14-1921-2014

Metcalfe, P., Beven, K., Hankin, B., & Lamb, R. (2017). A modelling framework for evaluation of the hydrological impacts of nature-based approaches to flood risk management, with application to in-channel interventions across a 29-km2 scale catchment in the United Kingdom. Hydrological Processes, 31(9), 1734–1748. https://doi.org/10.1002/hyp.11140

Miguez, M. G., Veról, A. P., De Sousa, M. M., & Rezende, O. M. (2015). Urban Floods in Lowlands—Levee Systems, Unplanned Urban Growth and River Restoration Alternative: A Case Study in Brazil. Sustainability 2015, Vol. 7, Pages 11068-11097, 7(8), 11068–11097. https://doi.org/10.3390/SU70811068

Ministerio de Ambiente. (2015). Estadísticas de Patrimonio Natural. In Estadísticas de Patrimonio Natural (p. 20). https://doi.org/10.1039/DT9960002403

Moriasi, D. N., Arnold, J. G., Van Liew, M. W., Bingner, R. L., Harmel, R. D., Veith, T. L., Harmel, D., & Veith, T. L. (2007). Model Evaluation Guidelines for Systematic Quantification of Accuracy in Watershed Simulations. Transactions of the ASABE, 50(3), 885–900. https://doi.org/10.13031/2013.23153

Nikolopoulos, E. I., Anagnostou, E. N., Borga, M., Vivoni, E. R., & Papadopoulos, A. (2011). Sensitivity of a mountain basin flash flood to initial wetness condition and rainfall variability. Journal of Hydrology, 402(3–4), 165–178. https://doi.org/10.1016/j.jhydrol.2010.12.020

Ochoa-Tocachi, B. F., Buytaert, W., De Bièvre, B., Célleri, R., Crespo, P., Villacís, M., Llerena, C. A., Acosta, L., Villazón, M., Guallpa, M., Gil-Ríos, J., Fuentes, P., Olaya, D., Viñas, P., Rojas, G., & Arias, S. (2016). Impacts of land use on the hydrological response of tropical Andean catchments. Hydrological Processes, 30(22), 4074–4089. https://doi.org/10.1002/hyp.10980

Olang, L. O., & Fürst, J. (2011). Effects of land cover change on flood peak discharges and runoff volumes: model estimates for the Nyando River Basin, Kenya. Hydrological Processes, 25(1), 80–89. https://doi.org/10.1002/HYP.7821

Pabón-Caicedo, J. D., Arias, P. A., Carril, A. F., Espinoza, J. C., Borrel, L. F., Goubanova, K., Lavado-Casimiro, W., Masiokas, M., Solman, S., & Villalba, R. (2020). Observed and Projected Hydroclimate Changes in the Andes. Frontiers in Earth Science, 8, 61. https://doi.org/10.3389/FEART.2020.00061/BIBTEX

Palomino-Lemus, R., Córdoba-Machado, S., Gámiz-Fortis, S. R., Castro-Díez, Y., & Esteban-Parra, M. J. (2017). Climate change projections of boreal summer precipitation over tropical America by using statistical downscaling from CMIP5 models. Environmental Research Letters, 12(12), 124011. https://doi.org/10.1088/1748-9326/aa9bf7

Perdigão, R. A. P., & Blöschl, G. (2014). Spatiotemporal flood sensitivity to annual precipitation: Evidence for landscape-climate coevolution. Water Resources Research, 50(7), 5492–5509. https://doi.org/10.1002/2014WR015365

Qi, W., & Liu, J. (2019). Studies on changes in extreme flood peaks resulting from land-use changes need to consider roughness variations. Journal of Hydrology, 64(16), 2015–2024. https://doi.org/10.1080/02626667.2019.1669039

Rogger, M., Agnoletti, M., Alaoui, A., Bathurst, J. C., Bodner, G., Borga, M., Chaplot, V., Gallart, F., Glatzel, G., Hall, J., Holden, J., Holko, L., Horn, R., Kiss, A., Kohnová, S., Leitinger, G., Lennartz, B., Parajka, J., Perdigão, R., … Blöschl, G. (2017). Land use change impacts on floods at the catchment scale: Challenges and opportunities for future research. Water Resources Research, 53(7), 5209–5219. https://doi.org/10.1002/2017WR020723

Rotger, D. V. (2018). Mitigación del riesgo de inundación a partir de la planificación del paisaje. Caso: Arroyo del Gato. Gran la Plata (Buenos Aires, Argentina). Urbano, 21(37), 44–53. https://doi.org/10.22320/07183607.2018.21.37.04

Rothman, K. (1976). The Estimation of Synergy or Antagonism. American Journal of Epidemiology, 103(5), 506–511. https://doi.org/10.1093/oxfordjournals.aje.a112252

Salazar, S., Francés, F., Komma, J., Blume, T., Francke, T., Bronstert, A., & Blöschl, G. (2012). A comparative analysis of the effectiveness of flood management measures based on the concept of "retaining water in the landscape" in different European hydro-climatic regions. Natural Hazards and Earth System Sciences, 12(11), 3287–3306. https://doi.org/10.5194/nhess-12-3287-2012

Sánchez, D., Merlo, J., Haro, R., Acosta, M., & Bernal, G. (2018). Soils from the Amazonia (J. Espinosa, J. Moreno, & G. Bernal (eds.); pp. 113–137). Springer. https://doi.org/10.1007/978-3-319-25319-0_4

Sarmiento, F. O., & Kooperman, G. J. (2019). A Socio-Hydrological Perspective on Recent and Future Precipitation Changes Over Tropical Montane Cloud Forests in the Andes. Frontiers in Earth Science, 7, 324. https://doi.org/10.3389/feart.2019.00324

Segarra, V. (2022). Evaluación de la oferta hídrica bajo escenarios de cambio climático en la microcuenca del río Colonso, Ecuador. https://repositorio.ikiam.edu.ec/jspui/bitstream/RD_IKIAM/627/1/TT-H-IKIAM-000011.pdf

SGR. (2018). Metodología para elaborar agendas de reducción de riesgos. SNGRE. https://www.gestionderiesgos.gob.ec/wp-content/uploads/downloads/2019/01/METODOLOGÍA-PARA-ELABORAR-ARR.pdf

SGR. (2019). Lineamientos para incluir la gestión del riesgo de desastres en el Plan de Desarrollo y Ordenamiento Territorial (PDOT). SNGRE.

Sharma, A., Wasko, C., & Lettenmaier, D. P. (2018). If Precipitation Extremes Are Increasing, Why Aren't Floods? Water Resources Research, 54(11), 8545–8551. https://doi.org/10.1029/2018WR023749

Sierra, R. (2013). Patrones Y Factores De Deforestación En El Ecuador Continental. Conservación Internacional Ecuador y Forest Trends, 1, 22.

Smart, G. M. (2018). Improving flood hazard prediction models. International Journal of River Basin Management, 16(4), 449–456. https://doi.org/10.1080/15715124.2017.1411923

Solman, S. A. (2013). Regional climate modeling over south america: A review. Advances in Meteorology, 2013. https://doi.org/10.1155/2013/504357

Sorribas, M. V., Paiva, R. C. D. D., Melack, J. M., Bravo, J. M., Jones, C., Carvalho, L., Beighley, E., Forsberg, B., & Costa, M. H. (2016). Projections of climate change effects on discharge and inundation in the Amazon basin. Climatic Change, 136(3–4), 555–570. https://doi.org/10.1007/s10584-016-1640-2

Soulsby, C., Dick, J., Scheliga, B., & Tetzlaff, D. (2017). Taming the flood—How far can we go with trees? Hydrological Processes, 31(17), 3122–3126. https://doi.org/10.1002/HYP.11226

Southgate, D., Sierra, R., & Brown, L. (1991). The causes of tropical deforestation in Ecuador: A statistical analysis. World Development, 19(9), 1145–1151. https://doi.org/10.1016/0305-750X(91)90063-N

Sriwongsitanon, N., & Taesombat, W. (2011). Effects of land cover on runoff coefficient. Journal of Hydrology, 410(3–4), 226–238. https://doi.org/10.1016/J.JHYDROL.2011.09.021

Teng, J., Jakeman, A. J. J., Vaze, J., Croke, B. F. W. F. W., Dutta, D., & Kim, S. (2017). Flood inundation modelling: A review of methods, recent advances and uncertainty analysis. Environmental Modelling and Software, 90, 201–216. https://doi.org/10.1016/j.envsoft.2017.01.006

Tian, J., Guo, S., Yin, J., Pan, Z., Xiong, F., & He, S. (2022). Quantifying both climate and land use/cover changes on runoff variation in Han River basin, China. Frontiers of Earth Science, 16(3), 711–733. https://doi.org/10.1007/S11707-021-0918-5/METRICS

Tobón, C. (2008). Los bosques andinos y el agua. In Publicación de ECOBONA (Serie#4). Programa regional ECOBONA - INTERCOOPERATION, CONDESAN. http://infobosques.com/portal/wp-content/uploads/2016/08/b6a77b5786ffc08556b4861b514e76d6.pdf

Tobón, C. (2021). Ecohydrology of Tropical Andean Cloud Forests. The Andean Cloud Forest, 61–87. https://doi.org/10.1007/978-3-030-57344-7_4

UNEP. (2019). Land and Soil - Global Environment Outlook (GEO-6): Healthy Planet, Healthy People Chapter 8. https://wedocs.unep.org/20.500.11822/27657

UNISDR. (2017). Words into Action Guidelines: National Disaster Risk Assessment Hazard Specific Risk Assessment 4. Flood Hazard and Risk Assessment. UNISDR.

VanLiew, M. W., Arnold, J. G., & Bosch, D. D. (2005). Problems and potential of autocalibrating a hydrologic model. Transactions of the ASAE, 48(3), 1025–1040. https://doi.org/10.13031/2013.18514

Vargas, D., Pucha-Cofrep, D., Serrano-Vincenti, S., Burneo, A., Carlosama, L., Herrera, M., Cerna, M., Molnár, M., Jull, A. J. T., Temovski, M., László, E., Futó, I., Horváth, A., & Palcsu, L. (2022). ITCZ precipitation and cloud cover excursions control Cedrela nebulosa tree-ring oxygen and carbon isotopes in the northwestern Amazon. Global and Planetary Change, 211, 103791. https://doi.org/10.1016/J.GLOPLACHA.2022.103791

Vu, M. T., Raghavan, V. S., & Liong, S.-Y. (2017). Deriving short-duration rainfall IDF curves from a regional climate model. Natural Hazards, 85(3), 1877–1891. https://doi.org/10.1007/s11069-016-2670-9

Wasko, C., & Sharma, A. (2017). Global assessment of flood and storm extremes with increased temperatures. Scientific Reports, 7(1), 7945. https://doi.org/10.1038/s41598-017-08481-1

Wasko, C., Sharma, A., & Lettenmaier, D. P. (2019). Increases in temperature do not translate to increased flooding. Nature Communications, 10(1), 5676. https://doi.org/10.1038/s41467-019-13612-5

Yang, L., Feng, Q., Yin, Z., Wen, X., Si, J., Li, C., & Deo, R. C. (2017). Identifying separate impacts of climate and land use/cover change on hydrological processes in upper stream of Heihe River, Northwest China. Hydrological Processes, 31(5), 1100–1112. https://doi.org/10.1002/HYP.11098

Yin, J., Gentine, P., Guo, S., Zhou, S., Sullivan, S. C., Zhang, Y., Gu, L., & Liu, P. (2019). Reply to 'Increases in temperature do not translate to increased flooding.' Nature Communications, 10(1), 5675. https://doi.org/10.1038/s41467-019-13613-4

Yin, J., Gentine, P., Zhou, S., Sullivan, S. C., Wang, R., Zhang, Y., & Guo, S. (2018). Large increase in global storm runoff extremes driven by climate and anthropogenic changes. Nature Communications, 9(1), 4389. https://doi.org/10.1038/s41467-018-06765-2

Zhang, L., Nan, Z., Yu, W., Zhao, Y., & Xu, Y. (2018). Comparison of baseline period choices for separating climate and land use/land cover change impacts on watershed

hydrology using distributed hydrological models. Science of The Total Environment, 622–623, 1016–1028. https://doi.org/10.1016/J.SCITOTENV.2017.12.055

APPENDIX I

COVER PAGE OF PUBLISHED ARTICLES

water

MDPI

Article

Flood Hazard Assessment in Data-Scarce Watersheds Using Model Coupling, Event Sampling, and Survey Data

Jorge Hurtado-Pidal [1,*], Juan S. Acero Triana [2], Edgar Espitia-Sarmiento [3] and Fernando Jarrín-Pérez [4]

1 Department of Territorial Planning, Faculty of Environmental Sciences and EULA-Centre, Universidad de Concepción, 4070386 Concepción, Chile
2 Department of Agricultural and Biological Engineering, University of Illinois, 1304 West Pennsylvania Avenue, Urbana, IL 61801, USA; jsa2@illinois.edu
3 Water and Aquatic Resources Research Group (GIRHA), Universidad Regional Amazónica Ikiam, 150101 Tena, Ecuador; edgar.espitia@ikiam.edu.ec
4 Department of Biological & Agricultural Engineering, Texas A&M University, TX 77843, USA; fjarrin@tamu.edu
* Correspondence: jorgehurtado@udec.cl; Tel.: +56-9-6298-4586

Received: 8 July 2020; Accepted: 1 October 2020; Published: 4 October 2020

Abstract: The application of hydrologic and hydrodynamic models in flash flood hazard assessment is mainly limited by the availability of robust monitoring systems and long-term hydro-meteorological observations. Nevertheless, several studies have demonstrated that coupled modeling approaches based on event sampling (short-term observations) may cope with the lack of observed input data. This study evaluated the use of storm events and flood-survey reports to develop and validate a modeling framework for flash flood hazard assessment in data-scarce watersheds. Specifically, we coupled the hydrologic modeling system (HEC-HMS) and the Nays2Dflood hydrodynamic solver to simulate the system response to several storm events including one, equivalent in magnitude to a 500-year event, that flooded the City of Tena (Ecuador) on 2 September, 2017. Results from the coupled approach showed satisfactory model performance in simulating streamflow and water depths ($0.40 \leq$ Nash-Sutcliffe coefficient ≤ 0.95; $-3.67\% \leq$ Percent Bias $\leq 23.4\%$) in six of the eight evaluated events, and a good agreement between simulated and surveyed flooded areas (Fit Index = 0.8) after the 500-year storm. The proposed methodology can be used by modelers and decision-makers for flood impact assessment in data-scarce watersheds and as a starting point for the establishment of flood forecasting systems to lessen the impacts of flood events at the local scale.

Keywords: flood hazard assessment; data scarcity; model coupling; event sampling; survey data

1. Introduction

The assessment of natural hazards, such as flash floods, remains a challenging issue in environmental sciences [1]. Flash floods caused by extreme rainfall events associated with climate change have increased in the past few years [2–4]. Thus, the development and implementation of measures that diminish flash flood impacts and safeguard people and civil infrastructure are imperative. In this context, numerical models have been found to be reliable tools for flash flood hazard assessment. Specifically, hydrological and hydrodynamic models have been widely applied to describe flash flood dynamics at the watershed scale and project potential impacts on urban areas. Hydrological models (e.g., HEC-HMS, SWAT, MIKE 11, HBV, Top Model) have been widely used to simulate precipitation-runoff processes due to the ease of their implementation [1]. Although these

Ecological Engineering 183 (2022) 106764

Contents lists available at ScienceDirect

Ecological Engineering

journal homepage: www.elsevier.com/locate/ecoleng

Is forest location more important than forest fragmentation for flood regulation?

Jorge Hurtado-Pidal [a,*], Juan S. Acero Triana [b], Mauricio Aguayo [a], Oscar Link [c], Bryan G. Valencia [d], Edgar Espitia-Sarmiento [d], Bruno Conicelli [d]

[a] Department of Territorial Planning and EULA-Center, Universidad de Concepción, Chile
[b] Department of Environmental Sciences, University of California Riverside, USA
[c] Department of Civil Engineering, Universidad de Concepción, Chile
[d] Department of Water and Earth Sciences, Universidad Regional Amazónica Ikiam, Ecuador

ARTICLE INFO

Keywords:
TETIS
Overland flow
Stormflow
Land cover change
Tropical humid basin
Ecuador

ABSTRACT

Native forest deforestation has been identified as one of the main land cover changes affecting flood risk specially during small and moderate storm events. In this regard, forest protection and reforestation are considered a nature-based solution (NbS) for flood regulation. However, there is a lack of knowledge about the effects of different deforestation spatial patterns over floods. Effects of land cover changes on floods in a humid tropical basin within the Ecuadorian Amazon are assessed distinguishing forest location and forest fragmentation. The hydrological distributed model TETIS was applied to simulate the hydrological response of a basin to extreme storms having return periods of 1, 10 and 100 years, considering five land cover scenarios. The model was calibrated and validated using nine storm samples collected at a gauge station during the years 2018 and 2020. The simulated overland flow in hillslopes and stormflows within the river channel were analyzed to i) assess the statistical differences among all land use scenarios with the Kruskal-Wallis test; ii) assess the statistical differences among pairs of both location and fragmentation scenarios through the post-hoc evaluation Dunn test; iii) assess the statistical differences in relation to the baseline. Obtained results indicate that stormflow is less sensitive than overland flow to land cover changes. Forest location have more influence than forest fragmentation over both, overland flow and storm flows. Deforestation of the upper basin represents the worst scenario for flood regulation, thus protection of existing forest, as well as reforestation of deforested areas located in the upper watersheds is a priority for flood risk mitigation and forest conservation. The results enhance our understanding of ecosystem services provided by tropical Andean foothills forests.

1. Introduction

Between January 1975 and June 2002, freshwater floods, including flash floods, killed 176,864 people producing 2.27 billion losses worldwide (Jonkman, 2005; Merz et al., 2014; UNISDR, 2017). The synergy between land cover and climate change will likely increase, exacerbating flood risk (Chang and Franczyk, 2008; De Roo et al., 2003; Güneralp et al., 2015; Hirabayashi et al., 2013; IPCC, 2021; Yin et al., 2018). Native forest deforestation has been identified as one of the main land cover changes affecting flood risk (Gao and Yu, 2017). Consequently, there is a general concern in searching for land cover based solutions to approach flood risk management as land cover is a fundamental hydrological driver (Barbedo et al., 2014; Bin et al., 2018; Blöschl et al., 2007; Lane, 2017; Rogger et al., 2017).

Forest protection and reforestation are considered a nature-based solution (NbS) for flood regulation (Dadson et al., 2017; Ilieva et al., 2018; Seddon et al., 2020). NbS gained much attention in Tropical Andean regions as forests also provide ecosystem services, such as carbon storage, soil erosion control, and water regulation (Ataroff and Rada, 2000; Bonnesoeur et al., 2019; Tobón, 2021, Tobón, 2008). For instance, the forest can intercept up to 30% of the rainfall (FAO-CIFOR, 2005), returning it into the atmosphere through evaporation. Therefore, soil moisture is reduced by forests through evapotranspiration or enhanced infiltration, especially in tropical regions. Forests can also delay the overland flow acting as a water flow obstacle that increases the terrain roughness (Iacob et al., 2017; Shuttleworth et al., 2019; Yang et al.,

* Corresponding author.
E-mail address: jorgehurtado@udec.cl (J. Hurtado-Pidal).

https://doi.org/10.1016/j.ecoleng.2022.106764
Received 2 March 2022; Received in revised form 28 April 2022; Accepted 29 July 2022

APPENDIX II

RESUMEN PARA DIFUSIÓN

RESUMEN PARA DIFUSIÓN

El cambio climático con el aumento de la precipitación y el cambio de cobertura del suelo, como la deforestación, son dos de las principales razones por las cuales las inundaciones pueden ocurrir más seguido o ser de mayor magnitud. El efecto del cambio climático sobre el caudal de los ríos puede abarcar grandes regiones, mientras que la deforestación, tiene un impacto más localizado, por ejemplo, en cuencas hidrográficas pequeñas con menos de 100 kilómetros cuadrados de área. Por esta razón, la protección y reforestación de bosques, es considerado como una de las Soluciones Basadas en la Naturaleza (SbN) para regular inundaciones en cuencas pequeñas. Sin embargo, aun así, la capacidad del bosque para regular inundaciones es limitada, siendo efectiva solamente durante eventos de precipitación pequeños y medianos. Sin embargo, hay poca información sobre cómo el cambio climático y la deforestación actúan de forma combinada magnificando sus efectos sobre las inundaciones. Además, tampoco se conoce como las diferentes formas de puede tener la deforestación, impactan las inundaciones. En consecuencia, esto limita nuestra comprensión de cómo los bosques, ayudan a prevenir inundaciones en el contexto de las SbN y la adaptación al cambio climático. Para resolver este problema, este estudio analizó, en una cuenca tropical en la Amazonía Ecuatoriana, cómo la deforestación en diferentes partes de la cuenca afecta el régimen de caudales y las inundaciones. También se examinó, cómo el cambio climático y la deforestación se combinan para alterar los caudales en la cuenca.

En la primera parte del trabajo, se usaron modelos matemáticos que simulan el comportamiento del agua en el río, pero también cuando se desborda y produce inundaciones. De esta forma se pudo simular cómo la cuenca responde a diferentes intensidades de precipitación y eventos de inundación, incluido un evento que inundó la ciudad de Tena en la Amazonía Ecuatoriana, el 2 de septiembre de 2017. En la segunda parte del trabajo se construyeron escenarios hipotéticos de deforestación en la cuenca, para ver cómo cambian los caudales por este fenómeno. Se evaluó, el efecto que se produce en los caudales, la deforestación en la parte baja de la cuenca, en la parte alta o cabeceras, pero también la deforestación dispersa en toda la cuenca. Por último, en la tercera parte del trabajo, se analizó también el efecto que tiene en los caudales el cambio climático con el aumento de precipitación y también como se puede potenciar con la deforestación. Se evaluaron, así mismo, los efectos individuales y combinados del cambio climático y la deforestación en 42 puntos de la red hídrica de la cuenca (puntos de muestreo de caudales en la Figura 1).

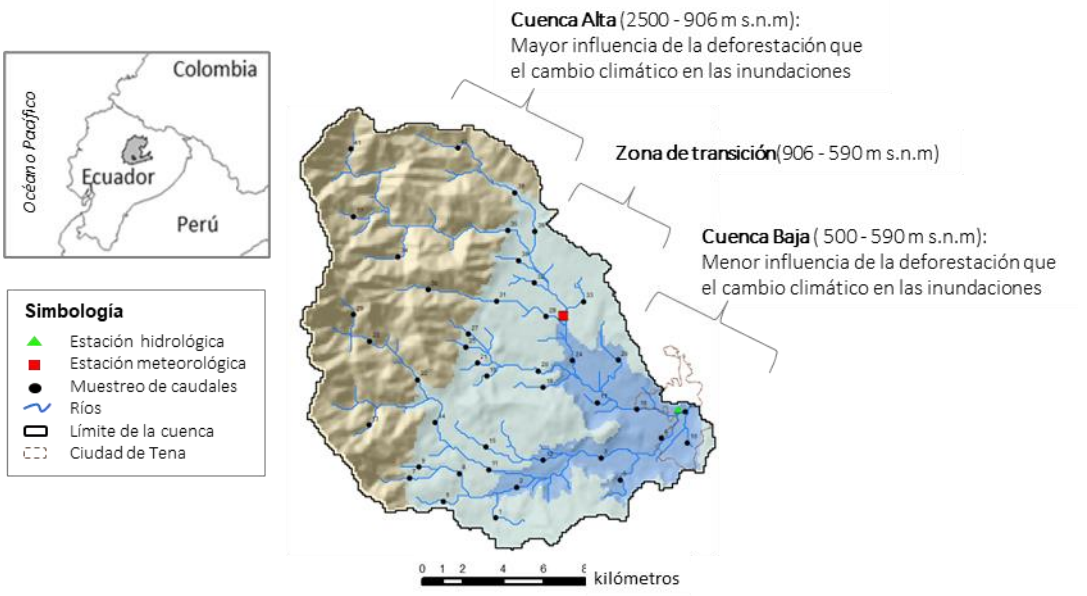

Figura AII. 1. Zonificación de la cuenca en función de la importancia del cambio climático y la deforestación en las inundaciones.

Se encontró que, independientemente de la superficie del bosque, la ubicación de la cubierta forestal si es importante para regular caudales durante tormentas. Específicamente, el bosque ubicado en la parte alta de la cuenca tiene más capacidad para regular caudales, respecto al bosque en la parte baja. Sin embargo, se observó que a medida que las tormentas se vuelven más intensas, el bosque pierde su capacidad de regulación de caudales, independientemente de su localización. Por otro lado, se verificó que el cambio climático afecta a los caudales de forma más homogénea, o similar, a lo largo de la cuenca. En general, el cambio climático tuvo más efecto en los caudales en la parte baja de la cuenca; mientras que la deforestación tuvo mas efecto en la parte alta. Ahora bien, cuando el cambio climático y la deforestación se combinaron, su efecto también fue mayor en la parte alta y disminuyó progresivamente hacia la parte baja, haciéndose casi imperceptible al final. En base a estos resultados se pudieron establecer tres zonas en función de la importancia del cambio climático y la deforestación en las inundaciones (cuenca alta, zona de transición y cuenca baja; Figura 1).

En resumen, la protección y reforestación de los bosques en la parte alta de la cuenca son esenciales para reducir el riesgo de inundaciones. Sin embargo, a medida que las tormentas se vuelven más intensas y el área de la cuenca se hace más grande, los bosques tienen menos capacidad para prevenir inundaciones. Por lo tanto, debemos combinar las SbN con otras estrategias para gestionar eficientemente las inundaciones.